NUCLEAR PHYSICS at GANIL - A COMPILATION 1989-1991

M. Bex, J. Galin

NUCLEAR PHYSICS GANIL 1989-1991

a COMPILATION

NUCLEAR PHYSICS at GANIL

A - COMPILATION

1989-1991

Editors : Monique BEX, Joël GALIN

Spring 1992

CONTENTS

FOREWORD.

This compilation deals with experimental and theoretical work performed at GANIL for the 1989-1991 years. During this period, the accelerator performances have been strongly increased, as well for the delivered energies and intensities as for the span of accelerated ions. In the experimental areas, a totally new data acquisition system has been set up, and the adding of a Wien filter to the Lise spectrometer results now in a versatile and efficient isotope separator, called LISE III.

In this foreword, it is not possible to refer to every result obtained during the considered period, but it is interesting to illustrate by few examples what is due to the improved qualities of the accelerator and of the experimental facilities.

The time structure and the large intensity of the beam were decisive in identifying, for the first time, kaon production in heavy ions collisions at the GANIL subthreshold energies. Nucleons have to undergo several collisions before inducing such a process, and the strange particle emission should be very sensitive to the physical conditions of the hot and compressed interacting zone.

Lead and Uranium beams, now available at the Fermi energy, have been used to study the nuclear disassembly of very large and heavy systems. New results have been obtained on the collective flow in heavy ion reactions, giving new insights on the Equation of State problematics.

In the field of nuclear structure, the magnetic spectrometer SPEG, coupled with large particle or gamma detectors shed light on new aspects of the giant resonance excitations. Exotic nuclei are extensively studied, with a particular emphasis on the 11Li nucleus. A new method of mass measurement, using the CSS2 as a mass separator, has been successfully tested; it will greatly improve the accuracy achieved on intermediate and heavy nuclei.

Last but not least, the theory group is actively working to include fluctuations in the description of the nuclear dynamics and to characterise the onset of the multifragmentation process in heavy ion collisions.

We thank the authors for the quality of their contributions.

Samuel HARAR
Director

Hubert DOUBRE
Deputy Director

I
COMPILATION

PART I : THEORY

PART II: EXPERIMENTS

A - NUCLEAR STRUCTURE

A1 - NUCLEAR SPECTROSCOPY

A2 - EXOTIC NUCLEI AND DECAY MODES

B - NUCLEAR REACTIONS

B1 - PERIPHERAL COLLISIONS. PROJECTILE-LIKE FRAGMENTS

B2 - DISSIPATIVE COLLISIONS - HOT NUCLEI

B3 - MULTIFRAGMENT EMISSION

B4 - MESONS AND PHOTONS

PART 1

THEORY

Inclusion of fluctuations in nuclear dynamics (I)*

G.F. Burgio[1,2,†], Ph. Chomaz[1,2,‡] and J. Randrup[1,3]

[1]) Nuclear Science Division, Lawrence Berkeley Laboratory
University of California, Berkeley, California 94720, USA

[2]) GANIL, B.P. 5027, F-14021 Caen Cedex, France

[3]) GSI, Postfach 11 05 52, D-6100 Darmstadt 11, Germany

1 Introduction

The development of quantitatively useful approximate methods for describing the dynamical evolution of many-body systems far from equilibrium forms an important part of modern physics. A complete treatment requires the consideration of the correlated evolution of a large number of degrees of freedom and is usually impractical.

One avenue towards reducing the problem to a tractable form is to retain only a small part of the dynamical information. In nuclear dynamics it often suffices to retain only the reduced one-body density matrix. In the mean-field approximation, a single average effective one-body density is considered, while fluctuations are completely neglected. The approximation is most useful when the particular ensemble involved displays only little diversity. But when the dynamical evolution contains branchpoints from which very different further developments can occur, such as when the system enters an unstable region, it is meaningless to employ a single "average" representative one-particle density.

One possible solution is to still represent the system in terms of a mean-field configuration which, at any particular time, can undergo a stochastic evolution, so allowing the system to experience different histories. Therefore the global description will be given in terms of "ensemble" of trajectories instead of an "average" one. In effect, this ensemble acts as the heat bath in Brownian motion and the equation of motion will be of the Langevin type.

*This work was supported in part by the Director, Office of Energy Research, Office of High Energy and Nuclear Physics, Nuclear Physics Division of the U.S. Department of Energy under Contract No. DE-AC03-76SF00098.

† Supported in part by INFN Sezione di Catania and LNS, I-95129 Catania, Italy.

‡ On leave from Division de Physique Theorique, Institut de Physique Nucleaire, F-91406 Orsay Cedex, France.

2 Illustration of the method

Our starting point is the socalled Boltzmann-Langevin (BL) equation, which is the stochastic version of the Boltzmann-Uehling-Uhlenbeck (BUU) approach. The BUU equation provides a semi-classical evolution of the one-nucleon phase-space density $f(r,p,t)$ taking into account the propagation in the mean field together with the average effect of Pauli-blocked two-body collisions between individual nucleons. Recently, the BUU theory has been extensively applied to nuclear collisions and has proven fairly successful for describing one-body observables.[4] The stochastic version of this model was proposed to describe large fluctuation phenomena, such as multifragmentation.[2] We have tested a specific implementation of the BL equation, which reads :

$$\frac{\partial f}{\partial t} + \{H[f], f\} = I[f] = \bar{I}[f] + \delta I[f] \ , \qquad (1)$$

where $H[f]$ is the self-consistent mean field Hamiltonian and $I[f]$ is the stochastic collision term, which acts as a random force on the one-body density $f(r,p,t)$. It is then reasonable to split the collision term $I[f]$ into an average part $\bar{I}[f]$ and a fluctuating part $\delta I[f]$.

In order to solve the above equation of motion, we represent $f(r,p)$ on a lattice of grid points in phase space.[3] The size of each lattice cell is given by $\Delta s = \Delta r \Delta p / h^D$, D being the dimension of the physical space, and the value f_k at the lattice point $s_k = (r_k, p_k)$ represents the average value of f over the cell k.

During a given small time interval Δt, the expected number of elementary two-body transitions $\bar{\nu}$ from within the phase-space subcells 1 and 2 into the subcells $1'$ and $2'$ is given by

$$\bar{\nu}_{1,2;1'2'} = \Delta t \Delta s^4 f_1 f_2 \bar{f}_{1'} \bar{f}_{2'} \delta(r_1 - r_2) \delta(r_1 - r_{1'}) \delta(r_2 - r_{2'}) \omega(p_1, p_2; p_{1'}, p_{2'}) \ , \quad (2)$$

where $\omega(p_1, p_2; p_{1'}, p_{2'})$ is the elementary transition rate and the Pauli blocking factors $\bar{f} \equiv 1 - f$ express the availability of the final one-particle states. When the phase-space density $f(r,p)$ is changed in accordance with the above expression the usual BUU evolution results. In order to include the noise term , we note that the actual number of elementary transitions ν is a stochastic variable, having a Poisson distribution characterized by the above mean value $\bar{\nu}$ and a variance $\sigma_\nu^2 = \bar{\nu}$. Therefore, the statistical properties of $I[f]$ are fully determined by the mean transition rates $\bar{\nu}$. In our particular numerical implementation, we simulate the distribution of ν by a Gaussian with variance $\sigma_\nu^2 = \bar{\nu}$. Consequently, the noise δI can be simulated by augmenting the mean value $\bar{\nu}$ with a fluctuation $\delta\nu$ chosen randomly from a normal distribution with a variance equal to $\bar{\nu}$. This manner of introducing the fluctuations at the elementary level preserves the correlations induced by the fact that each individual transition involves four phase-space locations.

3 Applications

In order to test the quantitative utility of the method, we have first studied a periodic two-dimensional system of free nucleons (i.e. without one-body field).[3] The interesting evolution then occurs in momentum space and a spatial average may be performed. The initial condition consists of two touching Fermi spheres of radius 275 MeV/c ($f(p)$ is 1 inside the spheres, 0 otherwise). We have followed an ensemble of 1100 trajectories. We have found that the augmented simulation preserves the mean evolution towards the appropriate Fermi-Dirac distribution, as it should (see Fig.1). In order to study fluctuations and correlations in phase space, we have to discuss the properties of the associated correlation function of $f^n(p,t)$:

$$\sigma(p;p') = 4V(\prec f^n(p)f^n(p') \succ - \prec f^n(p) \succ \prec f^n(p') \succ), \tag{3}$$

which can be splitted in a variance and a covariance :

$$\sigma(p;p') = \sigma^2(p)h^2\delta(p,p') + \sigma_{cov}(p;p'). \tag{4}$$

It was shown that the variance of the phase-space occupancy must follow closely the predictions of the corresponding Fokker-Planck equation [1], $\sigma^2 = f(1-f)$, (see Fig.2). This relation remains valid throughout the evolution if it is fulfilled by the initial condition and represents a strong constraint for any fluctuation calculation.

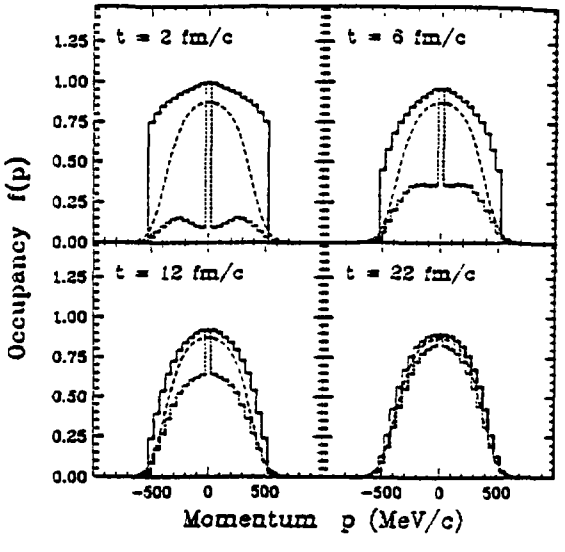

Figure 1 : Occupancy cuts

Cuts along the axes of the ensemble-averaged phase-space occupancy $f(p_x,p_y,t)$, shown at four different times t during the evolution from the initial configuration towards the corresponding Fermi-Dirac equilibrium.

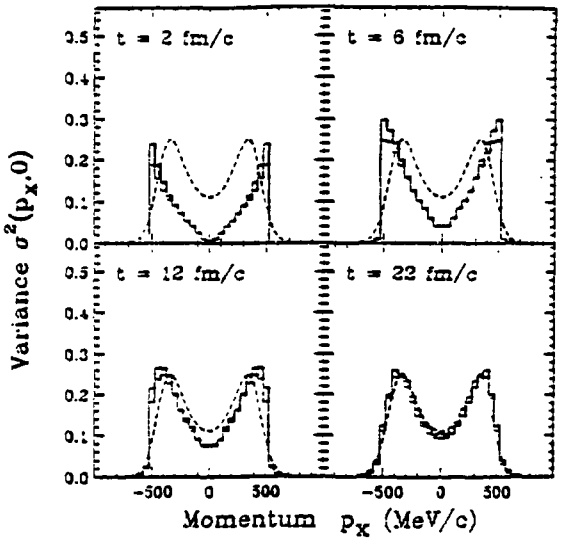

Figure 2 : Variance cuts

Cuts of the variance in phase-space occupancy $\sigma^2(p_x,p_y,t)$ along the axes in a display similar to Fig.1. The solid histogram is the calculated variance, while the dashed curve is the quantum-statistical limit towards which the variance is expected to relax. The thin histogram shows the instantaneous equilibrium variance $f\bar{f}$; it is seen that $\sigma \approx f\bar{f}$ throughout.

The covariance (fig.3 shows the "tagged" covariances, which are partially integrated over a domain of $\pm 45^o$ around the p_x-axis) displays the expected features. Indeed, the initial correlations reflect the only possible type of collision, namely a particle from one of the Fermi spheres scattering off one in the other Fermi sphere into the y direction. In the final pattern, the observed correlation is the superposition of two components: the strong positive correlation with the states around the Fermi surface, but on the opposite side, originated from the only states available as collision partners; secondly, an isotropic negative correlation with the accessible final states all around the Fermi surface.

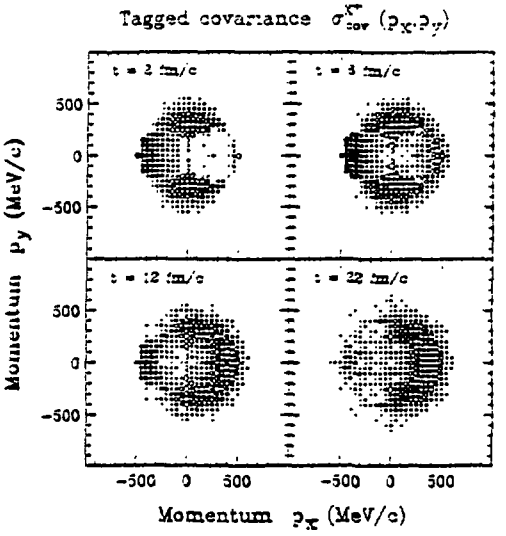

Figure 3 : Tagged covariance

The calculated results for the tagged covariances. The full circles represent positive correlations and the empty circles the negative ones. The radius of a circle is proportional to the magnitude of the correlation.

4 Conclusions

These findings support the validity of our method for treating fluctuations in a quantitatively reliable manner. It is therefore expected that the model may be useful for studying clusterization phenomena at low densities where the mean field is strongly attractive and will amplify the stochastic fluctuations of the individual trajectories in the one-body phase space.

References

[1] J. Randrup and B. Remaud, Nucl. Phys. **A514**, 339 (1990).

[2] S. Ayik and C. Gregoire, Phys. Lett. **B212**, 269 (1988).

[3] Ph. Chomaz, G.F. Burgio, and J. Randrup, Phys. Lett. **B254**, 340 (1991); G.F. Burgio, Ph. Chomaz, and J. Randrup, Nucl. Phys. **A529**, 157 (1991).

[4] G.F. Bertsch and S. Das Gupta, Phys. Rep. **160**, 190 (1988).

Inclusion of fluctuations in nuclear dynamics (II)*

G.F. Burgio[1,2,†], Ph. Chomaz[1,2,‡] and J. Randrup[1,3]

[1]) Nuclear Science Division, Lawrence Berkeley Laboratory
University of California, Berkeley, California 94720, USA

[2]) GANIL, B.P. 5027, F-14021 Caen Cedex, France

[3]) GSI, Postfach 11 05 52, D-6100 Darmstadt 11, Germany

1 Introduction

The Boltzmann-Langevin (BL) approach has recently gained interest in nuclear dynamics as a formally well-founded vehicle for extending the very successful mean-field description to more violent phenomena, such as heavy-ion induced nuclear multifragmentation processes.[1, 2] In the first part of this report we already discussed the numerical method we adopted in order to solve the BL equation and we summarized our efforts to test the method and compare it with others that have been proposed. In those test studies, we ignored the action of the effective one-body field by assuming that it remained constant throughout, thus reducing the interesting dynamics to momentum space alone.

Of course, the effective field plays a key role, since it adjusts itself selfconsistently to the density fluctuations generated by the the two-body collisions, and thus it acts to amplify instabilites. We have included the effective field, which corresponds to the collisionless (Vlasov) part of the evolution, by a standard matrix technique. Here we present a first application to a catastrophic process, namely the clusterization of matter at subsaturation density. Although the approach was developed within the context of nuclear dynamics [3], the method is quite general and may therefore be of much broader utility.

*This work was supported in part by the Director, Office of Energy Research, Office of High Energy and Nuclear Physics, Nuclear Physics Division of the U.S. Department of Energy under Contract No. DE-AC03-76SF00098.

† Supported in part by INFN Sezione di Catania and LNS, I-95129 Catania, Italy.

‡ On leave from Division de Physique Theorique, Institut de Physique Nucleaire, F-91406 Orsay Cedex, France.

2 Application to a Model System

We have studied a gas of Fermions situated on a two-dimensional torus. For the effective one-body field we employ a simplified Skyrme interaction averaged over the y-direction and we look at clusterization along the x-direction only. We then solve the stochastic *BUU* equation on a lattice of 21 cells in the x direction and 25×25 cells in momentum space. We chose a spatial resolution of 1 fm along the x-axis, while the length in the y direction was chosen to be large ($L_y = 5000$ fm) since the one-body field doesn't depend on y. The momentum resolution was 65 MeV/c. The interaction range in the collision integral was taken as 1.2 fm.

We have initialized the system as a uniform gas at half the saturation density, with Fermi-Dirac occupancies corresponding to the small temperature 3 MeV; this is in the mechanically unstable regime of the phase diagram. We analyze an ensemble of 100 trajectories; for each trajectory, the calculation was stopped at 90 fm/c.

In Fig. 1 we show the time evolution of the density vs. the position for one trajectory of the ensemble. Initially the system has a uniform density, but soon the fluctuations are breaking this initial symmetry. Subsequently, the fluctuations are rapidly amplified by the action of the effective one-body field, thus leading towards fragment formation. We note that the density distribution of each particular system keeps changing with time, with the clusters exhibiting fusion and fission. In this manner, each particular trajectory explores the various accessible configurations, while the distribution of trajectories quickly approaches the appropriate statistical limit.

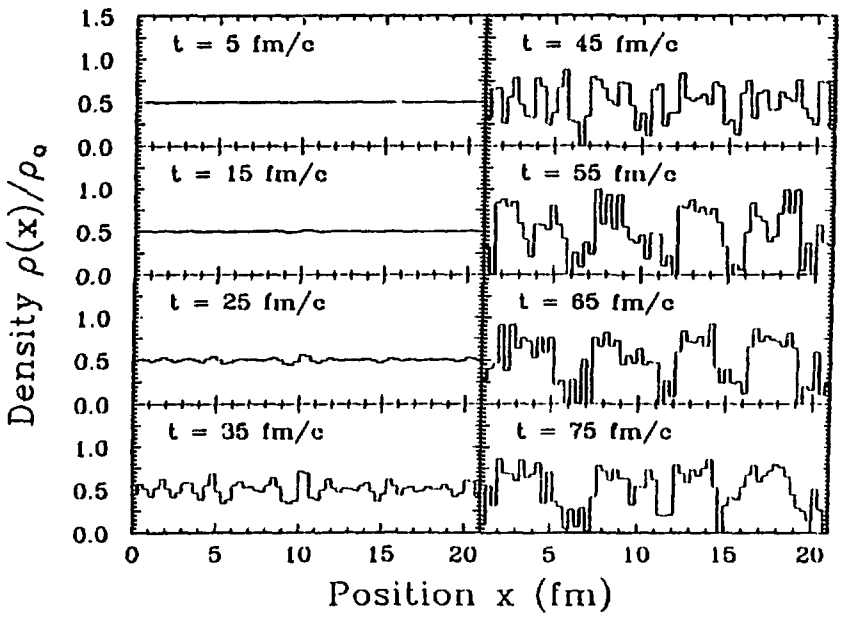

Figure 1

The density profile $\bar{\rho}(x,t)$ associated with one particular trajectory vs. the position x shown at eight different times t.

2.1 Instabilities

To get a deeper insight into the mechanism of fragmentation and the role of the instabilities, we can study the onset of the phenomenon within the linear response theory. If the system is unstable, some eigenmodes will be exponentially amplified with a characteristic time τ.

We have computed the actual dispersion relation by considering the *BUU* evolution (without fluctuations) of a uniform density at 3 MeV of temperature perturbed with a small (1%) harmonic variation in the x direction. In Fig. 2 we show the evolution of $1/\tau$ vs. the wave number k of the eigenmode. The curve is symmetric around $k = 0.75$ fm^{-1}, because a double step is used in the discretization of the gradients.

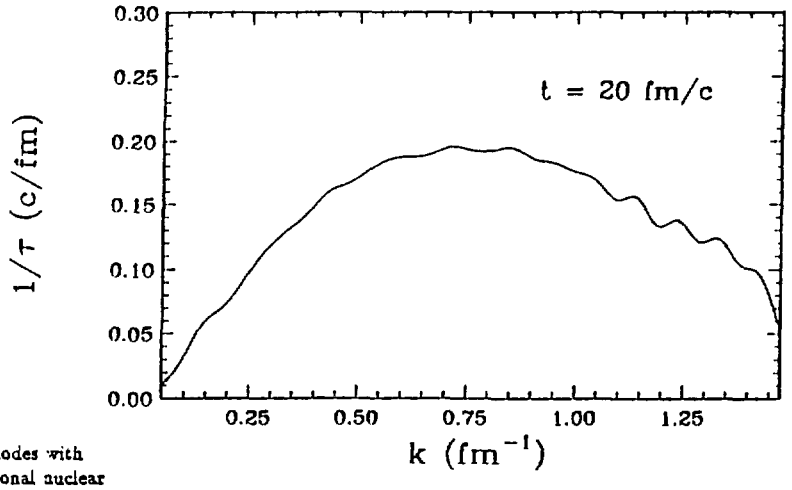

Figure 2

The growth rate $1/\tau_k$ of harmonic modes with reduced wave number k in two-dimensional nuclear matter at half the saturation density, as resulting from our numerical implementation of the *BUU* model.

2.2 The onset of multifragmentation

This normal mode analysis will allow us to study the interplay between instabilities and fluctuations. Indeed, considering the Fourier transform of the fluctuations of the density, $F(k,t) = \int dx e^{i2\pi kx} \delta\rho(x,t)$, we find

$$\sigma_k(t) = \prec |F(k,t)|^2 \succ = \int\int dx dx' \; e^{i2\pi k(x-x')} \; \prec \delta\rho(x,t)\, \delta\rho(x',t) \succ . \quad (1)$$

Fig. 3 displays the fluctuation σ_k vs. the reduced wave number k. At the early stage of the evolution one mainly observes the Fourier component of the noise, and indeed we observe that the spectrum at $t = 5$ fm/c is characteristic of a system where the fluctuations must be correlated over a domain of at least 1 fm in size. As the time goes on, one observes the interplay of the stochastic collisions and the exponentially increasing propagation due to the unstable effective field.

The continual action of both agents shifts the peak to slightly higher frequencies. However, it should be noted that the system is never fully dominated by the instabilities. This demonstrates that the system is keeping some memory of the physical processes that have induced the fluctuations.

After 30 fm/c the system enters into a non-linear regime, with frequency doubling leading soon to a chaotic transition stage, before reaching an equilibrium characterized by a statistical population of fragment configurations, which is independent of the specific early evolution.

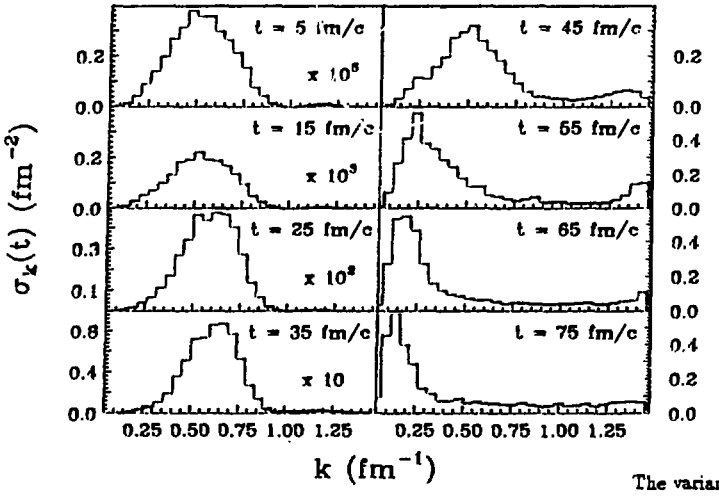

Figure 3

The variance σ_k vs. the reduced wave number k, shown at a number of times t.

3 Conclusions

In conclusion, using a recently developed nuclear BL model, we have made a first dynamical simulation of a catastrophic evolution leading to the multifragmentation of an initially uniform system. In the presented results, we have been able to discern two dynamical regimes: an early linear regime characterized by a competition between the stochastic creation of fluctuations and their exponential evolution due to the instability of the effective field, and a later complex one where the system behaves chaotically and seeks to condense into fragments. Since the detailed evolution towards equilibrium has been found to be sensitive to the specific treatment of the fluctuations, it appears that the inclusion of fluctuations is important for the quantitative description of fragment production in nuclear collisions, and consequently it may be expected that actual collision experiments can provide a means for testing the theory.

References

[1] S. Ayik and C. Gregoire, Phys. Lett. **B212**, 269 (1988);

[2] Ph. Chomaz, G.F. Burgio, and J. Randrup, Phys. Lett. **B254**, 340 (1991); G.F. Burgio, Ph. Chomaz, and J. Randrup, Nucl. Phys. **A529**, 157 (1991).

[3] G.F. Burgio, Ph. Chomaz, and J. Randrup, GSI-91-62, Preprint Dezember 1991, to be published in Phys. Rev. Lett.

CLASSICAL AND QUANTUM APPROACH TO LIGHT-PARTICLE CORRELATIONS IN INTERMEDIATE ENERGY HEAVY-ION REACTIONS

B. Erazmus, L. Martin, N. Carjan[1], R. Lednicky[2], M. Aboufirassi, D. Ardouin,

Laboratoire de Physique Nucléaire IN2P3/CNRS et Université de Nantes
2 rue de la Houssinière - 44072 Nantes - FRANCE
[1] Centre d'Etudes Nucléaires de Bordeaux-Gradignan, 33175 Gradignan Cédex - FRANCE
[2] permanent adress Joint Institut for Nuclear Research, Dubna, Russia

Abstract : *We present a classical and a quantum approach to light particle correlations. The calculations are compared with p-p and p-d correlation functions measured at backward angles in the reaction $^{40}Ar + ^{108}Ag$ at 44 MeV/nucleon. With reasonable lifetime values of the sources the predictions of the classical model is found to be in good agreement with experimental data. The quantum calculations give a good description of the two-proton correlation function while the result for the p-d data is fairly poor. In the quantum approach the Coulomb field of the residual nuclus is not taken into account. This explains most of differences between the two approaches.*

The correlation function of two particles with small relative momenta ($q < 50$ MeV/c) contains valuable information about the spatial and temporal extension of their emission source. However, this information is difficult to extract since the shape of the correlation function is usually due to several, difficult to separate, effects. In the case of identical particles the symmetrization or antisymmetrization of the wave function leads to a constructive or destructive interference in the correlation function. In addition, the outgoing particles interact through attractive nuclear and also, if they are charged, repulsive Coulomb forces.

The three effects occur in the same range of relative momenta and it is therefore useful to look for a situation in which at least one of these effects can approximately be neglected. In the case of light particles sequentially evaporated from a thermalized nucleus the nuclear interaction between two particles is strongly attenuated [1]. We have elaborated a classical and a quantum approach to light-particle correlations in intermediate energy heavy-ion reactions. The data used for comparison with our calculations come from an experiment performed at GANIL, where light particles were measured at backward angles (90° - 125°) in the reaction $^{40}Ar + ^{108}Ag$ at 44 MeV/nucleon [1].

Classical approach.

To describe two light charged particles sequentially evaporated from a residual recoiling nucleus, three body bidimensional trajectory calculations have been performed [2-4]. The two light particles were approximated by point like charges and the emitting nucleus was supposed spherical. An attractive Woods-Saxon nuclear interaction was included only between the residual nucleus and each of the light particles. The nuclear interaction between two particles was neglected since, at a time τ (emission of the second particle) of the order of 10^{-21}s, the distance from the nuclear surface of the first particle is much larger than the range of the nuclear

force. The emission of particles was supposed isotropic and radial with a maxwellian distribution for the initial energies.

The parameters describing the emitting nucleus, i.e. its temperature T, and the Gaussian mass distribution are extracted from the energy spectrum of single protons. A good reproduction of the experimental average proton energy and of the width, measured at backward angles in the reaction $^{40}Ar + ^{108}Ag$, has been obtained by choosing T = 4 MeV, A_0 = 120u and σ_A = 10 u as the emitter temperature and the parameter of its Gaussian mass distribution.

Once the main characteristics of the residual nucleus have been found, we have analyzed the sensitivity of the calculated correlation function to the value of τ, the mean time between two successive particle emissions. Our calculations reproduce the experimental data with a value of $\tau = 2. \times 10^{-21}$s for the two-proton correlation function and $\tau = 3.5 \times 10^{-21}$s for the proton-deuteron system (Fig. 1 a and b).

This classical approach describes the three-body Coulomb interaction and nuclear interaction between light particles and the residual nucleus. Quantum statistics effects as well as nuclear force between two particles are neglected. For a simultaneous treatement of these effects a quantum approach is the most appropriate.

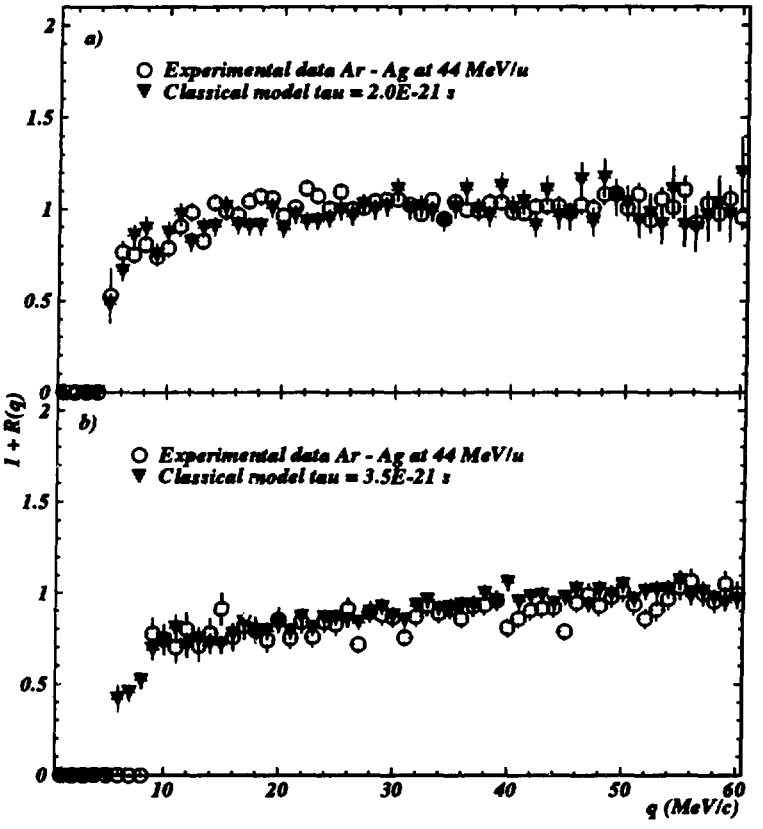

Fig. 1 (a) Two-proton and (b) proton-deuteron correlation functions calculated in the frame of classical approach, taking into account the final detector resolution and compared with the experimental data.

Quantum approach

The model was developped by R. Lednicky and V.L. Lyuboshitz to analyze the dependence of the two-particle correlation function on the space-time dimensions of the particle

production region [5]. The calculation provides simple analytical formulae for the correlation function of two particles with small relative momenta. The effects of quantum statistics and final state interations are taken into account. This model, initially developped for sufficiently fast particles does not take into account their interaction with the residual nucleus.

We have adapted this calculation to our problem of two particles sequentially emitted in intermediate-energy heavy-ion reactions [4]. In the quantum approach, the experimental two-proton correlation function is reproduced as well as by our classical model giving the same value of the mean lifetime of the residual nucleus $\tau = 2. \times 10^{-21}$s (Fig. 2a). This result confirms the strong attenuation of the nuclear force between the two particles.

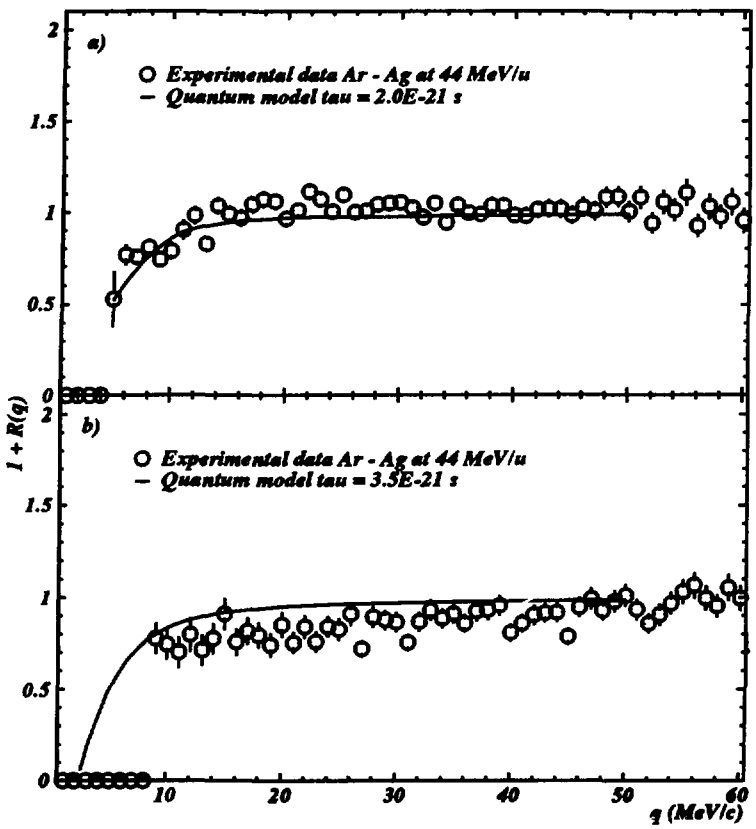

Fig. 2. Predictions of the quantum model compared with the experimental two-proton (a) and proton-deuteron (b) correlation functions.

In the case of proton-deuteron correlation function, the predictions of the quantum model differ from the experimental data (Fig. 2b). The p-d correlation function does not contain neither quantum statistics effects nor resonant nuclear interaction. Coulomb forces are, in this case, the main source of correlations. Moreover, the acceleration in the Coulomb field of the emitter is not the same for proton and for deuteron. The influence of the residual nucleus is certainly important for the correlation function of two particles with a different mass to charge ratio. This explains the disagreement of the experimental data with the quantum calculation. Figure 3 shows that the classical model taking into account the two-body Coulomb interaction only between proton and deuteron gives the same shape of the p-d correlation

function as in the quantum approach. The influence of the Coulomb force from heavy reaction residue was previously observed in α-p correlation measurement [6].

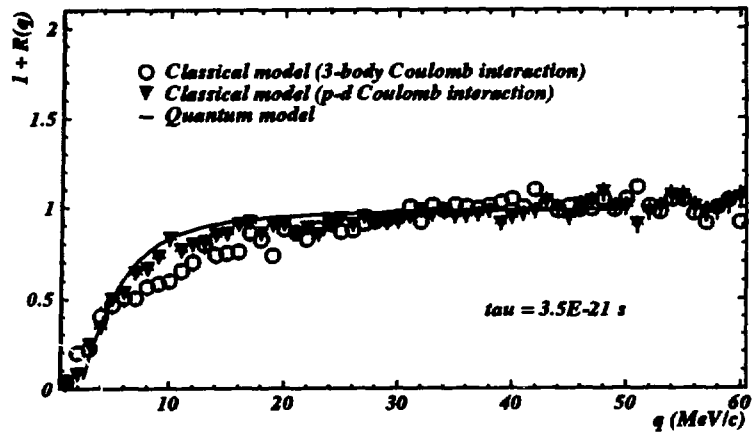

Fig. 3. Proton-deuteron correlation functions predicted by the classical model with and without the Coulomb field of the residual nucleus. The solid curve represents the quantum calculation.

A more precise comparison of these two different approaches will be possible by measuring particles with very small relative momenta. We are now setting up an experiment in which two protons will be detected by the magnetic spectrometer SPEG at GANIL [7]. The minimum value of the relative momentum and the resolution will be of the order of 1 MeV/c.

The first measurement will be performed at backward angles in order to attenuate the strong interaction between two protons and to allow a precise evaluation of the importance of quantum statistics effects. Later, by changing the reaction kinematics and the detection angle, we could be able to vary the characteristics of the emitting nucleus and therefore the shape of the correlation function.

Concerning the theoretical description of all effects giving rise to correlations, the most appropriate approach should be a quantum one taking into account the influence of the residual nucleus. This is a non trivial problem of two particles scattering in the nuclear and Coulomb field of the nucleus.

REFERENCES

(1) D. Ardouin, Nucl. Phys. A495, 57c (1989) ;
P. Lautridou, Ph. D. thesis, Université de Bordeaux (1989) ; J. Quebert, in Proceedings of the XXVII Winter Meeting on Nuclear Physics, Bormio, Italy, 1989.

(2) N. Carjan, B. Erazmus, D. Ardouin, in Proceedings of the International Workshop on Particle Correlations and Interferometry in Nuclear Collisions, Nantes, France, edited by D. Ardouin (World Scientific, Singapore, 1990), p. 192.

(3) B. Erazmus, N. Carjan, D. Ardouin, Phys. Rev. C44 (1991) 2663.

(4) B. Erazmus, L. Martin, N. Carjan, R. Lednicky, to be published.

(5) R. Lednicky, V.L. Lyuboshitz, in Proceedings of the International Workshop on Particle Correlations and Interferometry in Nuclear Collisions, Nantes, France, Edited by D. Ardouin (World Scientific, Singapore, 1990) p. 42, and references therein.

(6) J. Pochodzalla et al., Phys. Lett. 161B (1985) 256.

(7) B. Erazmus et al., Comité National d'Expériences du GANIL - Proposition d'experience n° E 193, juin 1991.

PROPERTIES OF THE NUCLEAR E.O.S. FROM INVESTIGATIONS ON COLLECTIVE EFFECTS IN HEAVY ION COLLISIONS

V. De la Mota, M. Farine, F. Haddad, D Idier, B. Remaud, T. Sami[1], P. Schuck[2], F. Sébille.

Laboratoire de Physique Nucléaire IN2P3/CNRS et Université de Nantes
2 rue de la Houssinière - 44072 Nantes - France
[1] Institut de Physique, BP 52, Bab-Ezzouar, Alger, Algérie
[2] ISN, 38026 Grenoble Cédex - France

I. Competition of mean-field and residual interactions in collective observables

A theoretical analysis of collective observables in Heavy-Ion reactions at medium energies have been performed in the framework of the semi-classical Landau-Vlasov approach. This work is a contribution to the analysis of two fundamental aspects of the nuclear dynamics, i.e. the mean-field and residual interaction effects. The investigation of observable sensitivity to the mean-field has been realized using various effective nuclear interactions. These interactions have been choosen in order to enlighten the influence of the infinite incompressibility modulus, the non-locality and the finite range of the nuclear forces. The sensitivity to the residual interaction has been studied considering different scalings of the in-medium nucleon-nucleon cross-section. An illustration of this work is given in figure 1.

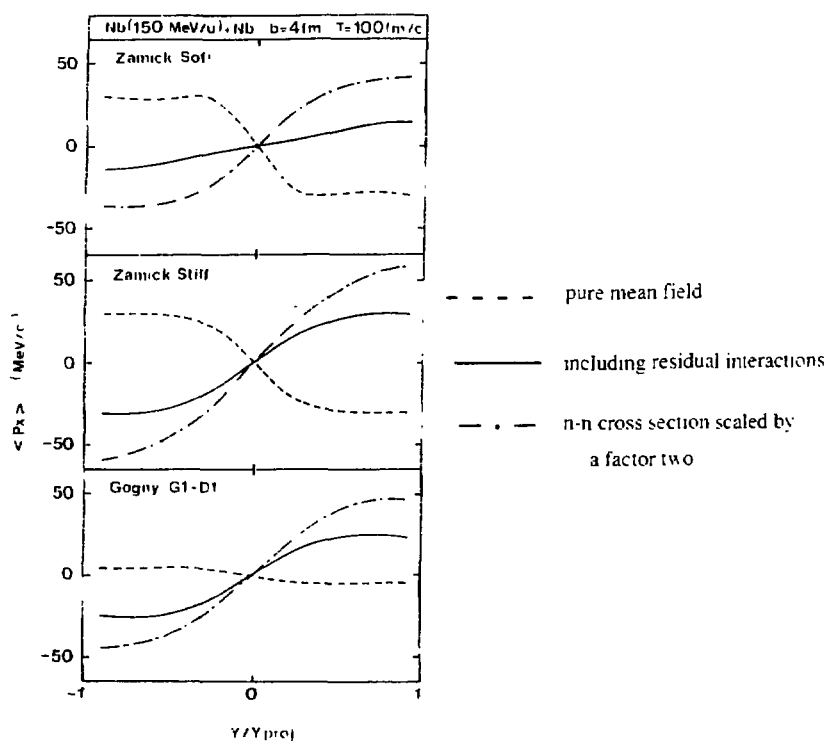

Figure 1. Transverse momentum per nucleon in the reaction plane as a function of the normalized rapidity, at time t = 100 fm/c.

Our results show that the behavior of the observables cannot be interpreted only from pure static considerations. It requires an analysis of the dynamical mechanisms governing their build up. In particular, the theoretical investigation of the transverse collective motion of nuclear matter underlines on one hand, the increasing role of non locality effects and residual interaction with growing incident energies, on the other hand the importance of out of equilibrium effects that must be properly taken into account if one wishes to extract information on the nuclear Equation of State.

2. The phenomenon of flow inversion at GANIL energies.

The study of Heavy-Ion collisions at incident energies above 400 MeV/u have evidenced a transverse collective flow of nuclear matter. More recent experiments performed in particular at GANIL have demonstrated a persistence of this collective effect at lower energies, with in addition the appearance of an inversion in the transverse direction. This inversion phenomenon presents a great interest for the knowledge of the nuclear matter properties, since it bears signatures of a transition between two different regimes. One in which the predominant behavior is repulsive, and another one where it is attractive. Due to the interest of this effect and to the quality of the experimental results obtained at GANIL, a theoretical study have been undertaken in the framework of the Landau-Vlasov approach.

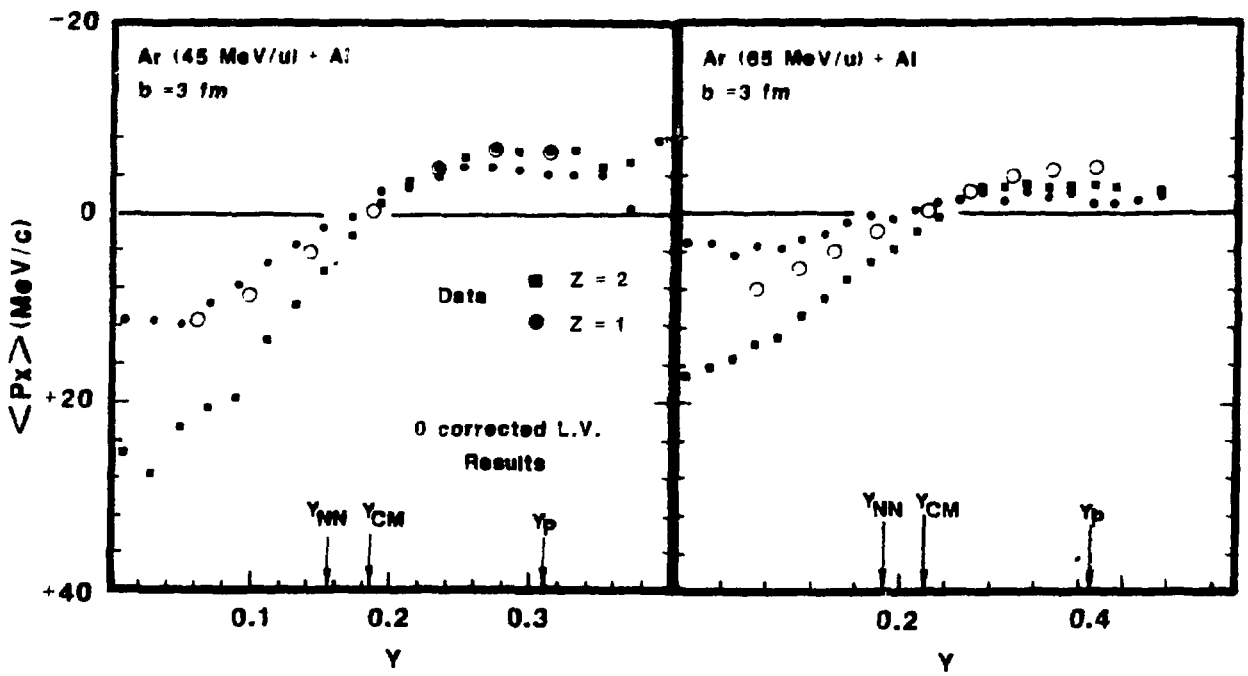

Figure 2. Mean transverse momentum in the reaction plane as a function of the longitudinal rapidity.

Comparisons between theoretical and experimental results have been performed, taking into account the main experimental biases. They permitted to check that the simulations of nuclear collisions should bring qualitative as well as quantitative informations. An illustrative example is given in figure 2. The theoretical analysis has also addressed the sensitivity of the transverse flow to the nuclear matter properties. Without entering the details, among the main results steming from this study, is that heavy ion collisions should not provide a direct access to the value of the infinite incompressibility modulus. This is coherent with the fact that the

nuclear matter properties do not restrict to this parameter alone. In addition, heavy-ion collisions provide the opportunity to explore large areas of the nuclear Equation of State, and to improve our knowledge on the nuclear properties in situations out of equilibrium.

3. Isospin effects on dynamics of heavy-ion collisions.

Heavy-ion physics with radioactive beams open new domains of research where properties of nuclei very far from the beta stability line can be explored. Calculations were carried out within the Landau-Vlasov model formalism, using an effective force which has an adjustable isospin dependent term. Our aim was to gain insight on two related questions :

- what are the effects of the isospin dependent component of the interaction on dynamics of reactions described within Landau-Vlasov formalism ?
- are there sizeable differences in dynamics of reactions induced by radioactive beams in comparison with reactions induced by comparable beams close to the beta stability line ?

After checking that static properties of different Ca isotopes could be correctly described by our model we investigated two types of heavy ion collisions.

We investigated peripheral collisions between various Ca isotopes at 15 MeV/u incident kinetic energy with an impact parameter b = 7 fm. Results of calculations show that inclusion of the isospin interaction is needed to achieve complete equilibration. Influence of the isospin on the dynamics can be seen in figure 3 which shows a plot of the density of matter at 2 times t = 160 fm/c and t = 240 fm/c for the ^{56}Ca (15 MeV/u) + ^{40}Ca, for 3 values of the adjustable isospin-strength parameter c. Reaction time and neck formation clearly depend on c.

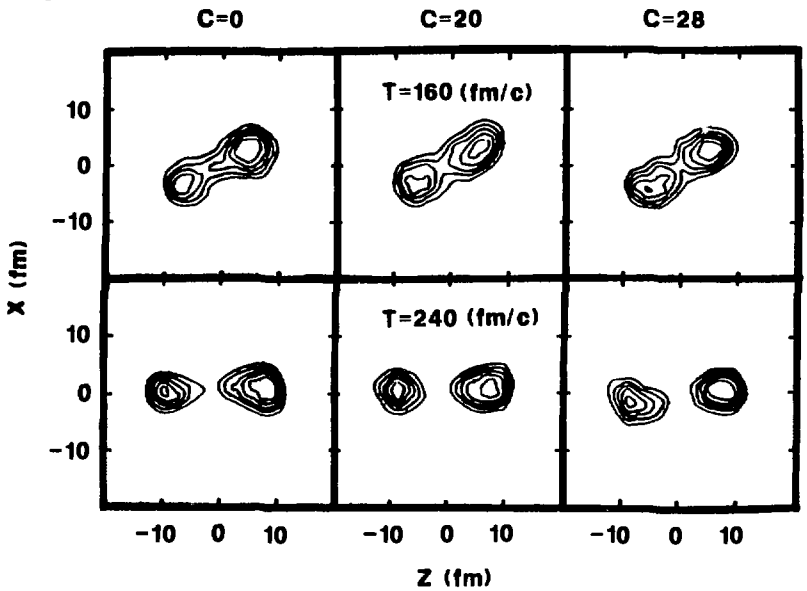

Figure 3. Influence of the isospin on the dynamics of the reaction ^{56}Ca (15 MeV/u) + ^{40}Ca at b = 7 fm.

In order to study isospin effects at higher energies we carried out calculations on central collisions (b = 2 fm) with the same Ca isotopes at 40 MeV/u incident kinetic energy. Preequilibrium emissions were shown to be very sensitive to the isospin-strength parameter c. We also looked at the instantaneous value of the I = (N-Z/A) coefficient of the emitted fluxes ; as expected, we have a net dependence of the time evolution of I on the value of c, with large initial fluctuations due to the small number of nucleons taken into account. With c growing, neutrons are less bound which favors an increase of I. Asymptotic values of I are quickly reached (around 140 fm/c) (figure 4).

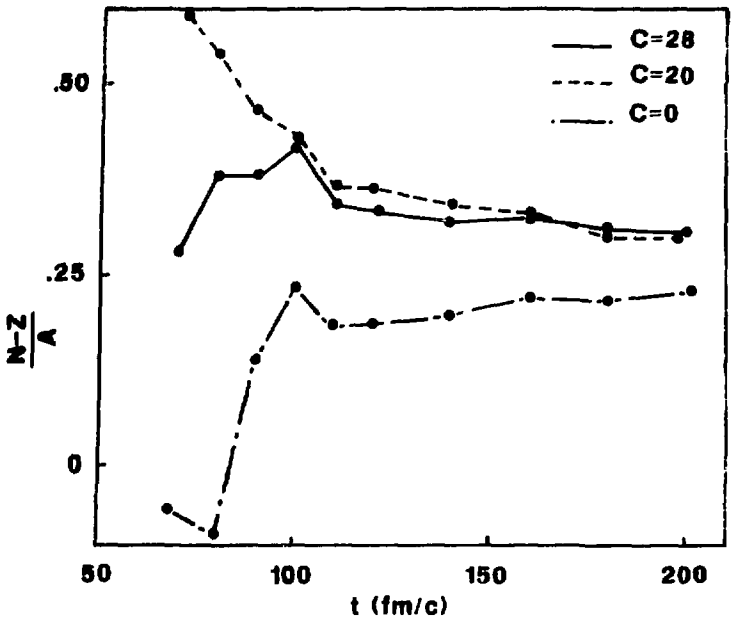

Figure 4. Time evolution of I = N - N/A for different values of c during the reaction ^{48}Ca (40 MeV) + ^{48}Ca.

Such calculations have shown that semi-classical models could also be used to study microscopic nuclear fluxes between interacting ions. Preliminary calculations were done in this direction, showing the sensitivity of this mechanisms vs the isospin strength parameter c.

References.

(1) J. Peter et al, Nucl. Phys. A519 (1990) 611, Phys. Lett. B2371 (1990) 187.
(2) P. Schuck, R.W. Hasse, J. Jaenicke, C. Grégoire, B. Remaud, F. Sébille and E. Suraud, Prog. in Part. and Nucl. Phys. 22 (1989) 181.
(3) V. de la Mota, F. Sébille, B. Remaud and P. Schuck, XXVII Winter Meeting on Nuclear Physics, Bormio, Italy (1990).
(4) F. Sébille, V. de la Mota, B. Remaud and P. Schuck, Second IN2P3-RIKEN symposium on Heavy-ion collisions, World Scientific (1990) 369.
(5) M. Farine, T. Sami, B. Remaud and F. Sébille, Z. Phys. A. 339 (1991) 363.

DYNAMICS OF FLUCTUATION THROUGH COMPUTER SIMULATIONS

B. Benhassine, M. Farine, E.S. Hernandez[1], D. Idier, B. Remaud, F. Sébille.

Laboratoire de Physique Nucléaire IN2P3/CNRS et Université de Nantes
2 rue de la Houssinière - 44072 Nantes - FRANCE
[1]) Depto de Fisica (UBA) Pabellon I. Ciudad Universitaria 1428 Buenos Aires, ARGENTINE

I. Dynamics of density fluctuations in nuclear matter.

Due to the structure of the effective nucleon-nucleon force, a spinodal region can be defined in the (Temperature, Density) plane of the Nuclear Equation of State. The matter instability against long wavelength density fluctuations which is expected to occur in this zone, has been tentatively associated with the experimentally observed increase of the yield of intermediate mass fragments, around 50 MeV/u incident energies.

We have undertaken a systematic study to compute the dynamics of such a process, first in infinite nuclear matter to get rid of the surface instabilities which could compete in finite nuclei. The process of bubble or droplet formation is an out-of-equilibrium process for which no formal theory is available : the Landau theory of Fermi liquids can predict only the birth conditions of the process but it fails as soon as the system enters the non-linear regime. We then use computer simulations, submitted to the constraint that they should reproduce at best the ground properties of nuclear matter close to equilibrium.

In this work, we address :

1) the conditions under which the Nuclear Equation of State in a large range of excitation energies can be accurately reproduced with a semi-classical model using test particles, for local as well as non-local nucleon-nucleon interactions. An illustrative example is given in figure 1.
2) the dynamics of fragment formation.
3) the effects of temperature, average density, screened Coulomb interaction, effective mass on the characteristic times for fragment formations.

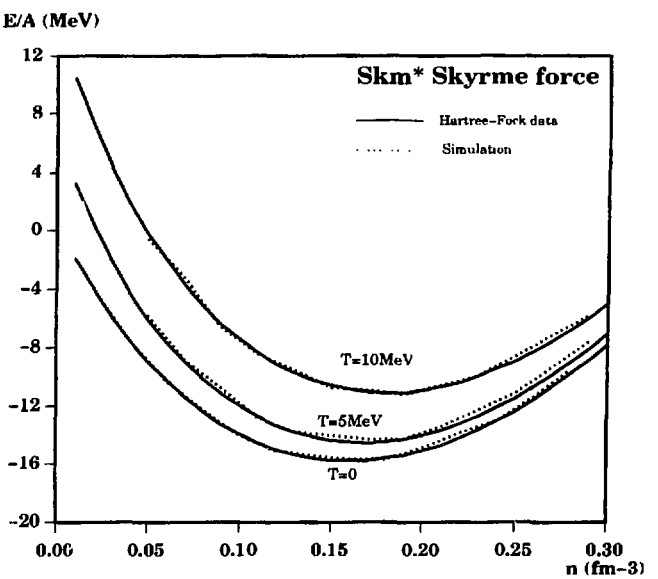

Figure 1 : Equation of State of the Skm* Skyrme force

In particular, our study show that the temperature and the average density strongly influence this characteristic time, which is about 2.7 10^{-22}sec in the most favoured case of a cold, dilute nuclear matter. At T = 6 MeV, it reaches 7.4 10^{-22}sec. By comparison with reaction durations, this could indicate that such a process would contribute to the fragment formation, only in the low energy regime of heavy ion reactions.

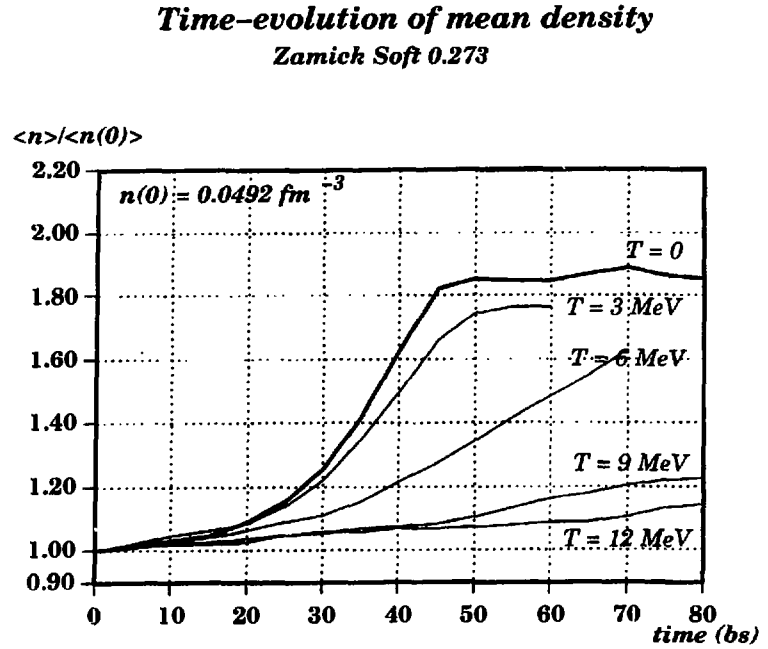

Figure 2 : time evolution of the mean density in infinite nuclear matter with a soft Zamick force.

II) Phase space fluctuations and dynamics of fluctuations of collective variables.

The theoretical studies of Ayik, Gregoire, Suraud and Randrup, Remaud have elaborated a framework for the study of phase space density fluctuations. However, much remains to be done to insure the procedures to compute them in cases of interest, such as nucleus collisions. Our work aims at casting a bridge between the formal theory and numerical simulations based on popular models as B.U.U. and Landau-Vlasov models.

In particular three directions of investigation have been tackled :

1) A formal deduction of the analytical form of the general covariance matrix for the phase space fluctuations of fermion systems in thermal equilibrium, and explicit expressions for the dispersions of collective variables (such as quadrupole moment or average transverse momentum).

2) For out-of-equilibrium systems, when the relaxation time approximation is valid, we establish the transport equations for the dispersion of collective variables and derive their equilibrium solutions to be compared with 1).

3) Using a Landau-Vlasov code for infinite nuclear matter, we compute microscopically the fluctuations for specific collective variables and show that they are in good agreement with those found with the above-sketched formal approaches. An illustrative example is given in figure 3.

From the first results, we demonstrate how numerical noise can be controlled in simulations. As already seen for the diagonal part (Randrup/Remaud), we show that the excitation energy is the leading term for the whole covariance matrix, whatever this energy is thermally equilibrated or not. Then, the equilibrium solutions of point 1) can be used to compute fluctuations in highly non-equilibrium solutions. This could provide a cheap method to estimate the width of the dispersion of collective variables around their averages.

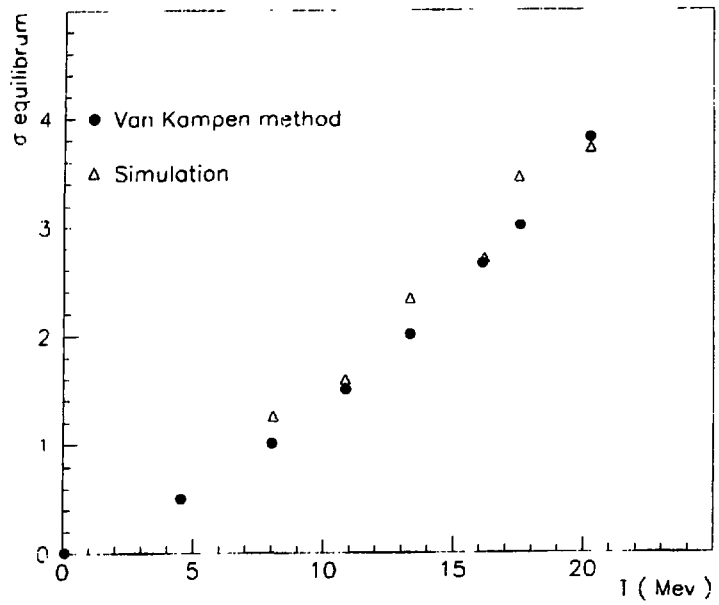

Figure 3 : Quadrupole moment equilibrium dispersion.

REFERENCE

(1) R.W. Hockney and J.W Eastwood, Computer simulations using particles, Adam Hilger, Bristol (1988).

(2) S. Ayik dans C. Grégoire, Nucl. Phys. **A513** (1990) 187.

(3) S. Ayik, E. Suraud, J. Stryjewski and Belkacem, Z. Phys. A. Atomic Nuclei **337**, 413 (1990).

(4) J. Randrup and B. Remaud, Nucl. Phys. **A514** (1990) 339.

(5) G.F. Burgio, Ph. Chomaz and J. Randrup. Nucl. Phys. **A529** (1991) 157

(6) N.G. Van Kampen, Stochastic Processes in Physics and Chemistry, North Holland (1991).

NUCLEAR MEAN FIELD AND TWO-BODY INTERACTIONS AT FINITE TEMPERATURE

J. Cugnon*, A. Lejeune*, P. Grangé**, U. Lombardo***, M. Baldo***

*Université de Liège, Institut de Physique au Sart Tilman, Bâtiment B.5,
B-4000 LIEGE 1 (Belgium)
**Laboratoire de Physique Théorique, Centre de Recherches Nucléaires (CRN),
B.P. 20 CRO, F-67037 STRASBOURG Cedex (France)
***Dipartimento di Fisica, Univ. di Catania, Corso Italia 57,
I-95129 CATANIA (Italy)

The description of the heavy ion collisions in the intermediate energy regime requires the knowledge of the nuclear mean field and of the effective interaction in non-equilibrium situations. We set out a whole program to calculate these physical quantities in nuclear matter at finite temperatures using a Brueckner-type approach.

We first calculated the nuclear mean field including (for the first time without any approximation) the second order term (in the g-matrix) at zero and finite temperature [1,2]. This term is repulsive (~ 20 MeV). The whole average field has a slow temperature dependence as indicated in fig. 1.

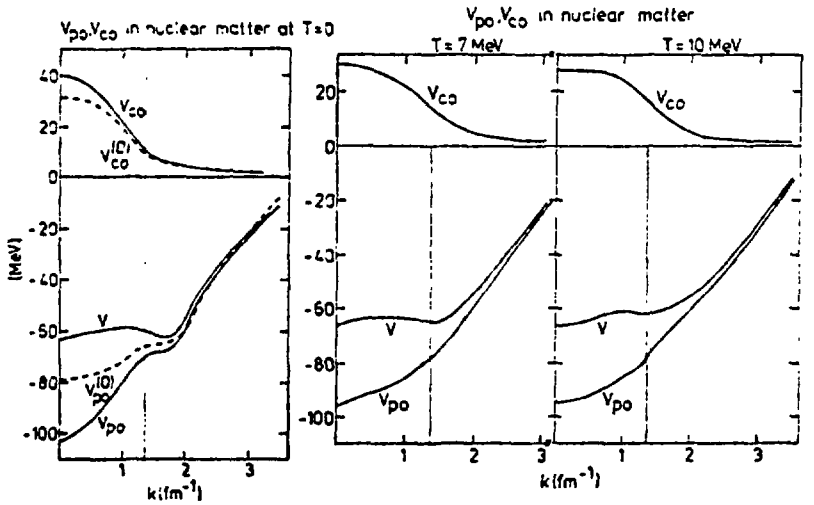

Fig. 1 : Mean field calculated in Brueckner theory for several temperatures. The quantity indicated V_{po} is the first order term, the one indicated V_{co} is the second order term. The full curve V is the sum of the two contributions (from ref. [1]).

We also calculated the effective interaction, identified to the g-matrix, for several densities and temperature. We extracted the corresponding effective interaction [3]. We showed that the temperature dependence exhibited in fig. 2 is quadratic and is less important however than the density dependence in the intermediate energy range.

Finally, the effective mass effect to medium corrections of the collision term is discussed in ref. [4].

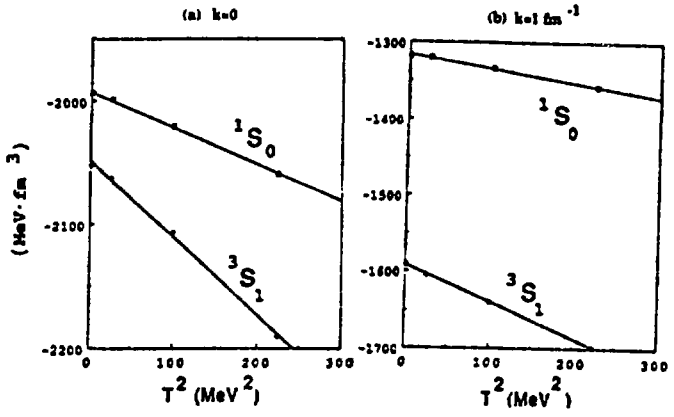

Fig. 2 : Temperature dependence of the NN effective interaction in two channels for two values of the relative nucleon-nucleon momentum.

[1] P. Grangé, J. Cugnon and A. Lejeune, Nucl.Phys. A473 (1987) 365-393

[2] J. Cugnon, P. Grangé and A. Lejeune, Journal de Physique Colloque C2, supplément au n° 6, 48 (1987) C2-282-C2-286

[3] A. Lejeune, J. Cugnon, M. Baldo and U. Lombardo, Nucl.Phys. A492 (1989) 173-186

[4] J. Cugnon, "The Nuclear Equation of State", part A, ed. W. Greiner & H. Stöcker, NATO ASI Series, Plenum Press, New York (1989) 257-271.

NUCLEAR MEAN FIELD IN NEUTRON RICH MATTER

J. Cugnon*, A. Lejeune*, M. Baldo**, U. Lombardo**

*Université de Liège, Institut de Physique au Sart Tilman, Bâtiment B.5,
B-4000 LIEGE 1 (Belgium)
**Dipartimento di Fisica, Univ. di Catania, Corso Italia 57,
I-95129 CATANIA (Italy)

The formation of more and more neutron rich nuclei and the investigation of the N/Z degree of freedom in heavy ion collision makes desirable a reinvestigation of the mean field properties for asymmetric matter. We report here on such a study based on Brueckner approach.

We especially pay attention to the mean field as a function of the asymmetry parameter $\beta = (N-Z)/(N+Z)$. We showed [1] that the mean field for a nucleon ($\tau = 1$, proton, $\tau = -1$ neutron) of momentum k is given accurately by

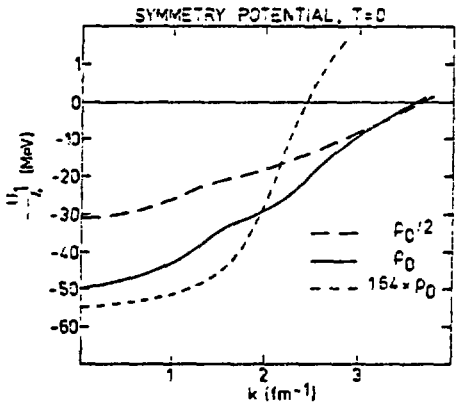

Fig. 1 : Isovector part $U_1/4$ of the mean field in nucleon matter for three densities.

$$U(k, \tau, \beta) = U_0(k) + \frac{\tau\beta}{4} U_1(k) ,$$

where U_0 is the mean field in symmetric nuclear matter. The quantity $U_1(k)$ is given in fig. 1 for several densities. The temperature dependence (in the GANIL regime) is rather weak. We also showed that the effective mass has a strong β-dependence.

We also investigate the superfluidity properties of neutron and nuclear matter [2]. The gap equation has been solved exactly (for the first time) for realistic interactions. The results are given in fig. 2. It is seen that the gap is smaller in nuclear matter than in neutron matter, but the dependence upon β is rather weak. We verified that the critical temperature for desappearance of the superfluidity is roughly given by $T_c = 0.57\ \Delta$,

where Δ is the gap at Fermi momentum and zero temperature.

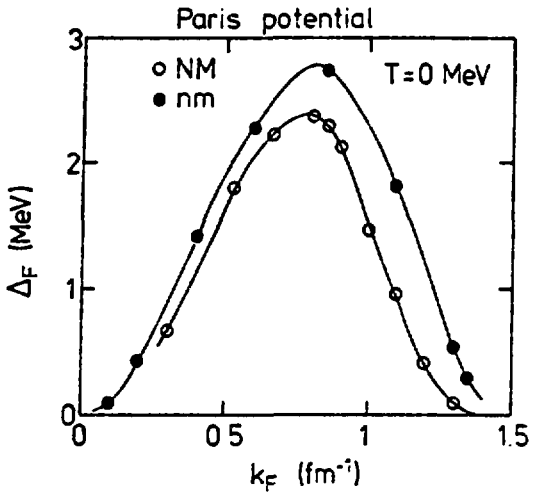

Fig. 2 : Gap Δ_F at Fermi momentum for nuclear matter (open dots) and neutron matter (black dots).

[1] J. Cugnon, P. Deneye and A. Lejeune, Zeit. für Phys. A328 (1987) 409-415

[2] M. Baldo, J. Cugnon, A. Lejeune and U. Lombardo, Nucl.Phys. A515 (1990) 409-432.

FRAGMENTATION IN MEDIUM ENERGY HEAVY ION COLLISIONS

M.COLONNA 1), N.COLONNA 2), A.BONASERA and M.DI TORO 1)

1) INFN-Lab.Naz.del SUD, Catania
2) LBL- Berkeley

We carefully analyse fragment production in heavy ion collisions at beam energies between 30 and 60 Mev/u. Solving the BNV equation we follow the entrance channel dynamics which shows an evolution of reaction mechanisms, from incomplete fusion to deep inelastic and participant spectator pictures, depending on energy, impact parameter and size of the colliding nuclei. An important increasing pre-equilibrium emission of nucleons is revealed with increasing beam energy. Eventually equilibrated primary sources are formed, whose deexcitation stage is followed within a quantum statistical cascade approach which includes all possible decay channels (GEMINI code). The input properties of the primary fragments are obtained from a suitable clustering procedure of the phase space distribution at some equilibration time, fixed on the time of the end of pre-equilibrium emission. From the mainly classical dynamics of the kinetic BNV evolution it will be never possible to get complex fragment production just following the dynamics at later times.
With this "conventional" coupling of non equilibrium and equilibrium features a large variety of data on fragment production are reproduced for the reactions Kr+Al at 34.4 Mev/u, Ca + Ca at 35 MeV/A, La+Al at 40 and 55 Mev/u and La+Cu at 55 Mev/u.
In particular, we focalise on the reaction Kr+Al at 34.4 MeV/A for the availability of nice data from an experiment perfomed at Ganil. The dynamics of the reaction is explained in fig.1. It is possible to observe an evolution from incomplete fusion to deep-inelastic. We show how our approach correctly describes the inclusive cross section behaviour. The IMF's production is in fact quite well reproduced (see fig.2). These fragments come from a fission mechanism of the compound primary sources created in the case of the more central impact parameters. In fact, without considering any possibility to undergo fission for the previous sources, i.e. just considering a dynamical stage, we don't get any IMF's production (dashed line).

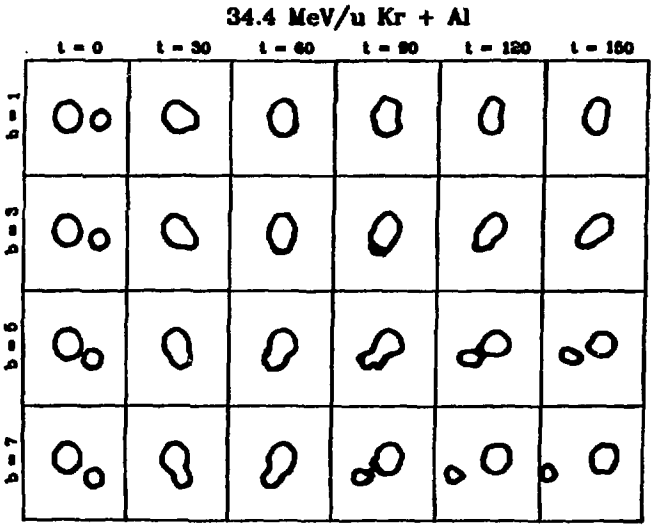

Fig.1

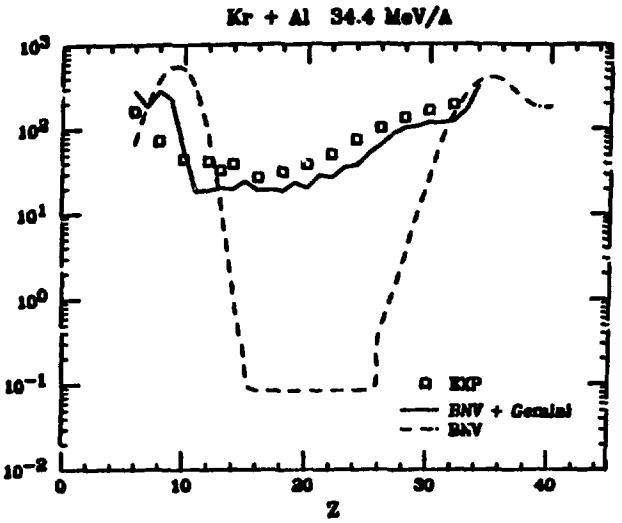

Fig.2

However some signatures of more exotic mechanisms are appearing at 55 Mev/u; in fact for the La + Cu case something is clearly missing also in the inclusive production of medium-light fragments (see fig.3). A microscopic study of the nuclear matter phase diagram seems to relate these discrepancies to dynamical instabilities. In fact, while in the La + Al case(where the entropy per nucleon value is s = 0.6) the spinodal region is only slightly touched, in the Cu case (s=1), where more energy is available and a larger compression is reached, the system deeply enters such instability region (see fig.4). When dynamical (surface or volume) instabilities are occuring the growing of fluctuations is the main mechanism of fragmentation: fluctuations are completely outside of the BNV picture, where only the mean phase space trajectory is described. Therefore the lack of the previous approach in describing some experimental results may be used as a signature of new exotic phenomena, like multifragmentation, a direct explosion of the nuclear system expected on the basis of the growth of nuclear instability.

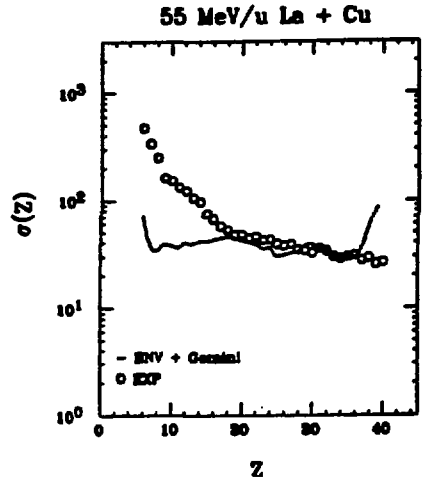

Fig.3

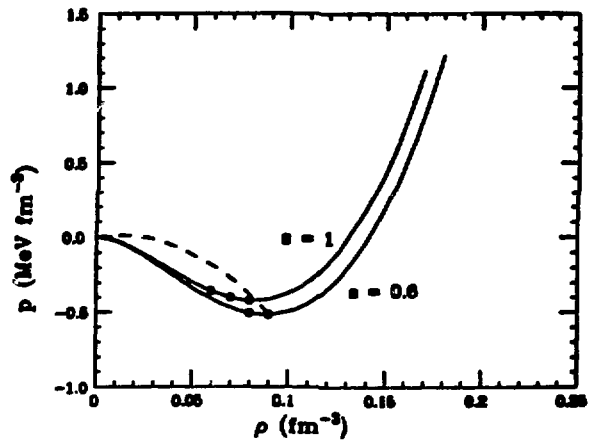

Fig.4

References

1) A.Adorno, M.Colonna, M.Di Toro and G.Russo, "Medium Energy Collisions and Multifragmentation" in "The Nuclear Equation of State", Ed.s W.Greiner and H.Stoecker, Plenum 1990, 413-420
2) A.Bonasera, M.Colonna, M.DiToro et al. Phys.Lett. 224B (1990) 169, Nucl.Phys. A519 (1990) 211c, Nucl.Phys. A529 (1991) 565
3) M.DiToro, "Macroscopic vs. Microscopic description of multifragmentation", Invited talk "Colloque GANIL" Giens 1990
4) A.Bonasera, M.Colonna, M.DiToro, "Time scales in complex fragment production at intermediate energies" in "Nuclear Dynamics" Ed.s W.Bauer and J.Kapusta, World Sci. 1991, 91-102
5) M.Colonna, N.Colonna, A.Bonasera and M.DiToro "Equilibrium features and dynamical instabilities in Nuclear Fragmentation" LNS preprint 92-04, Nucl.Phys.A, in press

DAMPING OF GIANT RESONANCES IN HOT NUCLEI

A. *Smerzi*, M. *Di Toro*

INFN – LNS, Catania, Italy

The effect of one- and two-body dissipation on the damping of giant dipole resonances (GDR) is studied in a semiclassical approach solving a Vlasov equation with a collision relaxation time [1]. The latter is microscopically evaluated from the equilibration of a distorted momentum distribution in a kinetic approach. Particle emission is also computed in the same picture. Without free parameters a good agreement whit data is obtained for GDR's on the ground state. In fig. 1) we show the collisional widths (dashed line) and the final FWHM's of the strength distribution solid line compared with data (shaded area). The large enhancement is explained as a interplay between collisional and Landau Damping. For collective vibration built on excited states we get a dramatic increase of the widths with excitation energy due to the increment of nucleon-nucleon collisions. In fig. 2) our results (dashed line) are compared with various experiments in the Sn region [2,3,4]. Our results are in very good agreement with the analysis of Yoshida et al. [4] based on a evaporation cascade code with fully excitation energy dependent widths. A saturation can be reproduced only including the neutron evaporation cooling mechanism (solid line of fig. 2). [5]

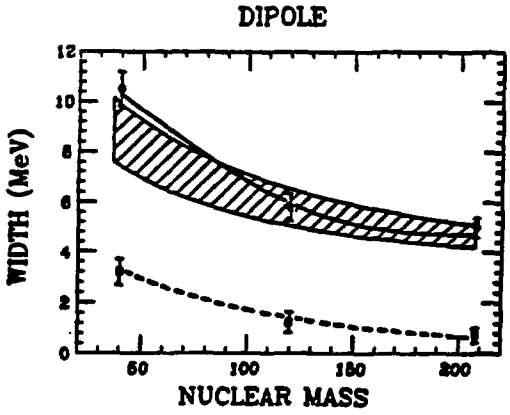

Fig.1

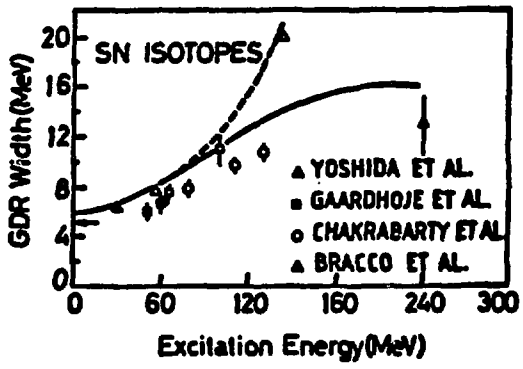

Fig.2

However experimental informations on the excitation energy dependence of the spreading widths are not conclusive, being very much model dependent: the experimental γ-spectra are equally well reproduced from different cascade analyses, using GDR spreading widths showing a saturation or a strong increase with excitation energy. This can explain the discrepancies in the data shown in fig.2 .

On the other hand there is a very clear experimental evidence which deserves a thorough explanation: a decrease of the dipole strength in the giant resonance region at high excitation energies, with consequent saturation of the number of emitted photons [4]. This observation has been recently associated to a pre-equilibrium mechanism [6]. Indeed if at high temperature the GDR cannot achieve a thermal equilibrium with the compound nucleus before it cools down by neutron evaporation, the GDR states will be depopulated and then a smaller strength will appear in the GDR region. This effect should be certainly taken into account in the evaluation of the photon decay probability: the point we would like to stress here is that this is not enough to account for the experimentally observed quenching of the GDR photon yield. A strong increase of the GDR width, as found in this paper, with a related smoothing of the resonant form factor of the γ-absorption cross section, is also necessary in order to get the saturation point at the correct experimental excitation energy.[9]

In order to make an accurate study of this effect we have to evaluate the probability of photon emission integrated over the resonance region. In fig.3 we report the excitation energy dependence of the probability and of the corresponding photon yield ($12 \leq E_\gamma \leq 20 M\epsilon V$) in the Sn case computed with increasing GDR spreading and total widths as described in this paper. We get a saturation of the GDR photon emission at $E^* \simeq 200 MeV$ in very good agreement with experiments. [4]. We can define a corresponding limit temperature $T \simeq 4.0 MeV$.

In fig. 4 we report the same quantities computed using a spreading width not depending on the excitation energy $\Gamma^\downarrow = 4.8 M\epsilon V$, fixed on the ground state value, and a total GDR width showing a saturation value $\Gamma_{GDR} = 12 M\epsilon V$, due to the effect only of angular momentum deformations, as suggested in ref.[6]. In this picture only a pre-equilibrium mechanism is envisaged to account for the GDR γ-yield reduction. The GDR photon quenching is reproduced only at very high excitation energies, which correspond to limiting temperatures $T \simeq 7 - 8 M\epsilon V$, in clear disagreement with data.

Our conclusions strongly support the picture of a slow disappearing of giant dipole

resonances with increasing excitation energy due to effect of nucleon-nucleon collisions. This process will clearly dominate the collective motion damping in the region above saturation of the angular momentum transferred to the hot fused system, and it has been probably understimated in other analyses [7,8].

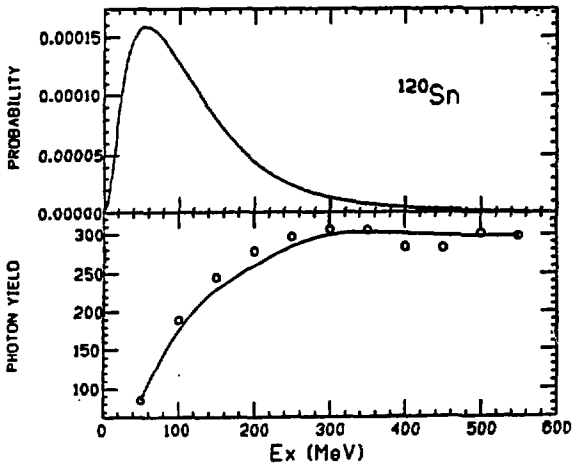

Fig. 3

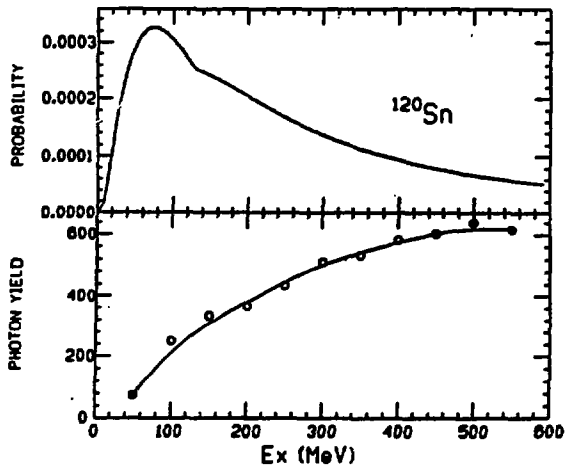

Fig. 4

1) G. F. Burgio and M. Di Toro, Nucl. Phys. A 476 (1988) 189

2) D.R. Chakrabarty et al., Phys. Rev. C36 (1987) 1886

3) J.J.Gaardhoje et al., Phys. Rev. Lett. 59 (1987) 1409

4) K. Yoshida et al., Phis. Lett. B245 (1990) 7

5) A.Smerzi,A.Bonasera, and M.Di Toro 'Damping of giant resonances in hot nuclei" Phys. Rev. C44 (1991) 1713

6) P.F.Bortignon, A.Bracco, D.M.Brink and R.A.Broglia, "Limiting temperature for the existence of collective motion in hot nuclei" NBI Preprint 91-36

7) F.V. De Blasio, W. Cassing, M. Tohyama, P.F. Bortignon and R.A. Broglia "Non perturbative study of damping of Giant Resonances in hot nuclei" NBI Preprint 91-38

8) P. F. Bortignon et al. Nucl. Phys. A495 (1989) 1550

9) A.Smerzi and M. Di Toro "Limiting temperature for giant dipole resonances", XXX Int. Winter Meeting on Nuclear Physics, Bormio 1992

BINARY AND TERNARY FISSION OF HOT AND ROTATING NUCLEI

G. ROYER and J. MIGNEN

Laboratoire de Physique Nucléaire IN2P3/CNRS - Université de Nantes
2 rue de la Houssinière - 44072 Nantes - FRANCE

Heavy-ion accelerators as GANIL allow the study of highly excited nuclei obtained by partial fusion of the projectile and the target. A large amount of thermal excitation energy and rotational energy is deposited in such systems and, nevertheless, the fission process remains an important decay mode besides the nucleon evaporation and fragmentation channels.

Within the rotational finite-range liquid drop model including the asymmetry and the temperature, we have studied[1-3] the deformation energy of such hot and rotating nuclei. The selected fission path goes through the compact and prolate shapes. In the ternary case, a very efficient two-dimensional shape sequence has been preliminarily defined.

The heating of a nucleus lowers strongly its fission barrier and the lowering is all the more important as the system is heavy since the main temperature effect is to diminish the surface tension. The fission barriers vanish for $A \approx 200$ at $T = 5$ MeV. The ternary fission barriers are much higher than in the binary case but their temperature dependence is the same. Due to the differences between the mass inertia, the barrier for light nuclei vanishes for

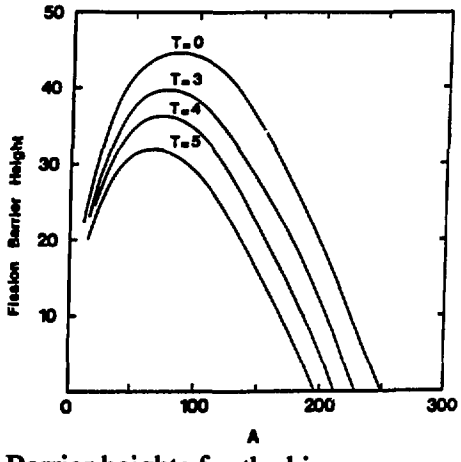

Barrier heights for the binary symmetric fission along the β-stability valley.

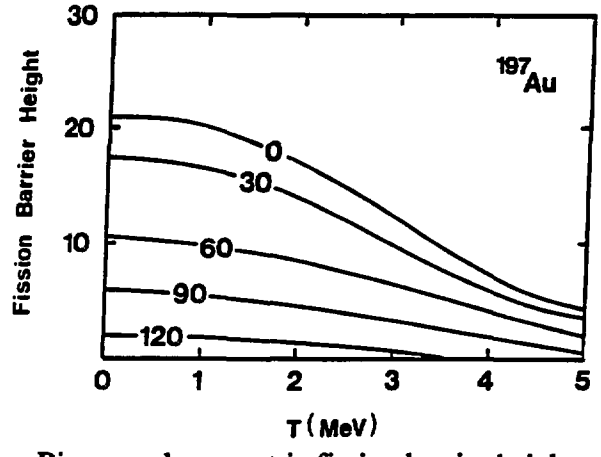

Binary and symmetric fission barrier heights as a function of the angular momentum (ħ unit).

low angular momenta, while, for heavy systems, the centrifugal forces compensate for the deformation energy only for very high angular momenta. In the symmetric ternary fission path the nuclei are able to sustain very high angular momenta without fissioning even at high

temperatures. This could perhaps explain the possible and unexpected detection of the Pb-like nucleus at T = 6 MeV and J = 160 ħ in peripheral collisions where the compression effects are small.

The lowering of the surface energy and, then, of the fission barrier by the temperature increases with the decay symmetry of the system and with its mass. The incorporation of the temperature maintains essentially the same topology of the Businaro-Gallone picture.

The macroscopic ternary fission barrier height and position depend strongly on the decay asymmetry. For light nuclei and for all the mass asymmetry values, the saddle-point corresponds to three separated fragments hold together by the nuclear proximity forces which counter balance the Coulomb repulsion. For heavier nuclei, the saddle-point shape has the same configuration, except for very high decay asymmetries (^{4}He emission as an example) where the barrier top corresponds to the one-body configuration at the beginning of the neck formation. With increasing asymmetry, double-humped barriers occur and, then, the possible existence of elongated but compact isomeric states. Naturally, such an approach supposes complete thermalisation of the system. An other limitation is the inability to describe the nucleon evaporation.

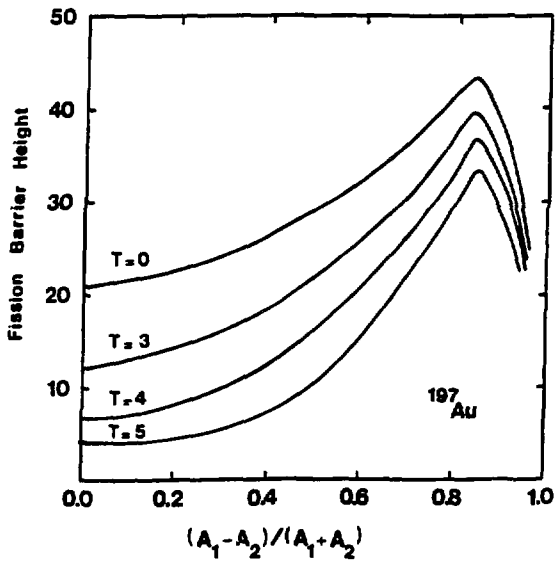

Binary fission barrier heights as fonctions of the temperature and the decay asymmetry.

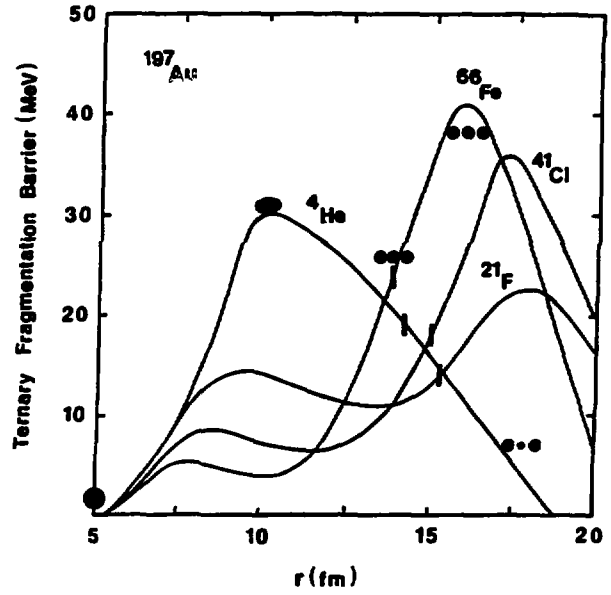

Ternary fission barriers (T = 0). The central fragment is indicated on the curves.

1) J. Mignen and G. Royer, J. Phys. G 16 (1990) L 227.
2) G. Royer and J. Mignen, 7 th Adriatic international conference on nuclear physics : Heavy-ion Physics - Today and tomorrow (Brioni, Yougoslavie : 27 may - 1 June 1991).
3) G. Royer and J. Mignen, J. Phys. G (1992)

SEMICLASSICAL SIMULATION OF SUDDEN NUCLEUS SCISSION

G. ROYER, B. REMAUD, F. SEBILLE, and V. DE LA MOTA

Laboratoire de Physique Nucléaire IN2P3/CNRS - Université de Nantes
2 rue de la Houssinière - 44072 Nantes - FRANCE

Heavy-ion beams in the intermediate energy domain allow the study of highly excited nuclei obtained by partial fusion of the projectile with the target. Unexpectedly, the fission process remains an important decay mode of such hot systems.

As a first step, the dynamics of a split nucleus has been simulated[1] within a semiclassical description based on the Landau-Vlasov equation with a Uehling-Uhlenbeck collision term. Initially, the spherical nucleus is suddenly divided into two parts boosted in opposite directions by a momentum per particle k_z. The resulting collective motion can be analyzed by following the time evolution of the quadrupole moment of the system and its collective energy estimated from the local collective velocity field.

For excitations below the breakpoint, the system swings in the potential energy pocket. The damping of the collective motion and its conversion into intrinsic kinetic energy is very slow when only the pure mean field acts. In contrast, when the two body collisions are effective, only one oscillation occurs and the transport between the collective and intrinsic degrees of freedom is a very rapid phenomenon, since the big hole dug in the velocity distribution weakens the Pauli blocking effects.

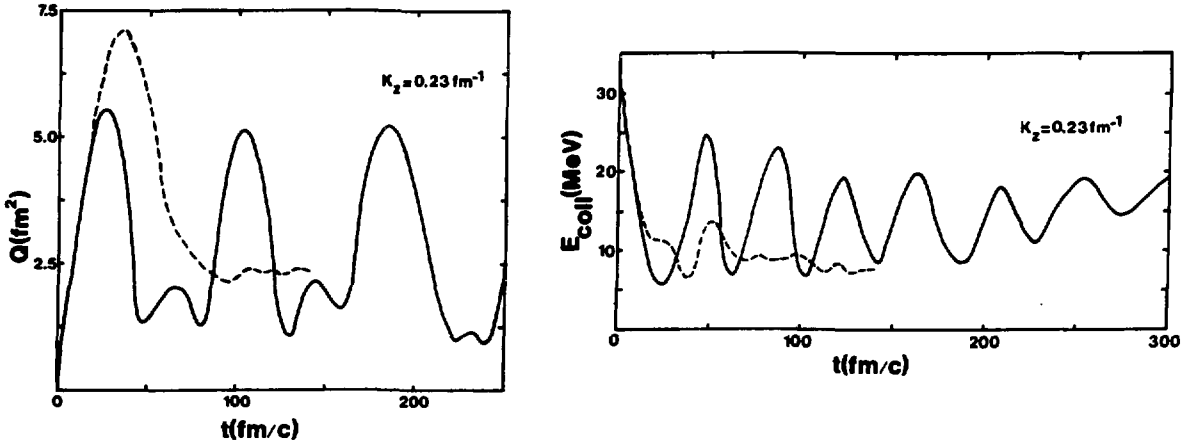

Time evolution of the quadrupole moment and the collective energy for an initial excitation k_z of the ^{40}Ca nucleus below the breakpoint. The solid curve corresponds to the mean - field effects while the dashed line incorporates the two - body collisions.

The same strong influence of the two-body collision effects is observed above the breakpoint ($|k_z| \geq 0.4\ f_m^{-1}$). The scission path is better reproduced when the nucleon-nucleon cross section is large. Changes in the nucleon-nucleon cross section do not affect strongly the mass quadrupole moment but lowers the potential barrier of about 15 MeV. An estimate of this barrier is found by looking at the time evolution of the kinetic collective energy which gives the amount of energy needed to overcome the potential barrier :

$$E_{barr} = \max_t [E_{coll}(t = o) - E_{coll}(t)]$$

The obtained barrier height is slightly higher than the macroscopic fission barrier height (≈ 35 MeV for the ^{40}Ca nucleus) determined from the liquid drop model. The reasons are that the splitting of a nucleus is a rough and sudden approximation of the fission process and that the prescription for the mean-field may not fully describe the surface properties of nuclei. Finally this semiclassical description points out the role of the nucleon-nucleon collisions which govern the damping of the collective energy and deformations and favor the evaporative deexcitation channel. Such a role has also been observed in the simulation of the dynamics of excited rotating nuclei[2]. The study of more fissile nuclei is in progress[3].

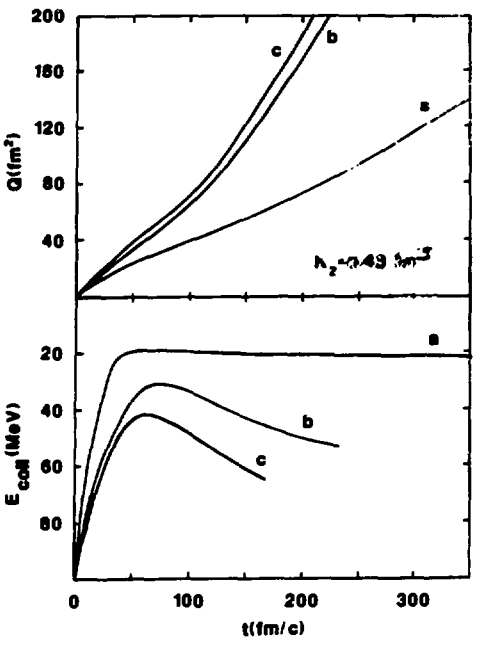

Time evolution of the quadrupole moment and collective energy due to pure mean field effects (a), inclusion of two body collisions (b) and two-body interactions with a double nucleon-nucleon cross section (c).

1) G. Royer, B. Remaud, F. Sébille, V. de la Mota, Phys. Rev. C44 (1991) 2226

2) F. Garcias, V. de la Mota, B. Remaud, G. Royer, F. Sébille, Phys. Lett. B255 (1991) 31

3) F. Haddad, G. Royer, B. Remaud, F. Sébille, in progress.

EVAPORATION, FISSION AND FRAGMENTATION OF HOT ROTATING NUCLEI

B. REMAUD, F. GARCIAS*, G. ROYER, F. SEBILLE, and V. DE LA MOTA

Laboratoire de Physique Nucléaire IN2P3/CNRS - Université de Nantes
2 rue de la Houssinière - 44072 Nantes - FRANCE
* Département de Fisica, Universitat de Ses Illes Balears, E- 07071 - Palma de Mallorca, Spain

The observation of very excited nuclei after the collisions of heavy-ions at intermediate energies raise two fundamental questions : what are the mechanisms of energy transfer from the initial motion to the intrinsic degrees of freedom and, once created, what are the deexcitation channels of hot nuclei ?

The evaporation of these hot rotating nuclei has been studied[1] within a semi-classical description based on the Landau-Vlasov equation with an Uehling-Uhlenbeck collision term to take into account the two-body interactions which play a major role in the rearrangement of these systems[2]. This framework allows to study the competition between particle evaporation, binary and ternary fission and multifragmentation as a function of initial angular momenta and excitation energies.

From the one body distribution, a velocity field is extracted and the collective energy E_{coll} (t) follows. The excitation energy is given by :

$$E^* = E_{tot} - E_{coll} - E_{esc},$$

where E_{esc} is the energy of the evaporated particles. For small excitation energies and angular momenta, the nucleus takes and oblate shape and increases its deformation, but, before passing the saddle-point, it has lost particles by evaporation and returns to the spherical shape. For larger rotations and excitations the system falls into the fission valley. At very large initial excitations the expansion of the system is quick and the system explodes keeping its initial oblate symmetry. This regime corresponds to fragmentation.

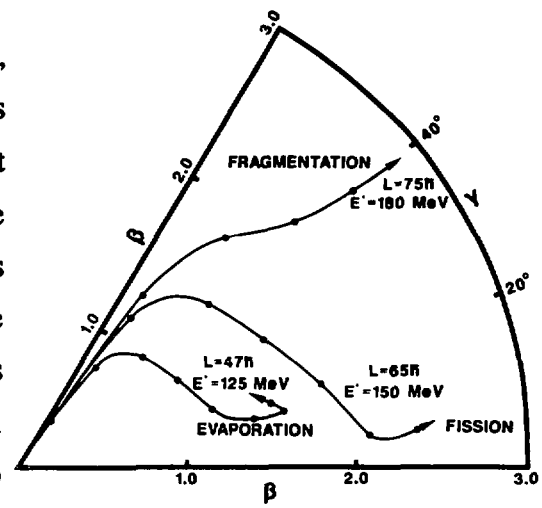

Three trajectories of a ^{40}Ca hot, rotating nucleus. Marks indicate the time steps (10^{-22} s).

The classification of the various deexcitation modes has been realized in the (L, E*) plane, variables in close relation to the experimental observables.The present method of boosting the initial rotation of nucleus does not allow to access the pure yrast lines (E* = 0, L > 0). Although a rough approximation to the nucleon efffective force is used, the critical angular momentum for (cold) fission is 45 $\hbar$ in correct agreement with Thomas-Fermi calculations. When E* increases the probability of a binary fission regime decreases regularly and completely disappears at E* = 300 MeV although the fission barrier lowers according to the same trend as in static calculations. A critical zone exists for high excitation energies where the nucleus passes directly from the evaporation regime to ternary fission and fragmentation. This dynamical competition between the fission, nucleon evaporation and fragmentation regimes is illustrated in the last figure for two initial conditions : L = 45 $\hbar$, E* = 44 MeV and L = 55 $\hbar$, E* = 201 MeV. The nucleus with higher angular velocity and excitation energy looses mass at much higher rate and its angular momentum relaxes much faster. Both systems yield an evaporation residue although static studies would have predicted vanishing fission barriers.

Studies are underway for more fissile nuclei[3] which could really explored all the regimes considered here in realistic nuclear reactions.

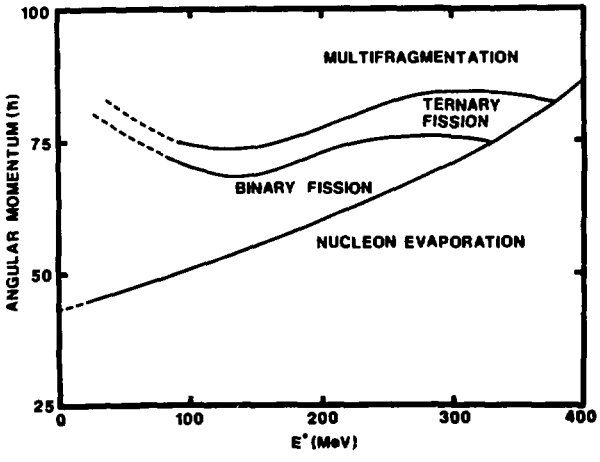

deexcitation channels of a ^{40}Ca excited nucleus.

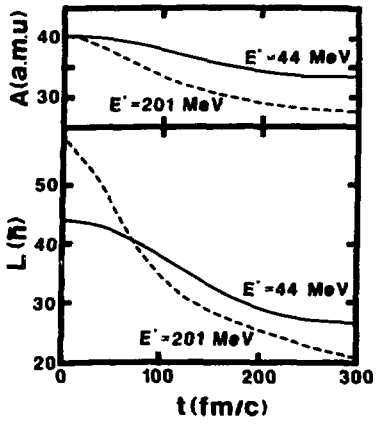

Evolution of mass and angular momentum of two ^{40}Ca nuclei with different initial excitations.

1) F. Garcias, V. de la Mota, B. Remaud, G. Royer, F. Sébille, Phys. Lett. B255 (1991) 311
2) G. Royer, B. Remaud, F. Sébille, V. de la Mota, Phys. Rev. C44 (1991) 2226
3) F. Haddad, G. Royer, B. Remaud, F. Sébille, in progress.

EXCITED NUCLEI AND TESTS OF NUCLEAR FRAGMENTATION MODELS

B. Elattari, J. Richert and P. Wagner
Centre de Recherches Nucléaires and Université Louis Pasteur
Strasbourg, France

Experiments on nuclei which are generated in energetic collisions show remarkable properties. Several routes which may lead to interesting information about highly excited nuclei formed in these experiments have been suggested. The study of their decay properties is one of them.

The analysis of experimental fragment distributions of ^{197}Au [1] and the comparison with a theoretical interpretation in the framework of percolation models [2] reveals the possible existence of several decay regimes and some sharp transition from one to the other which can be interpreted as a phase transition in the corresponding finite system. Experimental charge distributions of fragments also show an intermittent behaviour which may or may not be related to the phase transition.

In order to understand and to explain these facts we proposed different models which describe the decay of an excited nucleus as a step by step sequential process. We implemented this scenario by means of Monte Carlo simulations, generating sets of decay events [3]. In each event the nucleus proceeds via a chain of binary decays involving the successive sequentially generated excited aggregates. The dissociation process stops when there is no excitation energy left over in the final cold fragments.

This simple scenario has been applied to the study of excited nuclei in different regions of the mass table and over a large range of initial excitation energies. The relative weight of different binary decay channels was fixed by transition rates corresponding either to an inverse fusion process (detailed balance - Weisskopf [4]) or to the fission of a nucleus at finite temperature (transition state theory - Swiatecki [5]). Fig. 1 shows examples concerning ^{44}K and ^{197}Au. In the case of ^{197}Au the evolution of fragment multiplicities with excitation energy shows different regimes, i.e. from left to right, light particle evaporation, events with two large fragments (absent in the case of ^{44}K), decay into several large pieces, vaporisation into light particles.

Final charge (mass) distributions can be used in order to work out average moments of these quantities for fixed multiplicities of fragments (total number of particles and fragments of any size). The analysis of these moments can be compared to the results obtained in the experiment and percolation calculations obtained in the case of ^{197}Au. Fig. 2 shows a typical behaviour of the second moment m_2 as a function of the fragment multiplicity m. In general, all qualitative trends observed in the experiment and percolation calculation can be reproduced. It is however not possible to reproduce stringent constraints such as for example, the universally fixed location in m of the maximum of m_2. Furthermore there exists no sign for the existence of a power law behaviour of the charge (mass) distributions for some specific value of the relevant parameter

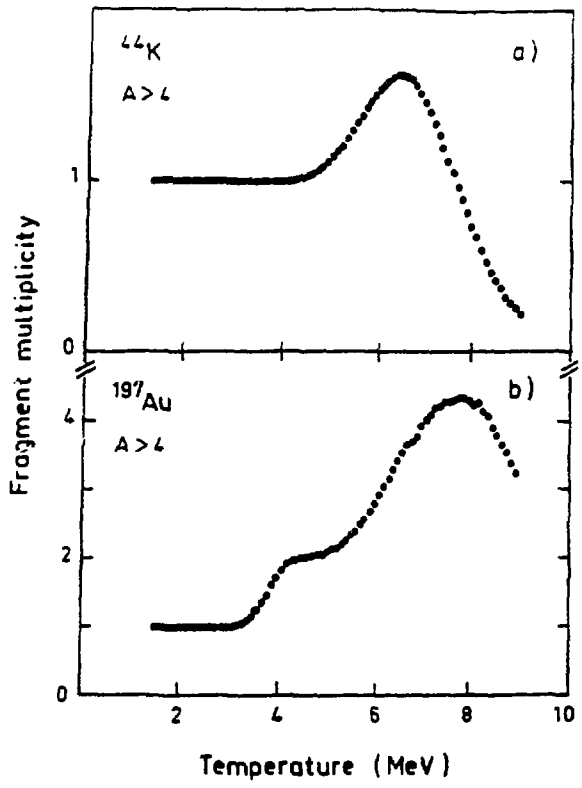

Fig. 1

Fig. 1 : Evolution of fragment multiplicities (mass larger than 4) with increasing excitation energy (here temperature). The decay channels with two large fragments (so called pseudo fission) is absent in the case of ^{44}K.

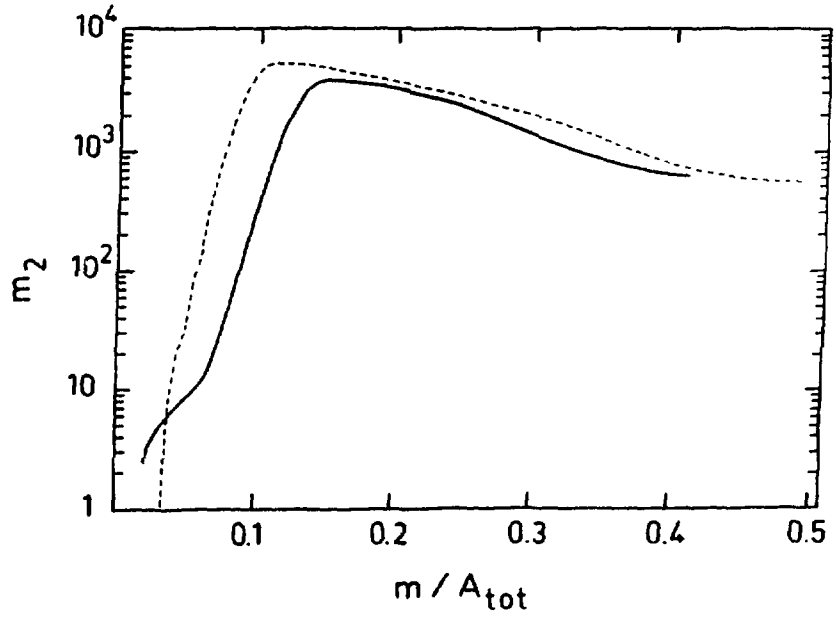

Fig. 2

Fig. 2 : Second moments from mass distributions of ^{197}Au as a function of reduced multiplicity (A_{tot} =197). Full line : detailed balance [4]. Dotted line : transition state theory [5]. The experimental maximum lies at $m/A_{tot} \simeq 0.25$

(here the excitation energy). Finally Fig. 3 shows that the so called factorial moments [7] F_i (i = 2, 3,...) do not show the expected scaling properties which characterise intermittency, i.e. $\ell n\, F_i \sim - f_i\, \ell n \delta s$ where δs is the length of equal charge (mass) intervals and the f_i's are real positive coefficients.

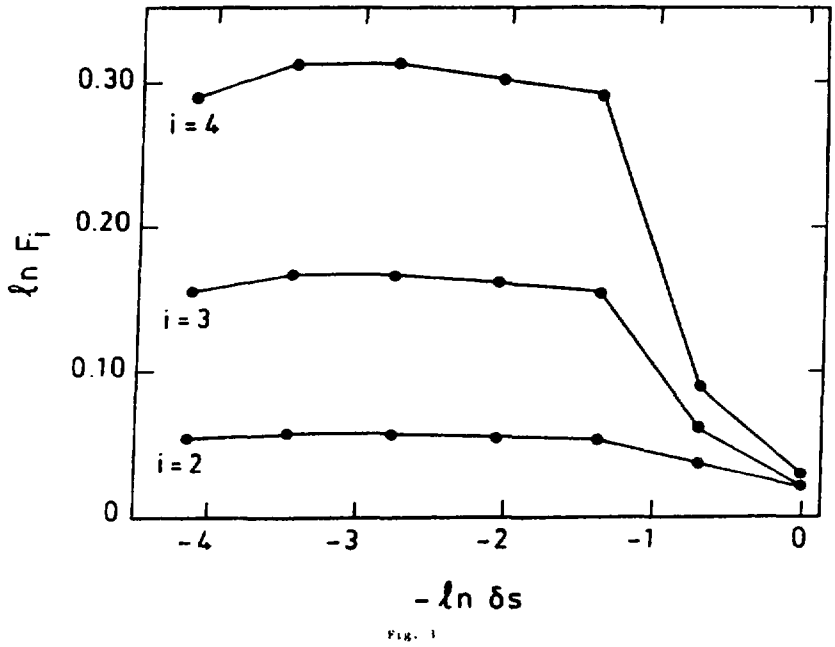

Fig. 3 : Factorial moments as a function of the mass interval length δs obtained from simulations. No intermittency can be observed.

In order to investigate this last point we introduced an analytical description of sequential decay. Production yields of fragments with fixed charge or mass evolve in time by means of rate equations [6] forming a set of coupled equations which are linear both in time and in the production yields. These quantities are fluctuating quantities as a consequence of the stochastic nature of the equations induced by the random properties of the transition rates which can be written in terms of averages and fluctuating parts. It is possible to show by means of analytical arguments which are corroborated by numerical checks that the distributions cannot exhibit an intermittent behaviour [8] . A typical example for this is shown in Fig. 4 where the linear dependence of the logarithm of moments with respect to $-\ell n \delta s$ is not observed. This is in agreement with the results of simulations, Fig. 3, where the evolution of the number of fragments of a given type depends also linearly on the number of fragments of all types present in the process. These results are general in the sense that they depend in no way on the specific expression of the transition rates and hence must be related to the linear character of the process described by these models.

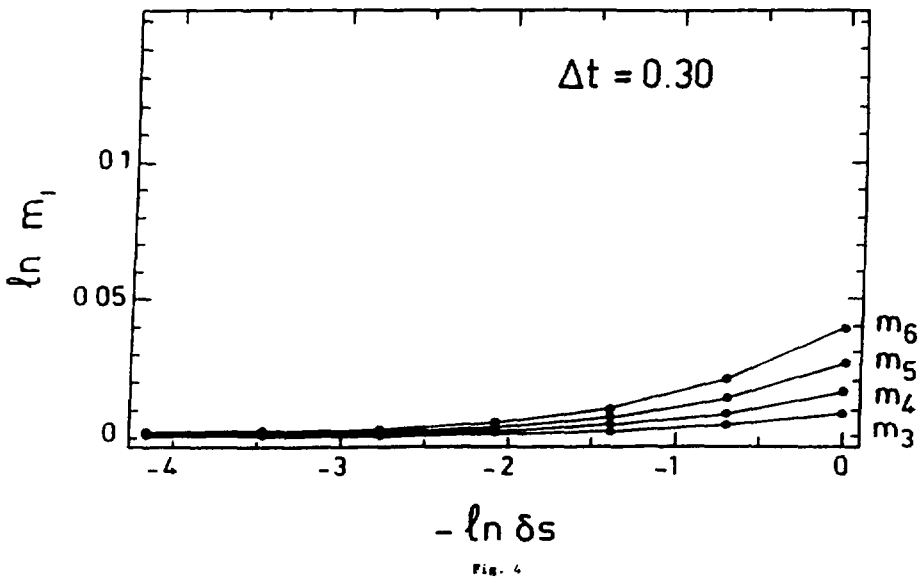

Fig. 4 : Normalised moments $m_j(\Delta t) = \sum_{k=1}^{M} \langle P_k^j(\Delta t)\rangle / \sum_{k=1}^{M} \langle P_k(\Delta t)\rangle^j$ at time $\Delta t = 0.3$ as a function of the interval length $\delta s = A_{tot}/M(P_k(t)$ = production yields of fragments in the mass interval k). No intermittency can be observed. For more details see ref. [8].

Intermittency has been observed on the experimental charge distributions of fragmented ^{197}Au. If this property gets confirmed in the case of other nuclei, sequential decay as described by means of models of the type presented above cannot stand as an adequate scenario of nuclear fragmentation. In the absence of an explicit theory other scenarii corresponding to other phenomenological processes must be considered.

[1] C.J. Waddington and P.S. Freier, Phys. Rev. **C31** (1985) 888
[2] X. Campi, Phys. Lett. **208B** (1988) 351
[3] J. Richert and P. Wagner, Nucl. Phys. **A517** (1990) 399
[4] V.F. Weisskopf, Phys. Rev. **52** (1937) 195
[5] W.J. Swiatecki, Aus. J. Phys. **36** (1983) 641
[6] C. Barbagallo, J. Richert and P. Wagner, Z. Phys. **A324** (1986) 97
[7] M. Ploszajczak and A. Tucholski, Phys. Rev. Lett. **65** (1990) 1539 and refs. therein
[8] B. Elattari, J. Richert and P. Wagner, preprint CRN/PHTH 91-18 December 1991

Kinetic Description of Nuclear Dynamics

A.Adorno,[1], A.Bonasera[1,2], F.Gulminelli[2,3] and P.Schuck[4]

1) Laboratorio Nazionale del Sud, v.A.Doria, 95125 Catania, Italy
2) Istituto Nazionale di Fisica Nucleare, Sezione di Catania, c.so Italia 57, 95129 Catania, Italy
3) Dipartimento di Fisica and INFN, v.Celoria 16, 20133 Milano, Italy
4) Institute des Sciences Nucleaires, F-38026 Grenoble-Cedex, France

ABSTRACT

Different problems that can be experimentally studied at the GANIL energies are addressed, i.e. subthreshold particle production, the computation of the variances in intermediate energy one body observables, and the widths of giant resonances. We solve an extension of the BNV (Boltzmann Nordheim Vlasov) equation including triple collisions and fluctuations, and compare the results to different analytical calculations and experimental data.

For a dynamical description of HI collisions, semiclassical methods have proved to be very successfull and transparent. In particular, the time evolution of the one body semiclassical Wigner function is very well described by the Landau Vlasov (LV) or Boltzmann Nordheim Vlasov (BNV) equation [1]. With the availability of HI experimental facilities at intermediate energy, it is now possible to build up portions of nuclear matter far away from equilibrium, at a density which is easily twice the saturation density and an excitation energy that can easily reach the binding energy per nucleon. In such a situation the incoherent binary scattering approximation given by the Boltzmann collision integral can be fairly inadequate and multiple scatterings have to be taken into account. Moreover in this dynamical regime critical phenomena are expected, and it is probable that high order correlations and the dynamical propagation of fluctuations in the nuclear medium can lead to critical behaviours, like nuclear multifragmentation and phase transitions.

One of the most stringent assumptions to be done in order to derive the BNV equation is that the gas is very rarified, so that all correlations except local incoherent two body scatterings can be neglected. If the density is high and the incident energy is such that Pauli blocking is not too important, one has to relax this approximation and an explicit form for the three body collision integral can be worked out under the same kind of approximations that lead to the Boltzmann equation [2,3].

We have devised [3] a numerical algorithm to sove the extended Boltzmann equation, and checked it against different analytical results and Enskog's theory.

In this approach, where we neglect genuine three body forces in the collision integral, a triple collision is a succession of three binary collisions occurring among particles that are at the same time inside the interaction sphere. In the spirit of Enskog's virial theory [4] the effect of many body correlations can be expressed by an expansion of the mean free path in powers of density, and this virial expansion can be used in the actual computation of the scatterings [3].

We have seen a considerable effect of triple collisions on collective flow observables, nucleon spectra and subthreshold pion production. In fact, incoherent nucleon-nucleon collisions are responsable for some of the

high energy particle production [5] but, when the total energy of the produced particle is very close to the kinematical threshold, the incoherent scatterings are not sufficient to explain the data and other mechanisms have to be invoked . One such mechanism could be the cooperation of three nucleons [3,6].

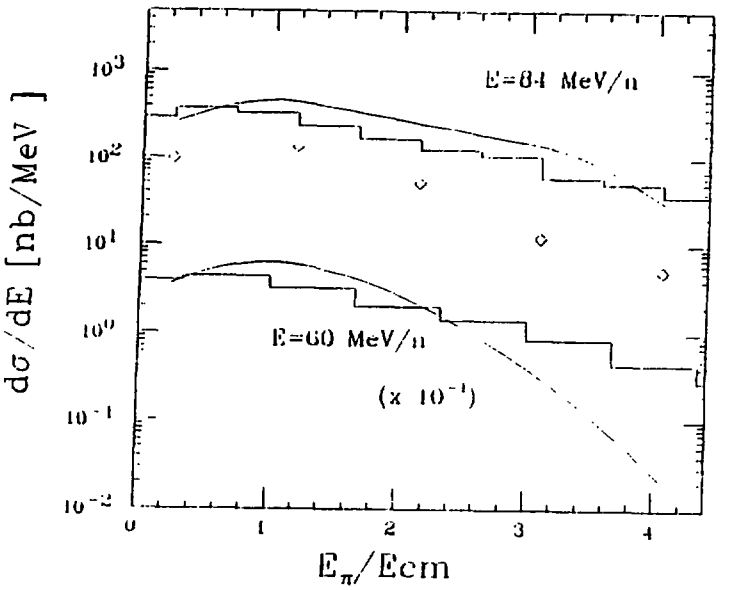

Fig.1

An example is shown in fig.1, which displays the differential π^0 spectrum obtained in a C+C collision at two different beam energies. The diamonds give the calculation with two body collisions only, the full line includes triple scatterings and the histograms represent experimental data [7]. A net increase of the yield is seen by considering three body collisions, and the reproduction of experimental data is very good except for the very subthreshold pions. The calculation [6] is perturbative and the elementary production cross sections are parametrized from experimental data. Pauli blocking is checked on the final states of the colliding nucleons.

The recent experimental findings about fragmentation and multifragmentation have raised a great interest about the problem of fluctuations in nuclear physics [8]. In principle the kinetic equations represent an ideal tool to analyze microscopically and self-consistently the dynamical evolution of a heavy ion collision, but the BNV equation ,being an average one body theory, presents serious drawbacks for an application in the critical regime. Even if in an actual HI collision no critical phenomenon is happening, it would be very useful to know the fluctuations of the exact microscopic distribution function, with respect to the Boltzmann approximation. As a matter of fact, in the computation of one body observables, the average distribution function $\overline{f}$ allows us to reproduce only mean values, while no informations on the variances of the observables is achieved. If the fluctuation δf is small it is possible to use the theory of quasi-stationary fluctuations [2,9]. Then the correlation function of fluctuations is the solution of a linearized Boltzmann equation, with an appropriate initial condition which can be easily computed from the Boltzmann approximation itself [9,10].This initial condition, i.e. the equal time correlation function, gives the variance of the distribution [9,10], while the behaviour of the correlation function with time is an exponential with a slope which gives the relaxation time of the perturbation [10,11].

An example is given in fig.2 for a quadrupole deformation of a Ca nucleus. The full line represents the correlation function of fluctuations integrated over momentum space in the homogeneous case, i.e. neglecting the mean field. The details of the calculation (amplitude of the deformation, treatment of Pauli blocking)are chosen such to compare to the analytical calculation ref.[12]. The slope of the correlation function, τ = 130 fm/c, gives the collisional relaxation time of the the deformation of the Fermi sphere, while the analytical

estimate [12] gives τ = 142 fm/c.

On the other hand, the dashed line in fig.2 refers to a Vlasov calculation (mean field only) for the same initial condition of the previous one. The correlation function of fluctuations has been integrated both over $\vec{r}$ and $\vec{p}$ space. In this case the slope results τ = 375 fm/c and is connected to one body dissipation mechanisms, the so called Landau damping. In ref.[10] we have shown that this damping is strongly connected to the escape of particles from the excited nucleus, and that the relaxation time is a linear function of the excitation energy.

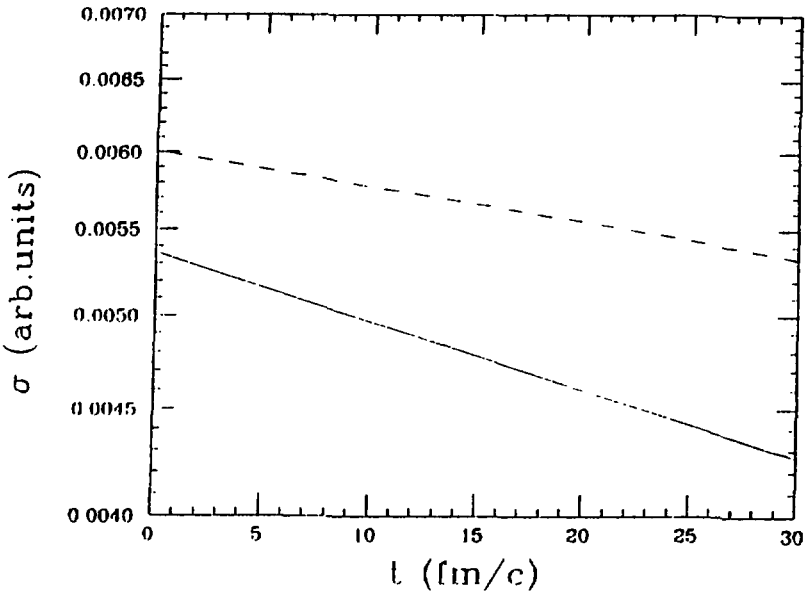

Fig.2

The widths that can be obtained from these relaxation times are in both cases much smaller than the ones shown by experimental data. Therefore the self consistent interplay between mean field and collisions has to play a very important role in order to build up the final widths, or some quantum effect that has been neglected in this semiclassical calculation has to be taken into account.

A complete self consistent BNV calculation for the GQR in Ca is presented in fig.3.

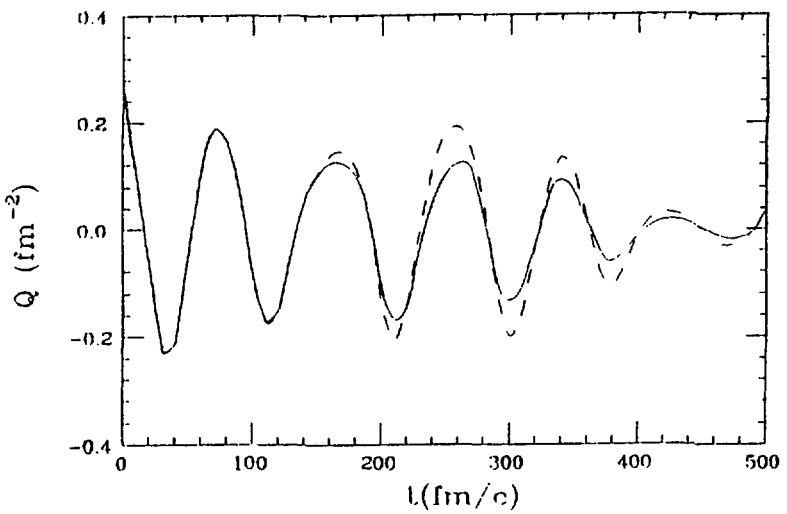

Fig.3

Here, the quadrupole in momentum space is displayied as a function of time (full line) and compared to a calculation where the collision integral was not included (dashed line). A clear effect of the collisions on the

damping of the collective motion can be seen. This effect is increased by the self consistent mean field: since most of the particles are in phase with the coherent field, the amplitude of the collective motion is enhanced and this opens some more free space for the collisions.

In conclusion, in this contribution we have focused on some applications of the kinetic theory in the high density, high temperature regime, where the BNV equation treatment does not represent an adequate approximation any more. We have shown that the inclusion of triple scatterings in the transport equation can shed some light on the problem of subthreshold particle production. We have also presented a new method to evaluate fluctuations in the time evolution of the average one body distribution function. This method can be used to compute the variances in one body observables, i.e. mass distributions and energy spectra, and to evaluate relaxation times of collective motions, both in the collisional regime and for the damping due to the mean field. The inclusion of two body collisions in a self consistent calculation for collective modes is seen to give a considerable contribution to the damping. Work is in progress to connect this effect to the computation of giant resonance widths. The model breaks down if the fluctuations get too large, i.e. approaching a critical region. A comparison with experimental widths of the distributions of one body observables will be very interesting, since it could give informations about the approach to critical phenomena.

References

[1] G.F.Bertsch and S.Das Gupta,Phys.Rep.160(1988)190 and ref.therein
P.Schuck, R.W. Hasse, J.Jaenicke, C. Gregoire, B. Remaud, F. Sebille,
and E. Suraud, Progr. in Part. and Nucl. Phys.22(1989)181 and ref. therein

[2] E.M. Lifshits and L.P. Pitaevskii, Physical Kinetics (Pergamon press, New York, 1981)

[3] A.Bonasera, F.Gulminelli, Phys.Lett. 259B (1991) 399
A.Bonasera, F.Gulminelli, Catania preprint 1-1991 and Phys.Lett.B, in press

[4] S.Chapman and T.G.Cowling, "The Mathematical Theory of Non-Uniform Gases" (Cambridge University Press, London 1970), chapter 16 and references therein

[5] A.Bonasera and C.Gregoire, Lett.Nuovo Cimento 102A(1989)1301

[6] A.Adorno and A.Bonasera, proc. of the IV Convegno di Fisica Nucleare Teorica, Marciana Marina (Elba)1991, and to be published

[7] H.Noll et al., Phys.Rev.Lett. 52(1984)284

[8] S.Ayik, C.Gregoire, Nucl.Phys. 513A(1990)187
E.Suraud, S.Ayik, J.Stryjewski, M.Belkacem, Nucl.Phys.A519 (1990) 171c
J.Randrup, B.Remaud, Nucl.Phys. 514A(1990)339
P.Chomaz, G.F.Burgio, J. Randrup, Nucl.Phys.514A(1990)339, 529A (1991)157

[9] L.D.Landau and E.M.Lifshits, "Statistical Physics", Pergamon Press, New York (1981) chap.12

[10] A.Bonasera, F.Gulminelli, P.Schuck, to be published

[11] S.Ayik, E.Suraud, J.Stryjewski, M.Belkacem, Zeit.Phys. 337A(1990) 413

[12] G.F.Bertsch, Z.Phys. 289A (1978)103

Towards theoretical descriptions of complex nuclear collisions *)

E. Suraud
GANIL, BP5027, F14021 Caen, cedex, France

*) *This contribution covers joint works with various colleagues and friends. The author is very grateful to them. A proper credit of the performed works is made in the appended list of references.*

The dynamics of heavy-ion reactions at energies below a few hundreds of MeV per nucleon is exceptionally rich, as well from the point of view of the behaviors of nuclear matter (clusterization, particle production, ...) as from the point of view of the properties of such dynamical systems (far from equilibrium situations, highly dissipative regimes, large fluctuations, ...). These difficulties are conversely stimulating in order both to understand the physics of these collisions and to have deeper insights into the dynamics of such processes. The latter aspect, in turn, may have a wide field of applications.

Along the years it has become obvious that the usual kinetic equation approches had to be complemented by a fluctuation component, in the spirit of the Langevin decsription of Brownian motion. In order to attack such a problem in the nuclear context we have explored on the same footing several levels of investigation :

1) *Formal developpments*. The intuitive Boltzmann-Langevin description has been derived on firm grounds [1]. Fluid dynamical reductions of the Boltzmann-Langevin approach have also been considered [2]. Finally a more general and flexible formalism (Stochastic TDHF) has been propounded and is actively studied [3].

2) *Developments of trustworthy algorithms for the simulation of realistic collisions*. Such a program started from formal considerations [4]. Comparison of available methods were performed with solvable models of the Boltzmann equation [5]. New methods of resolution were also proposed [6,7]. Finally an approximate resolution scheme of the Boltzmann-Langevin equation has been developed [8].

3) *Applications to physical problems*. After a reasonable understanding of collective modes [9, 10], fusion process [11] and related phenomena [12, 13] the new emerging stochastic extensions of kinetic equations were applied with success to realistic reactions [8]. Applications were performed to the production of subthreshold kaons [14] and are currently studied for multifragmentation and fission.

It is the usual conclusion of (any) paper to state that more work is needed, which is in fact generally true. But as a famous physicist said some time ago it is a chance :

"The diversity of the phenomena of nature is so great, and the treasures hidden in the heavens so rich, precisely in order that the human mind shall never be lacking in fresh nourishment"

J. Kepler

References

[1] The Boltzmann-Langevin equation derived from the real-time path formalism
P. G. Reinhard, E. Suraud and S. Ayik
Ann. Phys.(NY) **213**(1992)204-229

[2] From one-body to collective transport models
S. Ayik, E. Suraud, J. Stryjewski and M. Belkacem
Zeit. Phys. **A337**(1990)413

[3] Stochastic TDHF and the Boltzmann-Langevin equation
P. G. Reinhard and E. Suraud
Ann. Phys.(NY) (1992), in press, preprint GANIL P91-07

[4] Semiclassical and phase space approaches to dynamic and collisional problems of nuclei
P. Schuck, R. W. Hasse, J. Jaenicke, Ch. Grégoire, B. Rémaud, F. Sébille and E. Suraud
Progress of Nuclear and Particle Science **22**(1989)181-278

[5] Collisional relaxation in simulations of heavy-ion collisions using Boltzmann-like equations
G. Welke, R. Malfliet, Ch. Grégoire, M. Prakash et E. Suraud
Phys. Rev. **C40**(1989)2611-2620

[6] Weighted particle method for solving the Boltzmann equation
M. Tohyama and E. Suraud
Phys. Rev **C43**(1991) 1518-1521

[7] Stochastic and deterministic solutions of the 2-D Boltzmann equation
M. Tohyama and E. Suraud
Submitted to Nucl. Phys. **A**(1992)

[8] Applications of Boltzmann-Langevin equation to nuclear collisions
E. Suraud, S. Ayik, M. Belkacem and J. Stryjewski
Nucl. Phys. **A**(1992), in press, preprint GANIL P91-01

[9] Giant dipole modes in heavy-ion reactions
E. Suraud, M. Pi and P. Schuck
Nucl. Phys. **A492**(1989)294-314

[10] High Temperature giant dipole and isoscalar resonances
F. Garcias, M. Barranco, J. Navarro et E. Suraud
Zeit. Phys. **A337**(1990)261

[11] Quasi-fusion of La + C at intermediate energies. A study within the Landau Vlasov approach
M. Pi, E. Suraud et P. Schuck
Nucl. Phys. **A524**(1991)537-560

[12] Compressional effects in Heavy-ion collisions : Spinodal decomposition and thermal energy saturation
E. Suraud, M. Pi, P. Schuck, B. Rémaud, F. Sébille, Ch. Grégoire and F. Saint-Laurent
Phys. Lett **229B**(1989)359-363

[13] Birth, Life and Death of Hot Nuclei
E. Suraud, Ch. Grégoire and B. Tamain
Progress of Nuclear and Particle Science **23**(1989)357-467

[14] K^+ production far below the free nucleon-nucleon threshold
M. Belkacem, E. Suraud and S. Ayik
Submitted to Phys. Rev. Lett. (1992), preprint GANIL, P92-07

MULTIPARTICLE CORRELATIONS AND INTERMITTENCY

P. Bożek[1,2], M. Płoszajczak[1] and A.Tucholski[3]

[1] *GANIL, F-14021 Caen, France*

[2] *Institute of Nuclear Physics, PL-31-342 Krakow, Poland*

[3] *Soltan Institute for Nuclear Studies, PL-05-400 Swierk, Poland*

Intermittency is a manifestation of scale invariance and randomness in physical processes. Originally, it was discussed in a theory of turbulent flow . Since few years the intermittency analysis became a largely studied experimental observable in high energy phenomenology. Recently, it was proposed to apply the intermittency analysis to the studies of the fragment charge distribution following the decay of hot nuclear residuum [1] .

It has been conjectured that the multiplicity fluctuations in small bins can reveal important aspects of the multiparticle production or multifragmentation. To identify these fluctuations, Bialas and Peschanski proposed to calculate the scaled factorial moments (SFMs) [2] which measure dynamical fluctuations without the influence of Poissonian noise. The SFMs have also the advantage to select the spikes in the multiplicity distribution because the moment of rank i contains only contributions from bins with at least i particles (fragments). If non-statistical fluctuations (intermittency) exist at all scales then the SFMs F_i of a studied distribution rise like $F_i(\delta y) \propto (\delta y)^{-f_i}$ with decreasing the bin size δy . Several effects can modify this power-like behaviour strongly or even simulate its presence. These are in the first place various finite size effects which have been discussed recently in connection with the phase transition in finite size percolation and Ising models [3] . In the cluster size distribution of fragments , mixing of events of different dynamical origin including the critical and non-critical ones , may lead to the effects which paradoxically are quite similar to the effects of genuine scale-invariant correlations [4] . Also the dimensional projection can modify the phenomenon [5] and the underlying scale-invariance of the distribution in higher dimensions has to be deconvoluted by the method of finite-size scaling as discussed in [6] .

In the nuclear collisions at energies $E/A \leq 1GeV$, the particle production is strongly suppressed and the nuclear breakup into fragments dominates. Several authors, drawing the analogy between the distribution of either the droplet sizes at the critical point or the cluster sizes at the percolation threshold and the distribution of nuclear fragments in mass and charge [7, 8] suggested the possibility of a liquid-gas or percolation phase transition in the nuclear fragmentaton process. One of the additional features of the critical phenomenon could be the presence of the self-similar fluctuations.

In the case of nuclear fragmentation , the geometrical features of clusters are not directly measurable and it was proposed to search for a signal of the critical behaviour in the fragment-size distribution [1] . The intermittency analysis has been done for the bond percolation model at around the point $q_c = q_\times = 0.25$ of a second-order phase transition in the infinite ($A \longrightarrow \infty$) system [1] . The self-similarity of n_s and the intermittent pattern of fluctuations is seen only in the narrow range of bond activation parameters q between 0.21 and 0.27 with the intermittent pattern in the whole range of fragment sizes for $q \simeq 0.24$. This region of bond activation parameters corresponds to a region of

large fluctuations in both the size of clusters as well as in their multiplicity as expected around the critical point. One should stress, that the total fragment multiplicity which includes also the fragments with size $s = 1, 2$ is changing smoothly over the critical region and its dispersion is approximately constant.

The percolation model is not analytically solvable in more than 1D. By studying the 1D percolation , one can identify three main contributions to the correlations [4] :

- the upper mass bound $< n_j n_k >= 0$ for $j + k > A$, which is numerically not important,
- the repulsive correlations arising from the fact that the second fragment is chosen in a smaller system $(A - j)$, which influences mainly the fluctuations in large bins,
- the attractive correlations arising from the configurations where the two fragments have one or more common inactive links in their perimeters.

These contributions should also be present in the percolation in higher dimensions. For simplicity let us consider the correlations as measured by the second scaled factorial cummulant $f_{jk} =< n_j n_k > / < n_j >< n_k > -1$ between one large fragment of mass s and one fragment of mass $s' = 1$ ($\equiv f_{s1}$) in $D \geq 2$. The mean number of clusters of mass n_s is :

$$< n_s >= A \sum_t g_{st} q^s (1-q)^t \ , \tag{1}$$

where g_{st} is the number of clusters with size s and perimeter t per lattice site. Taking into account only the configurations where the two clusters have at most one common link in the perimeter one obtains :

$$f_{s1} \sim \frac{1}{A}\left(\frac{t}{1-q} - s - t\right) \tag{2}$$

The perimeter t at the percolating point takes the form :

$$t = s(1-q)/q + const\ s^{\zeta} \qquad (s \longrightarrow \infty) \ . \tag{3}$$

where the second term is not present below q_c. From (2) and (3) one obtains :

$$f_{s1} \sim \frac{const\ q}{A(1-q)} s^{\zeta} \ , \tag{4}$$

i.e. the attractive correlations whose appearance is directly linked with the apperance of the excess perimeter $\sim const\ s^{\zeta}$ at the percolating point. The perimeter t of the cluster is the continuous path of active bonds at a boundary which can be either external or internal to the cluster. If the size s of a cluster is identified with its mass then t is the quantity which defines the structure of this mass. At first sight one would expect that $t \propto s^{(1-1/D)}$ as in ordinary geometry for which $surface \propto volume^{(1-1/D)}$, where D is the dimension of the space. However, the perimeter is not a surface in the usual sense, because above the critical point the infinite cluster is not compact containing at their interiof many inactive bonds. Only the second term in eq. (3) may be interpreted as coming from the usual surface contribution, since for $q > q_c$ one has $\zeta = 1 - 1/D$ [9] . Interestingly, near the percolation point, in analogy to the usual cluster scaling , one

expects also that the perimeter distribution function obeys the scaling behaviour [10] and the scaling exponents can be related to those of the usual cluster scaling.

For $q > q_c$ the number of fragments of "finite" size decreases and , consequently, the importance of the correlation effects between those fragments diminish. This is not only true for the fragments of size s and $s' = 1$ but for any two fragments of "finite" size. The decrease of the total number of fragments in favour of the increasing mass of the infinite cluster could be responsible for the disappearance of the intermittency signal above the percolating point. Notice that the scaled factorial cummulant f_{s1} depends on the size of the fragmenting system and decreases with increasing A .

Contrary to the analysis in the percolation model, the experimental data cannot be analyzed as a function of the local connectivity parameter q and one has to look for other ways of selecting critical events. In recent publications [1] , we have shown an evidence for the intermittent behaviour in the charge distribution of fragments in the breakup of Au-nuclei of energy $E \sim 10 GeV/A$ in the nuclear emulsion. In ref. [1] it was proposed to select events according to the number of heavy fragments N_{fr} $(s \geq 4)$. Unfortunately, the experimental data , consisting of only about 400 events in which the charge of all fragments has been measured, exclude any more restrictive analysis including cuts in kinematical variables and/or in the multiplicity of fragments. Hence , at the moment, the predictions of the percolation analysis at around $q \simeq q_c$ as presented in the previous section, cannot be satisfactorily tested.

The experimental data was successfully simulated using the bond percolation model on a cubic lattice containing about the same number of sites as nucleons in the fragmentating Au -nucleus and with the randomly chosen value of the bond activation parameter q in each event [1] . These random - q events have been then filtered by the condition on N_{fr} analogously as in the experimental analysis. Both the intermittency slopes as well as the values of the SFMs have been reproduced well. Interestingly, the cascading model of nuclear fragmentation [11] which reproduces inclusive properties and the features of the conditional moments reasonably well, fails to reproduce the fluctuation properties as seen in the SFMs analysis. It remains to be seen whether this is a generic feature of all fragmentation equations or only of its linear versions.

As said before, the mixing of fragmentation events of different dynamical origin in one ensemble may lead to the intermittent-like bahaviour even though events of each set separately do not show any singular correlations. Hence, if possible one should try to avoid admixing events of distinctly different nature as they may lead to the non-Poissonian deformations of the uncorrelated distribution of fragments. The restrictive conditions on the total multiplicity could provide a more uniform in nature ensemble of fragmentation events. Even more attractive, though at present unfeasible, would be to select events by the kinematical criteria (cuts in p_T , excitation energy, impact parameter etc.) which would not introduce bias in selecting the fragmentation partitions.

The method of SFMs opens the possibility to study quantitatively the non-Poissonian fluctuations at small scales and in this way it provides a new source of informations about the highly excited nucleus undergoing the transition from the highly excited aggregate of nucleons to the final fragments. It is a long and challenging question whether this transition exhibits the properties of the critical phenomenon. However, independently of the precise answer to this question, the SFMs appear as new observables which characterize the particle (fragment) distributions in a more detailed way than the inclusive

observables.

In future studies one should also test the fluctuation properties of the fragment distribution in the phase-space variables. A possible presence of the scale-invariant distribution can then be studied using the finite-size scaling method for the one-dimensional spectra [6] . This method can be useful in extracting scaling indices and scale factors for different reactions at different collision energies helping in this way to understand the relation between scales and the mean-size of interaction region.

References

[1] M. Ploszajczak and A. Tucholski, Phys. Rev. Lett. **65** (1990) 1539;
M. Ploszajczak and A. Tucholski, Nucl. Phys. **A523** (1991) 651.

[2] A. Bialas and R. Peschanski, Nucl. Phys. **B273** (1986) 763;
ibid. **B308** (1988) 857.

[3] J. Dias de Deus and J.C. Seixas, Phys. Lett. **B246** (1990) 506;
P. Bozek, Z. Burda, J. Jurkiewicz and M. Ploszajczak, Phys. Lett. **B265** (1991) 133;
P. Bozek and M. Ploszajczak, Phys. Lett. **B264** (1991) 204; ibid. **B262** (1991) 383.

[4] P. Bozek, M. Ploszajczak and A. Tucholski, Nucl. Phys. **A539** (1992) 693.

[5] W. Ochs, Phys. Lett. **B247** (1990) 101;
A. Bialas and J. Seixas, Phys. Lett. **B250** (1990) 161;
P. Bozek and M. Ploszajczak, Phys. Lett. **B251** (1990) 623.

[6] P. Bozek, M. Ploszajczak, Ganil Report P 91-23.

[7] X. Campi, J. Phys. A Math. Gen. **19** (1986) 917;
X. Campi, Phys. Lett. **B208** (1988) 351.

[8] D.H.E. Gross et al., Z. Phys. **A309** (1982) 11;
J. Bondorf et al., Nucl. Phys. **A443** (1985) 321;
J. Randrup and S. Koonin, Nucl. Phys. **A356** (1981) 223.

[9] D. Stauffer, Introduction to Percolation Theory (Taylor and Francis, London and Philadelphia, Penn., 1985).

[10] R.M. Ziff, Phys. Rev. Lett. **56** (1986) 545.

[11] B. Elattari, J. Richert and P. Wagner, CRN-Strasbourg Report CRN/PHTH 91-08.

PART 2

EXPERIMENTS

A - NUCLEAR STRUCTURE

A1 - NUCLEAR SPECTROSCOPY

GIANT RESONANCES AND MULTIPHONON STATES IN HEAVY ION REACTIONS

Y. Blumenfeld[1], Ph.Chomaz[2]†, N.Frascaria[1], J.P.Garron[1], I.Lhenry[1], J.C.Roynette[1], J.A.Scarpaci[1], T.Suomijärvi[1] N.Alamanos[3], B.Fernandez[3], A.Gillibert[3], A.Lépine[4], and A.Van der Woude[5]

[1]*Institut de Physique Nucléaire, 91406 Orsay Cedex (France)*
[2]*GANIL, BP 5027, 14021 Caen Cedex (France)*
[3]*DAPNIA CE Saclay 91191 Gif-sur-yvette Cedex (France)*
[4]*Instituto di Fisica, Sao Paulo (Brazil)*
[5]*Kernfysich Versneller Institut, Groningen (Netherlands)*

1) Motivations

The search for multiphonon states built with giant resonances (GR) in nuclei is currently in full development. Three main avenues have been followed in this search. Evidence for the two phonon giant dipole resonance has been found in (π^+,π^-) double charge exchange reaction on several targets[1]. Very recent preliminary results from Darmstadt[2] show evidence for the same double giant dipole excited by the Coulomb interaction in relativistic heavy ion collisions. Since several years now we have initiated a program at GANIL to study multiple phonon states built with the giant quadrupole resonance (GQR) and excited by nuclear excitation in intermediate heavy ion reaction[3].

Intermediate energy heavy ion (HI) probes have provided recently some significant new insights into the properties of giant resonances in nuclei. Of particular importance are the very large differential cross sections and the excellent peak to continuum ratios obtained in such reactions which allow to study these collective states and particularly their decay under optimal conditions. The choice of the beam is of great importance. For example, for the study of the GDR and other isovector resonances such as the isovector quadrupole or the double GDR, the use of the most energetic and/or heaviest beam provide optimal conditions due to the presence of a strong Coulomb excitation. Conversely, the investigation of the GQR and higher multipolarity giant isoscalar modes will benefit from the use of moderate energy (40 MeV/n) "light" heavy probes for which the angular distributions retain a certain sensitivity [4,5].

At excitation energies above those of the known GR, low cross section structures superimposed on a large background have been observed. To get a better understanding of these structures, numerous experiments[3,6] have been performed. Up to now, the most consistent representation of these data is given by a multiphonon calculation[7,8]. But it is clear that for a better understanding of these states it is of paramount importance to understand the continuum of heavy ion spectra and to search for more direct signatures of multiphonon states.

Light particle-heavy fragment coincidence experiments should provide a unique tool,

† *On leave from Division de Physique Théorique, Institut de Physique Nucléaire, 91406 Orsay Cedex (France)*

both to disentangle the various mechanisms contributing to HI inelastic spectra and to progress towards the understanding of the microscopic structure of the excited states.

About simultaneously, we studied the neutron decay of GR and high lying states excited in the ^{17}O + ^{208}Pb, ^{120}Sn and ^{90}Zr reaction[9]. Since analysis of the data is still underway, we will concentrate in the following on the ^{40}Ca + ^{40}Ca experiment[10,11].

2) Experiments

We undertook at the GANIL facility a new generation of coincidence experiments. A first experiment[10-17] was performed by bombarding an evaporated self supporting 0.5 mg/cm ^{nat}Ca foil with a 50 MeV/N ^{40}Ca beam . ^{40}Ca was chosen because its collective states have been extensively studied and they decay statistically with a high probability by charged particle emission. The inelastically scattered heavy fragments were detected using the SPEG spectrometer. Coincident light charged particles were detected in 19 cesium iodide elements of the multidetector array PACHA[7].

2) Results and Discussion

In the inclusive inelastic spectrum, the GR is splitted into 2 components centered at 14 MeV and 17 MeV excitation energy, while some small bumps appear at high excitation energy. By comparison with DWBA calculations both components of the GR can be mainly attributed, in the studied angular range, to the excitation of the giant quadrupole resonance (GQR).

The angular evolution of the proton energy spectra obtained at different angles in coincidence with ^{40}Ca spectra vividely portrays the contributing mechanisms[10,11]. A strong enhancement of the proton cross section is observed in the direction of the recoiling nucleus. These protons are attributed to knock out reactions. All protons arising from pick-up break-up reactions are concentrated in a cone of approximately 30^0 centered around the beam direction. In particular, this experiment has allowed to measure the contribution of the pick-up break-up mechanism which accounts for at most half of the cross section in the excitation energy region around 60 MeV.

In the backward direction, the measurement of inelastic scattering in coincidence with light charged particles allows to unambiguously select target excitations. In fig. 1, the ^{40}Ca inelastic spectrum in coincidence with these backward emitted protons, corrected for the thresholds of the various evaporation channels, is displayed. In this spectrum, in addition to the GQR at 17 MeV, one can see a very prominent structure at twice the GQR excitation energy which is a good candidate for a two phonon quadrupole excitation. To confirm this interpretation a detailed study of the decay of both states is necessary.

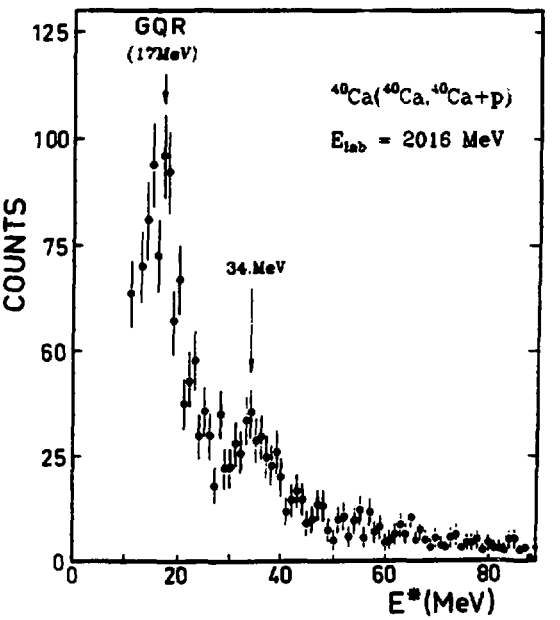

Fig. 1

Particle decay of GR can occur through various processes[18]. The coupling of the particle-hole (1p-1h) state to the continuum gives rise to direct decay into hole states of the A-1 residual nucleus with an escape width $\Gamma^{\uparrow}$. The spreading width $\Gamma^{\downarrow}$ arises from the fact that the 1p-1h doorway state can couple to 2p-2h states which couple again to 3p-3h to np-nh states untill finally a completely equilibrated system is reached.

Experimentally, the two decay modes can be distinguished by measuring the spectrum of the residual A-1 nucleus. Statistical decay can be inferred from a comparison of the experimental spectrum of the A-1 nucleus (or the corresponding particle spectrum) with the one calculated by means of the Hauser Feschbach formalism. The excess cross section is then attributed to non statistical decay of which the part decaying to hole states is considered as direct decay.

This calculation has been performed for the two components of the GQR using the code Cascade.

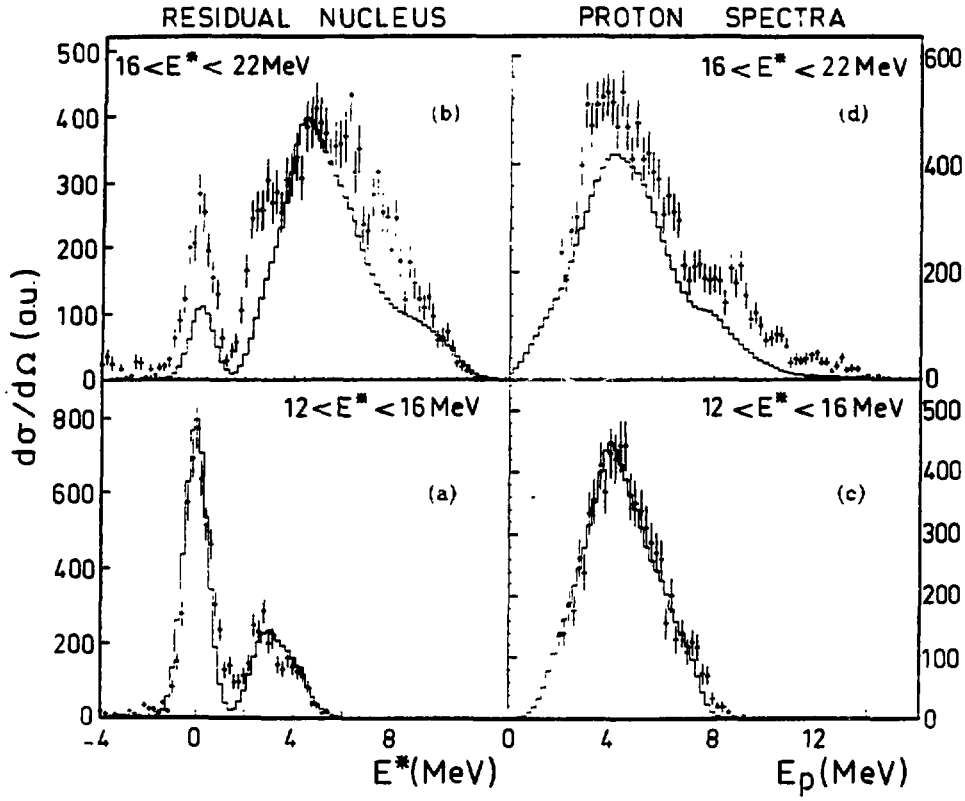

Fig. 2

Experimental final state spectra for the excitation energy range of : (a) 12 < E_x < 16 MeV and (b) 16 < E_x < 22 MeV in ^{40}Ca (c) and (d) are the corresponding proton spectra (see ref). The histogram represent statistical decay calculations using the code CASCADE

It turns out that the dominant decay mode for the low energy component of the GQR can be understood statistically (see fig 2 a and c) whereas the excess of high energy protons observed for the second component of the GQR can be identified with a direct decay to hole states in ^{39}K. In that case, the non statistical branch to low lying hole states accounts for about 30% of the total decay width (see fig. 2 b and d).

This result is of great importance for the following reason: the signature of a two phonon state can be given by the study of its decay. In principle, the multiplicity of

the emitted particles from a multiphonon state is expected to be proportionnal to the number of excited phonons, as far as we assume that all phonons decay independently. For example, the protons emitted by a two phonon state in ^{40}Ca built with the GQR will exhibit the same direct decay branch as for the GQR but with a multiplicity twice as large. We expect the proton kinetic energy spectra for the two phonon state to exhibit the same direct decay component as for the one phonon state. Instead, the direct decay of a high multipolarity GR excited in the same region is expected to be different since their decay will feed the hole states of the A-1 nucleus leading to very different proton energies.

The preliminary results obtained in the previously described experiment show that

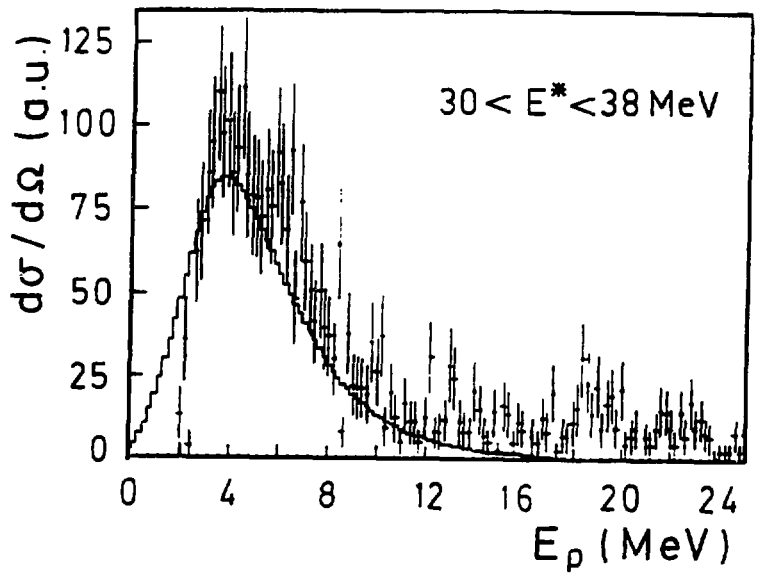

Fig. 3

Experimental and calculated (histogram) proton spectrum in coincidence with the excitation energy range of 30 < E_x < 38 MeV in ^{40}Ca

the proton spectra in coincidence with respectively the GQR and the bump at 34 MeV excitation energy seem to present a similar direct decay branch (see fig.3). Obviously, in this experiment, statistics are too weak to warrant definite conclusions, but these results are very promising. Also in the neutron decay experiment a non statistical decay branch is observed for very high lying states. An analysis of this component is currently underway.

4) Conclusion

This pionnering experiment has shown that light particle coincidences with inelastically scattered fragments provide a powerful tool for the understanding of heavy ion inelastic spectra at intermediate energies. The pick-up break-up mechanism is shown to account for at most half of the cross section at high excitation energies in the reaction studied. A sizable amount of this high energy cross section is due to excitations of the target, and in particular a prominent structure is observed at 34 MeV excitation energy, which is a good candidate for the double phonon excitation built with the giant quadrupole resonance.

Similar experiments using larger solid angle particle detection systems at backward angles will allow to obtain virtually background free spectra of inelastic excitations. Such an experiment has recently been performed on the $^{40}Ca + ^{40}Ca$ system in order to improve statistics concerning the 34 MeV structure. For heavier target nuclei, which decay preferentially by neutron emission, the EDEN neutron multidetector, recently completed at Orsay, has been tailored to this type of experiment[19].

References

1)For example Mordechai et al and references therein
2)For example The LAND collaboration GSI Report 09-91 (Dec.1991)
3)N.Frascaria, Nucl.Phys. A482(1988) 245c and references therein
4)T.Suomijärvi et al., Nucl.Phys. A491(1989) 314
5)T.Suomijärvi et al., Nucl.Phys. A509(1990) 369
6)N.Frascaria et al., Nucl.Phys. A474(1987) 253
7)Ph.Chomaz et al., Z.Phys. A318(1984)41
8)Y.Blumenfeld et al., Nucl. Phys. A455(1985)151
9)J. Blomgren and A.Van der Berg, private communication
10)Y.Blumenfeld and Ph.Chomaz, Phys. Rev.C 38(1988)2157
11)J.A.Scarpaci,PhD Thesis, Universite d'Orsay Report IPNO-T-90-04 (1990)
12)J.A.Scarpaci et al, Phys.Lett. B258(1991)279
13)J.C Roynette et al, XXVIII Intern. Winther Meeting on Nucl. Phys.
Bormio,(Italie) (Jan. 1990)
14)Y.Blumenfeld et al, IV Int. Conf. on Nucl. Nucl. Coll.
Kanazawa (Japon),(June 1991).
15)N.Frascaria, VI Int. Conf. on Nucl. React. Mechanisms.
Varenna (Italie),(June 1991)
16)J.C. Roynette, Intern. Conf. on New Nuclear Phys. with Advanced Technics.
Ierapetra (Greece) (June 1991).
17)N.Frascaria, G.R. and Related Phenomena. Notre Dame (USA) (Oct 1991)
18)A. van der Woude, Prog. Part. Nucl. Phys. 18 (1987) 217 and references therein
19)Y. Blumenfeld et al., Internal report Orsay IPNO-DRE 88/20 (1988)

Excitation of Giant Resonances in ^{208}Pb, ^{120}Sn, ^{90}Zr, and ^{60}Ni by 84MeV/nucleon ^{17}O Ions

R. Liguori-Neto [a,1], P. Roussel-Chomaz [a], L. Rochais [a], N. Alamanos [a], F. Auger [a], B. Fernandez [a], A. Gillibert [a], R. Lacey [a] and D. Pierroutsakou [a], J. Barrette [b], S. K. Mark [b], R. Turcotte [b], Y. Blumenfeld [c], N. Frascaria [c], J. P. Garon [c], J. C. Roynette [c], J. A. Scarpacci [c], T. Suomijarvi [c], A. Van der Woude [d] and A. M. Van der Berg [d].

[a] DAPNIA/SPN, Centre d'Etudes Nucléaires de Saclay, F-91191, Gif-sur-Yvette, France
[b] Foster Radiation Laboratory, Mc Gill University, Montreal, Canada H3A 2B2
[c] Institut de Physique Nucléaire, F-91406 Orsay, France
[d] Kernfysisch Versneller Instituut, NL-9747 AA Groningen, The Netherlands
[1] On leave from the University of São Paulo, supported by CNPq, Brasil.

Abstract: Elastic and inelastic scattering of 1435 MeV ^{17}O ions on ^{208}Pb, ^{120}Sn, ^{90}Zr and ^{60}Ni have been measured. Parameters of the isoscalar giant monopole and quadrupole resonances were obtained. The quadrupole resonance exhausts ~55% of the energy weighted sum rule while the observed monopole resonance corresponds to more than 100% of the sum rule.

Introduction

Giant resonances appears in all nuclei and are described as simple collective modes of excitation. They were the subject of intensive studies in the last decade [1-3]. These investigations used various complementary probes and nuclear reactions to isolate and identify the various resonances. In particular, inelastic scattering of light hadrons and low energy heavy ions have significantly contributed in our knowledge on electric giant modes.

The advent of heavy ion accelerators, providing beams in the energy region of 50 to 100MeV/nucleon, opened new perspectives and reactivated the experimental investigations in this field [4-12]. Inelastic scattering of heavy ions excites giant resonances with high differential cross sections and an excellent peak-to-continuum ratio. It is expected that new informations on the properties of electric giant resonances and possibly on higher multipole modes would be obtained. These probes could also contribute in the investigation of isovector giant modes since at these energies the Coulomb interaction is sufficiently strong to excite high excitation energy states [8,9]. Finally these advantages are well suited to study the decay properties of giant resonances, which provide unique information on their microscopic structure, experimental work in this direction is under way [8-11].

In this contribution we report on the excitation of giant resonances in ^{208}Pb, ^{120}Sn, ^{90}Zr, and ^{60}Ni using ^{17}O beam at an incident energy of 1435 MeV. The properties of giant resonances are discussed for the different mass regions.

Discussion

Typical inelastic spectra are shown in fig. 1 for the different targets. The large peak located between 10 and 20MeV arises mainly from the excitation of a few giant resonances, namely the isovector giant dipole (IVGDR), the isoscalar giant quadrupole (ISGQR) and isoscalar giant monopole (ISGMR) resonances [1-9]. Although other resonances are expected in this energy range, we will discuss here mainly the properties of these resonances and their evolution with the nuclear mass.

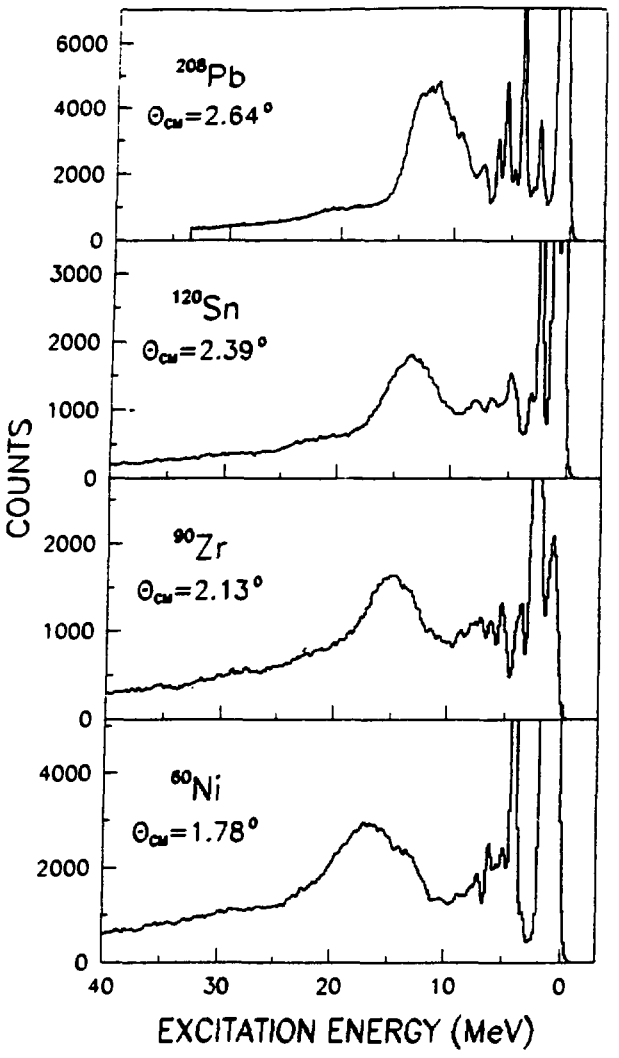

Fig. 1. Inelastic scattering spectra for the different targets.

1) ^{208}Pb

The measured angular distributions for the ISGMR and the ISGQR are shown in fig. 2. The results of the calculation are shown by the solid lines. They correspond to 52% of the EWSR for the ISGQR and 125% for the ISGMR. It was also attempted to reproduce these differential cross sections by adding some L=4 strength. Calculated angular distributions assuming pure L=4 excitations are show in fig. 2 (dotted lines). Even though the presence of L=4 strength is not necessary to reproduce the data, some L=4 strength (<10% of the EWSR) cannot be excluded by the present data partly due to the limited angular range of the present measurements.

2) ^{120}Sn

The percentage of the EWSR exhausted by the ISGQR is 50% in good agreement with the observed systematic [2]. This value is however smaller then the result of recent (a,a') inelastic scattering measurements in which 135% of the EWSR was found [13]. What is puzzling is the large percentage of the EWSR, 135 exhausted by the ISGMR.

Hexadecapole strength is observed in the region of the ISGQR with an upper limit of 5% on the EWSR [14,15]. Assuming here a peak exhausting 5% of the L=4 EWSR would lead to minor modifications, of the order of 5-10%, on the ISGQR and ISGMR strength. Although the large percentage of the EWSR exhausted by the ISGMR remains a puzzle it should be noticed that similar results were obtained in recent (^{17}O,^{17}O') inelastic scattering measurements [12].

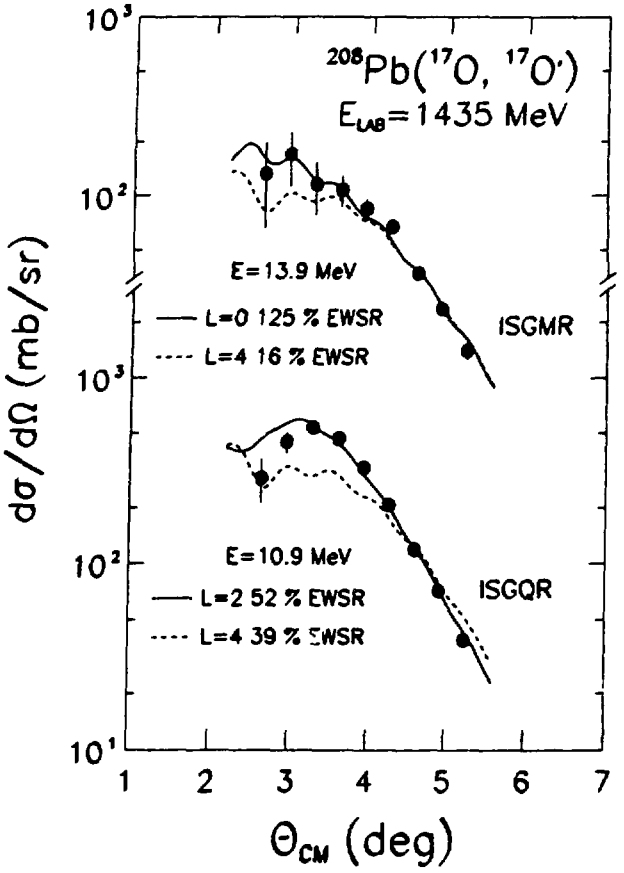

Fig. 2. Comparison of differential inelastic cross sections with coupled channels calculations. The dashed lines represent angular distributions calculated assuming pure L=4 transitions.

3) ^{90}Zr

The percentage of the EWSR exhausted by the ISGQR is 50%. The excitation of the ISGMR exhausts 118% of the EWSR. This value is quite large compared to the ISGMR strength observed in light ion inelastic scattering measurements [2]. It is close, however to the results of recent heavy-ion inelastic scattering experiments which report 80% [7] and 120% [6] depletion of the monopole EWSR.

4) ^{60}Ni

Few studies exist on giant modes in ^{60}Ni. The parameters of the ISGQR determined in an α particle inelastic scattering measurement are E=16.4 MeV, Γ=5.0 MeV and 63% of the EWSR [16]. The situation is quite ambiguous concerning the ISGMR. In the case of ^{58}Ni its observed excitation energy varies between 17 and 20 MeV with a strength ranging from 10% to 40% of the E0 EWSR.

In our experiment a peak centered at 16 MeV, with Γ=5.0 MeV, was assigned to the excitation of the ISGQR whereas the peak at 19.4 MeV to the excitation of the ISGMR. They correspond to 63% and 125% of the L=2 and L=0 EWSR respectively. The E2 EWSR percentage agrees with the α particle inelastic scattering results. In contrast, the E0 EWSR percentage is larger than the values observed in other Ni isotopes. However for this system, the E0 EWSR percentage depends on the assumed width of the ISGQR. For instance a fit of the spectra with Γ=3.8 MeV, although giving an as good description of the data, results in 180% of the E0 EWSR. A better fit of the data can be obtained if we assume hints of L=3 and L=5 strengts in the excitation region of the L=0 mode. In this case the percentage of EWSR drops down to ~ 100%.Because of the complexity of the spectra, the present data do not allow a precise determination of the ISGQR width and therefore the quoted L=0 EWSR percentage has a large uncertainty.

Conclusions

For all the nuclei we have studied, the giant resonance structure stands on a relatively low background compared to other probes, with a peak-to-continum ratio varying from 6 for ^{208}Pb to 3 for ^{60}Ni.

The giant resonance structure was decomposed into gaussian shape peaks describing giant modes of different multipolarity. The best defined giant resonance here is the ISGQR which exhausts of the order of 55% of the E2 EWSR in agreement with the systematics. The situation is different concerning the strength of the ISGMR for which we observed a strength varying between 100 and 135%. This mode was extensively studied in light ion inelastic scattering measurements and the observed strength seems to decrease almost linearly from a depletion of 100% E0 of the EWSR in A > 160 nuclei to about 10% in nuclei with A ~ 60 [2]. Recent charged particle decay studies of giant modes make this picture questionable, and reveal the presence of E0 strength close to 100% of the E0 EWSR in nuclei with A~ 24, 28 [17,18]. The present data support the presence of an important fraction of E0 strength for intermediate mass nuclei.

References

1) F. E. Bertrand and J. R. Beene Proceedings of the 1989 International Nuclear Conference, Sao Paulo, Bresil, Edited by M.S. Hussein, World Scientific.

2) A. Van der Woude, Prog. Part. Nucl. Phys. **18** (1987) 217.

3) F. E. Bertrand, Nucl. Phys. **A354** (1981) 129C.

4) J. Barrette et al., Phys. Lett. **B209** (1988) 182.

5) P. Roussel-Chomaz et al., Phys. Lett. **B209** (1988) 187.

6) T. Suomijärvi et al., Nucl. Phys. **A491** (1989) 314.

7) T. Suomijärvi et al., Nucl. Phys. **A509** (1990) 369.

8) J. R. Beene et al., Phys. Rev. **C41** (1990) 920.

9) J. R. Beene et al., Phys. Rev. **C41** (1990) 1332.

10) J. A. Scarpaci et al., to be published

11) M. Thoennesen et al., Phys. Rev. **C43** (1991) R12.

12) D. J. Horen et al., Phys. Rev. C42 (1990) 2412. and to be published

13) M. M. Sharma et al., Phys. Rev. **C38** (1988) 2562.

14) F. Bertrand et al., Phys. Lett. **B103** (1981) 326.

15) J. M. Moss et al., Phys. Rev. **C18** (1978) 741.

16) D. H. Youngblood et al., Phys. Rev. **C13** (1976) 994.

17) Y. Toba et al., Phys. Rev. **C41** (1990) 1417.

18) H. J. Lu et al., Phys. Rev. **C33** (1986) 1116.

EXCITATION AND FISSION DECAY OF ^{232}Th THROUGH THE (^{17}O,^{17}O') REACTION

J. BARRETTE, C. CABOT*, S. K. MARK, R. TURCOTTE, J. XING**,
Foster Radiation Laboratory, Mc Gill University, Montreal.

N. ALAMANOS, F. AUGER, B. FERNANDEZ, J. GASTEBOIS, A. GILLIBERT
R. LACEY, R. LIGUORI-NETO***, P. ROUSSEL-CHOMAZ****, A. MICZAIKA,
SEPN, Centre d'Etudes Nucléaires de Saclay.

Y. BLUMENFELD, N. FRASCARIA, J. P. GARRON, J. C. ROYNETTE,
J. A. SCARPACI, T. SUOMIJARVI,
Institut de Physique Nucléaire, Orsay.

A. VAN DER WOUDE, A. M. VAN DEN BERG, K. V. I., Groningen.

*on leave from Université Paris-XI, Institut de Physique Nucléaire, Orsay.
**on leave from Institute of Atomic Energy, Beijing.
***on leave from University of San Paulo, supported by FAPESP, Brasil.
****present address GANIL, BP 5027, 14021 CAEN Cedex

1- Motivation.

It is now well established that inelastic scattering of intermediate energy heavy ions is a powerful tool for the study of giant resonance excitation and of their decay. The measure of the fission probability of a giant resonance allows one to determine to what extent this resonance decays statistically. It has been shown that the fission probability of the Isovector Giant Dipole Resonance (IVGDR) in actinide nuclei is consistent with a pure statistical decay of this resonance.

On the contrary, the experimental situation concerning the Giant Quadrupole Resonance (GQR) fission decay has remained quite ambiguous for many years[1]. The situation has been clarified only recently in the case of ^{238}U, with the result of a fission probability consistent with the photofission data up to an excitation energy of 14 MeV[2,3]. In the case of ^{232}Th, the fission decay channel of GQR has been investigated only by using inelastic scattering of alpha particles [4]. In this work, no evidence for the fission decay of the GQR was found.

Our purpose was to take advantage of the large cross sections and the good peak to continuum ratio obtained with heavy ion projectiles, to study the excitation and fission deexcitation of the giant resonances in ^{232}Th, via inelastic scattering of 84 MeV/u ^{17}O ions. Due to its low particle emission threshold, it has already been shown that ^{17}O is particularly suitable for this type of studies, since it does not contribute to the inelastic spectra [5,6].

2- Giant resonance excitation.

The experiment was performed at the GANIL facility. The scattered particles were detected and identified in the energy-loss magnetic spectrometer SPEG[7], associated with its standard detection system for position measurements and particle identification. The experimental procedure has been extensively described elsewhere[8]. The angular acceptance of the spectrometer allowed the simultaneous measurement of inelastically scattered particules between 2.6° and 6.5°, with an angular resolution equal to 0.1°. The overall energy resolution was equal to 500 keV.

Fig 1 presents a typical energy spectra for the inelastic scattering of ^{17}O on ^{232}Th obtained near the grazing angle. The low energy part of the inelastic spectrum is dominated by the Coulomb excitation of the low-laying states in ^{232}Th. The broad peak centered around 12 MeV arises from the excitation of several giant resonances. The peak/continuum ratio is excellent compared to the data obtained with light probes such as protons or alphas (e.g. fig. 2 in ref [9]).

The energy and width obtained for the different resonances are presented in **table 1**. They are in good agreement with the values previously reported for this nucleus concerning the GQR) and the Giant Monopole Resonance[11]. The relatively low background in the energy spectra allows one to reduce ambiguities in the extraction of Giant Octupole Resonance parameters and leads to a somewhat lower energy position than in ref 9: (17.9±1.0) MeV instead of (19.6±1.0) MeV. The quality of the fit obtained with our method is illustrated on **fig.1**.

The percentage of the Energy Weighted Sum Rule (EWSR) exhausted by a resonance can be extracted from the comparison of the corresponding experimental angular distributions and the results of coupled channel calculations(**table 1**). The errors on the EWSR reported in **table 1** arise from the uncertainty on the absolute normalization and from the subtraction of the continuum underlying the resonances .

For the ISGQR in ^{232}Th, a rather precise value (65±15)% is obtained, whereas the result obtained in the previous light-ion experiments was strongly dependant on the choice made for the background [10] .

3- Fission decay of the Giant Resonances.

The fission fragments were identified by their energy and time-of-flight using a set of 10 (300 mm2) Si detectors placed in and out of the reaction plane. The anisotropy parameters extrated from angular correlations have been used to correct the fission probability near the fission threshold.

The inelastic spectrum, corresponding to the whole acceptance of the spectrometer is displayed on the upper part of **fig. 2**. Simultaneously to the singles measurements, coincidences between the scattered ^{17}O and fission fragments were recorded. The narrow peak observed near 6 MeV on the coincidence spectrum (medium part of **fig. 2**) is due to the fact that the fission barrier (B_f=6.15 MeV) is slightly below the neutron binding energy (S_n=6.4 MeV). Just above the opening of the neutron exit-channel, and because of the competition between fission and neutron decay of the excited nucleus, the coincidence rate suddenly decreases. Then the spectrum becomes rather flat before a distinct decrease between 12 and 13 MeV. Because of the second chance fission barrier, the spectrum rises up at an excitation energy slightly higher than 12.5 MeV. It rises again around the third chance fission threshold near 18 MeV.

The most interesting feature in this coincidence spectrum is the structure around 10 MeV which can be attributed to the decay of GR (both GDR and GQR). In the coincidence spectrum previously measured[4], no bump was observed around 10 MeV. This is probably due to the fact that, in the alpha singles spectrum, the GR peak is not very well defined and is small compared to the background. In **fig. 2**, the lower plot represents the evolution of the crude fission probability obtained from the ratio of the ^{17}O coincidence spectrum to the singles one. The fission probability fluctuations are mainly due to the statistics. These data, corrected for the non-isotropic angular distribution are reported in **fig. 3.**

The fission probability can be compared to the fission probability obtained from (γ,F) experiments[12], which gives in fact the fission probability of the GDR and then represents also the statistical fission probabiiity. In the region of GR, around 10 MeV, the agreement is quite good. At higher energies, our results are somewhat smaller than the statistical fission probability, but this region is largely dominated by the continuum.

The region between 8 and 13 MeV corresponds, in the singles spectrum, to cross sections for the GDR and the GQR excitation in respective proportions of around 2/3, 1/3. In this energy region, a mean fission probability value of (6.8±0.4)% was deduced, which is in good agreement with the 7.3% mean value for GDR fission obtained by photoabsorption measurements[12]. The good agreement between our data and the GDR fission means that the fission probability of the GR reported here, which is in fact, the fission probability of both GDR and GQR, is coherent with a statistical fission decay.

If one assumes that the GQR does not decay at all by fission, the fission probability of the GDR would be (8.5±0.4) %, i.e. sizebly larger than the photoabsorption results. Therefore, it is not possible in this experiment to conclude to an inhibition of the fission decay mode for the GQR. The GQR fission decay is found to be consistent with a statistical process.

4- Conclusion.

Intermediate energy heavy-ions have been used to study GR excitation and fission deexcitation in ^{232}Th. For the GQR and GMR excitation, the energy and width, as well as the corresponding sum-rule fraction obtained are in good agreement with the adopted values for this nucleus.

Concerning fission decay, the picture that emerges from our Th analysis is different from the one obtained with light-ion projectiles where no evidence for the fission decay of the GQR was found. We believe that this previous conclusion is due to an improper discrimination, in light ion scattering reactions, between the GR and the very large background. In the work we report here, the good peak-to-continuum ratio allows one to point out a bump in the coincidence spectrum around 10 MeV which can be attributed to both GDR and GQR decay. The analysis of the corresponding fission probability is in agreement with a main statistical fission decay of the GQR.

References

1 A. Van Der Woude, Prog. Part. and Nucl. Phys., Ed. A. Faessler Pergamon press, 18 (1987) 217.
2 R. L. Auble et al, Phys. Rev. 41, 6 (1990) 2620.
3 T. Weber et al Nucl. Phys. A 510 (1990) 1.
4 J . Van der Plicht et al, Nucl. Phys. A346 (1980) 349.
5 J. Barrette et al, Phys.Lett. B, 209 (1988) 182.
6 J. R. Beene et al, Phys, Rev.C 41, 3 (1990) 920.
7 L. Bianchi et al, Nucl. Instr. Meth. A276 (1989) 509.
8 C. Cabot et al, proceedings of XXV Int. Winter Meeting on Nuclear Physics, Bormio, (Italy), january 1991, p 273.
9 H. P. Morsch et al, Phys.Rev. C 25, 6 (1982) 2939.
10 M. N. Harakeh et al, Phys. Rev. C21 (1980) 768.
11 M. Buener et al, Phys. Rev. Lett. 45, 21 (1980) 1667.
12 T. Caldwell et al,. Phys. Rev. C, 21, 4 (1980) 1215.

Table 1	Parameters for giant resonances		
	E* (MeV)	Γ (MEV)	% EWSR
GDR1	11.5	4.3	115 ± 15
GDR2	14.4	4.5	
GQR	10.6±0.3	4.5±0.5	65±15
GMR	13.9±0.4	3.0±0.6	100-130
GOR	17.9±1.0	5.5±1.1	≤75

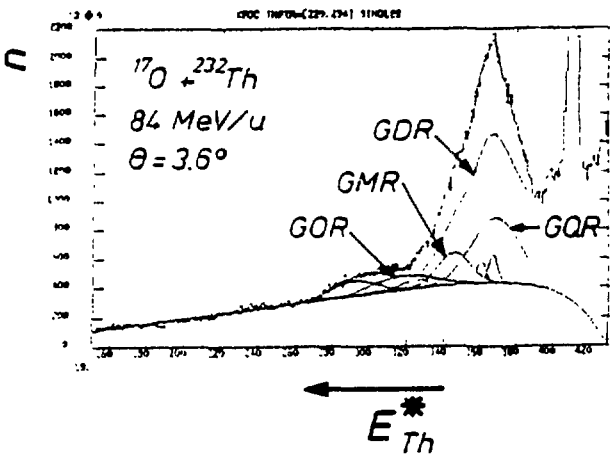

fig. 1 Inelastic scattering spectra at theta lab =3.6 degrees from the ^{232}Th (^{17}O, ^{17}O') reaction at 84 Mev/u. The solid curves show a decomposition of the spectra into resonance peaks and an underlying continuum as explained in the text.

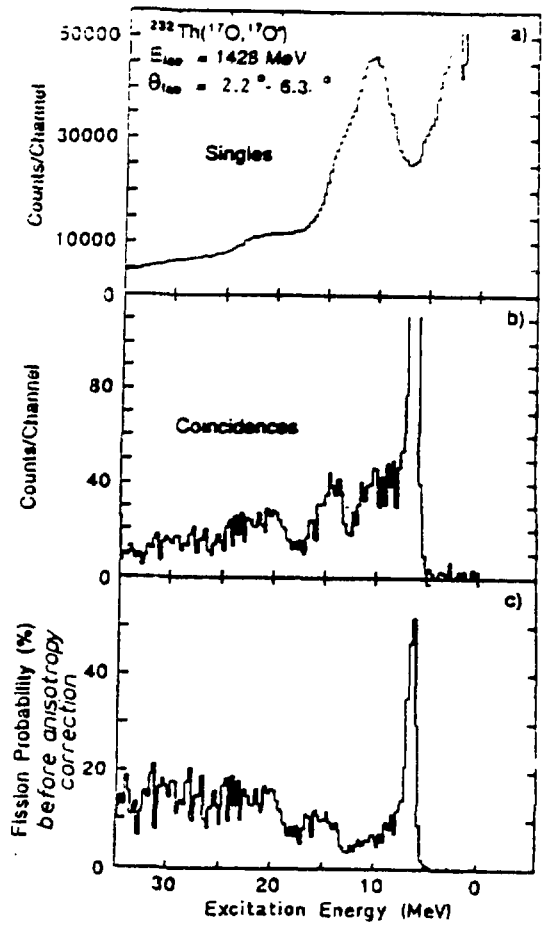

fig 2 a) Single inelastic scattering spectrum from the ^{232}Th(^{17}O, ^{17}O') reaction. It corresponds to the whole angular aperture of SPEG.
b) Same spectrum in coincidence with fission fragments.
c) Fission probability distribution before anisotropy correction. It has been obtained by dividing the coincidence data by the singles spectrum.

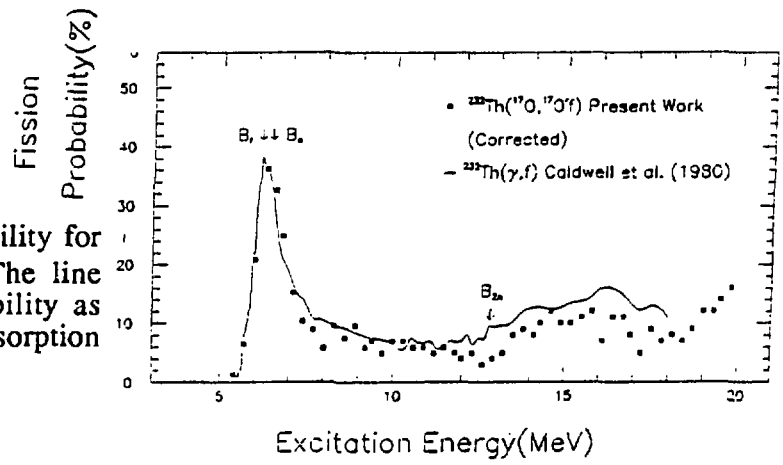

fig 3 Measured fission probability for the ^{232}Th(^{17}O, ^{17}O') reaction. The line represents the GDR fission probability as obtained in ref 12 through photoabsorption measurements.

ONE NUCLEON TRANSFER REACTIONS ON NON-CLOSED SHELL NUCLEI

D.Beaumel[1], Y.Blumenfeld[1], Ph.Chomaz[2]†, S.Fortier[1], N.Frascaria[1], S.Galès[1], J.P.Garron[1], H.Laurent[1], I.Lhenry[1], J.C.Roynette[1], J.A.Scarpaci[1], T.Suomijärvi[1], A.Gillibert[3], G.Crawley[4], J.Finck[4], G.Yoo[4], J.Barreto[5] and Nguyen van Giai[6]

[1]*Institut de Physique Nucléaire, 91406 Orsay Cedex (France)*
[2]*GANIL, B.P.5027, 14021 Caen Cedex (France)*
[3]*DAPNIA CE Saclay, 91191 Gif-sur-yvette Cedex (France)*
[4]*NSCL MSU, East Lansing, Michigan 48824 (USA)*
[5]*Universidade Federal,Rio de Janeiro 21945 (Brasil)*
[6]*Division de Physique Théorique, Institut de Physique Nucléaire, 91406 Orsay Cedex (France)*

1) Motivations

The availability of intermediate energy heavy ion beams has prompted the studies of the high excitation energy region in transfer reactions. In several experiments on one nucleon transfer reactions, a broad structure has been observed in the energy spectrum at 10-20MeV depending on the target nucleus [1,2,3]. It has been suggested that these structures are due to the excitation of high-spin single particle states. The width of the bumps has been explained by the coupling of these states to the low lying collective states [2,3].

However, the excitation energy of observed structures roughly varies as $A^{-1/3}$ for different nuclei and corresponds approximately to that of the well known giant resonances. Their width, few MeV, is also comparable to that of the giant resonances. Furthermore, in several experiments it has been shown that giant resonances are strongly excited in inelastic heavy ion collisions. These considerations raise the interesting question of whether the structures seen in the heavy ion induced transfer reactions could be due to collective particle-hole excitations such as giant resonances.

2) Experiment and Experimental Results

In order to study high energy excitations in one nucleon transfer reactions and to see if collective strength can be excited, an experiment with non-closed shell target nuclei has been performed at GANIL using the spectrometer SPEG. The transfer on a non closed shell target allows to excite particle-hole excitations in a one step process and thus should enhance the possibility to excite collective strength. In this experiment, several one nucleon stripping and pick-up reactions leading to closed shell nuclei in the exit channel were studied with two different projectiles: ^{20}Ne at 48MeV/A and ^{36}Ar at 42MeV/A. Fig.1 shows the transfer spectrum obtained for the following reactions:

neutron stripping: $^{20}Ne + ^{207}Pb \rightarrow ^{19}Ne + ^{208}Pb$

† *On leave from Division de Physique Théorique, Institut de Physique Nucléaire, 91406 Orsay Cedex (France)*

proton pick-up: $^{20}Ne + ^{209}Bi \rightarrow ^{21}Na + ^{208}Pb$
proton stripping: $^{20}Ne + ^{59}Co \rightarrow ^{19}F + ^{60}Ni$.

In the case of the stripping reaction (fig.1a,fig.1c), the spectra are dominated by a large bump centered at about the projectile velocity. This cross section mostly corresponds to projectile break-up reactions and to excitation of the non-resolved continuum states of the target. For the pick-up reaction (fig.1b), the spectrum is very different. This can be attributed to the absence of the projectile break-up background. Moreover, the matching conditions in the pick-up channel enhance the excitation of low excitation energy states.

In the spectrum measured for the reaction $^{207}Pb \rightarrow ^{208}Pb$ a bump at about 13.5MeV excitation energy is clearly observed as well as a second bump aroud 20MeV. On the contrary, in the case of the reaction $^{59}Co \rightarrow ^{60}Ni$, the spectrum presents less structures, in the high energy region, only a small shoulder can be seen at about 18MeV corresponding approximately to the $A^{-1/3}$ scaling of the excitation energy.

3) Calculations

To explain the energy spectra observed in several one nucleon transfer reactions either on closed or non-closed shell nuclei, a semiclassical model has been proposed by Bonaccorso and Brink[4]. This model reproduces the overall shape of the stripping spectra by including both the excitation of quasi-bound and non-bound states in the target nucleus and the projectile break-up background. However, this model has several free parameters and does not take into account particle-hole correlations.

In the case of the $^{207}Pb \rightarrow ^{208}Pb$ reaction we have performed microscopic calculations based on the RPA strength function and the DWBA transfer cross section [5-7]. In a microscopic model, giant resonances are described by a coherent sum of particle-hole excitations. In a transfer reaction on a non-closed shell nucleus such as ^{207}Pb, by adding a particle, a part of the ph-configurations contributing to the giant resonance strength can be populated. The amount of the collective strength exhausted in a given transfer reaction depends on the number of accessible ph-configurations and on the transfer cross section leading to these configurations. The final transfer cross section in this model is then given by

$$\frac{d\sigma}{d\omega}(E,\theta,L) = \sum_n |\sum_{ph} A_{ph}(ph,E,\theta) X_n^{ph}(ph,E_n)|^2 \delta(E-E_n)$$

where A_{ph} is the DWBA transition matrix, X_n^{ph} is the RPA amplitude and $n = (E_n, L_x, \pi, M_x)$.

In the calculation, the contribution of all ph-configurations obtained by coupling the neutron hole 3p1/2 in ^{207}Pb to different quasi-bound neutron particle levels have been considered and all isoscalar and isovector multipolarities from L=0 to L=9 have been included. It should be noted that this calculation has no free parameters.

Fig.2 presents a comparison of the calculated spectrum (fig.2b) with the experimental spectrum (fig.2a) for the reaction $^{207}Pb \rightarrow ^{208}Pb$. The calculation reproduces rather

well the low lying peaks in the spectrum. Furthermore, between 12 and 16MeV, a strong concentration of the cross section can be seen corresponding to the bump at about 13.5MeV in the experimental spectrum. The cross section in this excitation energy region is due to the excitation of high multipolarities 9^-, 7^-, 6^+ and 4^+. Due to the matching conditions in heavy ion reactions the high spin states are preferentially populated and, when a target with a low spin hole like ^{207}Pb is used, high multipole modes are excited selectively.

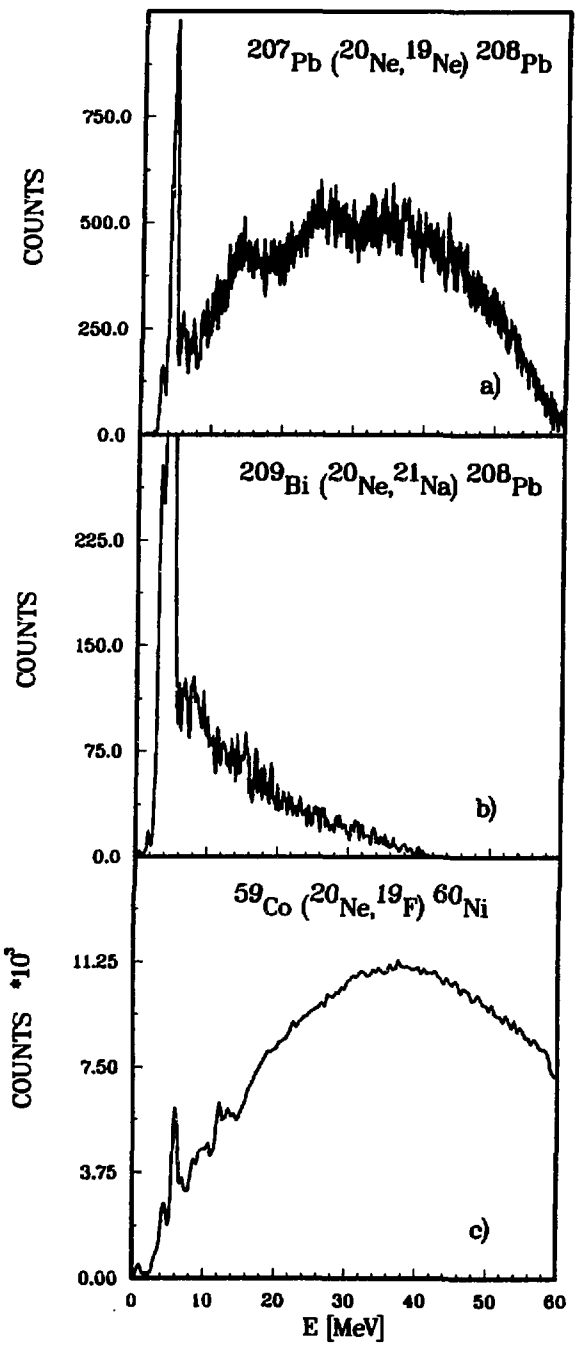

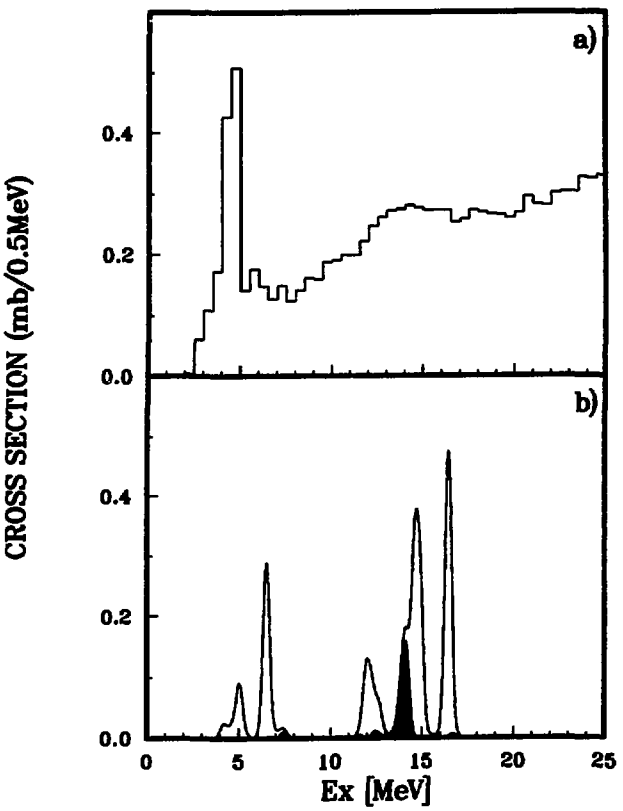

Fig.1. (Right) Experimental spectra obtained for different one nucleon transfer reactions with ^{20}Ne beam at 48 MeV/A.

Fig.2. (Left) Comparison of the calculated spectrum (fig.2.b) and the experimental spectrum of the fig.1.a.

An RPA state is generally considered collective if several particle-hole configurations contribute to this state. In fig.2b the colored part corresponds to the strength where more than 5 configurations contribute to a given RPA state and which can be considered as collective. The amount of collective strength excited in the studied reaction is small compared to the single particle strength. In fact, the strength of high multipole modes, which are favoured in this reaction, is mostly of single particle type while only the low multipole modes like the giant monopole, dipole and quadrupole resonances can be considered collective.

In the case of the reaction $^{59}Co \rightarrow^{60} Ni$ the excitation of low multipole collective modes should be less disfavoured due to the high spin of the proton hole in ^{59}Co. Calculations on this reaction are currently in progress.

4) Conclusion

Energetic heavy ion beams together with the spectrometer SPEG offering a high energy resolution and a wide momentum acceptance, are powerful tools to study the high energy region of the transfer spectra. In order to see if collective strength can be excited in transfer reactions, we have studied several one nucleon transfer reactions on non-closed shell target nuclei. These reactions allow particle-hole excitations in a one step process and thus give direct access to the collective particle-hole strength.

In the case of a neutron stripping on ^{207}Pb, a bump has been observed at about 13.5 MeV superimposed on a large projectile break-up background. A microscopic calculation coupling the DWBA transfer cross section and the RPA response function indicates a strong excitation of high multipole modes in this energy region. In this reaction, the cross section for collective strength is small due to the dominance of high multipole modes which are mostly single particle excitations.

This result indicates that in some cases transfer reactions could be used to study high multipole response functions which are very difficult to extract in the inelastic channel due to the dominant excitation of low multipole modes.

References

1)Ph. Chomaz et al., Rap.Ann.IPN (1990)
2)S. Fortier et al.,Phys.Rev.C41(1990)2689
3)S. Galès et al.,Phys.Rep. 166(1988)126
4)A. Bonaccorso and D. Brink, Phys.Rev. C44(1991)1559
5)I. Lhenry, PhD Thesis, Universite d'Orsay (to be published in 1992)
6)I. Lhenry et al, IV Int. Conf. on Nucl. Nucl. Coll. Kanazawa (Japan), (June 1991)
7)N. Frascaria, VI Int. Conf. on Nucl. React. Mechanisms. Varenna (Italy), (June 1991)

Giant Resonances and Intermediate Energy Heavy Ions: Electromagnetic Decay Experiments

This brief summary was prepared by
J. R. Beene and F. E. Bertrand
Oak Ridge National Laboratory, Oak Ridge, Tennessee 37831*

Collaborators on various parts of the research program have been:
ORNL – **D. J. Horen, J. Lisantti, M. L. Halbert, D. C. Hensley, D. Olive, M. Thoennessen, R. L. Auble, R. O. Sayer, and Gomez del Campo**
GANIL – **W. Mittig, Y. Schutz, H. Delagrange, F.Lefèvre, R.Ostendorf, R.Merrouch**
Saclay – **J. Barrette, N. Alamanos, F. Auger, B. Fernandez, and A. Gillibert**
Strasbourg – **B.Haas and J. P. Vivien**
University of Illinois – **A. M. Nathan**
Giessen – **W. Kühn**
GSI – **R. Holzmann**

1. INTRODUCTION

The study of the wide variety of collective modes that exist in the continuum region of the nuclear spectrum continues to be one of the most interesting, and productive areas of nuclear physics. Even the isovector giant dipole resonance (GDR), the first collective mode identified in the nucleus, remains an object of intense study.

More than a decade ago, when use of heavy-ion scattering as a quantitative tool for study of giant resonances was first being contemplated, it was already realized that such reactions suffered from a number of disadvantages compared to lighter hadronic probes [1]. The characteristic dependence of light-ion scattering angular distributions on angular momentum transfer is almost model-independent, and is qualitatively reproduced by models which take into account strong absorption. For heavier probes, the increasing importance of the Coulomb potential results in angular distributions for inelastic scattering which exhibit almost no sensitivity to multipolarity.

We now know that there are some compensating advantages of heavy-ion reactions. Early work confirmed [2,3,4] the expectation that heavy ions might provide an improvement in the ratio of excitation cross section for resonances to that of the underlying nuclear continuum when compared with light-ion probes [5,6]. This fact, together with the much larger absolute excitation cross sections provided by heavy ions, made such probes especially promising for coincidence experiments [6]. It was not clear how this peak-to-continuum ratio might evolve with increasing bombarding energy, but it was obvious (if sometimes overlooked) that absolute cross sections for low multipoles, should increase rapidly above about 50 MeV/nucleon, as Coulomb excitation of giant resonances became increasingly important. Since Coulomb excitation excites isoscalar and isovector states equally well, heavy-ions also promised to be an important tool for study of isovector strength, which had been very difficult to study with light-ion scattering, because of the relative weakness of the isovector nucleon-nucleus interaction.

Our work at GANIL has taken advantage of the very large cross sections from Coulomb excitation of the giant resonances to measure the photon decay of the resonances. The strength of electromagnetic transitions generally decreases rapidly with increasing multipolarity. Low energy E1 transitions between bound states are usually strongly suppressed compared to single-particle estimates because most E1 strength is concentrated in the GDR; nevertheless, these E1's generally compete favorably with higher multipoles. For higher transition energies, near the peak of the E1 strength distribution, E1 transitions overwhelm even strongly enhanced decays by other electromagnetic multipoles. E1 transitions, especially near the peak of the GDR, are even strong enough to compete to an easily observable extent with particle emission from states in the continuum. These features make electromagnetic decay studies of continuum states practical, and, in particular cases, a highly selective tool for isolating resonance strength.

2. DECAY EXPERIMENTS WITH 84 MeV/NUCLEON ^{17}O

Experiments to investigate giant resonance excitation and decay with the (^{17}O,$^{17}O'\gamma$) reaction at 84 MeV/nucleon were carried out at GANIL, using the SPEG facility to detect and identify inelastically scattered ^{17}O ions, and arrays of multiple BaF_2 crystals to detect γ-rays. (Experimental details are given elsewhere [7]). Figure 1 shows the resulting inelastic singles spectrum on a ^{208}Pb target, compared to a corresponding spectrum taken at 22 MeV/nucleon. (The ^{36}Ar spectrum will be discussed in the next section.) The total cross section in the GR peak at a scattering angle of ~2.5° is more than 3 b/sr, of which the GDR accounts for ~2 b/sr and the ISGQR ~0.7 b/sr. But more impressive, the continuum cross section above the resonance cross section (E^*~30 MeV) amounts to only about 60 mb/sr/MeV, or only about twice that at 22 MeV/nucleon, compared to a sixty fold increase in resonance cross section.

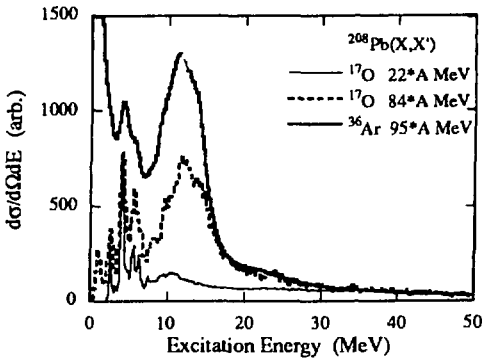

Figure 1. Comparison of the excitation of ^{208}Pb by the inelastic scattering of ^{17}O at 22 (thin solid curve) and 84 (dotted curve) MeV/nucleon, and ^{36}Ar at 95 MeV/nucleon (heavy solid curve). Spectra are normalized to match yields in the 35-40 MeV region.

The spectrum corresponding to the 84 MeV/nucleon data in Figure 1 in coincidence with single photon decays to the ground state is shown in Figure 2. Various ^{17}O-γ angular correlations demonstrated that the ground state γ-coincidence spectrum above E^*~9 MeV can be accounted for entirely in terms of decay of the GDR, within the limits of experimental accuracy. Furthermore, the excitation of the GDR can be accounted for very accurately in terms of pure Coulomb excitation. An example of one such correlation is shown in Figure 3. The solid line is a pure Coulomb excitation calculation. From these data it was determined that the integrated ground-state γ-decay branching ratio of the ^{208}Pb GDR is a rather large 0.019±0.002. It turns out that this value and, in fact, the energy dependence of the ground-state coincidence spectrum are well accounted for by parameter-free calculations, based on pure Coulomb excitation, the GDR strength distribution from photonuclear data, and the ideas of the multistep compound emission (MSCE) model [7-9]. The usefulness of the MSCE approach was further explored in reference [10] with a comparison of the GDR decay in ^{208}Pb to that in ^{209}Bi.

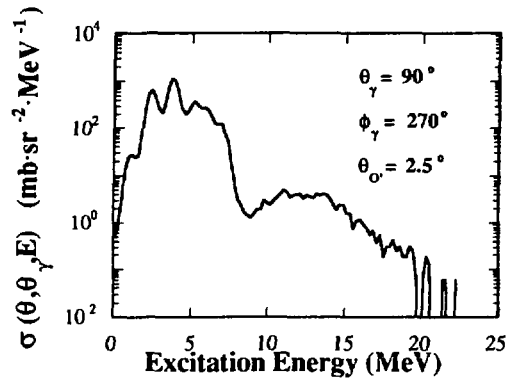

Figure 2. The ground state γ-decay coincidence spectrum corresponding to the 84 MeV/nucleon singles spectrum in Figure 1.

A wide variety of other results were obtained from the analysis of these data, ranging from an experimental verification of the isoscalar character of the 10.6 MeV GQR in ^{208}Pb, to information on the IVGQR strength distribution. These results have been discussed in detail elsewhere [7,10,11].

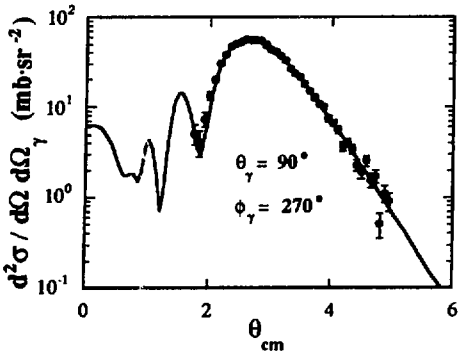

Figure 3. $^{17}O'$-γ_0 angular correlation for fixed γ detection angle, and an excitation energy rage from 9 to 12 MeV. The solid curve is a pure E1 Coulomb excitation calculation.

3. EXPERIMENTS WITH AR AND KR BEAMS

Cross sections for Coulomb excitation of giant resonances increase rapidly with both the velocity and nuclear charge of the projectile (we will, for simplicity consider only target excitation). At high enough energies, the excitation probabilities, particularly for the GDR, become large enough that multiple excitation of the giant modes might be expected.

A singles spectrum for 95 MeV/nucleon ^{36}Ar scattering is included along with the ^{17}O scattering results in Figure 1. A further dramatic increase in peak to continuum is seen. The total cross section in the GR bump is almost 15 b/sr while the continuum cross section is only about 120 mb/MeV at 30 MeV of excitation.

Figure 4 shows the total (angle integrated) cross section as a function of bombarding energy for Coulomb excitation of a selection of one-, two-, and three-phonon states in ^{208}Pb with ^{86}Kr beams. All the multiple excitations shown involve the GDR, but the mixed two phonon $2^+ \otimes$ GDR state is included along with multiple GDR excitations. The $3^- \otimes$ GDR state involving the low lying (2.61 MeV) octupole state has a similar energy dependence, with a slightly smaller cross section. It is clear that, provided sensitive and definitive enough detection and identification methods are available, the mixed two-phonon states and even the two-phonon GDR $\otimes$ GDR state, might be profitably studied with relatively low-energy beams, where high-resolution spectroscopic studies can be performed using the magnetic spectrometers available at facilities like GANIL. Data on the excitation strength, width, and decay properties of such states are of great interest, as they carry potentially new information about resonance damping, anharmonicities, and phonon-phonon interactions.

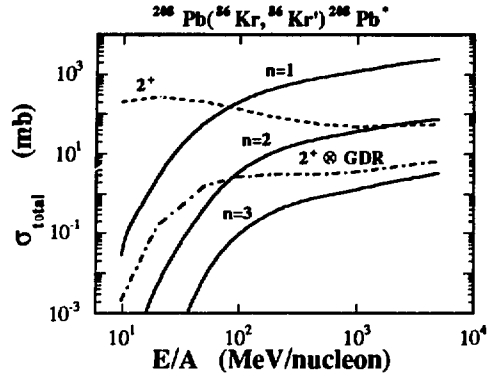

Figure 4. Total cross section for Coulomb excitation of some one-, two-, and three-phonon states in ^{208}Pb by ^{86}Kr scattering. The excitations involving only the GDR (solid lines) are labeled by the phonon number, n.

Our intermediate-energy experiments on two-phonon states rely on two tools for identification of the states. One is the expected Z of the projectile dependence of the excitation cross section. Two-phonon excitation cross sections at a given projectile velocity scale as Z^4, while one-phonon excitations scale as Z^2 [12]. Consequently we acquired data with the highest energy ^{36}Ar and ^{86}Kr beams available at GANIL (95 and ~60 MeV/nucleon, respectively). Our existing ^{17}O data provides a third Z point. To illustrate this point, the calculated peak differential cross sections for these three projectile combinations for excitation of the GDR $\otimes$ GDR state are ~1 mb/sr (^{17}O), ~50 mb/sr (^{36}Ar) and 60 mb/sr (^{86}Kr) and ~1 mb/sr, ~30 mb/sr and 160 mb/sr, respectively, for the $2^+ \otimes$ GDR. The other identification tool is the electromagnetic de-excitation of the GDR phonon, which has already been discussed extensively in the preceding sections.

Figure 5 illustrates schematically how we use the electromagnetic decay of the GDR phonon to isolate and identify two-phonon strength. The horizontal scale (excitation energy) is obtained from the energy of the inelastically scattered ion.

The coincident total γ-ray energy (ΣE_γ) measured in the BaF_2 arrays is plotted on the vertical axis. The locus along which all the excitation energy is accounted for by detected γ-radiation is the 45° dash-dotted line. The region expected to be occupied by events corresponding to decay of the various one- and two-phonon states involving the GDR are indicated on the figure along with numbers which are relative yields in our experimental geometry (including γ-detection efficiency) for ^{208}Pb (^{86}Kr,$^{86}Kr'$) at 60 MeV/nucleon, normalized to the Kr-γγ triple coincidence yield for the decay of the n=2 GDR in Pb.

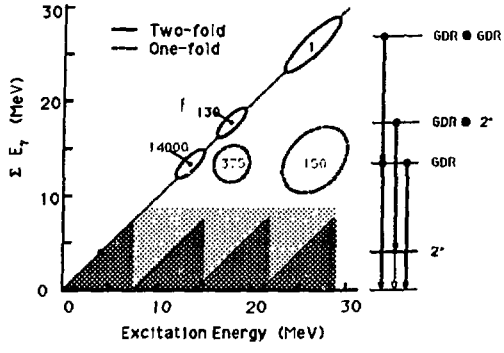

Figure 5. A schematic illustration of the experimental method employed to isolate two phonon strength in a heavy-ion scattering spectrum by γ-decay coincidence. The shaded region at the bottom of the plot represents a region of intense γ background from decays following emission of one or more neutrons.

Some very preliminary results of the analysis of these data are shown in Figure 6. The upper panel shows the one fold γ yield from $^{208}Pb(^{86}Kr,^{86}Kr'\gamma)$ in the range of Eγ from 12 to 18 MeV, as a function of excitation energy. This corresponds to a rectangular slice of Figure 5 projected onto the horizontal axis. Unfortunately the resolution in excitation energy is poor resulting from a combination of difficulties in the determination of $^{86}Kr'$ momentum and from target inhomogeneities, and as a result the mixed two-phonon states (2^+ x GDR expected at about 17.5 MeV and the 3^- x GDR at ~15.6 MeV) are not resolved from the GDR. However, a distinct structure centered at an excitation energy of 25 MeV is observed. Its properties are more clearly seen in the lower part of Figure 6 from which γ decays consistent with direct decays to the ground state (i.e., all excitation accounted for by Eγ) have been removed. We interpret the structure at ~2.4 MeV as resulting from the two phonon GDR ⊗ GDR state – as would be expected from the qualitative picture in Figure 5. The distribution of coincidence yield in Figure 6 is not a direct representation of the GDR ⊗ GDR strength distribution, but is related to it in a direct and straightforward way by the dynamics of the Coulomb excitation process. From a preliminary analysis of the data in Figure 6 we infer a GDR ⊗ GDR strength distribution centered at 26 MeV with a width of about 6 MeV.

Preliminary indications are that the γ-decay yield from the two-phonon GDR is somewhat higher than our simplest predictions. This would indicate that either the excitation cross section is larger than expected, or the γ-decay branch from the two-phonon state is larger than our simplest expectations based on a harmonic vibrator picture.

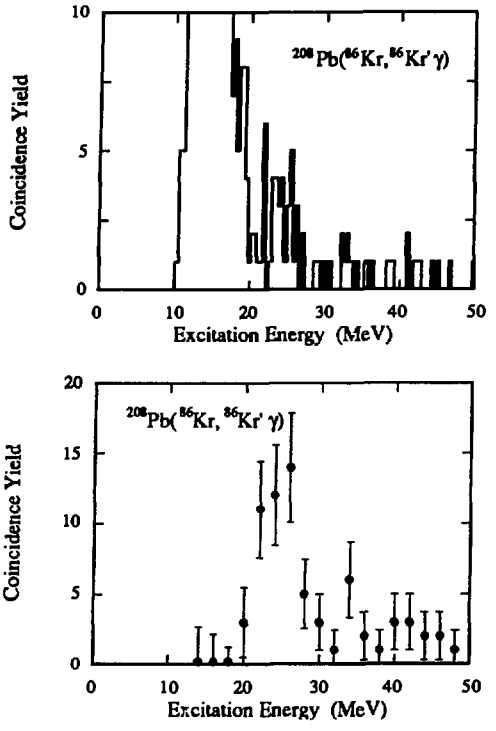

Figure 6. $^{208}Pb(^{*6}Kr,^{86}Kr'\gamma)$ coincidence spectra. See text for discussion.

4. SUMMARY

For heavy-ion bombarding energies above about 50 MeV/nucleon the excitation of low-multipolarity giant resonances proceeds mostly by Coulomb excitation. This leads to very large differential cross sections near the grazing angle, and to very large peak-to-continuum ratios. The available data are consistent with a steady and continuing improvement in this ratio both with increasing projectile velocity and Z. This observation has important implications for searches for exotic high-lying strength and for study of low-probability decay modes. We have demonstrated the importance of E1 dominance in the electromagnetic decay of giant resonance and have used this technique to observe a number of giant resonance phenomena such as the IVGQR and the two-phonon GDR.

Managed by Martin Marietta Energy Systems, Inc. under contract DE-AC05-84OR21400 with the U.S. Department of Energy.

5. REFERENCES

[1] C. K. Gelbke in Giant Multipole Resonances, Vol. 1 (ed. F.E. Bertrand), p. 33, Hardwood Academic Publishers, New York (1979).
[2] H. J. Gils et al., Phys. Lett. **68B** (1977) 427.
[3] K. T. Knöpfle and G. J. Wagner, "Nuclear Interactions," Lectures Notes in Physics Vol. 92, ed. B. A. Robson, Springer, New York (1979) p. 445.
[4] T.P. Sjoreen et al., Phys. Rev. C **29** (1984) 1370
[5] F.E. Bertrand, Nucl Phys. **A482** (1988) 287c.
[6] J.R. Beene et al, Phys. Rev. C **38** (1989) 1307.
[7] J.R. Beene et al., Phys. Rev. C **41** (1990) 920.
[8] H. Feshbach et al., Ann. Phys. (N.Y.) **125** (1980) 429.
[9] M. Hussein et al., Phys. Rev. Lett. **43** (1979) 1645.
[10] J.R. Beene et al., Phys. Rev. C **41** (1990) 1332.
[11] J.R. Beene and F.E. Bertrand, Understanding the Variety of Nuclear Excitations (3rd Int. Spring Seminar on Nuclear Physics, Ischia, Italy, May 21-25, 1990), ed. Aldo Covello, p. 685, World Scientific, Singapore (1991); F.E. Bertrand and J.R. Beene, Nucl. Phys. **A520** (1990) 627c.
[12] A. Bertulani and G. Baur, Phys. Rept. **163** (1988) 299, and references therein.

A2 - EXOTIC NUCLEI and DECAY MODES

REACTION STUDIES OF THE NEUTRON HALO

R. Anne[1], S.E.Arnell[2], R. Bimbot[3], S. Dogny[3], H. Emling[4], D. Guillemaud-Mueller[3], P.G. Hansen[5], P. Hornshøj[5], F. Humbert[6], L. Johannsen[5], B. Jonson[2], M. Keim[7], A. Latimier[3], M. Lewitowicz[1], S. Mattsson[2], A.C. Mueller[3], P. Møller[5], R. Neugart[7], T. Nilsson[2], G. Nyman[2], F. Pougheon[3], A. Richard[3], A. Richter[6], K.Riisager[5], M.G. Saint-Laurent[1], G. Schrieder[6], O. Sorlin[3], O.Tengblad[8],K. Wilhelmsen[2], D. Wolski[9]

[1]GANIL, BP 5027, F-14021 CAEN cedex, France
[2]Fysiska Institutionen, Chalmers Tekniska Högskola, S-41296 GÖTEBORG, Sweden
[3]Institut de Physique Nucléaire, F-91406 ORSAY cedex, France
[4]Gesellchaft für Schwerionenforschung, Postfach 11 05 52, D-6100 DARMSTADT, FRG
[5]Det fysiske Institut, Aarhus Universitet, DK-8000 AARHUS C, Denmark
[6]Institut für Kernphysik, TH Darmstadt, Schlossgartenstrasse 9, D-6100 DARMSTADT, FRG
[7]Institut für Physik, Universität Mainz, Staudingerweg 7, D-6500 MAINZ, FRG
[8]CERN, CH-1211 GENEVE 23, Switzerland
[9]D. Wolski, Soltan Institut for Nuclear Studies, PL-05400 SWIERK-OTWOCK

Neutron halos appear in nuclei close to the neutron drip line. What happens is that the low separation energy of the last neutron (or neutrons) allows them to move away from the attractive nuclear potential and into free space by quantum-mechanical tunneling, thus leading to a considerably extended surface region. The neutron halo was discovered through reaction experiments with very unstable nuclei, and this type of experiments still provides the best method to study it.

The neutron halo gives rise to an increased nuclear matter radius (quite different from the charge radius), this was used as the first signal of its existence. Later experiments, including the present work, have looked at the reaction channels that are most sensitive to the appearence of the halo, namely the one or two neutron removal channels. The cross section for these processes is much larger than usual, especially for high-Z targets: the physical separation of the neutron(s) from the nuclear core leads to the appearance of strong electric dipole excitations at very low energy which in turn gives a large cross section for neutron removal via Coulomb dissociation. We have measured the cross section for the process for several light drip-line nuclei and have at the same time looked at the angular distribution of the emerging neutrons. The large spatial extension of the halo neutrons should correspond to a narrow momentum distribution, that can be expected to be reflected in the angular distribution of the fragments. This was earlier shown to be the case for the charged core; we have confirmed this by looking directly at the neutrons.

Both one- and two-neutron halos have been studied here. The latter ones are the most intriguing as the n-n interaction in the halo must play an important role for their structure. We have therefore measured several of these nuclei with different two-neutron separation energy - ^{11}Li, ^{14}Be and ^{8}He - in order to see how the halo-specific features emerge. By far the largest effects are found for ^{11}Li with a 2n separation energy as low as 250 keV. As an example of a one-neutron halo we have taken ^{11}Be with a 1n separation energy of 506 keV.

An ^{18}O primary beam of 55-65 MeV/u bombarded a Be production target; the secondary beams were separated by means of the doubly-achromatic spectrometer LISE and focussed on a secondary target in the middle of a silicon counter telescope. The experiment with ^{11}Be was made with LISE3. The velocity filter allowed to obtain an isotopic purity of the secondary ^{11}Be beam of 99.99%. Both the incoming beams and the outgoing charged fragments were identified on an event-by-event basis, the total intensity of the secondary beams being kept at about 1000/s. The secondary targets used were rather thick in order to obtain a reaction probability of about 1%. In this way, the major reaction channels could even be studied in some detail.

Table 1: Cross sections and widths of neutron distributions.

Beam	Observed fragment	Cross-section (barn) Be	Ni	Au	$\theta_{1/2}$ (deg.)[a] Be	Ni	Au
^{8}He	^{6}He+n[b]	0.41±.15	$1.5^{+1.0}_{-0.5}$	$2.9^{+5.0}_{-2.5}$	6.2±1.2	7.1±2.0	7±5
^{11}Li	^{9}Li + n[b]	0.65±.12	2.1±0.4	10.8±1.9	3.2±0.2	2.9±0.3	3.4±0.2
	^{9}Li	0.47±.10	1.3±0.4	5.0±0.8			
^{14}Be	^{12}Be + n[b]	0.37±.08	$0.60^{+0.30}_{-0.21}$	$1.3^{+1.3}_{-0.6}$	4.8±0.5	6.4±1.8	6.6±2.3
	^{12}Be	0.44±.10	1.0±0.3	2.1±0.6			
^{9}Li	n					8.5±0.9	

[a]*Observed opening angle corresponding to half intensity*
[b]Calculated as an integral over the neutron distribution

For interpretation it is important to clarify to what extent the results reflect the reaction mechanism and to what extent they carry the desired information about the groundstate wave function of the halo nucleus, we shall discuss this using ^{11}Li as example. There is strong direct and indirect evidence that the stripping reactions of ^{11}Li proceed entirely through three mechanisms. We have mentioned above the Coulomb dissociation. In addition to this, two inseparable *nuclear* contributions exist: absorption and diffraction dissociation which dominate for light targets. A simple model which takes these three mechanisms into account is able to reproduce the caracteristic features of the observed cross-sections.

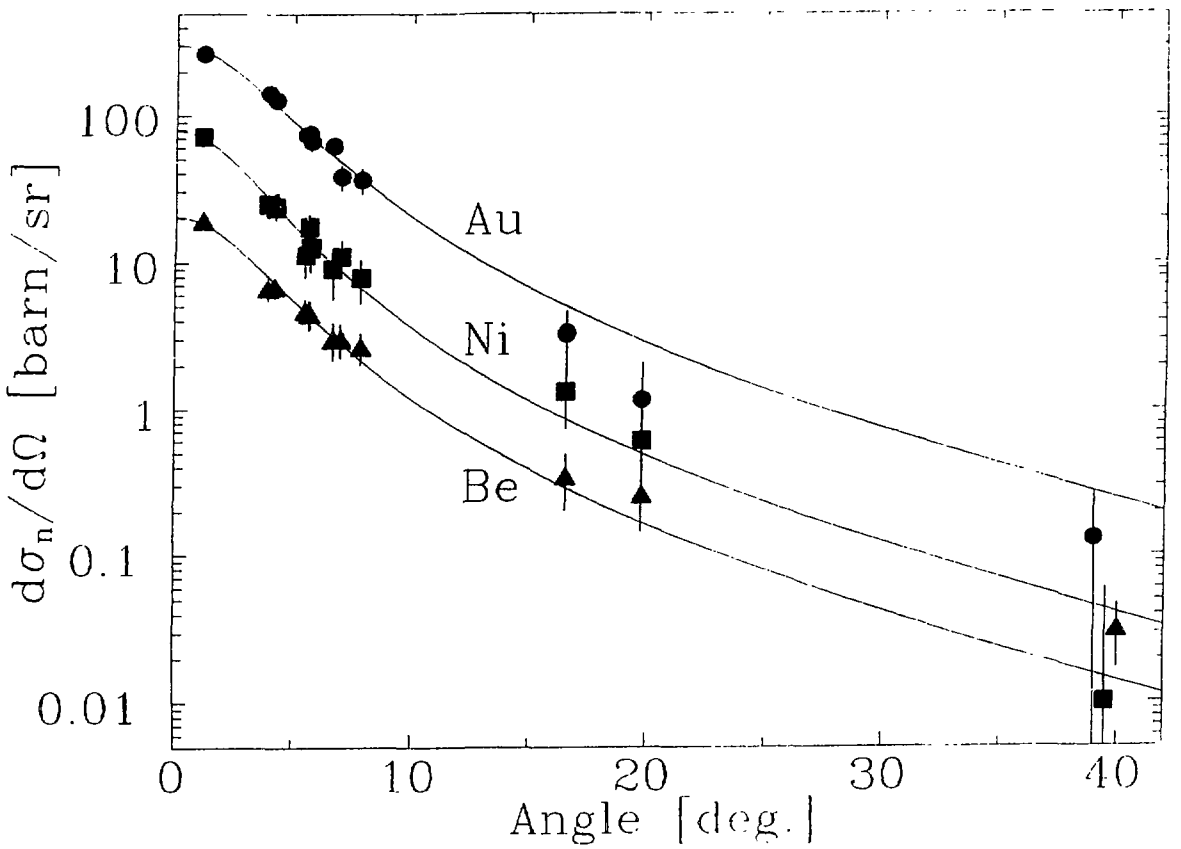

Figure 2: Single neutron angular distributions for (^{11}Li,^{9}Li) reactions on Be, Ni and Au. The differential cross-section is shown versus the angle of the emerging neutron relative to the incoming beam as measured in the laboratory frame. The two points above 15° are averages over three and four detectors, respectively. The curves are fits with a Lorentzian distribution.

Neutrons produced in the reactions were detected in an array of liquid-scintillation counters placed 3 m from the target, see figure 1. Our main interest was to study the "gentle" break-ups which yield fragments emerging with the beam velocity. The analysis of the ^{11}Be data is still going on, the results for the other isotopes are presented in the following.

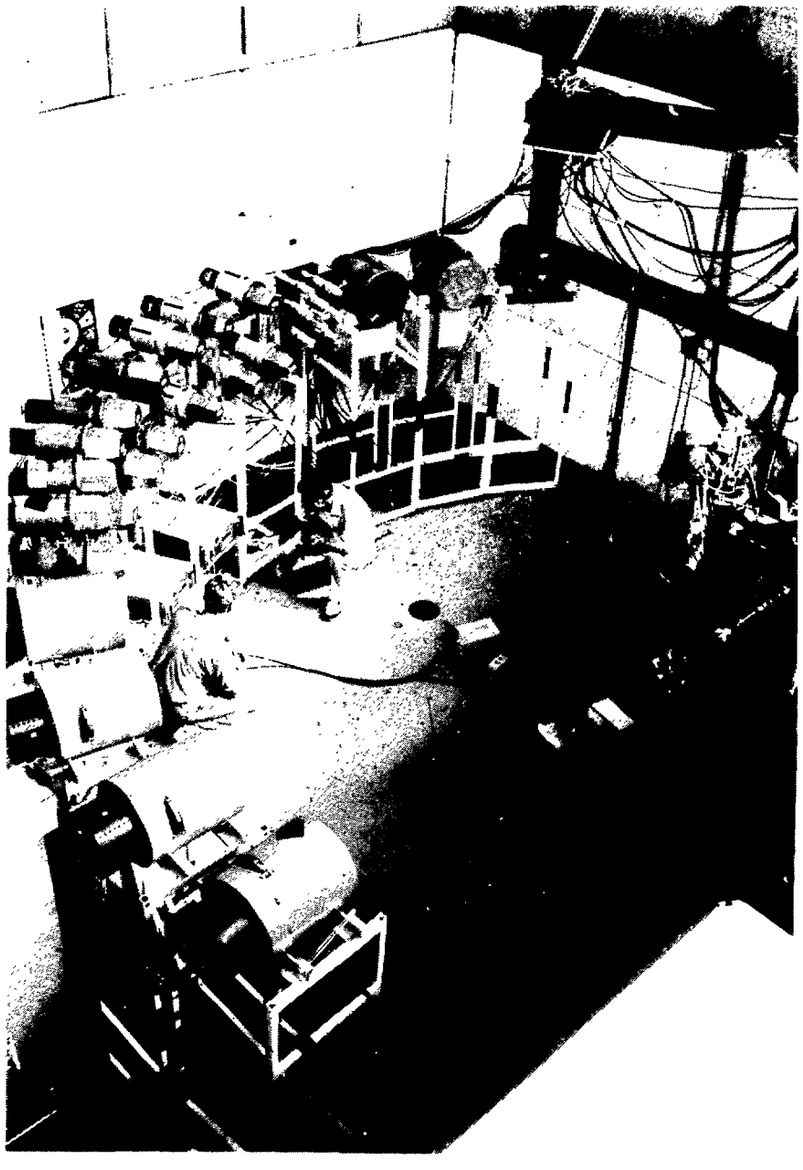

Figure 1: Photograph of the neutron detection array at the end of the LISE spectrometer

The cross sections for the 2n removal channels could be determined both by detecting the charged fragment, in the silicon telescope, and by detecting the neutrons. The cross sections obtained in this way are given in the table, note that the ratio of the cross sections determined in the two different ways gives the average number of neutrons from the break up.

The most striking feature of the experiment is that the neutron angular distributions for ^{11}Li are very narrow (see table 1 and fig.2) and also remarkable similar for different targets. The deduced spread of transverse momentum is an order of magnitude lower than the typical Fermi momentum of normally bound nucleons. Since the reaction mechanisms seem not to affect significantly the momentum distributions it is tempting to conclude that they correspond to the one in the halo. The number of observed nn coincidences is still small at present time, their angular dependance suggests however that there is no strong correlation between the neutrons.

The effects seen for ^{11}Li are also present in ^{14}Be and ^{8}He but less pronounced as expected from the 2n separation energies. One of the challenges of future radioactive beam experiments will be the study of the neutron halo for heavier drip-line nuclei where cases with extremely low 2n separation energies might be found.

The results of the experiments have been published in the following journals:

(1) R. Anne et al., Phys. Lett. **B250** (1990) 19
(2) K. Riisager et al. Nucl. Phys. A (1992) in press

The results were reported as invited talks in the following conferences:

(3) A. C. Mueller, RIKEN-IN2P3 Symposium, Obernai (France), April 9-12 1990
(4) M. Lewitowicz et al., Nuclear Shapes and Nuclear Structure at low excitation Energies, Cargèse (France), June 3-7 1991
(5) A. C. Mueller, Fourth International Conference on Nucleus Nucleus Collisions, Kanazawa (Japan), June 10-14 1991
(6) K. Riisager et al., International Symposium on Properties of Unstable Nuclei, Niigata (Japan), June 17-19 1991
(7) P. G. Hansen, Gordon Conference, New London, NH (USA), June 24-28 1991
(8) A. C. Mueller, Gordon Conference, New London, NH (USA), June 24-28 1991
(9) R. Anne et al., Second International Conference on Radioactive Beams, Louvain la Neuve (Belgique), August 19-21 1991

ELASTIC SCATTERING OF 29MeV/n ^{11}Li IONS ON A ^{28}Si TARGET

M.Lewitowicz[1], C.Borcea[1], R.Anne[1], A.G.Artukh[2], R.Bimbot[3], V.Borrel[3], F.Carstoiu[4], Z.Dlouhy[5], S.Dogny[3], D.Guillemaud-Mueller[3], A.Kordyasz[6], S.Lukyanov[2], A.C.Mueller[3], Yu.Penionzhkevich[2], F.Pougheon[3], P.Roussel-Chomaz[1], M.G.Saint-Laurent[1], N.Skobelev[2], J.Svanda[5], K.Terenetsky[7], S.Tretyakova[2], V.Verbisky[7]

[1] *GANIL,BP 5027,F-14021 Caen,France,*
[2] *LNR,JINR,PO Box 79,Dubna,Russia*
[3] *IPN,F-91406 Orsay,France*
[4] *Cent. Ins. of Phys., P.O.Box MG6,Bucharest,Romania*
[5] *Nucl. Phys. Inst., CS-25068 Rez,Czechoslovakia*
[6] *IFD UW,Hoza 69,PL-00_681 Warsaw,Poland*
[7] *Inst. for Nucl. Res., Prosp. Nauki 47, Kiev,Ukraine*

1. INTRODUCTION

In a recent experiment at GANIL[1)], the original ^{11}Li interaction cross-section data obtained by Tanihata et al. at Berkeley[2)] have been complemented by a measurement of the Coulomb dissociation cross section and the neutron angular distribution at lower energy (30 MeV/n). This new data have provided further support for the neutron halo hypothesis. Nevertheless, although they give information about the extent of the neutron cloud and the degree of correlation between the two extra-core neutrons, these experiments are unable to provide detailed information about the proton and neutron distributions in ^{11}Li. Such information can, however, be obtained from measurements of the elastic-scattering angular distributions. In this way, it should be possible to test various theoretical descriptions of ^{11}Li. The aim of the present experiment was to advance the idea of a "nondestructive" study of ^{11}Li, by measuring its elastic scattering from a ^{28}Si target.

2. EXPERIMENT

The secondary beams of 29MeV/n ^{11}Li (150pps) and 25.4MeV/n ^{7}Li (1000pps) were produced in a reaction of a 76MeV/n ^{18}O primary beam bombarding a 360mg/cm^2 Be+2900mg/cm^2 C production target. The outgoing fragments were separated by means of the LISE3 spectrometer[3)] and identified by their energy loss and time of flight. The purity of the secondary beams was better than 98%. An energy width of the secondary beam was defined by a momentum acceptance of the LISE spectrometer and was set to 2.3% in the case of ^{7}Li and to 9.4% in the case of ^{11}Li.

A low intensity (100-1000pps) and a big angular and energy spread of the secondary beams imply an application of a detection system in which a high efficiency of registration of diffused particles is complemented by measurement of angle and position on a target for each particle. A schematic view of the set-up used in the present experiment is shown in figure 1. A trajectory of each incident particle was reconstructed by means of two position-sensitive X-Y silicon detectors, 71mg/cm^2 and 104mg/cm^2 thick respectively, placed at the final focal point of the spectrometer. The second detector was simultaneously used as a secondary target. Angles and energies of diffused ions were measured with help of two circular silicon strip detectors. The angle between the trajectory of incident and diffused particle in a plane parallel to the beam axis was measured by the first detector with 16 circular strips. The second detector with 8 radial strips allowed for a rough determination of the angle in a plane perpendicular to the main axis of the beam. A distance between the secondary target and the strip detectors was adjusted to cover the center-of-mass diffusion angles between 5° and 17° for ^{7}Li and between 5° and 22° for ^{11}Li.

A matrix of seven BGO cristals[4)] was used to determine a residual energy of each particle. The overall energy spread of diffused particles including energy width of secondary

beam, internal resolution of the detectors and energy straggling was a 7% for ^{7}Li and a 20% for ^{11}Li ions.

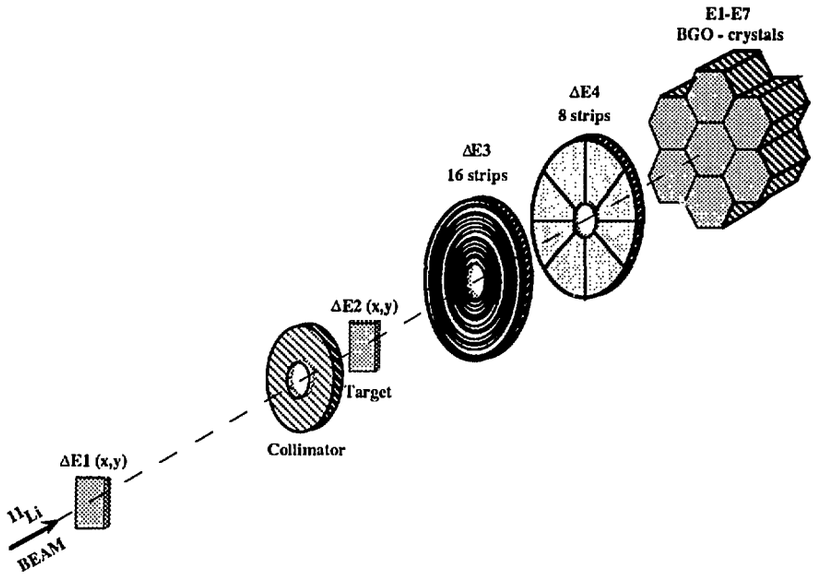

Figure 1. Experimental set-up

3. RESULTS

Angular distributions of elastic scattering of ^{7}Li and ^{11}Li measured in this experiment are shown in a figure 2. A use of the thick target, an angular resolution of about 1.5° and a lack of separation between elastic and inelastic scattering result in a flattering of diffractional structure of the spectra.

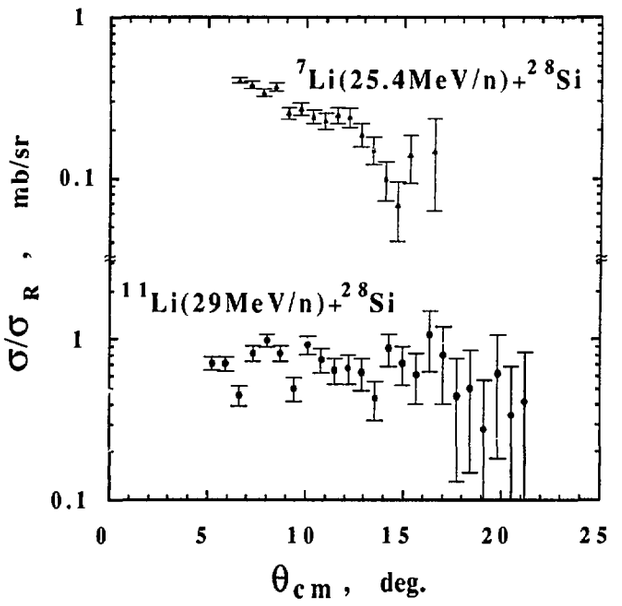

Figure 2. Angular distributions of elastic scattering of ^{7}Li and ^{11}Li on a ^{28}Si target.

The obtained σ/σ_R distribution of ^{7}Li is in agreement with previous measurements performed for similar systems[5-7]. At the same time the distribution of σ/σ_R for ^{11}Li lies higher and decrease slower with angle than the analogical distribution measured at the same energy for the ^{6}Li[5].It seems that these differences in the angular distributions can be hardly explained by a mass difference between the two nuclei.

Another observation comes from the analysis of energy spectrum of diffused ^{11}Li ions. If the scattering of ^{11}Li is at low impact parameters (e.g. at high diffusion angles) accompanied by a break-up of this nucleus ^{11}Li->^{9}Li+2n one should observed in the energy spectrum ,shown in figure 3, a peak corresponding to the 29MeV/n ^{9}Li ions. A careful mathematical analysis set an upper limit of the contribution of ^{9}Li nuclei to about 5%.

A full interpretation of the data in a framework of optical model with a double folding potential is currently in progress.

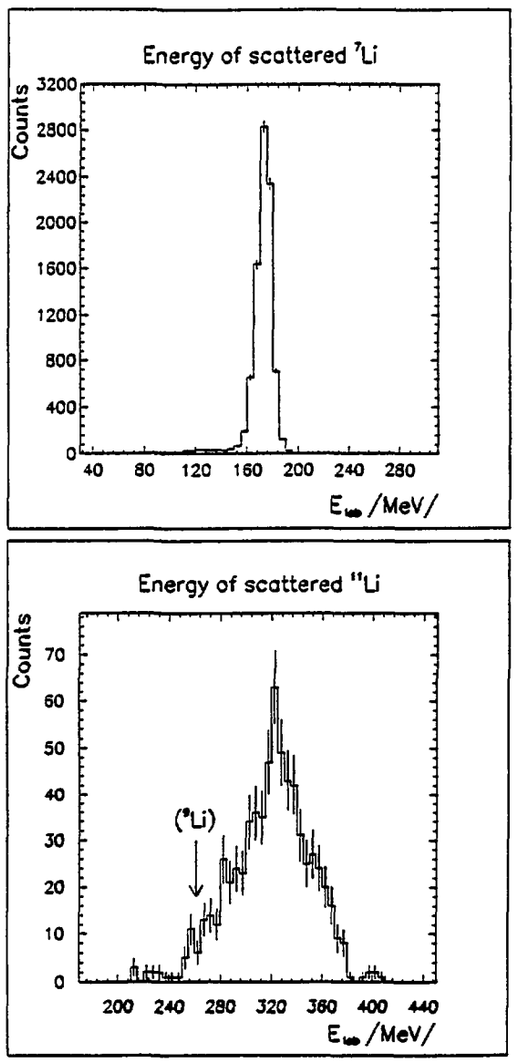

Figure 3. Energy distributions of elastcally diffused ions of 25.4MeV/n ^{7}Li ions (upper part) and of 29MeV/n ^{11}Li ions (lower part) on a .^{28}Si target

4. CONCLUSIONS

The results of present experiment proofed that a measurement of elastic scattering of very exotic nuclei although technically difficult can be performed even at a very low (several hundred particles per second) intensity of a secondary beam. For a complete explanation of the obtained angular and energy distributions of diffused ^{11}Li ions particular properties of the ^{11}Li nucleus due to a presence of a neutron halo should be taken into account.

Similar experiments performed with a higher energy and angular resolution are possible and necessary to confirm and to study the phenomena of neutron halo for other light neutron-rich nuclei as ^{11}Be, ^{14}Be and ^{17}B.

REFERENCES

1) R.Anne et al., Phys. Lett. B250(1990)19 and K.Riisager et al. Nucl. Phys in press

2) I.Tanihata et al., Phys. Lett. 160B(1985)380

3) R.Anne and A.C.Mueller, Inter. Conf. EMIS-2, Sept. 2-6, 1991, Sendai, Japan, NIM in press and references contained therein

4) Z.Dlouhy et al., submitted to NIM

5) A.Nadasen et al., Phys. Rev. C39(1989)536 and references contained therein

6) Y.Sakuragi, Phys. Rev. C35(1987)2161

7) K.Katori et al., Nucl. Phys. A480(1988)323

MASS MEASUREMENTS WITH THE GANIL CYCLOTRONS

G.Auger[1], M.Bajard[1], E.Baron[1], D.Bibet[1], P.Bricault[1], A.Chabert[1], J.Ferme[1], K.Fifield[1], L.Gaudart[1], A.Gillibert[2], A.Joubert[1], M.Lewitowicz[1], W.Mittig[1], N.Orr[1], E.Plagnol[1], C.Ricaud[1], Y.Schutz[1] and A.C.C.Villari[3].

[1]GANIL, BP5027, 14021 Caen Cedex, France
[2]D.Ph.N, CEN Saclay, 91191 Gif sur Yvette Cedex, France
[3]IFUSP, Sao Paulo, Brasil

1. INTRODUCTION

The GANIL facility has now an established tradition in the domain of the study of exotic nuclei. Two beam lines are devoted to this physics : LISE [1] and SPEG [2]. Both have been able to identify and study numerous new nuclei. When the existence of exotic nuclei have been established, the first step of their study is to measure their mass. Different methods can be used, one of the simplest being a measurement of their time of flight along a given flight path. The length of the flight paths used is 40 meters in Lise (upgraded from 17m in the previous LISE setting) and 82 meters for SPEG. With the usual time resolutions that can be obtained, typically a few hundred picoseconds, the resolution in mass obtained is given by the formula :

$$\frac{\Delta M}{M} = 2.\left[\frac{\Delta T}{T} + \frac{\Delta L}{L}\right] + \frac{\Delta E}{E} \qquad (1)$$

where M is the mass to be measured, T the time of flight over a path of length L and E the kinetic energy) With the different factors involved, the precision which can be reached is of the order of 10^{-4}.

In order to reach a higher level of resolution a new method has been suggested by W.Mittig and tested recently.

2. THE GENERAL METHOD OF MASS MEASUREMENTS WITH THE GANIL CYCLOTRONS

The basic idea is to make use of the specific features of the GANIL Cyclotrons to extend the time of flight. The GANIL facility is made up of three successive cyclotrons : C0, CSS1 and CSS2, see figure 2. C0 is essentially linked to the ECR source and is used as an injector into CSS1. This cyclotron accelerates the injected beam up to energies ranging from ≈5 A.MeV for heavy ions to ≈13 A.MeV for light ions. These energies are already above the Coulomb barriers for a large variety of targets : nuclear reactions can therefore be used at this stage to produce exotic nuclei. After production, these nuclei can be injected into CSS2 for further acceleration. The time of passage in the cyclotron is obtained using the time difference between a "start" detector placed in front of the injection and a stop detector placed at the exit of the cyclotron. The same detector, a ΔE-E silicon detector, is also used to identify in charge and in energy the outgoing nuclei.

Because of the strong selectivity of the CSS2 a measure of the field B of this cyclotron will give a measure of the mass of the nuclei.The basic equation of a cyclotron is :

$$\frac{B}{\omega} = \frac{M}{q} \qquad (2)$$

where ω is the rotation frequency and q the ionic charge of the nuclei accelerated.

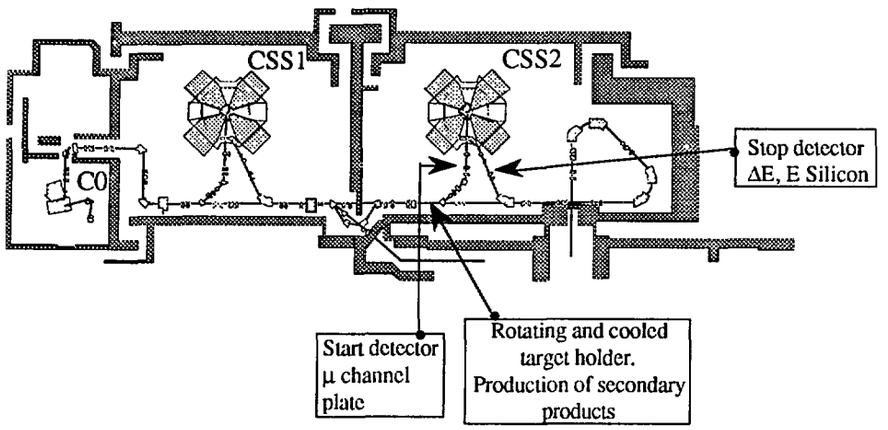

Figure 2. Schematic diagram of the GANIL cyclotrons and the different apparatus necessary for the mass measurement method.

In practice this method is not used for absolute measurements but the masses can be deduced from the comparison of the difference of phase (≈time of flight) between a known nucleus and the nucleus studied for a given setting of the CSS2 field or, because the acceptance in "mass" at a given field setting is of the order of $\approx 10^{-4}$, from the differences in both phase and field if different settings of the CSS2 are necessary.

3. PRACTICAL ASPECTS

There are two main problems that have to be solved before this method can be applied. The first is related to the conditions that have to be met for a given nuclei to be injected into CSS2, the second has to do with the tunning of the field of CSS2.

Indeed, the CSS1 and CSS2 cyclotron must be operated at the same radio frequency (RF). For a given frequency only different harmonics, let us call them H_1 and H_2 where both are integer numbers, can be used for either cyclotron. If R_1 and R_2 are the ejection radius of CSS1 and the injection radius of CSS2 and V_1 and V_2 the velocity at ejection from CSS1 and at injection into CSS2, these parameters must satisfy the following relationship :

$$\frac{H_1 \cdot V_1}{R_1} = \frac{H_2 \cdot V_2}{R_2} \qquad (3)$$

Typically for normal use of the accelerator, $H_1=5$, the ratio $R2/R1=2/5$ and $V_1=V_2$, requires that $H_2=2$. However the production of secondary nuclei by nuclear reactions, between CSS1 and CSS2, will invariably be associated with a loss in velocity and hence we must consider solution to eq.3 for which $V_2<V_1$. The most favorable case is $H_2=3$, for which :

$$V_2 = \frac{2}{3} V_1 \qquad (4)$$

Other combinations are of course possible as long as H_1 and H_2 are integer numbers.

The second problem is to set the isochronous magnetic field of CSS2. Even with prior knowledge of the mass and charge of the injected fragment, it is not possible to pre-tune the proper field for the injection,ejection in CSS2. It is therefore necessary in most cases to use a similar beam to tune CSS2 . By similar beam we mean one that has the same q/m and velocity. If this beam can be obtained with a measurable intensity (≈10nA), the tunning is straightforward because the different diagnostics, inside CSS2, are built to respond to these intensities. If however, this minimum intensity cannot be obtained, the

tunning will have to be done using different diagnostic tools. These diagnostics is made using ΔE-ESilicon detectors. These detectors are implemented inside the CSS2 vaccum chamber under the very difficult conditions found inside the cyclotron, high magnetic field and RF power.

4. RECENT TESTS

A first test run was performed in July 1990, in order to test the viability of this method and to obtain the precision of the measurement.

A beam of 40Ar (9^+) is ejected out of CSS1 with an energy of 13.3 A.MeV (Frequency HF=13.2 MHz ; Harmonic = 5), and its velocity is then degraded by a carbon target, see fig 2. The exact $V_2 = 2V_1/3$ velocity is obtained using the "α" spectrometer. Fine tuning of the velocity was obtained using the angle of the degrader with respect to the beam direction.

Once this is done, the beam (≈20 enA, $q = 16^+$; $q/m=2.5$) is sent to CSS2 and ejected after proper setting of the field.

Following this, a very thick production target is inserted in place of the degrader. The thickness is such that it will stop the ^{40}Ar beam but allow the secondary products to pass through. After some adjustement in the setting, nuclei of $^{25}Na(10^+)$ and $^{20}Ne(8^+)$ are observed. Figure 3a. shows these nuclei : the horizontal axis represents the difference in phase (time) between the "Stop" detector and the RF signal and the vertical axis the energy response of the ΔE stop detector.

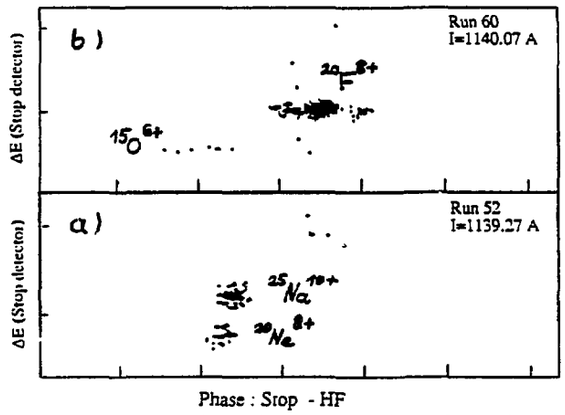

Figure 3. 2 dimensionnal representation of the signal detected in the ΔE (Stop) detector versus the difference between Stop timing signal and the radio frequency (HF) signal. The different nuclei identified are shown on the figure.

The difference in phase can therefore be related to the difference in q/m of these two nuclei and their relative masses can be deduced. A straightforward calculation yields, assuming the mass of ^{25}Na to be known :

Mass excess of : ^{20}Ne = -7.026±0.060MeV

which has to be compared to the known value of : -7.043±0.001 MeV. The precision of the method can therefore be estimated to be :

$$\Delta M/M \approx .06/18600 \approx 3.2 \times 10^{-6}$$

The uncertainty in this measurement is essentially related to the statistical uncertainty in measuring the centroids of the peaks. A significant increase in the statistics would be followed by a subsequent improvement in the precision obtained.

Figure 3b. shows, at a different field setting, the observation of $^{20}F(8^+)$. In order to obtain the mass from this measurement one has to take into account not only the change in phase but also the change in field, here measured by the intensity set in the main coils. This has been done by a prior calibration of ΔB/B versus ΔI/I.

Mass excess of ^{20}F = 0.113±0.200 MeV

to be compared with the known value of -0.015±0.0001 MeV. The resolution in this case is therefore only of $\approx 10^{-5}$. The explanation for this is essentially the limited accuracy of the relation between B and I. This is easily remedied by a proper magnetic field measurement.

5. FUTURE PROSPECTS FOR THIS METHOD.

Inspection of the mass tables of A.H.Wapstra et al. [3] show that the precision with which masses are measured range from 10^{-5} to 10^{-9}. A large fraction of exotic nuclei, those that are at the limit of the strong nuclear interaction drip line, are measured with precision in the range 10^{-5} to 10^{-7}, which is typically the one this method can reach. The range of possible application is therefore extreemely large.

Because of the high intensities that can be obtained by the C0 + CSS1 accelerator system and which will be further increased with the future O.A.I transformation, production of nuclei with very low cross sections can be considered. Three interesting range of nuclei will be considered in the near future : a precise measurement of mass of ^{11}Li is extremaly important in all theoretical considerations of a neutron halo, an attempt will be made to reach ^{100}Sn whose doubly magic nature is of great importance in nuclear physics. The region of very heavy nuclei, Z≥100 produced for example by G.Munzenberg et al. [4] at GSI with reactions of the type ^{54}Cr + ^{208}Pb at ≈5 A.MeV which is typically the range of reactions which one can access by this method is also of great interest.

6. CONCLUSIONS

The method suggested for mass measurements using the GANIL cyclotrons turns out to be a very powerful and precise tool. The CSS2 is a very efficient mass spectrometer whose mode of operation is well understood and can be used to push this method to its limit. After some modifications, a final precision of the order of 10^{-7} or better could be acheived. The limiting factor of this method is the rather low energies obtained with the CSS1, which could however be compensated by the increase in intensity which is programed in the near future and the use of a higher collection efficiency in reactions with inversed kinematics. With such an apparatus, the scope of possible measurements turns out to be extremely large.

REFERENCES

[1] R.Anne et al. NIM A257(1987)215
[2] A.Gillibert et al. Phys. Lett B192(1987)39
[3] A.H.Wapstra et al., Atomic Data and Nuclear Data Tables 39(1988)281.
[4] G.Munzenberg et al., Z.Phys. A328(1987)49

SYNTHESIS AND PROPERTIES OF NEUTRON-RICH NUCLEI AT GANIL WITH THE LISE SPECTROMETER

R. Anne[1], A. G. Artukh[2], D. Bazin[3], A. V. Belozyorov[2], C. Borcea[1], V. Borrel[4], P. Bricault[1], C. Détraz[5], S. Dogny[4], L.K. Fifield[1], H. Gabelmann[6], D. Guillemaud-Mueller[4], W. Hillebrandt[7], K.L. Kratz[6], M. Lewitowicz[1], S.M. Lukyanov[2], Yu. S. Lyutostansky[8], A.C. Mueller[4], Yu. E. Penionzhkevich[2], B. Pfeiffer[6], F. Pougheon[4], M.G. Saint-Laurent[1], V.S. Salamatin[2], F. Schäfer[6], W. D. Schmidt-Ott[9], H. Sohn[6], O. Sorlin[4], F.K. Thielemann[10], A. Wöhr[6], M. V. Zverev[8]

[1]GANIL, BP-5027, F-14021 Caen, France
[2]Laboratory of Nuclear Reactions, JINR, PO 79, Dubna, USSR
[3]CEN Bordeaux, Le Haut Vigneau, F-33170 Gradignan France
[4]Institut de Physique Nucléaire, F-91406 Orsay, France
[5]LPC, ISMRa, F-14032 Caen, France
[6]Institut für Kernchemie, Universität Mainz, D-6500 Mainz, Germany
[7]MPI für Astrophysik, D-8046 Garching, Germany
[8]Moscow Engineering Institute,Moscow, USSR
[9]II Physikalisches Institut, D-3400 Göttingen, Germany
[10]Harvard-Smithsonian Center for Astrophysics, Cambridge, MA, USA

1. INTRODUCTION

The synthesis and investigation of the properties of the extremely neutron-rich or proton-rich nuclei for the light elements present considerable interest both for the localization of the drip-lines and for the test of the theories describing the exotic nuclei.The possibility of producing secondary nuclear beams by means of heavy-ion projectile fragmentation has been discovered in the late 1970s by Symons, Westfall and co-workers at Berkeley [1,2]. During the 80s Tanihata et al. have pioneered the study of secondary nuclear reactions induced by these relativistic-energy beams from the BEVALAC[3]. The persistence of the characteristic features of the high-energy fragmentation in the Fermi-energy domain[4], allowed, since 1984, the development of a large experimental program at the spectrometer LISE at GANIL[5].

It is the scope of the present contribution to highlight some recent experiments at LISE on the neutron-rich side of the valley of stability.

2.IDENTIFICATION OF DRIP-LINE NUCLEI

Using the fragmentation of the primary GANIL beams for the production of exotic isotopes called for the use of a dedicated spectrometer with the following properties:

1) detection around 0° with a large collection angle, and very low background, in particular a complete elimination of the primary beam, in order to detect small cross section events;

2) good particle identification properties in order to discriminate without ambiguity the great number of produced nuclei;

3) a sufficient number of degrees of freedom in the ion optics in order to provide secondary beams of reasonable optical quality.

The LISE spectrometer made up of two identical dipoles (D1 and D2) in a double achromatic arrangement fulfills these requirements. The flight path through the instrument is to first order (correct to better than 10^{-4}) independent of the angle. This allows a very easy time-of-flight measurement. A Z-dependent selection criterion can be introduced by inserting an

energy degrader in the intermediate focal plane between D1 and D2. The achromatism of the line is then restored only for the wanted isotope by lowering the magnetic rigidity of D2 to the corresponding energy loss. The "original" spectrometer[6] LISE ended at the first achromatic point. An extension including a Wien filter has been added. This introduces another selection criterion in velocity[7]. The identification of the produced projectile-like fragment beams is readily performed by semiconductor telescopes installed at the (first) achromatic focus. The combined measurement, event-by-event, of energy loss ΔE, total energy E and time-of-flight TOF through the spectrometer allows an easy determination of Z, A.

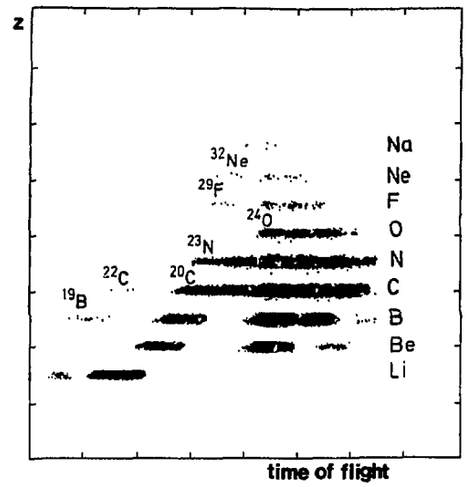

Figure 1: Neutron-rich nuclei along the drip-line from the fragmentation of a ^{48}Ca beam at 44 MeV/u on Ta.

Concerning the mapping of the neutron drip-line, all the neutron-rich isotopes of the light elements up to nitrogen (Z=7) which are predicted to be particle-stable have been synthesized. In order to look for the stability of isotopes of higher elements up to neon we have performed an experiment with a ^{48}Ca beam at 44 MeV/A aiming at the production of ^{26}O, ^{29}F, ^{32}Ne. Figure 1 shows the bi-dimensional representation of ΔE versus TOF for the fragments from the ^{48}Ca beam impinging onto a 173 mg/cm^2 Ta target. The most neutron-rich fragments observed correspond to the predicted[8] neutron drip-line isotopes ^{11}Li, ^{14}Be, ^{22}C, ^{23}N, and ^{29}F.The latter nucleus as well as ^{32}Ne were observed for the first time. No counts were observed for the isotopes ^{13}Be, ^{16,18}B, ^{21}C, ^{25}O, ^{28}F and ^{31}Ne, predicted to be particle-unstable. No counts corresponding to ^{26}O were observed. The cleanness of these particle-identification spectra underlines the quality of LISE, in particular the excellent rejection of the primary beam.

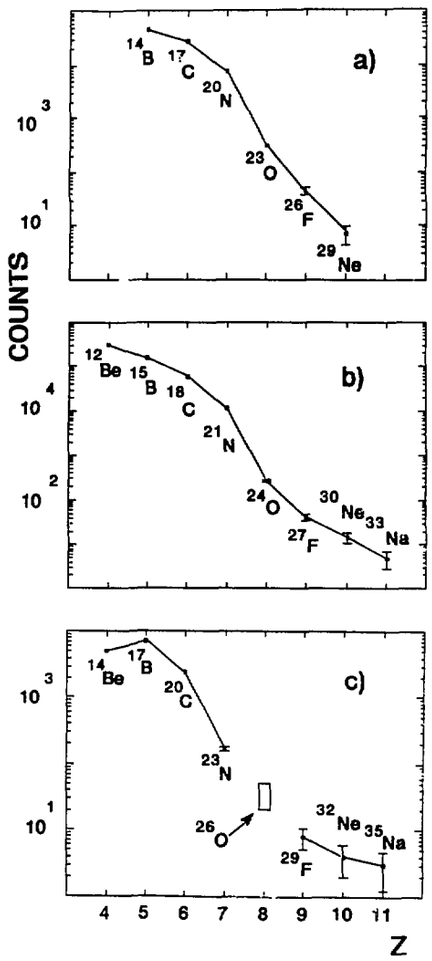

Figure 2: Isotopic production along lines with neutron numbers N+2Z-1 (a), N=2Z (b), N=2Z+2 (c). The error bars correspond to one-sigma statistical errors. From the smooth monotonous drop along these lines and the absence of any ^{26}O event, one can conclude to the particle-unbound character of this isotope (see text).

Figure 2 shows the isotopic production along lines which proceed parallel to the drip-line with neutron numbers N+2Z-1 (a), N=2Z (b), N=2Z+2 (c) (note that the N+2Z+1 line essentially consists of isotopes known to be particle unbound). A smooth monotonous drop is observed along these lines. From this trend one may expect a production rate of about 30 counts for ^{26}O. Since it is almost impossible to explain this absence by statistical fluctuations, this experiment gives strong evidence for concluding that the isotope ^{26}O is particle unstable. An interesting speculation has been brought forward by P.G. Hansen concerning the stability of the ^{26}O. If this isotope is particle stable but only very weakly bound, then it could exhibit an extremely extended neutron halo which would give rise to a very large break-up cross-section (in the production target).

More cross-disciplinary, the interpretation of (anomaleous) isotopic abundancies found in the Allende meteorite as nuclear structure origin has become possible by the measurement of the β-delayed neutron decay of exotic S and Cl nuclei produced by LISE[9]. Progress in nuclear astrophysics is intimately related to continued experimental and theoritical efforts in nuclear-structure physics. Already in 1986, Hillebrandt at al[10] had requested to measure the missing β-decay properties of the "key"-isotopes influencing the low production of ^{46}Ca as compared to ^{48}Ca in their β-delayed neutron model, i.e. ^{44}S and $^{45-47}$Cl. By fragmentating on a ^{64}Ni target (116 mg/cm^2) the ^{48}Ca beam of the GANIL it has been possible to produce and study these isotopes. A thick energy degrader (180mg/cm^2) of aluminium was used in order to reduce the number of unwanted nuclei. The fragments were identified using the method described above in three silicon detectors (300μ,300μ,5500μ).The implantation of the nuclei of interest was made in the third detector, which served also for the β-detection with an efficiency of ε_β=60 ±6%. The telescope was surrounded by a 4π neutron-long counter,. The long-counter device was composed of two concentric rings of ^{3}He-proportional counters embedded in a polyethylene moderator matrix. This detector has a nearly energy independent efficiency of ε_n = 27 ± 2% up to $E_n \approx 2$ MeV and has no low energy cut-off as do scintillators.Each isotope under study was on-line identified by a combined measurement of its time of flight through the spectrometer and its energy loss in the first silicon detector.Two single-channel analysers examined the ΔE and TOF pulses and each time that a wanted nucleus was identified, the primary beam was switched off for a time interval related to the expected half-life.During this time, a second data acquisition performed the registration of β-neutron coincidence at low background. A set of plastic scintillators was used as shieldings on top of and below the neutron long-counter to detect cosmic muons. Thus, in the subsequent off-line analysis it was possible to discriminate between true β-neutron coincidences and muon induced background. With this set-up, each β-delayed neutron could be directly correlated to its implanted neutron precursor.

Results on $T_{1/2}$ and P_n values of ^{44}S and ^{45,46}Cl are shown on figure 3. The $T_{1/2}$ of ^{47}Cl could not be deduced from the β-neutron coincidences because of the very few events which, nevertheless, allowed to limit the P_n(^{47}Cl) to the surprisingly low value of ≤ 3%.

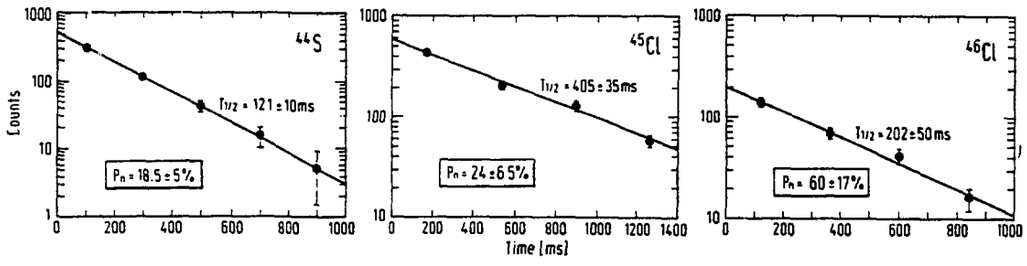

Figure 3: Beta-decay half-lives ($T_{1/2}$) and β-delayed neutron emission probabilities (P_n) of ^{44}S, ^{45}Cl and ^{46}Cl, obtained at GANIL.

With the $T_{1/2}$ of ^{44}S ans ^{45}Cl being considerably shorter than the predictions of Klapdor[11] used in ref.10, together with the higher, respectively lower P_n values of ^{46}Cl and ^{47}Cl, the conclusions of Hillebrandt et al. concerning the low production of ^{46}Ca are in principle strenghtened. As can be seen from figure 4 the experimental values may even turn out to be more favourable for a β-delayed neutron process than assumed. Successive neutron capture in the S and Cl chains is halted at the N=28 turning point nuclei where β-decay starts to dominate $T_{1/2}(\beta) < T_{1/2}(n)$. Of particular importance is the result that due to the short $T_{1/2}(^{45}Cl)$ feeding of $^{46,47}Cl$ is reduced. These isotopes were found to be the main progenitors of ^{46}Ca in the 1986 approach[10]. Moreover, even if the neutron capture in the Cl chain would proceed up to $^{46,47}Cl$, their P_n values would again result in a low ^{46}Ca abundance (see fig. 4). Hence with the present data, the problem of producing "very little" ^{46}Ca seems to be solved. But, on the other hand, may moderate the rather strict constraint on the neutron-exposure time requested in ref.10.

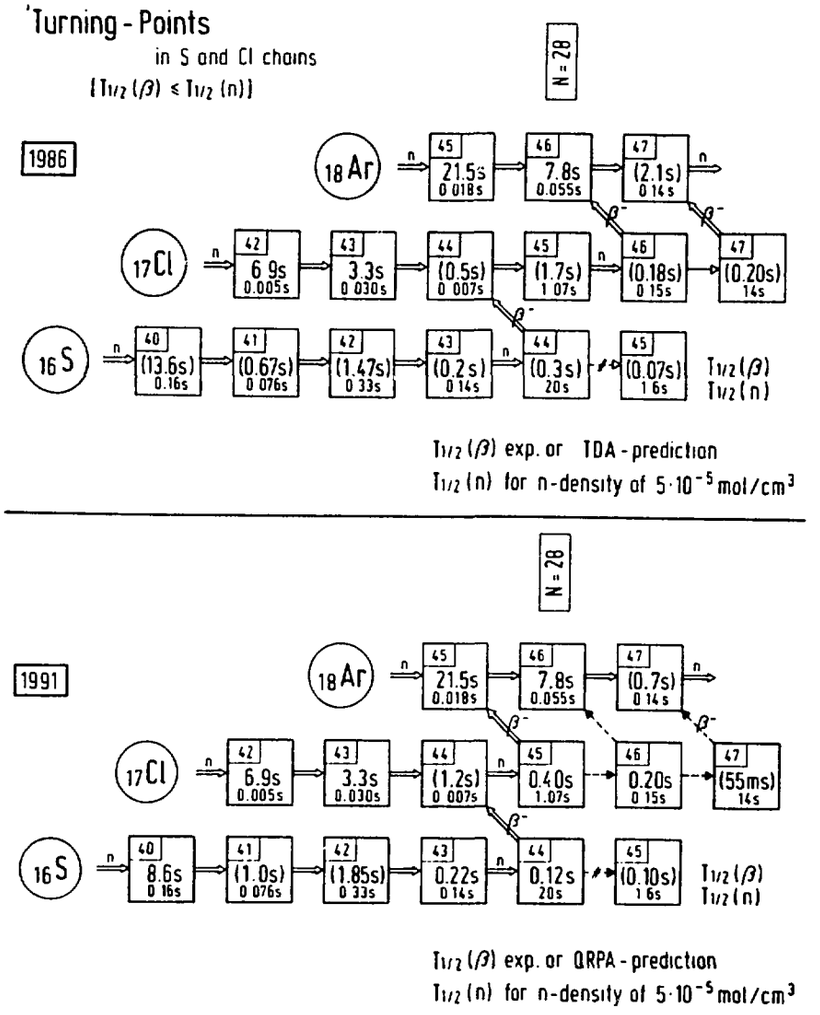

Figure 4: Neutron-capture path in the S to Ar chains for a stellar temperature of $T=8.10^8$ K and a neutron density of 5.10^{-5} mol.cm^{-3}; upper part: status in 1986, lower part: present status. With our new experimental data, at both N=28 "turning point" isotopes, ^{44}S and ^{45}Cl, β-decay back to stability starts to dominate over further neutron capture. Hence, the possible A=46,47 progenitors of ^{46}Ca will be produced in small amounts only. With this, large $^{48}Ca/^{46}Ca$ ratios can be obtained, as required to explain the observed abundances in meteorites.

4. CONCLUSION

The LISE spectrometer and now the LISE3 spectrometer, with its WIEN filter, operating after the achromatic spectrometer, offers an excellent isotope separation. With such a device heavier neutron-deficient species as well as neutron-rich one are now within the reach of experiments performed with GANIL heavier beams as krypton or xenon. Therefore a very broad domain of spectroscopic studies as well as secondary beam reactions is available.

6. REFERENCES

(1) T.J.M. Symons et al., Phys. Rev. Lett. **42** (1979) 40
(2) G.D. Westfall et al., Phys. Rev. Lett. **43** (1979) 1859
(3) See, e.g., I. Tanihata, Proceedings of the First International Conference on Radioactive Nuclear Beams, October 16-18, 1989, Berkeley, CA., USA, J.M. Nitschke ed., and references therein
(4) V. Borrel et al., Z. Phys. **A314** (1983) 91
(5) See, e.g., A.C. Mueller and R. Anne, Proceedings of the First International Conference on Radioactive Nuclear Beams, October 16-18, 1989, Berkeley, CA., USA, J.M. Nitschke ed., and references therein
(6) R. Anne et al., Nucl. Inst. Meth. **A257** (1987) 215
(7) A.C. Mueller, R Anne, Nucl. Inst. Meth. **B56/57** (1990) 559
(8) D. Guillemaud-Mueller et al., Phys. Rev. **C41** (1990) 937 and references therein
(9) K.L. Kratz et al., 1.European Workshop on Nuclear Physics, Megève 1991, IPNO-DRE 91-14 and O. Sorlin Thesis, Orsay (1991) unpublished IPNO-T 91-04 and to be published
(10)F.-K. Hillebrandt et al. Proc. of Weak and Electromagnetic Interactions in Nuclei,H.V. Klapdor ed., Springer Verlag (1986) 987
(11)H.V. Klapdor et al. At.Data Nucl. Data Tables **31** (1984) 81

7. OTHER REFERENCES

(12)Yu. E. Penionzhkevich et al., Z. Phys. **A 335** (1990) 117
(13) A. C. Mueller et al., Nucl. Phys. **A 513** (1990) 1
(14) A. C. Mueller, RIKEN-IN2P3 Symposium, Obernai (France), April 9-12 1990
(15)O. Sorlin et al., Nuclei in the Cosmos. International Symposium on Nuclear Astrophysics, Baden-Vienna (RFA) June 18-20 1990
(16)O. Sorlin et al., Sixth Workshop on Nuclear Astrophysics, Ringberg-Castle (RFA), February 19-22 1991
(17)O. Sorlin et al., Tagung der Deutschen Physikalischen Gesellschaft, Darmstadt (RFA), March 11-15 1991
(18)K.-L. Kratz et al., First European Biennal Workshop on Nuclear Physics, Megève (France) March 25-29 1991
(19)O. Sorlin et al., XVI European Geophysical Society Assembly, Wiesbaden (RFA), 22-26 April 1991
(20)A. C. Mueller, Gordon Conference, New London, NH (USA), June 24-28 1991
(21)A. C. Mueller, Fourth International Conference on Nucleus Nucleus Collisions, Kanazawa (Japan), June 10-14 1991
(22)M. Lewitowicz et al., Second International Conference on Radioactive Beams, Louvain la Neuve (Belgique), August 19-21 1991
(23)D. Guillemaud-Mueller, International Conference on Exotic Nuclei, Foros, Crimée (URSS), October 1-4 1991
(24)D. Guillemaud-Mueller, International Meeting on Nuclear Dynamics, Jackson Hole, Wyoming, (USA), 18-25 January 1992

STUDY OF LIGHT NEUTRON-DEFICIENT NUCLEI WITH THE LISE3 SPECTROMETER

V.Borrel[1], R.Anne[2], D.Bazin[3], C.Borcea[2], G.G.Chubarian[6], R.Del Moral[3], C.Detraz[4], S.Dogny[1], J.P.Dufour[3], L.Faux[3], A.Fleury[3], L.K.Fifield[2], D.Guillemaud-Mueller[1], F.Hubert[3], E.Kashy[5], M.Lewitowicz[2], C.Marchand[3], A.C.Mueller[1], F.Pougheon[1], M.S.Pravikoff[3], M.G.Saint-Laurent[2], O.Sorlin[1]

1 Institut de Physique Nucleaire, Orsay, France
2 GANIL, Caen, France
3 Centre d' Etudes Nucleaires, Bordeaux, France
4 Laboratoire de Physique Corpusculaire, Caen, France
5 Michigan State University, East Lansing, USA
6 Joint Institute for Nuclear Research, Dubna, USSR

1. Introduction

Over the last years, the use of projectile fragmentation of intermediate energy beams ^{36,40}Ar, ^{58}Ni, with 40 to 85 MeV/nucleon delivered by the GANIL facility, together with the selective LISE separator , has led to a rapid increase of information on light neutron-deficient nuclei. All existing neutron-deficient nuclei, up to titanium (Z=22) have been studied (1). Their half-lives and radioactive decay modes have been determined by measuring their emitted charged particles. Beta-delayed emission has been observed for ^{39,40}Ti (2). Beta-delayed proton emission occurs for ^{28}S and ^{31}Ar (3), (4) . Two-proton emission from the Isobaric Analog State has been observed for ^{31}Ar and ^{27}S (5) and other channels like beta-delayed three-proton emission also contribute (6). Experimental values for the ground-state mass excess of ^{31}Ar and ^{27}S have been deduced from the measured two-proton energy. The IMME has been checked in the case of ^{28}S.
The recent improvements of the GANIL accelerator, both in energy and in intensity, result in ^{58}Ni beams of 70 MeV per nucleon and 800 electrical nA. At the same time, the doubly achromatic spectrometer LISE was complemented with a WIEN filter. Thus, favorable experimental conditions become available for studying neutron-deficient nuclei with Z between 21 and 28. The present contribution, after describing the LISE3 spectrometer, reports on the production and study of several new neutron-deficient Cr, Mn and Fe isotopes.

2. The LISE3 spectrometer

The LISE spectrometer, essentially made of two identical dipole magnets D1 and D2 (figure1), is set at zero degree with a 1msr acceptance. The incoming beam is focused on the target by quadrupole lenses. The first dipole analyses the outgoing beam in A/Z. Moveable slits located in the dispersive focal plane limit the momentum acceptance, with a maximum equal to$\Delta p/p=\pm 2.5\%$.The second dipole compensates the dispersion of the first one: the set-up is doubly achromatic in angle and in position. As a consequence, the flight-path betveen the target and the final focal point is independant of the angle of entry in the spectrometer.After focalisation with quadrupole lenses the transmitted nuclei are collected in a small-size silicon detectors telescope in the final focal point. The time-of-flight parameter (t.o.f), obtained by comparing the time signal delivered by the first silicon detector with the radio-frequency signal of the cyclotron, is combined with the measured energy-loss in this detector (ΔE) and gives a clear identification in A and Z (figures 2 and 3).
The installation of a suitably shaped energy-degrader (a bent aluminium foil of variable thickness) in the dispersive focal plane separates the nuclei according to their slowing down in matter. The achromatism is restored only for the choosen isotope which is transmitted to the detector by tuning the second dipole to the corresponding magnetic rigidity. A few nuclides are collected instead of a few tens. The LISE set-up works as an isotope separator.

All the experiment so far have been performed at the first achromatic focal point. A means to improve the isotopic selection of the LISE spectrometer consists in using a third selection criterion: a velocity selection. Therefore the new-built extension is doubly achromatic in the horizontal plane and behaves as a WIEN filter which separates the nuclei in the vertical plane, according to their velocity. The selected isotopes are collected in a silicon detectors telescope located at the final focal point where they are identified and studied. The total flight-path is now 43 meters long, providing an easy mass-identification for heavy nuclei. Detailed reports on LISE and LISE3 are given in (7) and (8).

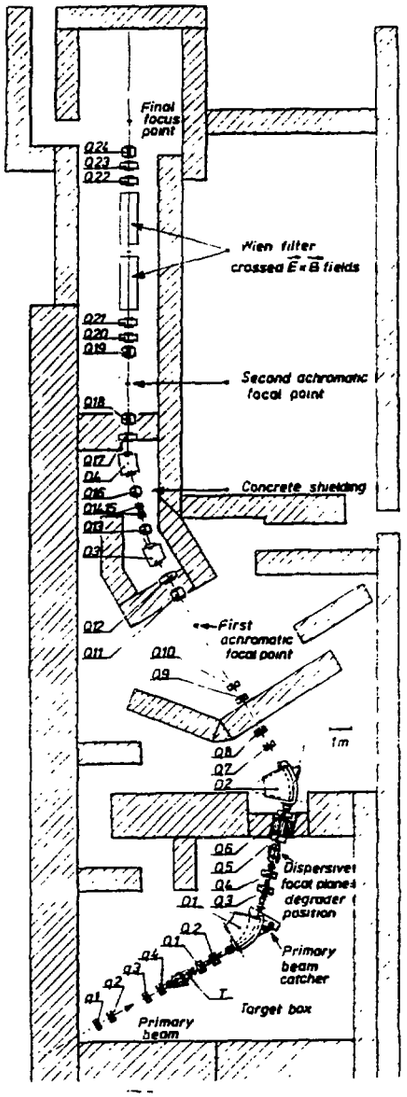

Fig.1. The LISE3 spectrometer

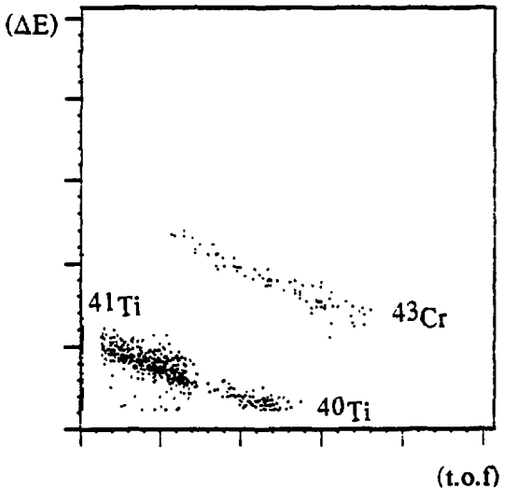

Fig.2. Nuclei transmited with ^{43}Cr

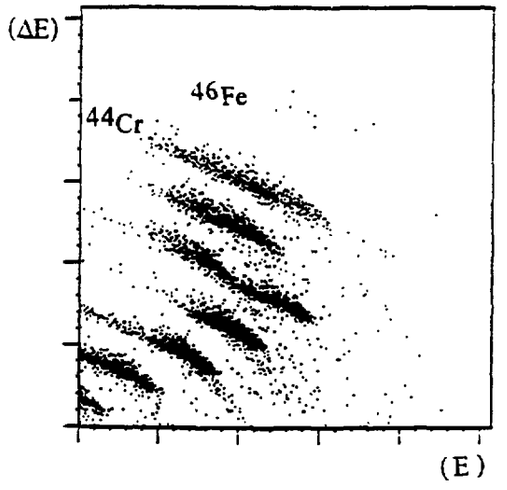

Fig.3. Nuclei transmitted with ^{46}Fe

3. Experimental set-up;production of new isotopes

A beam of 69MeV per nucleon ^{58}Ni projectiles impinges on a natural nickel target the thickness of which (150 mg/cm^2) is choosen so as to optimize the yield of interesting reaction products collected trough the LISE3 spectrometer. The average beam intensity is 400 electrical nA. A 72 mg/cm^2 aluminium degrader is installed.The detection telescope consists in three surface-barrier silicon detectors assembled together in a unique holder: they are 300 mm thick, the distance between two adjacent silicon surfaces is equal to 450 mm and the active area is equal to 300 mmA 4mm thick Si(Li) detector works as a veto detector for high-energy protons. A

remotely-controlled energy degrader preceeds the telescope and is adjusted so as to bring at rest the isotope of interest in the central silicon detector. The first and third detectors each form together with the central (second) one a telescope for the spectrosopy of the charged particles emitted by the implanted nuclei.
The two-dimensional identification diagrams shown on figures 2 and 3 are obtained for two different Bρ settings optimized for the collection of ^{45}Fe and ^{46}Fe, respectively. The magnetic rigidities and the electric field values are detailed in table1. The momentum acceptance is set to $\Delta p/p = \pm 2.5\%$ and the slits at the exit of the WIEN filter, which define the velocity acceptance, are opened to 30 mm. A third Bρ setting (see table 1) is used for the study of ^{47}Fe.

	Bρ1 (Tm)	Bρ2 (Tm)	E (keV)	Bρ3 (Tm)	Δt (ms)
^{45}Fe	1.842	1.645	± 90	1.645	250
^{46}Fe	1.857	1.653	± 90	1.652	800
^{47}Fe	1.927	1.732	± 100	1.730	250

Table1. Experimental conditions

The ^{43}Cr isotope is clearly identified (figure2) with 184 counts in a 24 hours long exposure, it is transmitted together with ^{40}Ti and ^{41}Ti (833 counts) whereas no counts are observed at the locations of ^{45}Fe and ^{42}V, respectively. 16 counts of ^{46}Fe are obtained in 15 hours, 1146 counts for ^{44}Cr and no event is observed at the location of ^{45}Mn (figure 3). The third experimental setting leads to the identification of ^{47}Fe with 23 counts in six hours, 294 counts of ^{46}Mn and 1886 events of ^{45}Cr are collected in the same time.The three nuclei ^{43}Cr, ^{47}Fe and ^{46}Fe are synthesized for the first time. The lightest known Cr isotope was ^{44}Cr (9) and ^{48}Fe had been produced and studied at GSI (10). ^{43}Cr and ^{46}Mn are collected in sufficient amounts to allow radioactive decay studies (see next section). These results allow us to consider that the ^{45}Fe half-life is shorter than the time-of-flight in the LISE3 spectrometer: 300 ns. This $T_Z = -7/2$ isotope is a candidate for two-proton decay with a two-proton separation energy calculated to be $S_{2p} = -820 \pm 200$ keV(1). It is also possible to conclude that ^{42}V and ^{45}Mn exhibit short half-lives (less than 300ns), and, thus, if they do exist, these nuclei may be direct proton emitters.

4. Decay studies

The ^{43}Cr and ^{46}Mn decay studies are performed on-line: two single-channel analysers examine the ΔE and t.o.f pulses. Each time that a ^{43}Cr (or ^{46}Mn) event is identified, the beam is stopped for a time Δt (see table1) five times longer than the expected half-life. During this time the heavy-ion data-acquisition system is turned off, while a clock an a second data-acquisition system are started. The energy deposited and the time of arrival of the ligth particles are recorded during the beam-off periods. The silicon detectors are calibrated before the experiment with an α source and during the experiment with the known beta-delayed protons emitted from ^{45}Cr (11). This experimental procedure has been described in (4) and in (5) .

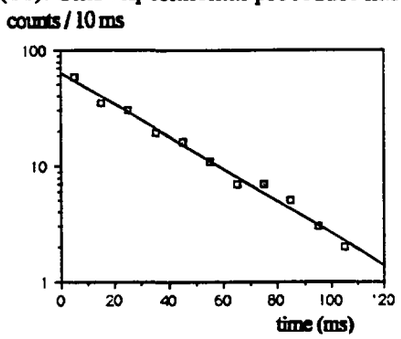

Fig. 4. ^{43}Cr time spectrum

$T_{1/2} = 20.9^{+3.8}_{-3.0}$ ms

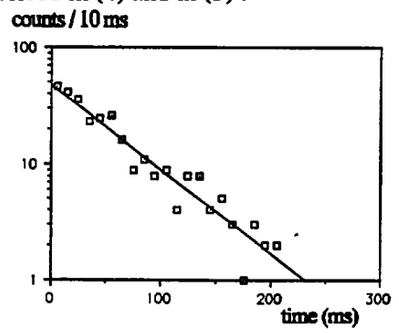

Fig. 5. ^{46}Mn time spectrum

$T_{1/2} = 41.4^{+7.1}_{-5.6}$ ms

Figures 4 and 5 display the time spectrum recorded for ^{43}Cr and ^{46}Mn, respectively. The $T_{1/2}$ values are obtained from a maximum-likelihood analysis of these experimental time distributions and the error bars correspond to a 70% confidence level. The masses of analogue states in an isospin multiplet are given to first order by a quadratic relationship: $M(A,T,T_z)=a(A,T)+b(A,T)T_z+c(A,T)T_z^2$. Table 2. summarizes the properties of the T = 2 levels which are members of the isospin quintet at mass A=43.

nucleus	T_z	mass excess (keV)	reference
^{43}K	5/2	-36592 ± 10	Wapstra et al. 1988
^{43}Ca	3/2	-30419 ± 19	Antony et al. 1986
^{43}V	-3/2	-9745 ± 50	this work
^{43}Cr	-5/2	-2135 ± 90	from IMME

Table 2. Properties of members of the T= 5/2 multiplet at mass 43

Two lines are identified on the energy spectrum of the charged particles emitted by ^{43}Cr, with total decay energies equal to 4320 ± 50 keV and 1870 ± 80 keV. They can be attributed to the beta-delayed emission of two proton and an alpha particle from the IAS in ^{43}V to the ground-states in ^{41}Sc and ^{39}Sc, respectively. An other line at 2290 ± 50 keV may correspond to the beta delayed two-proton emission to the first excited state in ^{41}Sc. The experimental value of the mass excess of the IAS in ^{43}V is deduced from these measured lines and from the known ground-state mass excess of ^{41}Sc which is equal to -14065 ± 1 keV (12). The value obtained is -9745 ± 50 keV and, applying the IMME to the T = 5/2 states in the three nuclei ^{43}V, ^{43}Ca and ^{43}K, one can deduce a value for the ground-state mass excess of ^{43}Cr : -2135 ± 90 keV.

nucleus	T_z	mass excess (keV)	reference
^{46}Sc	2	-41759 ± 13	Wapstra et al. 1988
^{46}Ti	1	-34928 ± 28	Antony et al. 1986
^{46}Cr	-1	-20236 ± 53	this work
^{46}Mn	-2	-12375 ± 120	from IMME

Table 3. Properties of members of the T= 2 quintet at mass 46

Three transitions are identified on the energy spectrum of the beta-delayed protons emitted by the 392 implanted ^{46}Mn nuclei: they correspond to total decay energies (since both the proton and the ion recoil energies are recorded in the telescope) of 4350 ± 50, 3560 ± 50 and 3000 ± 50 keV. The first experimental line matches the expected energy available for the proton decay of the isobaric analog state in ^{46}Cr to the ground-state in ^{45}V. The two others can be attributed to proton emissions from the IAS to excited states in ^{45}V (deduced from the level scheme of the mirror nucleus ^{45}Ti). The experimental energy for the proton decay of the IAS in ^{46}Cr (4350±50 keV), combined with the ground-state mass excess of the (^{45}V + p) system: -24586±17 keV (12), yields the mass of the IAS in ^{46}Cr to be -20236 ± 53 keV. The mass of the ^{46}Mn ground-state, derived with the IMME, is found to be equal to -12375 ± 120 keV. This value is in agreement with the prediction made by Wapstra et al. (12) of -12470 ± 400 keV.

5. Conclusion

The LISE3 spectrometer, with its WIEN filter operating after the achromatic spectrometer, offers an excellent isotope separation. Three new neutron-deficient nuclei are produced with the intense ^{58}Ni GANIL beam: ^{43}Cr, ^{47}Fe and ^{46}Fe.. Half-lives and mass excess values are measured in the present work for the neutron-deficient nuclei ^{43}Cr and ^{46}Mn. Heavier neutron-deficient species are now within the reach of experiments performed with GANIL heavy beams (krypton, xenon ...) and making use of the LISE3 set-up. Radioactive decay studies can be achieved in favorable experimental conditions.

6. References

(1) C. Detraz, Proc. Int. Conf. on nuclear physics 1990,World Scient.vol2 p 337
(2) C. Detraz et al., Nucl.Phys. **A519** (1990) 529
(3) F. Pougheon et al., Nucl.Phys. **A500** (1989) 287
(4) V. Borrel et al., Nucl.Phys. **A473** (1987) 331
(5) V. Borrel et al., Nucl.Phys. **A531** (1991) 353
(6) D. Bazin et al., Proc. of nuclear structure of light nuclei far from stability, ed G.Klotz, 1989 p 21 and Phys. Rev. in press
(7) R. Anne et al., Nucl.Instr.Meth. **A257** (1987) 215
(8) A.C. Mueller and R.Anne R Nucl.Instr.Meth. **B56** (1991) 559
(9) F. Pougheon et al., Z.Phys. **A327** (1989)17
(10) D. Schardt et al., Nucl.Phys. **A467** (1987) 93
(11) K.P. Jackson et al., Phys.Lett **49B** (1974) 341
(12) A.H. Wapstra , G. Audi, R. Hoekstra, At. Data Nucl. Data **39** (1988) 281
(13) M. S. Antony et al.,At. Data Nucl. Data **34** (1986) 279

7. Other references

V.Borrel et al., Second International Conference on Radioactive Nuclear Beams, Louvain-la-Neuve, Belgium, 19-21 August 1991, in press

BETA-DELAYED TWO-PROTON DECAY OF ^{31}Ar AND ^{27}S

V. Borrel[1], R.Anne[2], D. Bazin[3], R. Del Moral[3], C. Détraz[2], J.P. Dufour[3], D.Guillemaud-Mueller[1], F. Hubert[3], J.C.Jacmart[1], A.C. Mueller[1], F. Pougheon[1], M.S. Pravikoff[3], E. Roeckl[4]

1 Institut de Physique Nucléaire, 91406 Orsay Cedex, France
2 GANIL, BP5027, 14021 Caen, France
3 CEN Bordeaux, Le Haut Vigneau, 33170 Gradignan, France
4 GSI, Postfach 11 05 52, 6100 Darmstadt 11, Fed. Rep. Germany

At the proton drip-line light neutron-deficient nuclei exhibit several decay modes: a wide range of excited states, including the Isobaric Analog State, can be reached in the daughter nucleus through beta plus decay , and for these states proton and two-proton emissions are energetically possible .

This contribution reports on the experimental results obtained at GANIL with the LISE spectrometer on the decay of the T_z=-5/2 isotopes ^{31}Ar and ^{27}S .

Energy spectra of the beta delayed particles have been recorded and the halflives have been measured : $T_{1/2}$ = 15 ± 3 ms for ^{31}Ar and $T_{1/2}$ = 21 ± 4 ms for ^{27}S, leading to the branching ratios for beta decay towards the IAS: 4.8 ± 1.4 % and 4.0 ± 1.2 % respectively.

The observation of the two-proton emission from the IAS has led, through the Coulomb displacement energy systematics, to an evaluation of the ground-state mass excess for the two nuclei: 11425 ± 99 keV for ^{31}Ar and 17659 ± 114 keV for ^{27}S. These values are both 200 keV lower than the corresponding predicted values (ref.1). In the ^{31}Ar case, the deduced two-proton separation energy : S_{2p} = -7 ± 112 keV is in agreement with the non-observation of direct two-proton emission .

After corrections for the detection efficiency, the absolute branching ratios for beta-delayed two-proton emission have been calculated. They are equal to 2.4 ± 0.8 % and 2.0 ± 1.0 % respectively for ^{31}Ar and ^{27}S.

Since no beta-delayed proton emission via the IAS has been observed, other decay channels like beta-delayed three-proton emission should be searched for (ref.2).

REFERENCES

1) A.H. Wapstra, G. Audi and R. Hoekstra, At. Data and Nucl. Data Tables 3(1988) 281

2) D. Bazin et al, Proceedings of Nuclear Structure of Light Nuclei Far from Stability, Obernai, 1988 , ed. G. Klotz p 21 and Phys. Rev., in press

OTHER REFERENCES

V. Borrel et al., Nucl. Phys. **A473** (1987) 331

V. Borrel et al., Nucl. Phys. **A531** (1991) 353

V.Borrel, Proceedings of Nuclear Structure of Light Nuclei Far from Stability, Obernai, 1988, ed. G. Klotz p 7

Determination of the $^{13}N(p,\gamma)$ reaction rate through Coulomb break-up of a radioactive beam

J. Kiener[1], A. Lefebvre[1], P. Aguer[1], C.O. Bacri[2], R. Bimbot[2], G. Bogaert[1], B. Borderie[2], F. Clapier[2], A. Coc[1], D. Disdier[3], S. Fortier[2], C. Grunberg[4], L. Kraus[3], I. Linck[3], G. Pasquier[1], M.F. Rivet[2], F. St Laurent [4], C. Stephan[2], L. Tassan-Got[2], J.P. Thibaud[1]

1) C.S.N.S.M. IN2P3-CNRS, Bat 104-108, 91405 Orsay (France)
2) I.P.N. IN2P3-CNRS, 91406 Orsay (France)
3) C.R.N. IN2P3-CNRS, Univ. Louis Pasteur, B.P. 20, 67037 Strasbourg Cedex (France)
4) GANIL BP 5027 14021 Caen Cedex (France)

Abstract: *The $^{13}N(p,\gamma)$ reaction rate depends on the magnitude of the radiative width of the 5.17 MeV level in ^{14}O . That width has been measured using the Coulomb break-up technique. ^{14}O was excited in the Coulomb field of a ^{208}Pb target, the ^{13}N and proton fragments being recorded. The experimental value is $\Gamma_\gamma = (2.4 \pm 0.9)$ eV.*

1 Introduction

In numerous astrophysical environments, explosive hydrogen burning may occur at much higher temperatures and densities than are found in normal stellar environments. When the temperature increases, the waiting point of the CNO cycle shifts from the $^{14}N(p,\gamma)$ reaction to the next slow path which is the β^+ decay of ^{13}N , and the energy production limitation comes from the 14.4 min lifetime of ^{13}N . The next expected change should come when the $^{13}N(p,\gamma)$ reaction starts to compete with the ^{13}N decay because the proton capture lifetime

becomes shorter than the decay lifetime. However, until recently, no reliable experimental information was really available concerning the rate of the ^{13}N + p reaction, in spite of the importance of that reaction for stellar evolution models. Among the various consequences of that reaction, we can note tne possibility of by-passing the ^{13}C production, and then constraining the astrophysical models of stellar evolution involving $^{13}C(\alpha, n)$ as a neutron source. To help to solve those problems, large efforts have been made to produce a beam of radioactive ^{13}N and to get a direct measurement of that reaction rate.

Aware of the importance of the goal, many theoretical works as well as experimental ones have been achieved in order to evaluate the radiative width of the 5.173 MeV level in ^{14}O . This contribution reports results of an experimental radiative width determination using the new technique of Coulomb break-up.

2 The Coulomb break-up experiment

Studies of the dissociation of fast nuclear projectiles in the Coulomb field of a heavy target nucleus have been proposed as an alternative access to radiative capture cross sections of astrophysical interest [1]. Instead of measuring the direct fusion cross section process C + B $\rightarrow$ A + γ, one considers the time reversed photodissociation process A + $\gamma \rightarrow$ B + C taking advantage of the intense flux of equivalent photons produced by the interaction of the projectile A with the electric field of a heavy target nucleus. Together with the advantage of an usually larger phase space, the large number of photons result in a considerably enhanced cross section as compared with the capture reaction, giving access to very small cross sections.

2.1 Experimental conditions

We have studied the $^{13}N + p \rightarrow^{14} O + \gamma$ reaction by the Coulomb break-up technique, looking at the photo dissociation of a radioactive ^{14}O ($T_{1/2}$ = 1.2 min) beam at Ganil. The ^{14}O beam was produced by fragmentation and transfer processes of a 96 MeV/u primary beam of ^{16}O onto a 800 mg/cm^2 carbon target. The ^{14}O beam intensity was 10^6 particles.s^{-1} for a 2 μA electrical primary beam intensity. The secondary beam energy was 70 MeV/u with a resolution of about

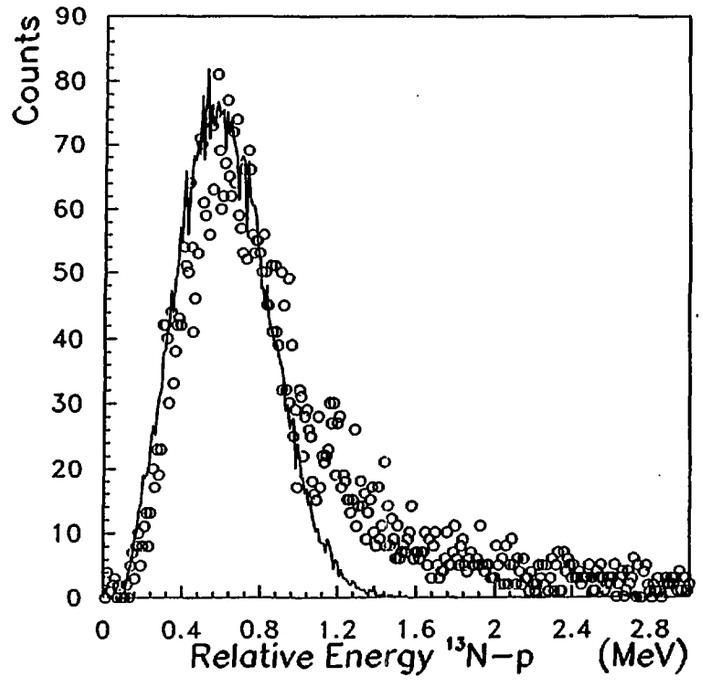

0.5 % and was delivered onto a target of 100 mg/cm^2 of ^{208}Pb, the high Z providing a higher Coulomb field and then larger excitation probability. The reaction products, such as ^{13}N and the other heavy elements were analysed by the magnetic spectrometer SPEG. Protons were detected by a set of five CsI detectors located in the reaction chamber, 70 cm downstream the lead target, and around the aperture of the SPEG spectrometer.

2.2 Experimental result

We obtain the spectrum of the relative energy of the p and ^{13}N (Figure) computed event by event, where is observed a large peak located at 540 keV. That spectrum was fitted using the peak shape provided by a Monte Carlo type simulation taking into account the beam energy resolution and emittance, scattering into the thick lead target and the

detector resolutions. The intensity of the peak was compared with the intensity obtained in a Coulomb excitation computation, using both a semi-classical type of calculation and a coupled channel code. Both computations are in agreement, and we infer a radiative width for the 5.173 MeV level in ^{14}O :

$$\Gamma_\gamma = (2.4 \pm 0.9) \text{ eV} \quad (1)$$

3 Conclusion

Our result is in close agreement with the value $\Gamma_\gamma = 2.44$ eV estimated by G.J. Mathews and F.S. Dietrich [2] looking at analogous transitions in neighbouring nuclei, and we can adopt their conclusions, specifically that the $^{13}N + p$ reaction rate is somewhat higher than is estimated in the data tables, the hot CNO cycle could be ignited at density low enough to prevent the collapse of a metal-rich supermassive star into a black hole [2].

An other conclusion of our work is that the Coulomb break-up of a radioactive beam can provide accurate and reliable information concerning unknown radiative widths. The method has implications in astrophysics as well as in nuclear physics. Concerning astrophysical reaction rate determination, that tool can offer a new way to get experimental information and should be used for other systems of astrophysical interest involving.

References

[1] G. Baur, C.A. Bertulani and H. Rebel, N.P. **A458** (1986) 188

[2] G.J. Mathews, and F.S. Dietrich, Ast. Jnal **287** (1984) 969

B - NUCLEAR REACTIONS

B1 - PERIPHERAL COLLISIONS
PROJECTILE LIKE FRAGMENTS

DEEP INELASTIC COLLISIONS IN THE SYSTEM AR + TH AT 31 MeV/u

R. Barth[1], Y. Cassagnou[2], M. Conjeaud[2], R. Dayras[2], S. Harar[3], R. Legrain[2], V. Lips[1], G. Klotz-Engmann[1], H. Oeschler[1], E.C. Pollacco[2] and C. Volant[2]

[1] *Institut für Kernphysik, Technische Hochschule Darmstadt, D-6100 Darmstadt, FRG*
[2] *D.Ph.N./SEPN, CEN Saclay, F-91191 Gif-sur-Yvette Cedex, France*
[3] *GANIL, BP 5027, F-14021 Caen Cedex, France*

1. Introduction

In heavy-ion reactions with incident energies below 10 MeV/u deep inelastic collisions (DIC) are a well known phenomenon, e. g. studying the reaction $^{40}Ar + ^{232}Th$ [1, 2]. As a by-product of an experiment using this collision system at intermediate energies to investigate the evolution of central collisions (see contribution in this volume) an interesting class of events has been observed: Triples coincidences with two medium-mass fragments and one rather light nucleus at forward angles. The events exhibit the characteristics of deep inelastic collisions. The relevant part of the experiment consisted of three parallel-plate avalanche counters, two of them at about 50^0 on both side of the beam axis and the third at 110^0.

2. Results

The main characteristics of these triple coincidences are summarized in fig. 1. Parts (a) - (d) show the velocity and charge distributions at 31 MeV/u incident energy for PPAC 1 and 2 at forward angles. (The atomic numbers of the fragments were determined from the energy-loss signal and the velocity with a resolution of 30%, using an iterative procedure [3].) The detection of a third fragment in PPAC 3 at backward angles introduces a strong asymmetry in the spectra of PPAC 1 and PPAC 2 despite their symmetric position relative to the beam. The fragments detected in counter 1 show a narrow velocity distribution, centered at 1.4 cm/ns, their charge distribution is peaked at Z≈40. In fig. 1(e) the relative velocity between the fragments detected in PPAC 1 and PPAC 3 is shown. The narrow distribution, centered at the Viola velocity, in addition to the corresponding charge and velocity distribution of the fragment detected in counter 3 shows that coincidences of two fission fragments were observed with these counters. The velocity and charge distributions observed for the fragments detected in counter 2 show properties characteristic for inelastically scattered projectiles observed in the low-energy regime. Namely, (i) the charge distribution is peaked at Z≈15, close to the projectile charge, (ii) the velocities are well below that of the beam (7.7 cm/ns), (iii) the angular distribution is forward peaked (fig. 1(f)), and finally (iv) the fragment in counter 2 lies preferentially in the plane spanned by the two fission fragments. In the picture of a deep inelastic collision this results through the transferred angular momentum, which favours a fission of the target nucleus mainly perpendicular to the spin axis. All these observations led us to conclude that the projectile-like partner - or the remaining part - of a DIC is observed.

Using the measured velocities and scattering angles of the projectile-like fragment the total kinetic energy loss (TKEL) was estimated to 700 MeV. The number of preequilibrium particles and the energy and linear momentum carried away by them has been calculated using Blann's code [4]. The experimental data show no dependence of the deduced TKEL

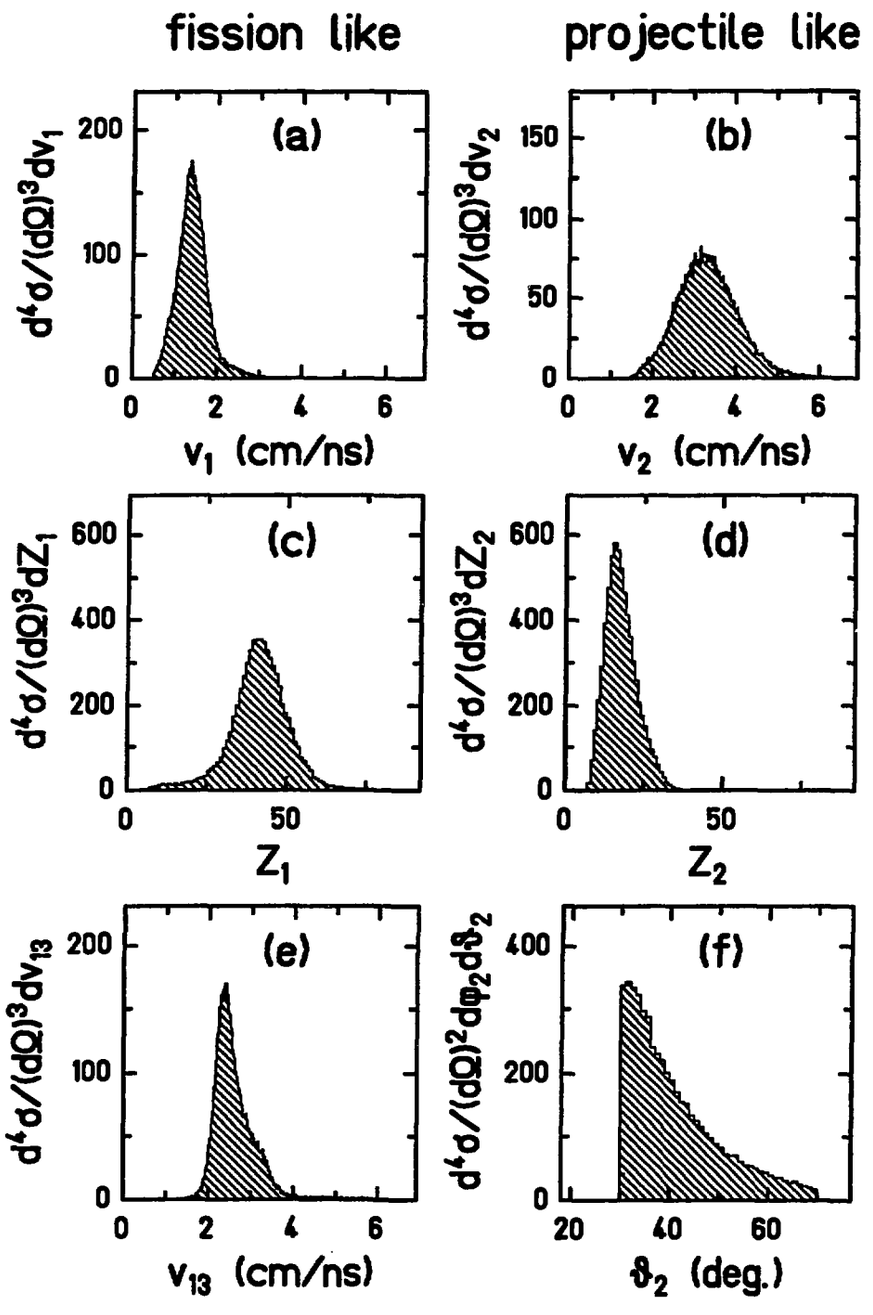

Figure 1: (a) Fragment velocities in triple coincidences measured with PPAC 1. (b) The same quantity measured with PPAC 2. (c) Fragment charges in triple coincidences measured with PPAC 1. (d) The same quantity measured with PPAC 2. (e) Relative velocity between fragments detected in PPAC 1 and PPAC 3 for triple coincidences. (f) Angular distribution of the fragments detected in PPAC 2 for triple coincidences.

value on the deflection angle of the fragments, similar to the system $^{40}Ar + ^{nat}Ag$ where such correlations were seen only in the vicinity of the grazing angle [5]. This suggests negative deflection angles for the projectile-like fragment, as observed for the system $^{14}N + ^{154}Sm$ at similar incident energies [6]. As for the excitation energy it is interesting to compare our results with the 4π neutron detector data for the system $^{40}Ar + ^{197}Au$ at 44 MeV/u incident energy [7]. High neutron multiplicities are found in reactions triggered by projectile-like fragments at 20^0, yielding values similar to those observed in our case.

The presence of DIC shows, that nuclei behave collectively, even for incident energies in the vicinity of the Fermi energy. This process must be taken into account when studying multiplicities and cross sections for IMF production in this regime.

References

[1] A.G. Arthuk, G.F. Gridnev, V.L. Mikeev, V.V. Volkov and J. Wilczynski, Nuclear Physics A215(1973)91

[2] J.C. Jacmart, P. Colombani, H. Doubre, N. Frascaria, N. Poffé, M. Riou, J.C. Roynette, C. Stéphan and A. Weidinger, Nuclear Physics A242(1975)175

[3] V. Lips, Diploma thesis, Technische Hochschule Darmstadt 1989; GSI Scientific Report 1987, p.309

[4] M. Blann, Physical Review C 31(1985)1245

[5] B. Borderie, M. Montoya, M.F. Rivet, D. Jouan, C. Cabot, H. Fuchs, D. Gardès, H. Gauvin, D. Jacquet, F. Monnet and F. Hanappe, Physics Letters B205(1988)26

[6] M.B. Tsang, W.G. Lynch, R.M. Ronningen, Z. Chen, C.K. Gelbke, T. Nayak, J. Pochodzalla, F. Zhu, M. Tohyama, W. Trautmann and W. Dünnweber, Phys. Rev. Letters 60(1988)1479

[7] J. Galin, J.L. Charvet, B. Cramer, E. Crema, H. Doubre, J. Frehaut, B. Gatty, D. Guerreau, G. Ingold, D. Jacquet, U. Jahnke, D.X. Jiang, B. Lott, C. Magnago, M. Morjean, J. Patin, E. Piasecki, J. Pouthas, F. Saint-Laurent, E. Schwinn, A. Sokolov and X.D. Wang, Proceedings of the symposium on nuclear dynamics and nuclear disassembly, Dallas, Texas, World Scientific (1989)320

Evaporation and Nonequilibrium Emission of Neutrons in Binary Au+Pb Collisions at 29 MeV/nucleon

B.M.Quednau, S.P.Baldwin, M.B.Chatterjee, W.U.Schröder, B.M.Szabo, J. Tõke, *University of Rochester*; D. Hilscher, U. Jahnke, H. Rossner, *HMI Berlin*; S. Bresson, J. Galin, D. Guerreau, M. Morjean, *GANIL*; B. Lott, *CRN Strasbourg*; D. Jacquet, *IPN Orsay*

1. Introduction

The purpose of the experiment was to study the characteristics of neutron-fragment correlations in an intermediate energy heavy-ion reaction. The analysis of the interdependencies of neutron emission patterns, neutron multiplicities and average atomic number and energy of coincident fragments produced in such a reaction allows one to identify the sources and mechanisms of neutron emission and, eventually, the reaction mechanism itself. The system Au+Pb was chosen for study because of its neutron richness and mass symmetry, facilitating the interpretation of the experimental data. The following outlines the kinematical coincidence method used to select energy loss bins by fragment angle-angle correlations and presents results of model calculations describing quantitatively the observed correlations.

2. Experimental Procedure

Charged reaction products were detected with 5 multi-element silicon telescopes and three large-area, 300-μm thick multi-strip silicon detectors. The telescopes positioned at $\theta = 6.5° + 8.5°$, and -21.5° were optimized to identify projectile-like fragments (PLF), while telescopes at $\theta = 61.5°$ and -141.5° were used to detect light charged particles and intermediate-mass fragments (IMF). The multi-strip detectors covering an angular range between 25° and 81° measured target-like fragments (TLF) in coincidence with the projectile-like collision partners measured at $\theta = 6.5°$. The neutron energies were measured using a time-of-flight method. The start signals were generated from the accelerator RF-period while stop signals were provided by 23 neutron scintillation counters placed at distances between 1 and 2 meters from the target, covering an angular range between $\theta_n = 163°$ and +165° in a common plane with the charged-particle detectors. Two of the neutron detectors were placed out of plane. The cylindrical NE213 scintillators were 1.5" to 4" thick and 5" or 10" in diameter. Discrimination between neutrons and gamma rays was accomplished employing pulse-shape analysis modules. A thin-walled stainless-steel reaction chamber was used in order to reduce absorption and scattering of neutrons. Furthermore, discrimination between neutrons and charged particles that had penetrated the thin walls of the scattering chamber and had been detected in the neutron detectors was accomplished using fast-plastic scintillation counters placed in front of forward-angle neutron detectors.

4. Experimental Results and Discussion

Binary collision events were selected using a kinematical coincidence method. PLFs were measured with a Si-telescope at $\theta = 6.5°$ while the coincident TLFs were detected in an angular

range of 25° to 81°. It was ascertained, based on characteristic correlations between the velocity vectors and masses of the coincident fragments, that the events with $76 \leq Z_{PLF} \leq 80$ and $25 \leq E_{TLF} \leq 200$ MeV used in the present analysis originated from binary collisions.

The upper left and right panels of Fig. 1 show the atomic number and energy distribution of the PLFs coincident with TLFs, respectively. The lower right panel shows the angular distribution of the coincident TLFs. The position of the relatively narrow peak at $\theta = 72°$ in the latter panel agrees with the average recoil angle for TLFs from binary damped collisions with a kinetic energy loss of $E_{loss} = 200$ MeV. The finite coincidence rate limited the energy loss studied to $E_{loss} \leq 500$ MeV.

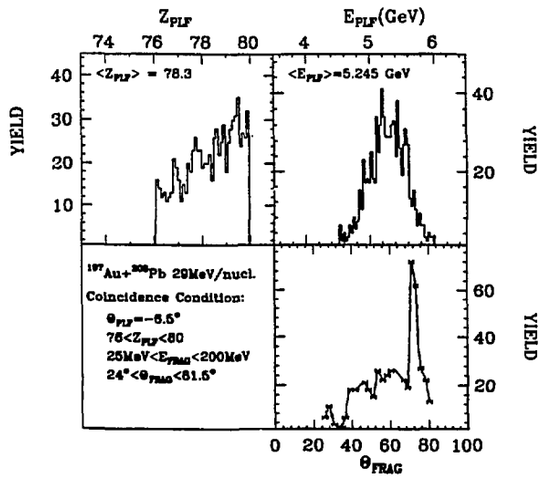

Figure 1: Energy and atomic-number spectra of PLFs coincident with TLFs (upper panels) and the angular distribution coincident TLF fragments (lower right).

A triple-coincidence measurement of kinematically identified PLFs and TLFs and neutrons allowed one to study the consistency of the reconstructed energy loss with the observed neutron multiplicities and slope parameters of neutron velocity spectra. In this measurement the kinetic energy losses were determined by selected angular correlation between PLF and TLF. Fig. 2 shows velocity spectra (dots) of neutrons, measured at 8 selected angles in coincidence with both, PLFs with $\langle Z \rangle = 78.3$ and $\langle E \rangle = 5.245$ GeV and TLFs at $\theta = +(73.5 \pm 1.1)°$. From the average energies, atomic numbers and angles it was determined that the average energy loss for the events included in Fig. 2 was $E_{loss} \approx 115$ MeV. The high-velocity component seen at $v_n = 7\frac{cm}{ns}$ at forward angles can be attributed to neutron emission from the fast-moving PLFs. The low-energy component, as well as the yield at backward angles, is due to the emission from the recoiling TLFs.

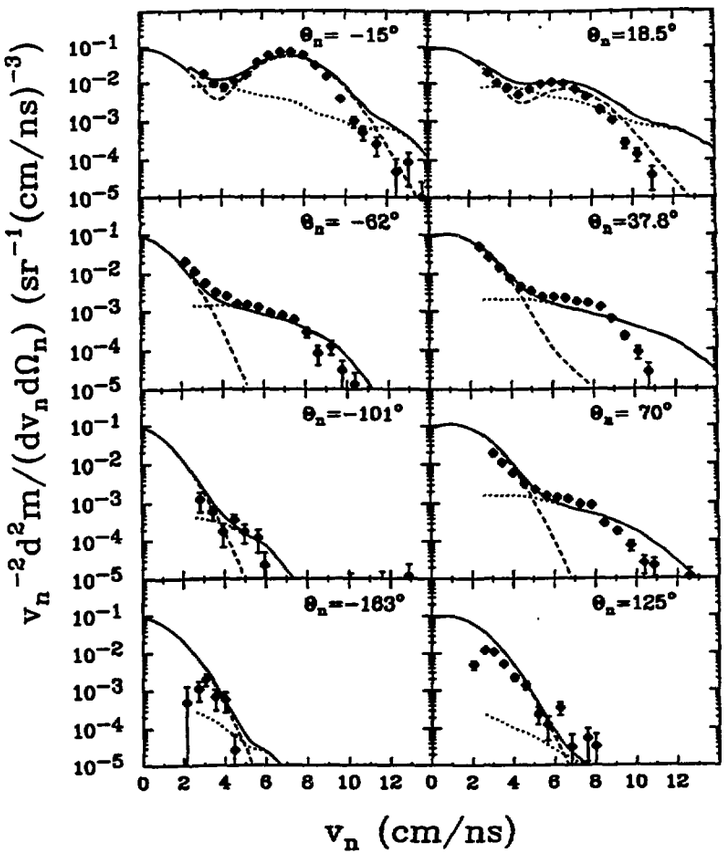

Figure 2: Velocity spectra of neutrons coincident with partially damped collisions events, i.e., fragments with $60 \leq Z \leq 90$ coincident with fragments detected at $+73.5 \pm 1.1°$.

In order to test the quantitative consistency of the assumption of sequential emission from excited primary PLFs and TLFs with the data, theoretical model calculations were performed. The dashed curves in Fig. 2 result from calculations assuming two effective sources, the fully accelerated PLF and TLF partners from a damped collision, evaporating isotopically neutrons in their rest frames. The neutron spectra are assumed to be given by Maxwell-Boltzmann distributions with inverse slope parameters reflecting an effective temperature of the evaporation cascade of $\tau \approx$ 1.7 MeV. The theoretical neutron velocity spectra shown as dashed curves in Fig.2 are consistent with the average properties of coincident fragments and with the average kinetic energy loss reconstructed from kinematics.

At medium forward angles, an additional component is seen in the neutron velocity spectra of Fig.2, which cannot be explained in terms of the above two-source emission scenario. The latter component can be modelled assuming nonequilibrium emission as predicted by a Fermi-jet mechanism[1]. As demonstrated by the comparison of the solid curves and the data in Fig.2, both, magnitude and gross structure of the measured neutron spectra is quite well explained, when this additional component is included.

5. Summary

In summary, a kinematical coincidence method was used to identify PLF and TLF produced in binary collision events. Based on the example of one particular coincidence condition, it was shown, that most of the neutron yield and associated fragment distributions can be described consistently assuming sequential neutron emission from primary fragments following a binary damped collision. An additional high-velocity neutron component is attributed to a nonequilibrium emission mechanism.

6. References

1. J. Randrup and R. Vandenbosch, Nucl. Phys. **A474**(1987)219.

PROJECTILE FRAGMENTATION EVOLUTION IN PERIPHERAL COLLISIONS

A Study of ^{16}O and ^{24}Mg on ^{197}Au over the Intermediate Energy Domain

L.Beaulieu[1], D.Doré[1], R.Laforest[1], J.Pouliot[1], R.Roy[1], C.St-Pierre[1], G.Auger[2], P.Bricault[2], S.Groult[2], É.Plagnol[2], D.Horn[3,4], J.L.Laville[4], O.Lopez[4], R.Régimbart[4] and J.C.Steckmeyer[4]

[1]*Laboratoire de Physique Nucléaire, Université Laval, Ste-Foy, Québec, G1K 7P4, Canada*
[2]*Grand Accélérateur National d'Ions Lourds, BP5027, 14021 Caen CEDEX, France*
[3]*AECL, Chalk River Laboratory, Chalk River, Ontario, K0J 1J0, Canada.*
[4]*Laboratoire de Physique Corpusculaire, Université de Caen, F-14032 Caen, France*

Physics Motivations

The general goal of these experiments was to study the evolution, with beam energy, of projectile fragmentation at intermediate energies by measuring all or most of the charged projectile-breakup products with a multi-element forward array. One of the important findings was to observe that the projectile excitation energy can become quite high, even from peripheral collisions. The specific physics questions explored can be summarized as follow:

1- BREAKUP CROSS-SECTION evolution: What is the role of transfer reactions ?
2- EXCITATION ENERGY in peripheral collisions: Have we reached the limit ?
3- EXCITATION ENERGY SHARING: What is the degree of thermalization ?
4- BREAKUP MECHANISM: Sequential or prompt ? $^{16}O \rightarrow \alpha\alpha\alpha\alpha$ at 32.5 A, 50 A and 70 A MeV, and $^{24}Mg \rightarrow \alpha\alpha\alpha\alpha\alpha\alpha$ at 50 A and 70 A MeV.

Experimental Setup

The reaction $^{16}O + ^{197}Au$ has been studied at 50 A and 70 A MeV [1]. The charged particles were detected in a close-packed forward array of 44 phoswich detectors. For the ^{24}Mg beam, a ring of 16 phoswiches and 32 time-of-flight scintillators (outer rings of the MUR) were added. The complete experimental setup is shown at Fig. 1. Two silicon telescopes have replaced two phoswiches to provide heavy mass resolution. The global polar angular range goes from 1.3° to 40° for all azimuthal angles, with a very good granularity, coverage and energy resolution needed to extract quantitative information from high multiplicity events. Any detector at θ_{lab} less than 24° was a trigger.

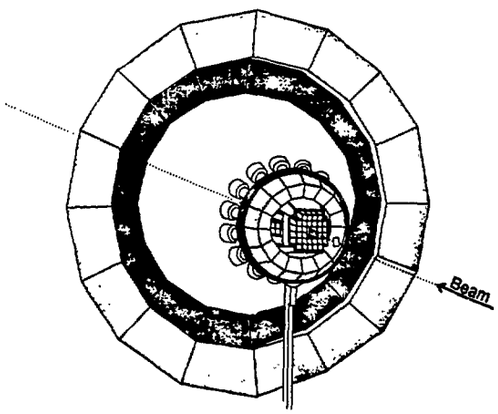

Figure 1.
Schematic view of the experimental setup.

Figure 2.
Calibration spectrum from secondary beams.

The energy calibration has been provided from secondary beams produced by beam fragmentation [2]. These were selected by the magnetic rigidity of the beam line elements and scattered on a Au target to give, in a short period of time, spectra as shown in Fig. 2. Up to twenty eight calibration points were obtained for most of the phoswich detectors.

Cross Sections

The absolute breakup cross sections, corrected for detection efficiency, for quasi-elastic (ΣZ=8) [1] and transfer reactions (ΣZ=5,6,7 and 9) [3] are shown in Fig. 3 for channels listed in Table 1. The similar trend of the cross sections at the three energies is striking, as manifested by the strong Q-value dependence already observed at 32.5 A MeV [4] and still present at 50 and 70 A MeV. The fluctuations around the strict exponential Q-value dependence (see for instance Q around -32 for ΣZ=8) present at the three energies can be explained by the different number of isotopic combinations contributing to a channel. One notices that the average slope of the Q dependence changes with energy. The yield for channels involving very negative Q values is increased relatively to the other channels. This suggests an evolution of the excitation energy distribution of the quasi-projectile with increasing beam energies. Transfer reaction cross sections remain quite high, even at the 70 A MeV.

Excitation Energy

The excitation energy of the primary projectile-like nuclei has been calculated event by event. We have retained channels involving charges equal to or greater than two. The excitation energy spectra of the primary projectile are shown in Fig. 4 for the decay into four He nuclei. Both the mean value and the inverse of the slope increase with beam energy. The same increases are also observed for all the other channels. The change of the mean values between either 32.5 and 50 A MeV, or 50 and 70 A MeV is roughly 23 % for all channels. This average increase is relatively modest compared to the gain of the available energy in the center of mass.

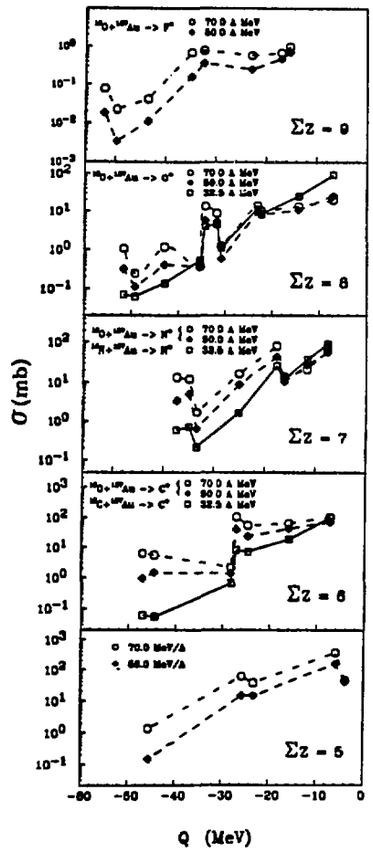

Figure 3
Quasi-elastic and transfer breakup cross sections

Table 1: Channels and their Q values (MeV) plotted in Fig. 3

Σ Z = 9		Σ Z = 7	
B He He	-15.3	C H	-7.6
Li He He He	-17.0	B He	-11.6
C H H H	-22.9	Li He He	-16.1
Li He He H	-32.4	He He He H	-17.6
He He He H H H	-34.9	B H H	-25.1
B H H H H	-43.5	Li Li H	-33.4
Li Li H H H	-49.7	Li He H H	-34.9
Li He H H H H	-52.2	He He H H H	-37.4
Σ Z = 8		**Σ Z = 6**	
C He	-7.2	He He He	-7.3
He He He He	-14.4	B H	-16.0
C H H	-22.3	Li He H	-24.6
B He H	-23.1	He He H H	-27.1
B Li	-30.9	Li Li	-28.2
Li He He H	-31.8	Li H H H	-44.5
He He He H H	-34.3	He H H H H	-46.9
Li Li He	-35.4	**Σ Z = 5**	
B H H H	-42.9	Li He	-3.9
Li Li H H	-49.2	He He H	-5.9
Li He H H H	-51.6	Li H H	-23.3
He He H H H H	-54.1	He H H H	-25.8
Li H H H H H	-71.4	H H H H H	-45.6

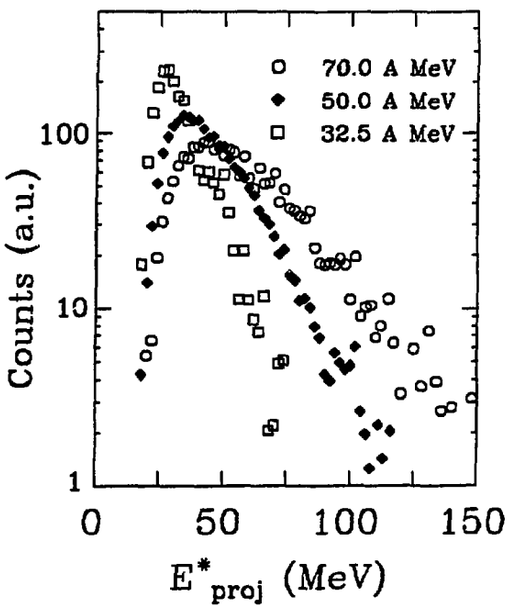

Figure 4
Experimental excitation energy spectra of the primary projectile-like nucleus breaking up into four helium nuclei. A comparison between three bombarding energies is shown.

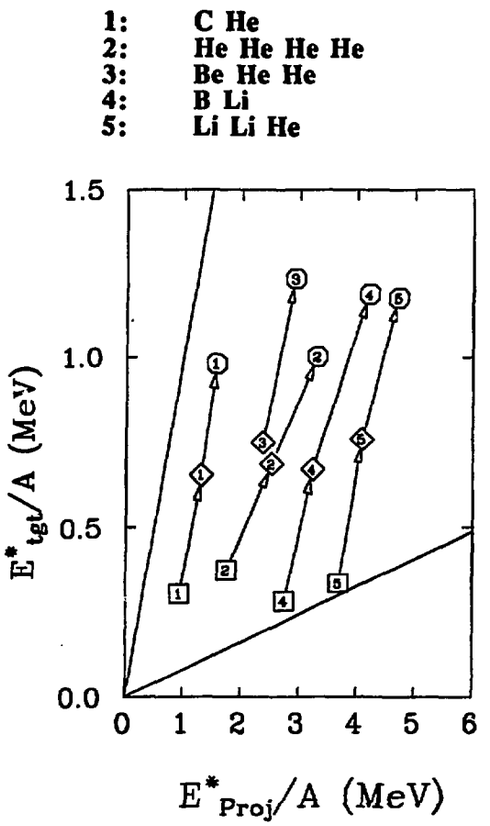

Figure 5
Target vs projectile excitation energy in MeV per nucleon.

Excitation Energy Sharing

The sharing of the total excitation energy between projectile and target is of great importance in understanding reaction mechanisms. The two extremes of this energy sharing are a fully thermally equilibrated system (equal temperature limit ETL, R=12) and a fast reaction (equal energy sharing EES, $R = E^*_{tgt}/E^*_{proj} = 1$). The large mass asymmetry is well adapted to discriminate between the two extremes.

The excitation energy of the target was deduced event by event from two-body kinematics. The most probable values for the excitation energy is plotted in Fig. 5 versus the values for the projectile. The arrows connect the results of a specific channel for the three bombarding energies. One can observe from the arrows that the change in excitation energy is roughly the same for all channels. The ratios, the excitation energy of the target divided by the one for the projectile, increase with bombarding energies but are still far from a thermally equilibrated target-projectile system.

At 32.5 MeV per nucleon, the maximum excitation energy of the projectile can become quite high (4-6 MeV per nucleon, see Fig.4). Although it still increases with higher bombarding energies, most of the new available energy is taken by the target-like nucleus. That seems to indicate that the excitation energy of the projectile-like is near saturation and can no longer increase significantly (Fig.5).

^{16}O --> α α α α: Prompt or Sequential ?

It has been predicted that the statistical emission of light particles via sequential decay at low energy would be replaced by a prompt breakup mechanism when the excitation energy becomes sufficiently high. This threshold was expected to be around 3 A MeV [5]. The four alpha breakup channel is appropriate to display kinematical differences between prompt breakup and sequential decay. Fig. 6 presents a comparison of the experimental distributions of relative angles to simulations of a sequential binary decay process (solid line) and to a simultaneous multifragmentation (dashed line). Graphs at 25 A and 32.5 A MeV are from ref. 6 and 7. The experimental results are well reproduced by a sequential mechanism, even when only highly excited events (E*/nucleon ≥ 4.4 MeV) are selected. No Coulomb suppressions predicted at small relative angles by the prompt decay model are observed. This indicates that sequential emission is responsible for the breakup of ^{16}O into four alpha particles over a large portion of the intermediate energy domain.

The analysis of the ^{24}Mg breakup into six alphas at 50 A and 70 A MeV is underway. It will be interesting to see how the breakup mechanism evolves with this higher multiplicity channel produced at most likely higher excitation energies.

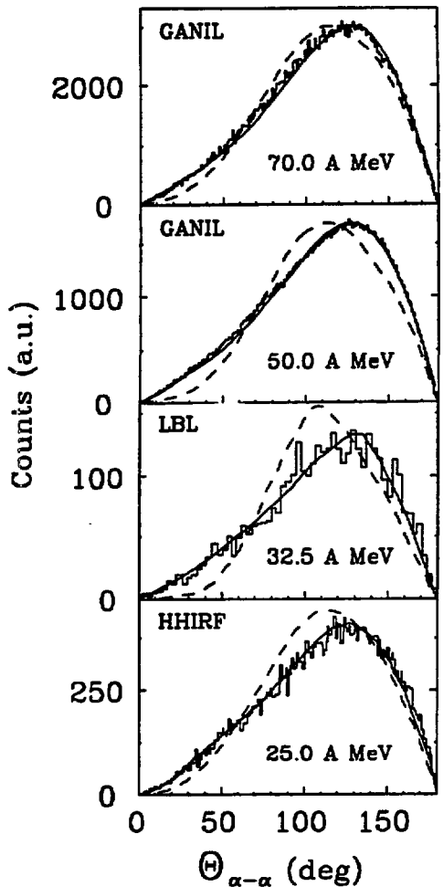

Figure 6

Relative angle distributions for the four helium channel. Data, sequential and prompt decay simulations are represented by the histograms,solid and dash-lines respectively.

Conclusions

The cross sections for the most negative Q-value channels increase with bombarding energies. Moreover, excitation energy distributions show that very excited projectiles are produced in peripheral collisions. Although the excitation energy of the projectile still increases with bombarding energy, that increase is accompanied by a much larger excitation energy gain for the target. One also observes that transfer reactions still play an important role in the intermediate energy domain. It is clear, from the last statement and from the predominance of sequential decay over the prompt breakup that low energy phenomena are still needed to describe the experimental results around and well above the Fermi energy. The ^{24}Mg data currently under analysis should strengthen many of these aspects and arise others.

References

(1) J.Pouliot *et al.*, Phys. Lett. B263(1991)18.
(2) D.Doré *et al.*, submitted for publication.
(3) R.Laforest *et al.*, submitted for publication.
(4) J.Pouliot *et al.*, Phys. Rev. C43(1991) 735.
(5) X.Campi *et al.*, Phys. Lett. B142 8 (1984).
(6) J.Barreto *et al.*, private communication and to be published.
(7) B.A.Harmon et al.,Phys. Lett. B235 (1990)234.

ARGON PROJECTILE FRAGMENTATION AT 60 MeV/nucleon

J. Barrette[1a], C. Beck[3], B. Berthier[1], Y. Cassagnou[1], J-L. Charvet[1], R. Dayras[1], H. Delagrange[4], B. Djerroud[3], B. Faure[1b], F. Gadi[1c], B. Heusch[3], G. Lanzano[2], R. Legrain[1], R. Lucas[1], C. Mazur[1], A. Pagano[2], E.C. Pollacco[1], J-E. Sauvestre[1], U. Sparti[2], S. Urso[2], C. Volant[1], J-P. Wieleczko[4]

[1]*DAPNIA/SPN CEN.Saclay, 91191 Gif-sur-Yvette Cedex, France*
[2]*INFN, Corso Italia 57, 95129 Catania, Italy*
[3]*Centre de Recherches Nucléaires, 67037 Strasbourg Cedex, France*
[4]*GANIL, BP 5027, 14021 Caen Cedex, France*

1. Motivations

Projectile fragmentation at intermediate energy has been extensively investigated by inclusive measurements[1,2] and the data have been generally interpreted in the framework of the abrasion-ablation model[2]. Nevertheless, data obtained from exclusive experiments, $^{40}Ar + {}^{27}Al,{}^{nat}Ti$ at 44 MeV/u[3], $^{40}Ar + {}^{nat}Ag$ at 27 MeV/u[4] and 30 MeV/u[5], measuring either the correlations between projectile-like (PLF) and target-like fragments (TLF) or the excitation energy partition between fragments, showed very clearly the persistence of dissipative collisions where the nuclear mean field still plays an important role. In order to follow the evolution of the projectile fragmentation with the incident energy we studied the reaction $^{40}Ar + {}^{nat}Ag$ at 60 MeV/u in two separate experiments. The first measured the correlations between projectile-like and target-like fragments[6]. In the second one coïncidence measurements between PLF and light charged particles (LCP) have been investigated[7].

2. PLF-TLF correlations

In the first experiment the set-up included a silicon telescope, located at 3.5°, which identified PLF's by their energy, charge and mass using a time of flight spectrometer. A battery of 8 silicon detectors, positionned between 15° and 85° in the same plane as the PLF telescope on the other side of the beam, measured the energy and the time of flight of the TLF's. The energy threshold of the TLF's was less than 1 MeV. The mass calibration of the TLF's was obtained by measuring the recoil energy and velocity of the target in the following elastic reactions: ^{40}Ar + Ni , Ag at 44 MeV/u and ^{40}Ar + Ag at 60 MeV/u. Due to the low kinetic energy of the recoil target the pulse-height defects in the detectors were important and corrected for by using the procedure established by Kaufman et al.[8].

The data were analysed by selecting every PLF's charge detected at 3.5 degrees, calculating the mean value of the associated PLF mass, and by looking at the evolution of the corresponding mean values of the TLF's angular, velocity and mass distributions. Figs.1-3 display the trends of these correlations as a function of the mean value of the PLF mass. Note that the mean velocities of each PLF measured in coïncidence with TLF were between 5 to 10% lower than the beam velocity in agreement with single measurements. As the detected PLF's mass decreases, the TLF's are emitted more and more in the forward direction and their velocity increases. This correlation bears close resemblance to

what is expected in binary dissipative collisions. On the other hand, the mass-mass correlation in fig.3 appears to be relatively flat. Although in the $^{40}Ar + Ag$ reaction at 60 MeV/u a large range of PLF fragments are produced, down to very light fragments, the corresponding masses of the TLF's remain close to the target one.

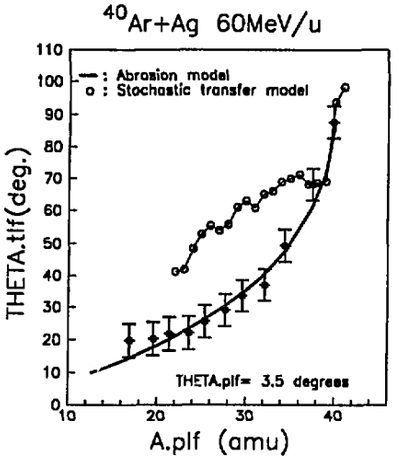

Fig.1: TLF's average recoil angle as a function of the mass of the associated PLF (full circles). Bars represent 5° deviations. Open circles and curve are the results of calculations described in the text.

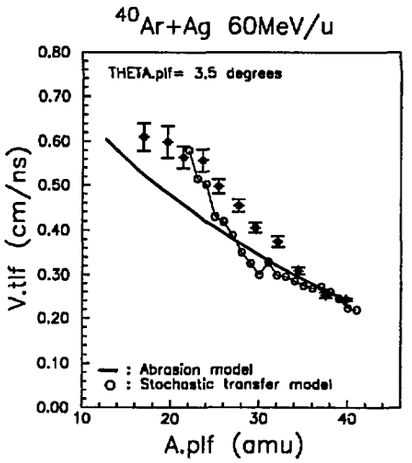

Fig.2: TLF's average recoil velocity as a function of the mass of the associated PLF. Error bars are statistical. The symbols have the same meaning as in Fig.1.

The data were compared with the predictions of two calculations. The first, represented by full curves in figs.1-3, is the abrasion model which includes dissipation[2]. In this case, the detected PLF and TLF are the quasi-cold spectators and the undetected fireball carries all the excitation energy. The second corresponds to a calculation by Tassan-Got[9] (open circles in figs.1-3) following the prescription of Randrup[10]. Briefly, it is an event-by-event Monte Carlo simulation based on the stochastic exchange of nucleons between projectile and target. It is to be noted that in general the exchange results in a small net mass transfer, thus the detected PLF and TLF are the evaporation residues of projectile and target sources, carrying an amount of excited energy depending on the impact parameter. We can see that, except for the PLF-TLF velocity correlation (fig.2), none of the two calculations is able to reproduce the totality of the PLF-TLF correlations. In particular, the discrepancy between the abrasion model prediction and the experimental PLF-TLF mass correlation has to be underlined (fig.3). On the other hand, the stochastic exchange model fails to reproduce the PLF-TLF angular correlation (fig.1). In this last calculation the pre-equilibrium particle emission has not been taken into account although it should play an important role in the first step of the $^{40}Ar + Ag$ reaction at 60 MeV/u.

3. PLF-LCP correlations.

In a second experiment, with the same system at 58 MeV/u, we measured the coïncidences between the PLF and the light charged particles (LCP) emitted in the forward direction. The charge and the energy of the PLF were measured in six ΔE-E silicon

telescopes located on each side of the beam at 2.8°, 4.8° and 11.4°. A hodoscope of 22 BaF_2 crystals covering the polar angles between 2.8° and 10° was placed on one side of the beam to detect the LCP. Pulse shape discrimination was achieved by integrating separately the fast and slow component of the light signal in the crystals. The combination of the pulse shape discrimination and the LCP time-of-flight measurement allowed the determination of the energy, charge and mass of the LCP[11].

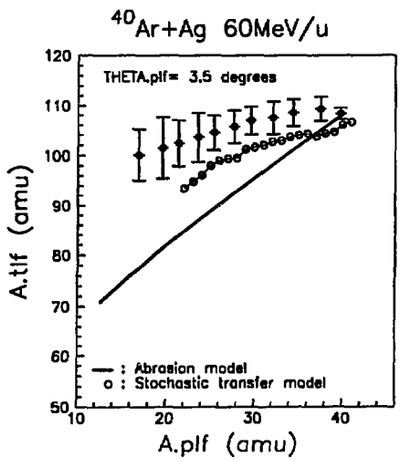

Fig.3: Detected mass of the TLF's vs the detected mass of the associated PLF's. Error bars are statistical. The symbols have the same meaning as in fig.1.

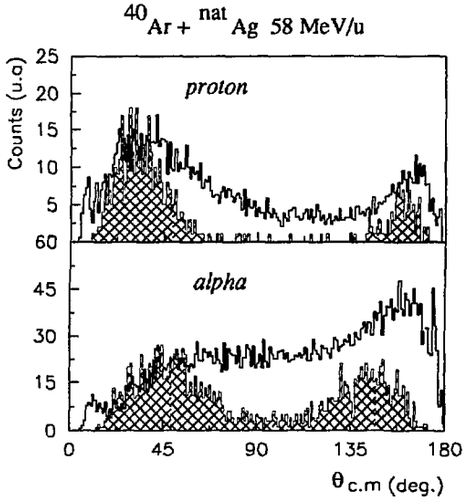

Fig.4: Angular distributions of proton and alpha particles plotted in the emitter reference frame. Comparison is made between experimental (histogram) and simulated (hatched area) data. PLF are detected at 2.8°.

The average multiplicity of LCP's with velocities close to the beam velocity increases almost linearly when the charge of the PLF's decreases, in agreement with the data of Steckmeyer et al.[12]. This trend suggests an emission from an excited quasi-projectile, the excitation energy of which increases as the mass of the observed PLF decreases. Such a sequential emission process is substantiated by the double-hump in the LCP energy spectra.

From the velocities of the PLF's and of the associated LCP's, it is possible to reconstruct the recoil velocity and direction of the emitting nucleus and to get the LCP angular distributions and energy spectra in the frame of the emitter. The resulting angular distributions of proton and alpha particles associated with PLF, detected at 2.8°, are represented by histograms in fig.4 in the emitter reference frame. In order to take into account the effects of the detection system acceptance we performed a simulation by using the event-by-event Tassan-Got[9] code based on the stochastic transfer model as mentionned in the previous section. The simulated data, normalised on the experimental angular distributions of protons and alphas emitted in the forward hemisphere in the emitter frame, are denoted by hatched areas in fig.4. From this comparison we can see that the whole proton data angular distribution is consistent with an emission by a hot equilibrated

projectile as it is supposed in the code. In contrast, the experimental alpha angular distribution shows an excess of particles emitted in the backward hemisphere in the emitter frame which enhances strongly a possible contribution from pre-equilibrium emission. This non-equilibrium component seems to increase with the mass of the emitted LCP.

In the emitter reference frame, the shape of the energy spectra is the same for the forward and backward emitted protons and is also consistent with the simulation. The experimental α-particle energy spectra are consistent with the simulation in the forward direction but extend to much higher energies in the backward direction, suggesting again a large non-equilibrium contribution in the backward hemisphere.

4. Conclusions.

Fragments of a 58 MeV/u ^{40}Ar bombarding a silver target seem to result essentially from the sequential decay of an excited quasi-projectile, the excitation energy of which increases as the mass of the detected fragments decreases and can reach temperatures as high as 5 MeV. This conclusion rules out the validity of the abrasion-ablation model at this intermediate energy and strengthens the strong dissipative binary character of the projectile fragmentation process. However, a sizeable contribution from pre-equilibrium emission is associated to the fragmentation process. In this case we can envisage that before the binary process takes place, a prolific pre-equilibrium particle emission could change the initial conditions of the two colliding nuclei by lowering the projectile mass and could explain the PLF-TLF mass correlation we measured in the ^{40}Ar + ^{nat}Ag at 60 MeV/u.

REFERENCES

(1) D. Guerreau , Nucl. Phys. A447(1985)37 and references therein
(2) R. Dayras et al., Nucl. Phys. A460(1986)299
(3) R. Dayras et al., Phys. Rev. Lett. 62(1989)1017
(4) B. Borderie et al., Ann. Phys. Fr. 15(1990)287
(5) F. Gadi-Dayras, Thèse d'Université n°611, Orsay, Juin 1988
(6) J-L Charvet et al., Proc. of the XXVIII International Winter Meeting on Nuclear Physics (Bormio 1990) p.351
(7) J-E Sauvestre et al., Proc. of the XXIX International Winter Meeting on Nuclear Physics (Bormio 1991) p.91
(8) S.B. Kaufman et al., Nucl. Inst. and Methods 115(1974)47
(9) L. Tassan-Got, Thèse d'Etat, Orsay, Juin 1988
(10) J. Randrup, Nucl. Phys. A383(1982)468
(11) G. Lanzano et al., Nucl. Inst. and Methods (accepted for publication)
(12) J.C. Steckmeyer et al. , Nucl. Phys. A500(1989)372

present address:
a- Foster Radiation Laboratory, Mac Gill University, Montreal, P.Q. Canada H3A2B2
b- Institut de Physique Nucléaire, BP 1, 91406 Orsay, France
c- DTA/CEREM CEN.Saclay, 91191 Gif-sur-Yvette Cedex, France

THE INTERACTION OF 93 MEV/NUCLEON ^{36}Ar WITH ^{197}Au - PARTICIPANT - SPECTATOR PHYSICS?

K. Aleklett[1], J.O. Liljenzin[2], W. Loveland[3], L. Sihver[1]

[1]*Studsvik Neutron Research Laboratory, S-611 82 Nyköping, Sweden*
[2]*Chalmers University of Technology, S-412 96 Göteborg, Sweden*
[3]*Oregon State University, Corvallis, OR 97331, USA*

1. Motivation

Previous studies[1,2] of the Ar + Au and C + Au systems intermediate energies have shown the increasing importance of heavy residue formation (relative to fission) with increasing projectile energy (Figure 1). We thought it would be interesting to extend our studies to a significantly higher energy where "participant-spectator" mechanisms for producing target fragments might begin to operate. Accordingly we present, in this report, preliminary results from a radiochemical measurement of the target fragment yields, angular distributions and energy spectra for the interaction of 93 MeV/nucleon ^{36}Ar with ^{197}Au.

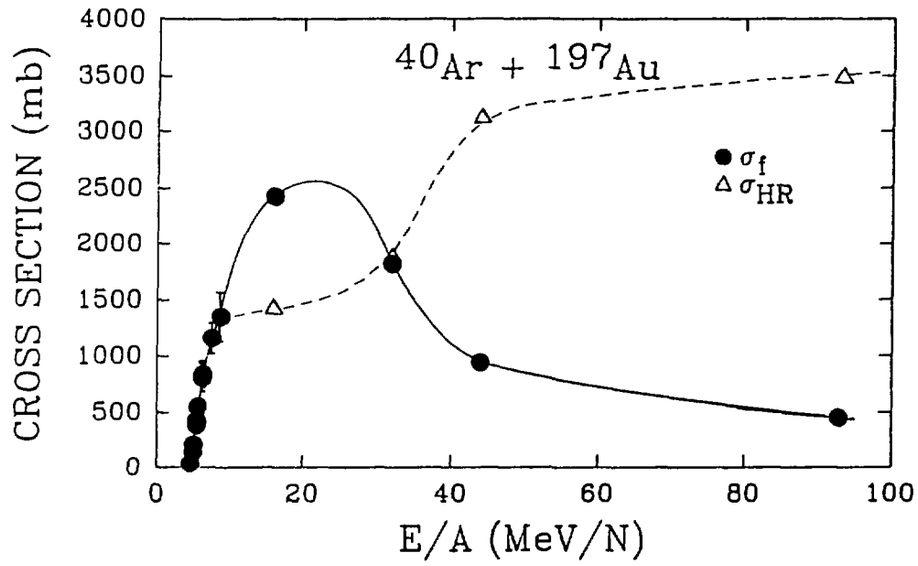

Figure 1. Variation of the fission cross section (solid points) and the heavy residue formation cross section (triangles) with projectile energy for the Ar + Au system. The points at 93 MeV/A are from this work.

2. Results

These single particle inclusive measurements took place at GANIL. The entire experiment took 13 minutes of beam, in which 3.1×10^{13} ions were delivered to the target. Following procedures that have been described elsewhere,[3,4] we calculated the fragment isobaric yield distribution from the measured nuclidic yields. The resulting fragment mass distribution is shown in Figure 2a. The fragment mass yields decrease essentially

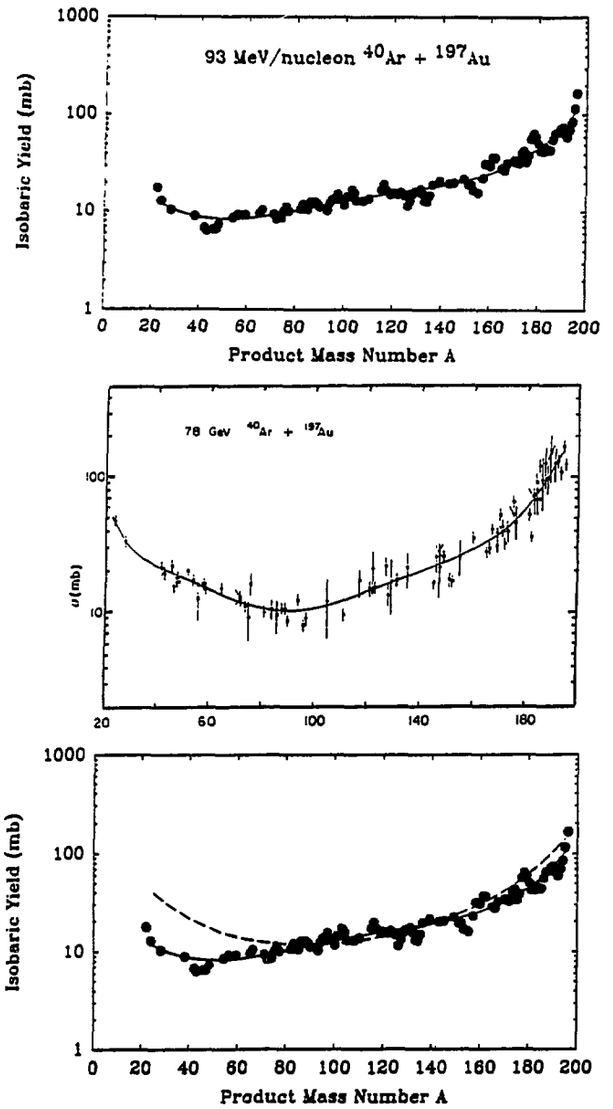

Figure 2. (a) Measured fragment isobaric yield distribution for the interaction of 93 MeV/nucleon ^{36}Ar with ^{196}Au. (b) Same as (a) except reaction is 1.95 GeV/nucleon ^{40}Ar + ^{197}Au (ref. 5). (c) Comparison of distributions in (a) and (b).

exponentially from massnumbers near the target to the lightest observed product mass numbers. Qualitatively this is characteristic of reactions[5] at much higher energies (Figure 2b). In Figure 2c, we directly compare the fragment isobaric yield distributions from the interaction of 93 MeV/A ^{36}Ar (solid points, solid line) and 1.95 GeV/A ^{40}Ar (dashed line) with ^{197}Au (ref. 5). Apart from the yields of the intermediate mass fragments A < 60), there are remarkably similar shapes for the fragment isobaric yield distributions for these two reactions induced by projectiles of disparate energy. This agreement appears to be yet another example of the concepts of total projectile kinetic energy scaling of fragment yields and limiting fragmentation. (It is well-known that the fragment yield distributions are similar for the interaction of 3 GeV and 78 GeV protons with ^{197}Au.)

Because of this similarity in mass-yield distributions between the reaction of 93 MeV/nucleon and 1.95 GeV/nucleon Ar with ^{197}Au, we felt we should look at other characteristics of the two reactions to see how they compare. In Figure 3 we compare the measured angular distributions for A ~ 125 nuclei from the interaction of 93 MeV/nucleon ^{36}Ar (solid triangles), 85 MeV/nucleon ^{12}C (solid line), 400 MeV/nucleon ^{20}Ne (dashed line) with ^{197}Au. The distribution from the Ar induced reaction is more forward-peaked than the reactions induced by the 1-8 GeV projectiles. Similarly, the longitudinal momentum transfer in the ^{40}Ar induced reaction is much greater than that seen in typical relativistic heavy ion reactions (Figure 4).

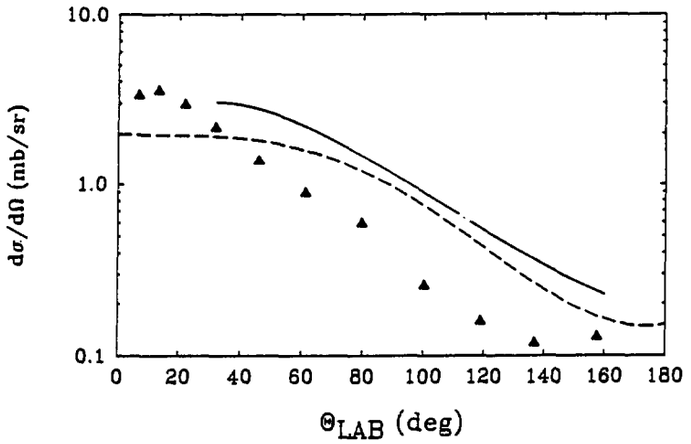

Figure 3. Comparison of A ~ 125 fragment angular distributions for the interaction of 93 MeV/nucleon ^{36}Ar (solid triangles), and 85 MeV/nucleon ^{12}C (ref. 7) (solid line) and 400 MeV/nucleon ^{20}Ne (dashed line) with ^{197}Au.

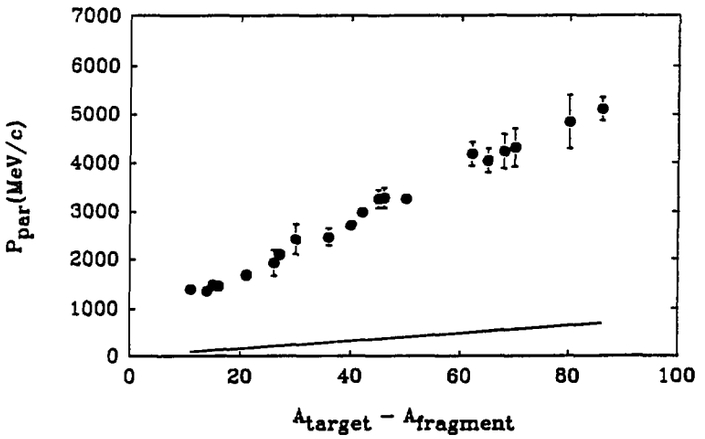

Figure 4. Comparison of the average longitudinal momentum transfer as a function of mass loss for the interaction of 93 MeV/nucleon ^{40}Ar with ^{197}Au (solid points) and that predicted by the systematics[8] of momentum transfer in projectile and target fragmentation at relativistic energies (solid line).

Yet another demonstration that the "participant-spectator" conditions have not been met in the 93 MeV/nucleon ^{40}Ar + ^{197}Au reaction are the observed widths of the momentum distributions (Figure 5) which are much larger in the reaction under study than typically observed in relativistic heavy ion reactions. Thus, despite the similarity in mass-yield distributions between the reaction of 93 MeV/nucleon ^{46}Ar + ^{147}Au with typical relativistic heavy ion induced fragmentation of ^{197}Au, a "participant-spectator" mechanism is not consistent with other aspects of the data.

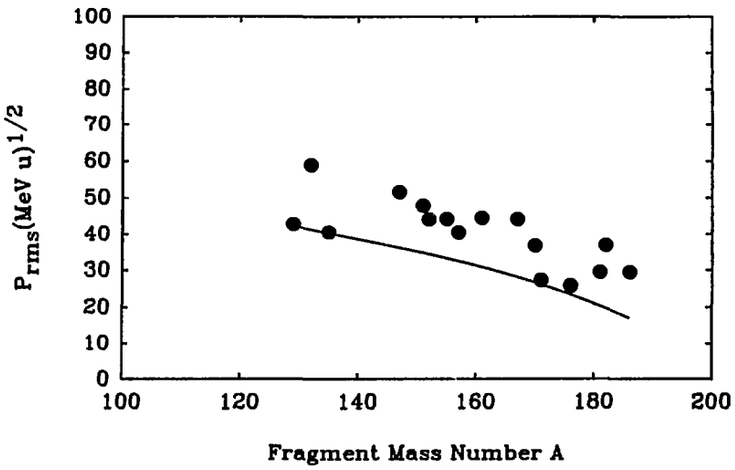

Figure 5. Comparison of the average rms fragment momentum from the interaction of 93 MeV/nucleon ^{36}Ar with ^{197}Au (solid points) with that expected from the systematics[8] of relativistic heavy ion reactions (dashed line).

REFERENCES

1. W. Loveland, K. Aleklett, L. Sihver, Z. Xu, C. Casey, D.J. Morrissey, J.O. Liljenzin, M. de Saint-Simon, and G.T. Seaborg, Phys. Rev. C41, 973 (1990).

2. K. Aleklett, M. Johansson, L. Sihver, W. Loveland, H. Groening, P.L. McGaughey, and G.T. Seaborg, Nucl. Phys. A499, 591 (1989).

3. D.J. Morrissey, D. Lee, R.J. Otto, and G.T. Seaborg, Nucl. Inst. Meth. 158, 499 (1978).

4. D.J. Morrissey, W. Loveland, M. de Saint-Simon, and G.T. Seaborg, Phys. Rev. C21, 1783 (1980).

5. Wenxin Li, W. Loveland, K. Aleklett, and G.T. Seaborg, Oregon State University Nuclear Chemistry Progress Report DOE/ER/70035-7, September, 1984.

6. R.H. Kraus, Jr. et al., Nucl. Phys. A432, 525 (1985).

7. J.B. Cumming, P.E. Haustein, and R.W. Stoenner, Phys. Rev. C33, 926 (1986).

8. D.J. Morrissry, Phys. Rev. C39, 460 (1989).

DEEPLY INELASTIC COLLISIONS IN 32 MEV/NUCLEON KR INDUCED REACTIONS ON AU AS VIEWED BY 4π NEUTRON MULTIPLICITY MEASUREMENTS.

E.Crema[a,b], S.Bresson[a], H.Doubre[a], J.Galin[a], B.Gatty[c], D.Guerreau[a], D.Jacquet[c], U.Jahnke[d], B.Lott[e], M.Morjean[a], E.Piasecki[a,f], J.Pouthas[a], F.Saint-Laurent[a], E.Schwinn[d], A.Sokolov[a], X.M.Wang[a,g]

[a] *GANIL, B.P.5027, F-14021 Caen Cedex, France*
[b] *Instituto de Fisica da Universidade de Sao Paulo, Sao Paulo,Brazil*
[c] *IPN, B.P.1, F91406 Orsay Cedex, France*
[d] *Hahn Meitner Institute, W-1000 Berlin 39, Germany*
[e] *CRN Strasbourg, B.P. 20 CRO, F-67037 Strasbourg Cedex, France*
[f] *Institute of Experimental Physics, Warsaw University, Hoza 69, PL-00-681 Warsaw, Poland*
[g] *Institute of Modern Physics, P.O. Box31, Lanzhou, China*

1. Motivations

At bombarding energies of about 30 MeV/nucleon, deep inelastic collisions have been shown to still represent a sizeable fraction of the reaction cross section and constitute a very efficient way to heat up nuclei[1]. Measurements have been undertaken on a rather heavy system (Kr+Au) for which, at low bombarding energy, fusion is known to occur with a very small probability and deep inelastic reactions exhaust a large fraction of the total reaction cross section. The aim of the experiment was two fold. First, we wanted to see to what extent the available energy could be dissipated in these deep inelastic collisions, and then, where this dissipated energy could be found.

2. Experimental approach

Projectile-like residues having suffered a deep inelastic collision have been detected and identified in Z by means of a high resolution silicon telescope, set close to the grazing angle (7°). Neutrons were measured in correlation, using the 4π ORIONI detector, a $3m^3$ liquid scintillator tank, loaded with Gd. In addition to the total multiplicity of neutrons measured event wise, the segmentation of ORIONI in four adjaccent sectors, centered on the beam axis, allowed significant measurements of the spatial distribution of the neutrons. As it will be shown, this information is crucial in order to infer the origin of the neutrons.

3. The data

The most interesting part of the data, in so far as the influence of impact parameter is considered in these peripheral reactions, is well shown on the scatter plots of Fig.1 for some representative projectile-like fragments. For the highest Z's, down to Z about Z=20, two distinct blobs of data points can be distinguished, characterized by different kinetic energies and neutron multiplicities, M_n. Whereas the most dissipative collisions (E<1GeV) are always characterized by very large Mn values, it is shown that, for the less dissipative ones, there is a strong correlation between kinetic energy of the projectile remnant and associated neutron number. Similar patterns were observed in Ar induced reactions.[2] Many different impact parameters must contribute to generate such different projectile residues detected at a unique angle. For the largest impact parameters, dissipation is weak and the trajectory is essentially governed by Coulomb forces leading to a scattering angle close to the grazing angle. On the contrary, for the inner impact parameters involved here the energy damping is huge and the projectile must have orbited towards negative angles before being released. These two components are best observed for fragment Z's close to the projectile Z. They are parts of the two branches distinguishable in a Wilczinski plot[3], when the yields are represented in an energy versus emission angle space. The neutron multiplicity provides a very sensitive

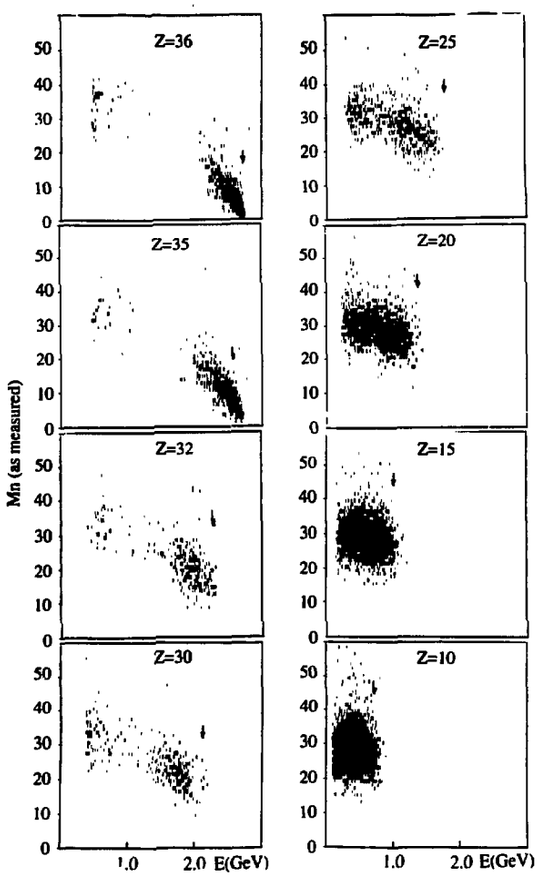

Fig.1 Scatter plot of projectile-like fragments detected at 7° in the 32 MeV/u Kr+Au reaction as a function of E and neutron multiplicity (as measured). The arrows correspond to fragments with the beam velocity.

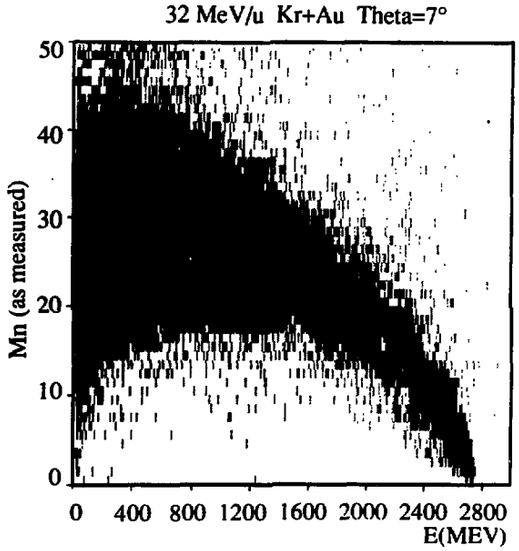

Fig. 2 Correlation between the kinetic energy of nuclei with $2 \leq Z \leq 37$ detected at 7° and neutron multiplicity (as measured i.e. without detection efficiency correction)

measurement of energy dissipation as this is well illustrated in Fig.2, where all data ($2 \leq Z \leq 37$) obtained at 7° have been summed up irrespective of Z.

The second question raised by the neutron data concerns the origin of these neutrons and the quantitative information they can provide relative to heat. In order to be illustrative, the exit channel with Z=28 has been selected, with events of average kinetic energy E=1600 MeV (i.e. roughly 26 MeV/u, to be compared with the 32 MeV/u Kr beam). Although the projectile has been relatively weakly slowed down, one can demonstrate that the target nucleus has been strongly heated up. The distribution of the neutrons in the four sectors of ORION are shown in Fig.3, as well as Monte Carlo calculations considering the detected fragment and its target partner (assuming two-body kinematics) as the main sources of neutrons. The detection efficiency is folded in the simulation code. Due to the large velocity of the projectile-like fragment, its evaporated neutrons can never reach the backward sector (A). One can thus use this selectivity to infer, from the data point of A, the total multiplicity of those neutrons emitted by the target-like fragment (open area) and show that there are much fewer neutrons that can be emitted by the projectile-like fragment (hatched area). It can also be seen that in the most forward sector (D) the simulation underestimates the number of measured neutrons. This is understandable since preequilibrium neutrons have been simply neglected in the simulation. In order to assess an excitation energy of the target-like nuclei from the deduced multiplicity of 30 evaporated neutrons, evaporation codes have been used, leading to $E \geq 700$ MeV or $T \geq 6$ MeV (assuming the level density parameter a=A/10). This example proves that pretty hot nuclei can be formed in rather peripheral collisions. Indeed, for the collisions leading to Z=28, as

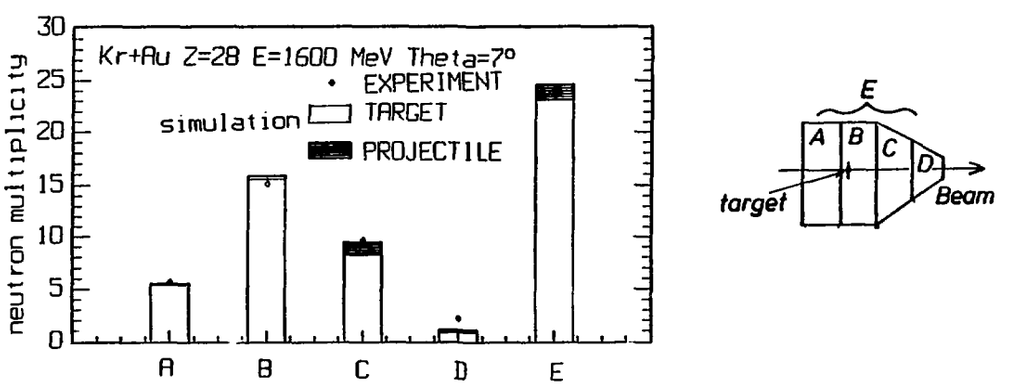

Fig.3 Number of neutrons detected from backward (A) to forward (D) and in the whole detector (E). The experimental data are given by open dots. Emission from projectile- and target-like nuclei is given by histograms after Monte Carlo simulation

considered above, the projectile-like nucleus has retained on the average 90% of its initial velocity. This implies that projectile and target nuclei have very little overlapped, as this was well illustrated by Rivet et al[1] in Landau-Vlasov calculations performed on a different system but at similar beam velocity. Because of the high impact parameters involved and the large observed dissipation, one also expects fairly large amounts of the initial angular momentum to be found as intrinsic spins of the partners in the exit channel. Indirect clues of such effects were obtained in Pb induced reactions when bombarding Au at comparable velocities. [4]

REFERENCES:

(1) M.F.Rivet et al. Phys. Lett. **B215**, 55 (1988)
(2) M.Morjean et al. Phy,s. Lett. **B203**, 215 (1988) and Nucl. Phys.**A524**, 179 (1991)
(3) J.Wilczynski Phys. Lett. **B47**, 484 (1973)
(4) S.Bresson et al. submitted to Phys. Rev. Lett. and contribution to the present volume

BINARY FISSION OF SPIN-ALIGNED PROJECTILE-LIKE NUCLEI IN THE $^{208}Pb+^{197}Au$ REACTION AT 29 MEV/NUCLEON

S.Bresson[a], M.Morjean[a], L.Pienkowski[a,b], R.Bougault[c] J.Colin[c], E.Crema[a,d], J.Galin[a], B.Gatty[e], A.Genoux-Lubain[c], D.Guerreau[a], D.Horn[c,f], D.Jacquet[e], U.Jahnke[g], J.Jastrzebski[b], A.Kordyasz[h], C.Le Brun[c], J.F.Lecolley[c], B.Lott[i], M.Louvel[c], C.Paulot[a], E.Piasecki[h], J.Pouthas[a], B.Quednau[j], W.U.Schroeder[j], E.Schwinn[g], W.Skulski[b], J.Tökej

[a] *GANIL, B.P. 5027, 14021 Caen-Cedex France*
[b] *Heavy Ion Laboratory, Warsaw University, ul. banacha 4, 02-097 Warszawa, Poland*
[c] *Laboratoire de Physique Corpusculaire, Bd du Maréchal Juin, 14032 Caen-Cedex France*
[d] *Instituto de Fisica, Universidade de Sao Paulo, Brazil*
[e] *Institut de Physique Nucléaire B.P. 1, 91406 Orsay-Cedex*
[f] *Chalk River Laboratories, Atomic Energy of Canada Limited, Chalk River, Ontario, Canada KOJ IJO*
[g] *Hahn Meitner Institut, D1000 Berlin 39, Germany*
[h] *Institut of Experimental physics, Warsaw University, Hoza 69, 00-681 Warszawa, Poland*
[i] *Centre de Recherches Nucléaires Strasbourg, B.P.20 CRO, 67037 Strasbourg France*
[j] *University of Rochester, Rochester, New York 14627 USA*

1. Motivations

In a recent paper, Piasecki et al.[1] have reported on the presence of strong correlations between character of a collision, between 29 MeV/nucleon Pb and Au, and associated neutron multiplicity, M_n. In particular, in a certain range of neutron multiplicities, binary fission of the projectile-like nucleus appears to be a dominant exit channel. By choosing Pb as a projectile, the heaviest beam then available at GANIL, a nucleus with a rather high fission barrier, the most peripheral collisions could not be probed by means of fission. The most central collisions could not be probed either by this channel since the system disassembles into a large number of light particles and intermediate mass fragments.

By investigating in some details the characteristics of the fission fragments it is possible to gain relevant information on the fissioning nuclei, and this sheds light on the dissipative process for the corresponding impact parameters. In particular the transfer of relative angular momentum into intrinsic spin of the fissioning nuclei can be investigated since fission is well known to be very sensitive to this parameter.

2. The experimental approach

At variance with many previous experiments[2] which have used the kinematical characteristics of the *two* correlated fission fragments to infer the violence of a collision, in the present experiment one has detected a *single* fragment and utilized the associated neutron multiplicity as a filter on the impact parameter. Once such a filter is applied, all interesting properties of the considered fissioning nuclei can be inferred from the measured characteristics (Z, E, θ) of this unique fragment.

The experimental set-up has been described in details by Piasecki et al.[1]. The fission fragments of the projectile-like nucleus were detected by means of a position-sensitive telescope subtending a detection angle of 14°, between 6° ad 20°. It consisted of two silicon detectors (200μm and 500μm thick for ΔE and E respectively), each divided into strips which provided us with the position in X and Y. Atomic numbers could be resolved up to Z=50. Target-like fission could not be measured because of the high energy threshold of this detector. As for the neutrons, they were counted eventwise by the 4π detector, ORION, whose global detection efficiency was Monte Carlo estimated at 65% for the collisions under study.

3. The experimental data

The Galilei invariant cross-sections of the fragments are presented in Fig.1 in the plane of the velocities, parallel and perpendicular to the beam direction for three different Z's and four neutron multiplicity gates (as they were registered i.e. without any detector efficiency correction). For M_n smaller than 35, well known Coulomb rings are visible that have been fitted in order to carry out the main characteristics of the fissioning nuclei. As shown in Fig.2, the average recoil velocity and deflection angle of the fissioning nuclei remain essentially constant for a given neutron multiplicity gate: as expected, the characteristics of the fissioning nuclei do not depend on the mass asymmetry of the splitting.

It is worth noticing that the fissioning nuclei are deflected at an angle slightly inside the grazing angle of 6.2 deg., whatever the considered neutron gate. This is a signature of the peripheral character of the corresponding collisions, that could also be expected from the rather modest values of corresponding M_n. One will come back on this particular aspect of the collision (Θ finite) in order to show that this allows gaining information on the spin of the fissioning nuclei.

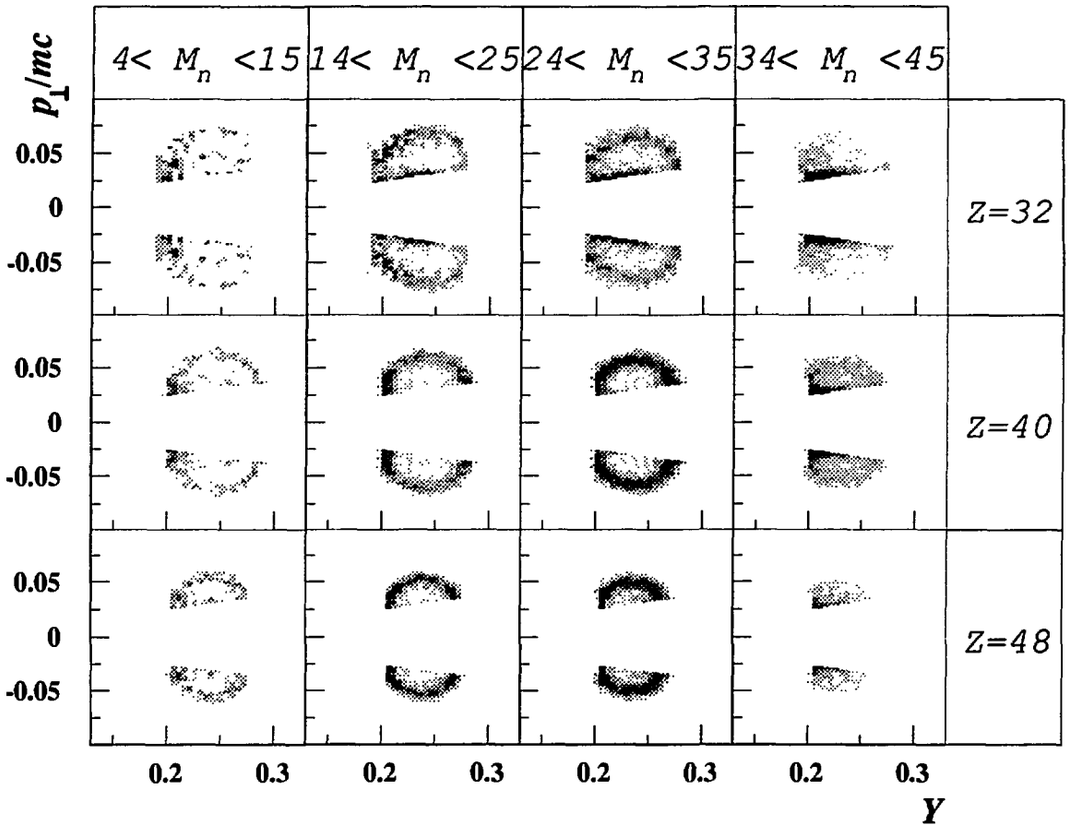

Fig 1 Invariant cross sections for several fission fragments characterized by their Z and gated by the associated neutron multiplicity.

The second point worth being stressed is related to the velocity of the fissioning nuclei. As expected, it slightly decreases with increasing M_n, as the collision becomes more dissipative. However, it remains in all cases fairly close to the beam velocity. This is a good signature of the rather peripheral character of the corresponding collisions. The dissipated energy can be inferred either from the deduced velocity of the projectile-like nucleus using a two-body kinematics or from the neutron multiplicity itself. Both approaches lead to consistent values of about 150, 360 and 550 MeV for the first three neutron gates considered in Fig.1. Taking into account the nearly symmetric character of the entrance channel, one is led to 75, 180 and 275 MeV excitation energies for the considered fissioning nuclei. This is rather small when

compared to the energy of 3 GeV available in this system. Again, this stresses the peripheral character of the corresponding collisions. The data from gate Mn=35-44 cannot be easily exploited because of the absence of well marked rings (Fig.1), which will be discussed further later on.

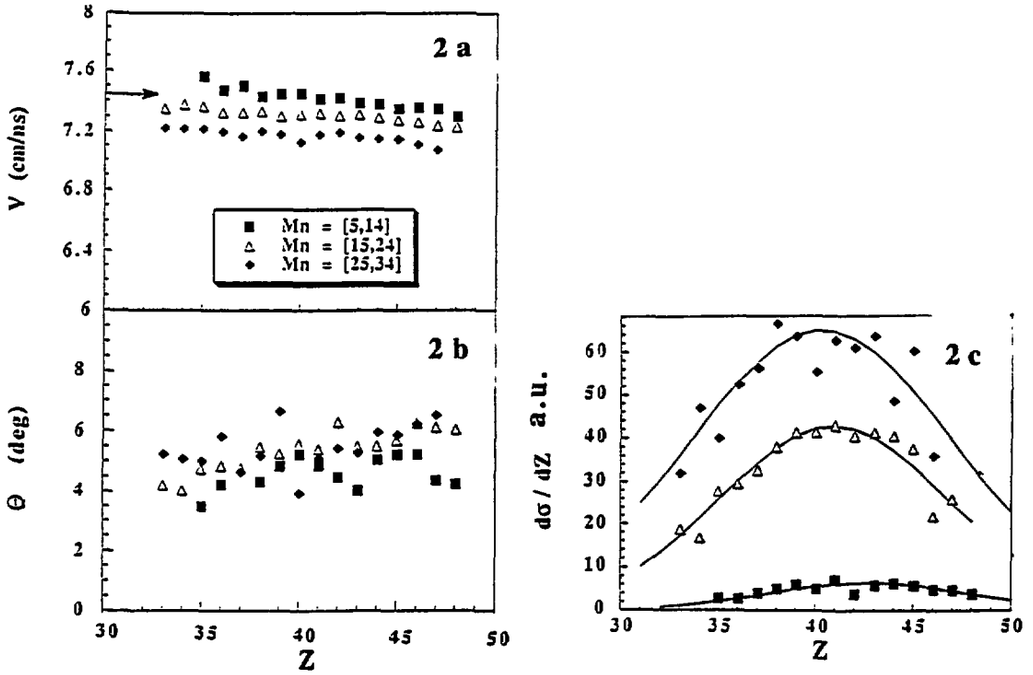

Fig.2a-b Characteristics of the fissioning nuclei (recoil velocity and deflection angle) as deduced from different Z's for several neutron multiplicity gates. Fig2c Fission fragment Z distribution.

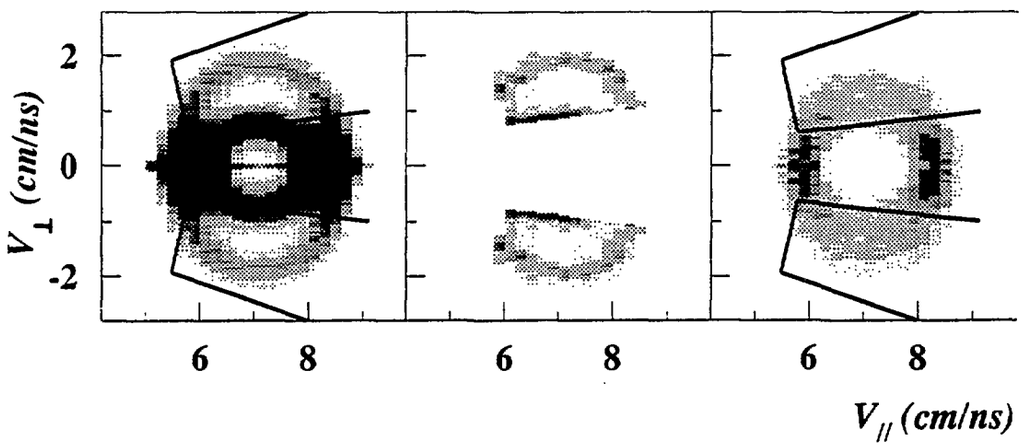

Fig.3 Monte Carlo simulations of the invariant cross sections for fission fragments assuming either high spin with strong alignment (left) or no spin (right) and comparison with experimental data (center). The area where experimental data are available is indicated by lines.

As a matter of fact, it is remarkable that the ring pattern of the invariant cross sections could be preserved with a fissioning nucleus not recoiling in the beam direction. This can be taken as an unmistakable evidence of strong spin effects. To show this, Monte Carlo simulations have been performed under two extreme and opposite assumptions. In these simulations, a fissioning nucleus with recoiling properties as derived from the above fitting procedure has been given either no spin at all or, on the contrary, high spin with strong spin alignment. In the first case the fragments are emitted isotropically in the emitter frame, in the second case emission is strictly restricted to the plane perpendicular to the spin axis i.e. to the reaction plane. The results of the simulation with large spins is qualitatively much closer to the experimental data than the calculated data under the assumption of low spin (Fig.3). One can easily guess that, if the fissioning nuclei had recoiled in the beam axis, such spin effects could not have been evidenced since one would have seen rings in any case.

Another information carried out from the experimental data are the differential cross sections $d\sigma/dZ$ once they have been integrated over the whole space. They exhibit gaussian shapes, roughly centered at half of the projectile Z. The small downward shift of the centroid with increasing M_n reflects mainly the onset of charged particle emission when the excitation energy increases[3]. Indeed, for such a nearly symmetric system in the entrance channel, no change is expected, on the average, in the mean Z of the pojectile-like nucleus, but only a broadening in the distribution[4]. The projectile-like fission cross section integrated over neutron multiplicities smaller than 35 amounts to 880 mb. Even when considering in the next M_n window events that can still be considered as binary fissions, the total fission cross section amounts at best to 20% of the reaction cross section. This provides an additional hint for the rather peripheral character for all collisions leading to fission.

Why does the ring pattern evolves towards a disk pattern for the high neutron multiplicities? Can this be taken as a clue for smaller spins or weaker spin alignment?. As a matter of fact, other effects can blur the ring picture. The first one is linked to the influence of temperature: thermal fluctuations as well as the evaporation of particles prior and after fission tend to broaden the fission fragment distribution out of the reaction plane. The second effect is related to the dynamics of the collision. As discussed earlier, an average deflection angle of the target-like fissioning nucleus could be determined, but not the fluctuations around the mean value. The more inelastic the collisions, the larger these fluctuations are known to be[4]. As a consequence the ring pattern can be blurred and appears more like a disk pattern. Finally when M_n increases there is no evidence that all the detected fragments are still of binary fission origin. There are even clues that some are not, however in absence of coincidence measurements between two fragments, it is difficult to make any selection.

4. Conclusions

Sequential fission of projectile-like nuclei originating from rather peripheral collisions have qualitatively shown the importance of spin effects (high spins and strong spin alignment) in such collisions. More quantitative information would require a good knowledge of the reaction plane which was not provided in the present experiment. This type of collisions appears very promising to generate moderately excited nuclei in high spin states and could be an alternative to the more conventional compound nucleus approach.

REFERENCES

[1] Piaseki et al. Phys. Rev. Lett. **66** (1991) 1291 , and contribution to this volume
[2] See for instance D.Jacquet et al.Nucl. Phys. **A511** (1990) 195
[3] D.X.Jiang et al., Nucl. Phys. **A503** (1989) 560
[4] R.Charity et al., Z. fur Physik **A341** (1991) 53
[5] S.Bresson et al., to be submitted to Phys. Rev. Lett.

The Study of Isotopic Distribution of Dissipative Fragmentation Reaction Induced By 44MeV/u ^{129}Xe At SPEG

Feng Jun[a], Shen Wenqing[a], Ma Yugang[a], Zhan Wenlong[b], L.Tassun-Got[c], C.Stephan[c], A.Gillibert[c], Y.Schutz[c], P.Juzun[c], W.Mittig[c]

[a] Shanghai Institute Of Nuclear Physics, 201800, P.R.China
[b] Institute of Modern Physics, 730000, Lanzhou, P.R.China
[c] GANIL, CAEN, France

The isotopic distribution of heavy ion peripheral and half-center collision at intermediate energy can not only give useful information about nuclear property and nuclear reaction mechanism but also be important for developing secondary beam technology and searching new nuclides[1]. The isotopic distribution of dissipative fragmentation reaction of ^{129}Xe on ^{90}Zr target in the magnetic spectrometer SPEG is measured. A focal plane detector of measuring the energy, range, position and TOF of reaction products is used to get particle identification by the way of certain software modification.[2] The experimental data are recorded on magnetic tapes in event-by-event mode through the GANIL data acquisition system. The off-line analysis of the data is performed at the institute of modern physics, china. Fig.1 shows the particle identification spectrum (a: charge Z spectrum, b: charge state Q spectrum, c: mass spectrum). On the base of particle identification, the isotopic distribution can be obtained. The cross mark in fig.2) shows the isotopic distribution of 44MeV/u ^{129}Xe+ ^{90}Zr reaction. A modified abrasion-ablation model with considering the thickness of neutron -skin predicated by the Droplet model and empirical one body dissipation theory at intermediate energy is used to fit the experimental results (the circle mark in fig.2). From this study, the following results can be obtained: when using a heavy projectile at intermediate energy, the reaction process is not a pure fragmentation process but a complex process including the transfer reaction, fragmentation and dissipation process, so that the excitation energy of the reaction products will be important for isotopic distribution and the reaction products will be moved in the direction of β- stability line by evaporating more nucleons and particles. N/Z ratio of the reaction system and the diffuseness of nucleon distribution in the projectile also play certain role in isotopic distribution. Therefore to get secondary beam of heavy exotic nucleus or to synthesize new heavy isotopes, the yields could be improved by choosing the type and thickness of target and the energy of projectile.

Reference:
[1]: D.Guerreau, Int. Conf. on HINC in Fermi energy domain, CAEN, France, C4-207, 1988
[2]: Feng Jun, PH.D. Dissertation, 1991

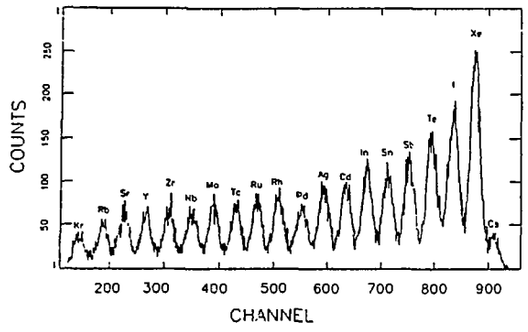
COUNTS
CHANNEL
200 300 400 500 600 700 800 900
Kr Rb Sr Y Zr Nb Mo Tc Ru Rh Pd Ag Cd In Sn Sb Te I Xe Cs

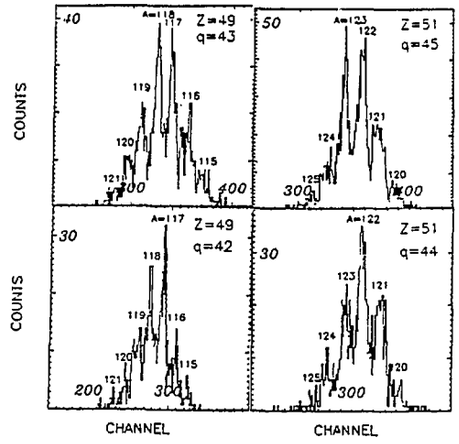
COUNTS
CHANNEL
CHANNEL
Z=49
q=43
Z=51
q=45
Z=49
q=42
Z=51
q=44

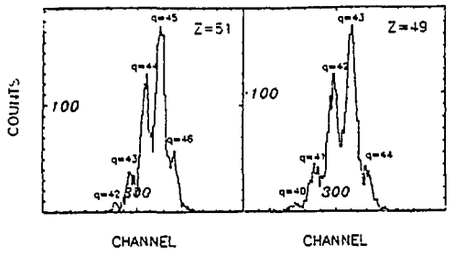
COUNTS
CHANNEL
CHANNEL
Z=51
Z=49

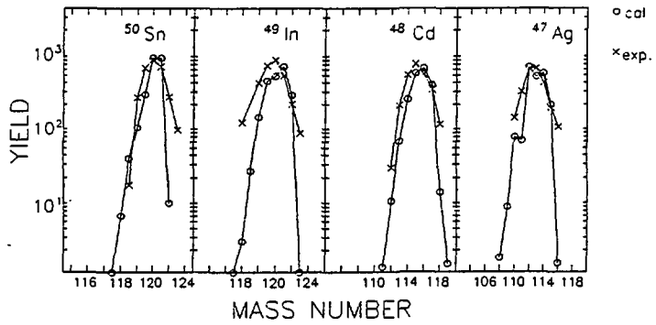
YIELD
MASS NUMBER
50 Sn
49 In
48 Cd
47 Ag
o cal
×exp.

B2 - DISSIPATIVE COLLISIONS-HOT NUCLEI

EVOLUTION OF CENTRAL COLLISIONS IN THE SYSTEM AR + TH

R. Barth[1], B. Berthier[2], E. Berthoumieux[2], Y. Cassagnou[2], S. Cavallaro[3], J.L. Charvet[2], M. Conjeaud[2], A. Cunsolo[3], R. Dayras[2], E. De Filippo[3], A. Foti[3], S. Harar[4], G. Klotz-Engmann[1], G. Lanzano[3], R. Legrain[2], V. Lips[1], C. Mazur[2], E. Norbeck[5], H. Oeschler[1], A. Pagano[3], E. Pollacco[2], S. Urso[3], C. Volant[2]

[1] *Institut für Kernphysik, Technische Hochschule, D-6100 Darmstadt, FRG*
[2] *D.Ph.N./SEPN, CEN Saclay, F-91191 Gif-sur-Yvette Cedex, France*
[3] *Istituto Nazionale di Fisica Nucleare, I-95129 Catania, Italy*
[4] *GANIL, BP 5027, F-14021 Caen Cedex, France*
[5] *University of Iowa, IA 52242 Iowa City, U. S. A.*

1. Motivation

One of the outstanding results of the experiments at intermediate energies is the rapid disappearance of fission in central collisions [1]. This result was obtained by measuring the folding angle distribution of the two fission fragments emitted in the system Ar + Th at incident energies between 31 and 44 MeV/u. While the fission cross section of peripheral reactions remain nearly constant with energy, the fission yield from central collisions decreases by 50% within this small energy interval. The question which decay channel takes over the missing part of the reaction cross section, remains open until now.

Possible answers are: (i) A transition from binary fission to multifragmentation, an idea supported by many experiments which report increasing yields of intermediate mass fragments (IMF) in this energy regime. (ii) A fission process accompanied by the emission of IMF's reducing the detection probability of fission in the quoted experiment. (iii) A transition from fission to another decay mechanism, e.g. the production of heavy residues. This could be caused by an increasing number of preequilibrium and/or evaporated particles. The remaining lighter nuclei survive due to their higher fission barriers.

We have performed two experiments to shed light on this question. The first one was oriented towards the study of possibilities (i) and (ii) and the second one, carried out very recently, was focussed on the study of heavy residues.

2. Experiment studying fission and correlated IMF emission

Figure 1 exhibits the experimental setup consisting of three large-area parallel-plate avalanche counters (PPAC) and eight telescopes.

Coincidences between fission fragments are measured with three PPAC's, two of them labelled 1 and 2 had an active area of $30 \times 30 cm^2$ and PPAC 3 with a surface of $15 \times 17 cm^2$, all at a distance of 30 cm from the target. Combination $1 - 2$ selects fission events from central collisions with folding angles close to 100^0, while combination $1 - 3$ favours the peripheral ones. In contrast to the previous experiment [1] the out-of-plane distributions are measured directly.

In the backward hemisphere eight telescopes were installed to detect the IMF's, either using Si-diodes or ionization chambers as ΔE-counters. They were installed 14 cm apart from the target at angles between 120^0 and 180^0. Two of them were placed out of plane.

The first question to answer is whether the out-of-plane width of the fission fragment angular correlations changes with incident energy. The widths for the pe-

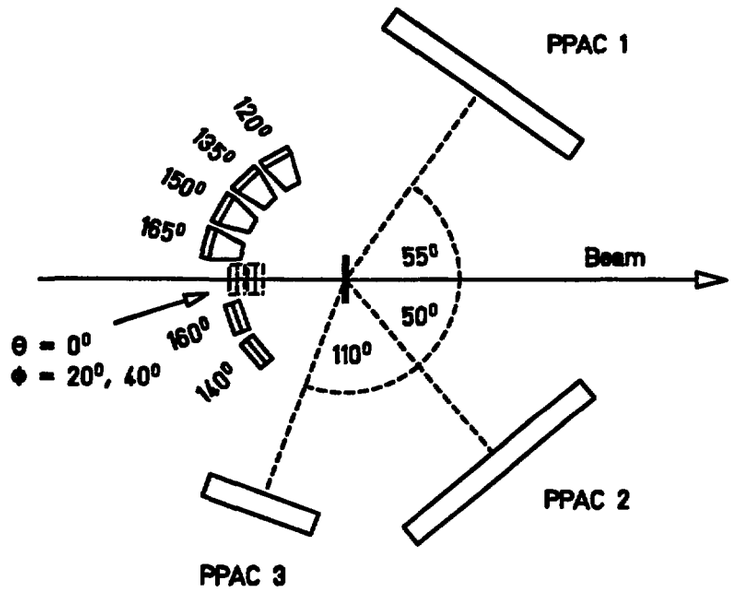

Figure 1: Setup consisting of three PPAC and eight telescopes

ripheral collisions do not vary with incident energy, while for central fission reactions the width increases by 25% with the incident energy. This difference has not been considered in ref. [1]. Yet, it only slightly reduces the drastic effect reported, the main problem still remains open.

Next, the multiplicity M_{IMF} of IMF (A>4) emitted in coincidence with fission was measured as a function of the transferred linear momentum for the two incident energies 31 and 44 MeV/u. An IMF emitted into the backward hemisphere implies an additional momentum onto the fissioning nucleus. This effect has been taken into account in the calculation of $p_{||}$ from the folding angle of the fission fragments. The angular distribution of the IMF has been found isotropic for the measurements at backward angles and such a shape has been assumed also for the forward angles to calculate the IMF multiplicity. This probably is an underestimation. As expected the IMF multiplicity is highest for central collisions. But at the two incident energies the same transferred linear momentum corresponds to different IMF multiplicities. It is argued that the key parameter for the IMF emission is the deposited energy [2, 3]. Therefore, we have converted the transferred linear momentum $p_{||}$ into an excitation energy E_x using the rather general relation [4],

$$E_x/E_i = \alpha \;\; p_{||}/p_i$$

E_i and p_i are the energy and momentum of the beam respectively. This relation holds for various mechanisms from the massive transfer up to individual nucleon-nucleon collisions, only the coefficient α varies slightly. From ref. [5] a coefficient $\alpha = 0.7$ was deduced for the system Ar + Th at the incident energies considered here. After this conversion the two curves as shown in fig. 2 coincide and prove that M_{IMF} is proportional to the excitation energy. At the higher incident energy higher values for M_{IMF} are observed in central collisions reflecting increasing excitation energies. This result is in contrast to the saturation observed in the neutron multiplicity measurements and favour our previous conclusion of still increasing excitation

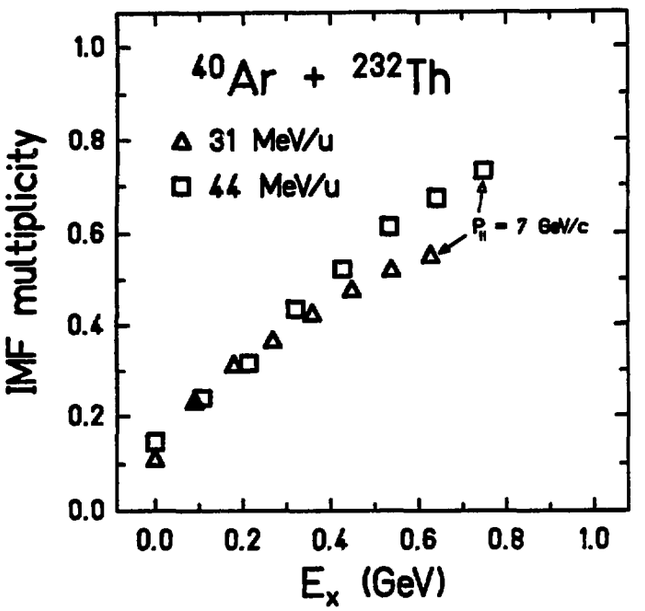

Figure 2: Multiplicity of the IMF emission as a function of the excitation energy

deduced from the fission fragment masses [1].

A quantitative analysis of the cross sections and multiplicities for central collisons from this experiment is given in table 1.

Energy/nucleon (MeV/u)	$\sigma_{fission}^{central}$ (mb)	σ_{IMF} (mb)	$M_{IMF}(fission)$	$\sigma_{fission} \times M_{IMF}$ (mb)
31	760±76	570±85	0.54±0.05	410±110
44	493±50	600±90	0.74±0.07	365± 86

Table 1: Summary of the cross sections and multiplicities. The cross sections for fission are taken from ref. [1] but corrected for the out-of-plane width and renormalized to the reaction cross section of ref. [6].

In the last column the cross section for the IMF produced in central collisions leading to fission is given. It can be seen, that a part of the IMF cross section, measured in single, must originate from another process. The most likely answer is the production of heavy residues in central collisions and hints were already reported in ref. [6]. This has led us to conceive a dedicated experiment for studying heavy residues.

3. Experiment studying heavy residues and correlated IMF emission

Very recently an experiment has been performed to detect heavy residues in coincidence with IMF and light particles. The main goal of the experiment was to investigate quantitively the role of heavy residue production in central collisions.

The setup consisted of 32 PIN-diodes of $3 \times 3cm^2$ size installed between 6^0 and 42^0 to measure the heavy residues, 8 telescopes of the TEGARA type (prototype for INDRA) to detect IMF's and fission fragments, 35 BaF_2 at backward angles to

measure the light particle multiplicities and various other detectors to characterize the centrality of the events. The data analysis of this experiment is still in progress.

References

[1] M. Conjeaud, S. Harar, M. Mostefai, E.C. Pollacco, C. Volant, Y. Cassagnou, R. Dayras, R. Legrain, H. Oeschler and F. Saint-Laurent, Physics Letters 159B(1985)244

[2] R. Trockel, U. Lynen, J. Pochodzalla, W. Trautmann, N. Brummund, E. Eckert, R. Glasow, K.D. Hildenbrandt, K.H. Kampert, W.F.J. Müller, D. Pelte, H.J. Rabe, H. Sann, R. Santo, H. Stelzer, R. Wada, Phys. Rev. Lett. 59 (1987) 2844.

[3] G. Klotz-Engmann, H. Oeschler, J. Stroth, E. Kankeleit, Y. Cassagnou, M. Conjeaud, R. Dayras, S. Harar, R. Legrain, E.C. Pollacco, C. Volant, Nucl. Phys. **A499** (1989) 392

[4] N.T. Porile, Phys. Rev. 120 (1960) 572

[5] U. Jahnke, J.L. Charvet, B. Cramer, H. Doubre, J. Frehaut, J. Galin, B. Gatty, D. Guerreau, G. Ingold, D. Jacquet, D.X. Jiang, B. Lott, C. Magnago, M. Morjean, J. Patin, J. Pouthas, Y. Pranal, E. Schwinn, A. Sokolov, J.L. Uzureau, Proceedings of the 20th International Summer School on Nuclear Physics, Mikolajki, Poland 1988, p. 171

[6] J. Galin, J.L. Charvet, B. Cramer, E. Crema, H. Doubre, J. Frehaut, B. Gatty, D. Guerreau, G. Ingold, D. Jacquet, U. Jahnke, D.X. Jiang, B. Lott, C. Magnago, M. Morjean, J. Patin, E. Piasecki, J. Pouthas, F. Saint-Laurent, E. Schwinn, A. Sokolov and X.D. Wang, Proceedings of the symposium on Nuclear Dynamics and Nuclear Disassembly, Dallas 1989, published by World Scientific, p. 320

Mean thermal energy produced in Ar-induced highly dissipative collisions

B. Lott[1], S. Bresson[2], J.L. Charvet[3], E. Crema[2], G. Duchêne[1], H. Doubre[2], J. Fréhaut[2], J. Galin[3], B. Gatty[4], D. Guerreau[2], G. Ingold[5], D. Jacquet[4], U. Jahnke[5], D.X. Jiang[6], C. Magnago[3], M. Morjean[2], Y. Patin[3],E. Piasecki[7], J. Pouthas[2], Y. Pranal[3], F. Saint-Laurent[2], E. Schwinn[5], A. Sokolov[2], J.L. Uzureau[3], X.M. Wang[2]

1) CRN Strasbourg, B.P.20 Cro, 67037 Strasbourg Cedex, France
2) GANIL, B.P.5027, 14021 Caen Cedex, France
3) CE Bruyères-Le-Châtel, B.P.12, 91680 Bruyères-Le-Châtel, France
4) IPN, B.P.1, 91406 Orsay Cedex, France
5) HMI Berlin, D 1000 Berlin 39, Germany
6) Inst. of Mod. Phys., PO Box 31, Lanzhou, China
7) Inst. of Exp. Phys., Warsaw Univ., Hosa, 69 00-681, Warsaw, Poland

1. Motivation

Assessment of the total excitation energy generated in a nuclear reaction is one of the major experimental problems in the study of hot nuclei. The thermal energy, E_{th}, can be evaluated by measuring the multiplicities of evaporated light particles and by estimating the excitation energy removed through this emission. In the following, the most probable E_{th} value for the highly dissipative collisions is inferred from the neutron multiplicity alone using the statistical model, with reasonable assumptions about the reaction mechanism.

2. Experimental Procedure

The neutron multiplicity distributions were measured in two different experiments using the Gd-loaded liquid-scintillator 4π detectors of CE Bruyères-Le-Châtel (ϕ 1 m, 500 l) and of HMI Berlin (ϕ 1.4m, 1500 l). A beam of 44 MeV/u Ar was used to bombard a total of seven different targets.The neutron counting was triggered by a prompt signal due to the detection in the scintillator of protons elastically scattered by neutrons and of reaction γ-rays. Owing to the very low detection threshold ($E\gamma$=2 MeV), the trigger condition was fulfilled for almost all the collisions leading to nuclear reactions, even for very peripheral ones.

The detection efficiency for neutrons emitted in highly dissipative collisions was calculated with the Monte-Carlo code DENIS2 [1], taking into account the geometry of the neutron detectors.

3. Experimental Results

Examples of neutron multiplicity distributions, corrected for background but not for the detector efficiency, are presented in Fig. 1 for different systems. These distributions exhibit clearly two components: a shoulder at low multiplicity corresponding to the most peripheral collisions, and a Gaussian-like bump at higher multiplicities. Remarkably, similar quantitative features are deduced from such distributions for systems of different mass asymmetry. These include a constant proportion (about 55%) of the total reaction cross section represented by the high multiplicity bump and a similar slope of the distributions for the highest multiplicities. The understanding of these features, although challenging, has not been achieved, as yet. The multiplicity value corresponding to the maximum yield in this bump, $< M_n^{dis} >$, (represented by

arrows in Fig. 1) is highly interesting because it has been observed to be very close to the most probable neutron multiplicity (or to the mean value as the distribution is almost symmetrical) measured in very dissipative collisions. Such collisions were selected by requiring detection of two coincident fission fragments exhibiting small correlation angles [2] or of light charged particles (lcp) at backward angles [3,4].

The values of $< M_n^{dis} >$, corrected for the detector efficiency, are presented in Fig. 2 (left-hand scale) as functions of the target mass, for the seven systems studied.

4. Thermal energies

The statistical code Gemini [5] was used to compute the thermal energies corresponding to the observed values of $< M_n^{dis} >$. The extracted values of E_{th} were found to be virtually independent of whether the emitter is assumed to be either the target nucleus or a system formed in an incomplete fusion reaction. Using the statistical model allows to take into account the competition between neutron and lcp emission. The calculated values of E_{th} (Fig. 2, right-hand scale) show that the observed strong increase of $< M_n^{dis} >$ with the target mass is mainly due to the enhanced dominance of neutron over lcp emissions when the emitter N/Z ratio is large, i.e., for heavy nuclei. An independent confirmation of the extracted values of E_{th} can be obtained by comparing the predicted lcp multiplicities to those actually measured for some systems [3, 6]

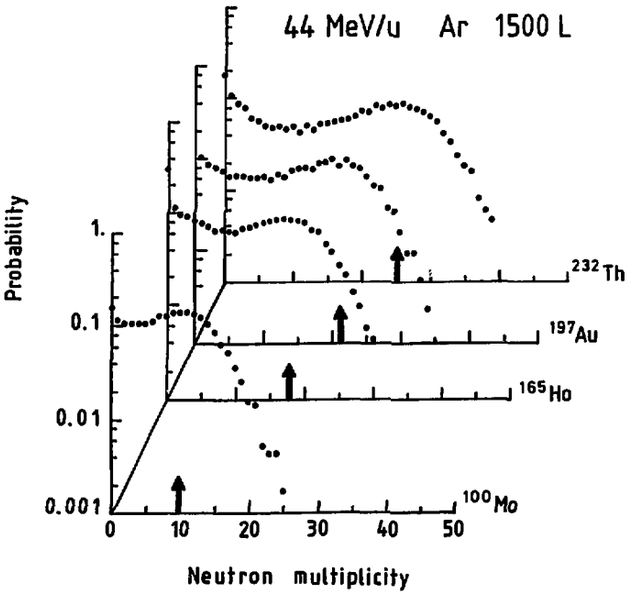

Figure 1

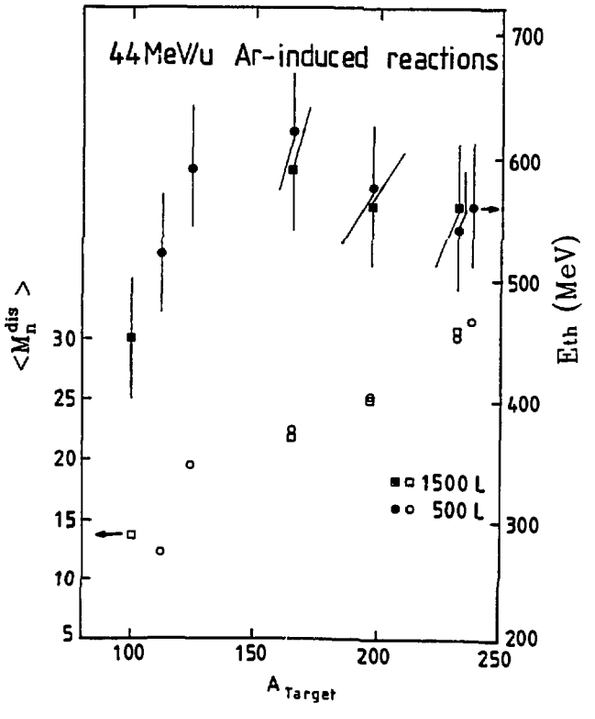

Figure 2

(Table). A reasonable agreement is observed, suggesting the that the assumed scenario is realistic. The inferred energies are about 500-600 MeV and vary only weakly with the target mass, specially for large masses. These values are significantly lower than those predicted in the massive-transfer picture (≡ 890 MeV for Ar+Au, assuming 60% of the full linear momentum transfer). This picture, although fairly useful for asymmetric systems at bombarding energies below 30 MeV/u is probably no longer adequate at higher energies.

System	Mp Exp.	Mα Exp.	Mp calc.	Mα calc.
Ar+Au	4.9	2.4	5.7	2.4
Ar+Th	3.8	2.3	3.6	1.6
Ar+Ag[6]	7.3	2.4	8.9	2.7

References

[1] J. Poitou and C. Signarbieux, *Nucl. Instr. Mes.* 135 (1976) 511.

[2] U. Jahnke et al., Proceedings of the 20th Mikolajk in Summer School on Nuclear Physics, Mikolajki, Poland, September 1988.

[3] D.X. Jiang et al., *Nucl. Phys.* A503 (1989) 560.

[4] E. Crema et al., *Phys. Lett.* 258 (1991) 266.

[5] R.J. Charity et al., *Nucl. Phys.* A483 (1988) 37

[6] G. Bizard et al., *Nucl. Phys.* A456 (1986) 173.

THE INTERACTION OF 35 AND 45 MEV/NUCLEON ^{129}Xe WITH ^{197}Au

K. Aleklett[1], J.O. Liljenzin[2], W. Loveland[3], A. Srivastava[3], R. Yanez[1]

[1]*Studsvik Neutron Research Laboratory, S-611 82 Nyköping, Sweden*
[2]*Chalmers University of Technology, S-412 96 Göteborg, Sweden*
[3]*Oregon State University, Corvallis, OR 97331, USA*

1. Motivation

At low energies (10 MeV/nucleon), the fusion of a heavy nucleus such as ^{129}Xe with another heavy nucleus ^{197}Au is not possible because the Coulomb repulsion between the interacting nuclei is too large to be counteracted by the nuclear attractive forces. As a result, even central collisions lead to deep inelastic scattering. At high energies (>100 MeV/-nucleon) we know[1] that the interaction of ^{139}La + ^{197}Au is dominated by "participant-spectator" dynamics, in which deep inelastic scattering does not play a role. It is an interesting problem in the study of nuclear reaction dynamics to be able to understand this transition in behaviour.

We[2] have previously shown the importance (and persistence) of deep inelastic scattering in the reaction of 21 MeV/nucleon ^{129}Xe + ^{197}Au. We thought it would be important to push these studies to higher energies to see how the deep inelastic scattering reaction mechanism evolves with energy. Accordingly, we measured the yields, angular distributions and recoil properties of the target-like fragments for the interaction of 35 and 45 MeV/nucleon ^{129}Xe with ^{197}Au using radiochemical techniques[3].

2. Results

The experiment was performed at GANIL utilizing the 45 MeV/nucleon ^{129}Xe beam. For the measurements with 35 MeV/nucleon ^{129}Xe, the primary beam was degraded using carbon foil degraders.

In the angular distribution experiment, we measured $d\sigma/d\Omega$ (Θ) for >100 target-like fragments at laboratory angles of 7.1, 13.6, 21.9, 32.3, 46.2, 61.5, 79.8, 100.2, 118.5, 135.6 and 155.5°. Preliminary results from the interaction of 45 MeV/nucleon ^{129}Xe with ^{197}Au (Figure 1) show some interesting trends. In these distributions, one observes a gradual evolution of the fragment angular distributions from a sidewise peaking (A ~ 195) to peaking at intermediate angles (~60° for A=183) to a forward peaking (0°for A ~ 160). Presumably this change represents a transition from quasi-elastic scattering to a two body inelastic process to incomplete fusion.

The target-like fragments are substantially more forward-peaked than would be expected from current models incorporating dissipative effects. For example, the model of Bonasera et al.[4] would predict the mean laboratory angles of emission of the TLF's to be ~67° for A=140 and 77° for A=181, for the 45 MeV/nucleon ^{129}Xe + ^{197}Au reaction while we observe the A≤ fragments to be strongly forward peaked and the A=183 fragments be emitted at a mean angle of 60°. The onset of fragmentation processes may be occurring at lower energies than expected from that model.

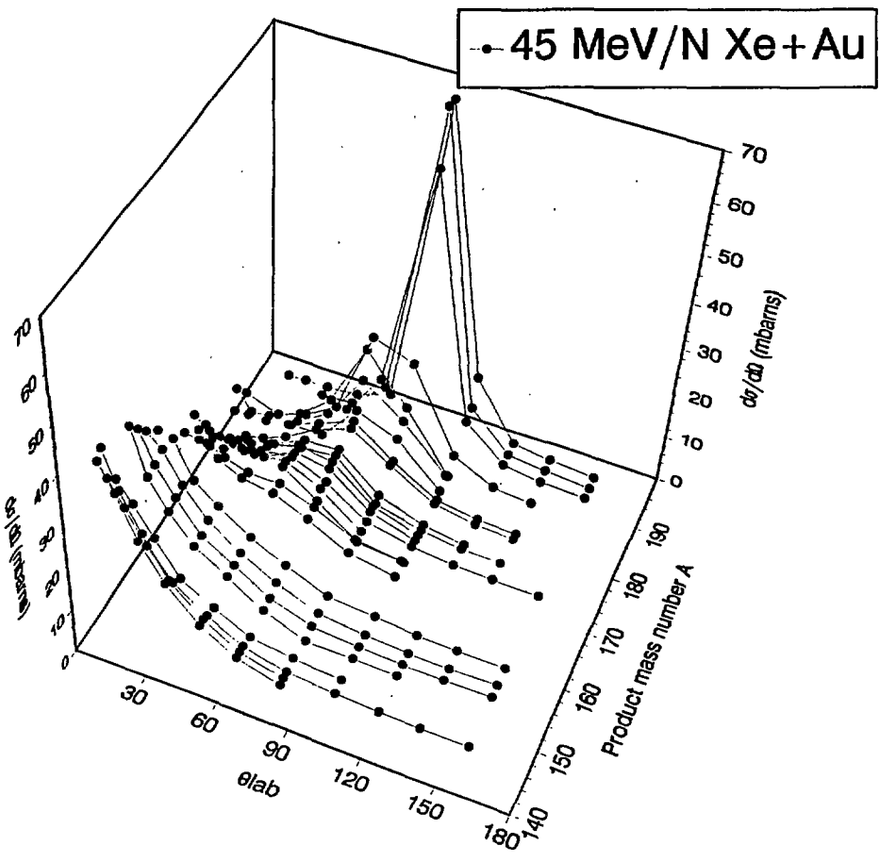

Figure 1. Three dimensional representation of the target-like fragment angular distributions for the interaction of 45 MeV/nucleon ^{129}Xe with ^{197}Au.

The fragment isobaric yield distributions (Figure 2) show the evolution of reaction mechanisms with increasing projectile energy. One observes the decrease in sequential fission of the TLF with increasing projectile energy along with a dramatic increase in the formation of the intermediate mass fragments ($A < 60$). A detailed analysis[2] of the latter trend shows a threshold for the production of A=20-40 IMFs to correspond to a projectile energy of ~30 MeV/nucleon (E ~950 MeV, T~7 MeV). This estimate of the threshold energy for IMF production is more consistent with the evaporative decay of the composite system (which could produce the larger IMFs seen in our observations) rather than cluster formation[5] from low density nuclear matter (which requires T~15 MeV and leads to smaller fragments).

At 21 MeV/nucleon, the observed values[2] of the fragment N/Z ratios, the fragment spin distributions (as deduced from isomer ratios); the shapes of the heavy fragment yield distributions and the fragment energies (as reduced from recoil measurements) are essentially the same as observed[6] in the interaction of 6.6 MeV/nucleon Xe with Au where deep inelastic scattering is known to be the primary source of TLFs. Thus we concluded[2] that primary mechanism responsible for the production of heavy target residues in the higher energy reaction was deep inelastic scattering.

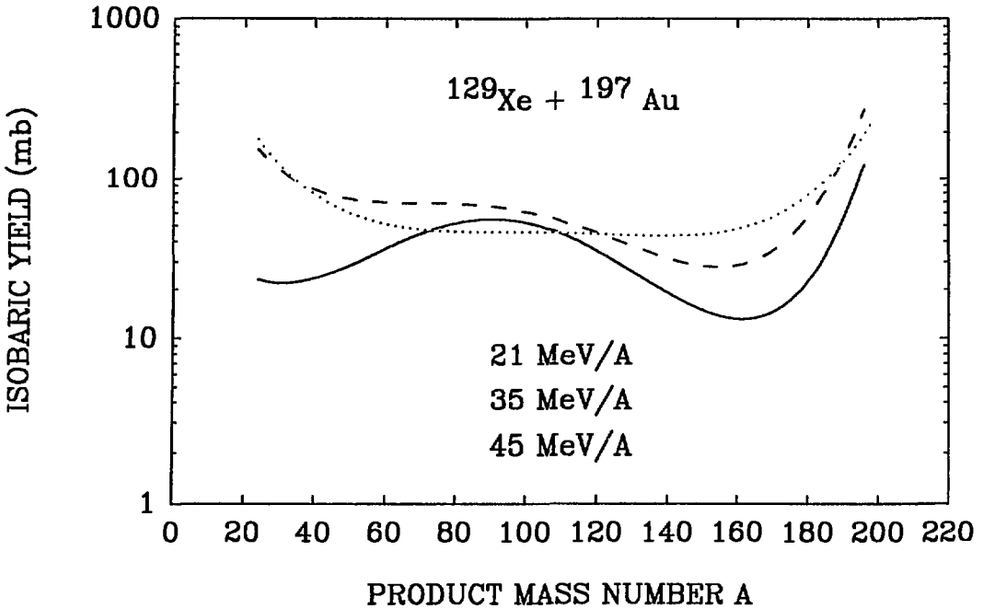

Figure 2. Fragment isobaric yield distributions (represented as smooth curves) for the interaction of 21, 35 and 45 MeV/nucleon ^{129}Xe with ^{197}Au.

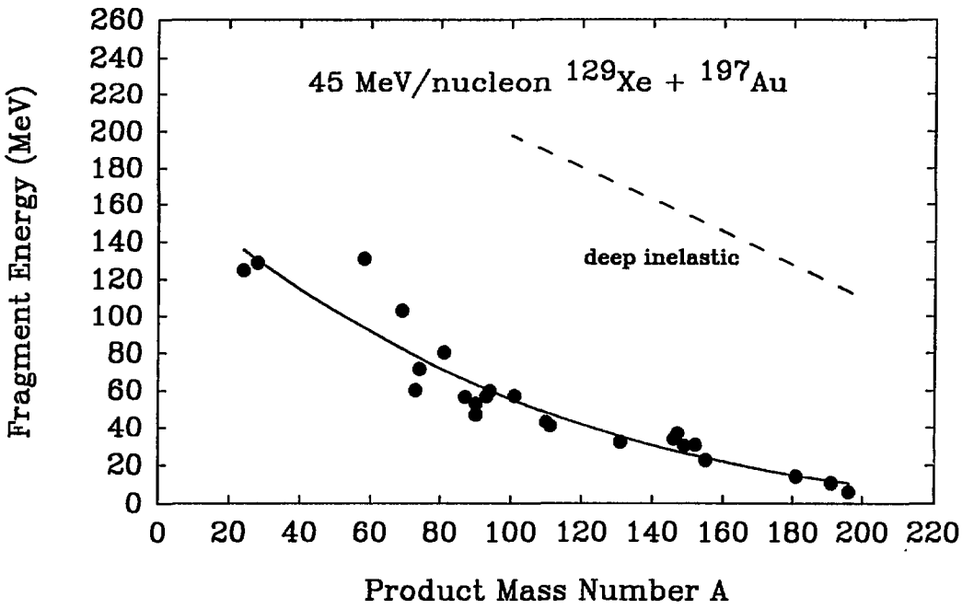

Figure 3. Target-like fragment energies for the interaction of 45 MeV/nucleon ^{129}Xe with ^{197}Au. Also shown as a dashed line are the fragment energies expected for the repulsion of touching spheres, which describes the TLF energies for the 6.8 MeV/A Xe + Au reaction.

At 35 and 45 MeV/nucleon, while the fragment N/Z ratios and spin distributions are essentially the same as seen in the interaction of 6.6 MeV/nucleon Xe with Au, the fragment energies (as deduced from recoil measurements) are too low to be consistent with deep inelastic scattering (Figure 3). The deduced fragment energies are a small fraction of what one calculated for completely damped events (and much less than those observed for TLFs in 6.6 MeV/A Xe + Au reactions). It would seem that while dissipative processes may be operating in the reaction of 35 and 45 MeV/nucleon ^{129}Xe with ^{197}Au, the amount of the momentum being transferred to the target-like fragment is very small.

REFERENCES

1. W. Loveland et al., Phys. Rev. C28, 2092 (1988).

2. A. Yokoyama et al., Phys. Rev. C (submitted for publication).

3. D.J. Morrissey, D. Lee, R.J. Otto, and G.T. Seaborg, Nucl. Inst. Meth. 158, 499 (1978).

4. A. Bonasera, M. di Toro, and C. Gregoire, Nucl. Phys. A463, 653 (1987).

5. W.A. Friedman, Phys. Rev. C42, 667 (1990).

6. J.V. Kratz et al., Nucl. Phys. A357, 437 (1981).

INFLUENCE OF THE FERMI MOTION ON SEQUENTIAL EMISSION SPECTRA

G. Rudolf[1], J.C. Adloff[1], B. Bilwes[1], R. Bilwes[1], M. Glaser[1], F. Scheibling[1], L. Stuttgé[1], S. Tomasevic[1], G. Bizard[2], R. Bougault[2], R. Brou[2], F. Delaunay[2], A. Genoux-Lubain[2], C. Le Brun[2], J.F. Lecolley[2], F. Lefebvres[2], M. Louvel[2], J.C. Steckmeyer[2], G.M. Jin[3], A. Péghaire[3], J. Péter[3], E. Rosato[3], F. Guilbault[4], C. Lebrun[4], B. Rastegar[4], Y. Cassagnou[5], R. Legrain[5], J.L. Ferrero[6].

[1] *Centre de Recherches Nucléaires, IN2P3-CNRS/Université Louis Pasteur B.P.20, 67037 Strasbourg Cedex, France*
[2] *Laboratoire de Physique Corpusculaire, ISMRA, IN2P3-CNRS 14050 Caen Cedex, France*
[3] *Ganil, B.P.5027,14021 Caen Cedex, France*
[4] *Laboratoire de Physique Nucléaire, IN2P3/CNRS et Université de Nantes 44072 Nantes Cedex 03, France*
[5] *DPhN/SEPN CEN, Saclay 91191, Gif sur Yvette Cedex, France*
[6] *IFIC, CSIC, Universidad de Valencia, 46100 Burjasot, Spain*

1. Motivations

Recent coincidence measurements showed that the Kr + Au collisions remain strongly dissipative up to 44 MeV/u [1]. Indeed, the velocities of projectile-like and target-like fragments suggest a dissipation of about 1.5 GeV for mid-central collisions. This experiment aimed at studying the deexcitation of the fast projectile-like fragment produced in these collisions.

2. Experiment

The 44 MeV/u ^{84}Kr beam delivered by GANIL bombarded 500 mg/cm^2 self-supporting Au targets. Three multidetectors were operated in the scattering chamber Nautilus: XYZt [2] which measures fragments with Z>7 in forward direction, MUR [3] which measures particles with Z<8 between 3 and 30° and one hemisphere of TONNEAU [4] which measures particles with Z<4 between 30 and 90°. The data acquisition was triggered by double or higher order coincidences between two modules of XYZt. For each event, the velocity vectors and the atomic number Z of all coincident fragments and the associated light particles were recorded.

3. Results

As a scale on the impact parameter, we shall use Z_{LP} which is the sum of the charges of all particles with Z<3 detected in TONNEAU and MUR. A maximum value of 30 was

observed for Z_{LP}. When $Z_{LP} < 18$, a fast fragment ($V/V_P > 0.67$, where V_P is the beam velocity) was observed in a large fraction of the events. It has been shown that this fast fragment is the secondary projectile-like nucleus [1], and that the coincident slower fragment has been emitted by the target. When Z_{LP} increases from 0 to 17, the charge of the fast fragment decreases from Z=33 to about 10 while its velocity decreases from V_P to about $0.7V_P$. In the hypothesis of two-body kinematics and no mass-drift, this corresponds to a dissipation of about 1.5 GeV [1]. In the present work, double coincidences in which one fast fragment is present and for which $Z_{LP}<18$ have been selected.

The light particle spectra have been considered in a system bound to the fast fragment. The z-axis has been oriented along the direction of the quasi-projectile in the c.m. system. In this system, the velocity V_{sys} of the light particle is the relative velocity between the particle and the fast fragment. The projections $V_{//sys}$ and $V_{\perp sys}$, the kinetic energy E_{sys} and the angle θ_{sys} were determined for all light particles event by event. It was checked that particles emitted at $\theta_{sys}<90°$ are emitted sequentially by the projectile-like nucleus. This is demonstrated by circular isocontours observed in $d^2M / \sin\theta_{sys}\, dV_{//sys}\, dV_{\perp sys}$ spectra [5]. Particles emitted by other sources contribute significantly at $\theta_{sys}> 90°$ only. The multiplicities of the sequential component (Fig.1) were therefore obtained by integrating the range θ_{sys}=0-90° and multiplying it by a factor 2.

In fig.1 are shown the energy distributions of Z=1, 2 and 3 particles in successive bins on Z_{LP}. To calculate E_{sys} from the measured V_{sys}, it was supposed that the particles with Z=1, 2 and 3 have masses 1, 4 and 6, respectively. That the production mechanism is not pure statistical evaporation is demonstrated by two observations. First, the shape of the spectra depends little on Z_{LP}. Since the collisions are more central when Z_{LP} increases, one would have expected that the deposited excitation energy and the temperature T would increase. The measured multiplicities increase indeed, but the shapes of the distributions vary little. Second, trying to extract T from the slopes of these spectra yields unrealistic temperatures of the order of 15 MeV for Z=2 and 25 MeV for Z=3 particles, while $T \cong 6$ MeV for Z=1 particles.

The evaporation component is indicated in fig. 1 by the dotted curves and has been calculated with the code PACE [6]. The calculations have been performed for ^{84}Kr nuclei with excitation energies of 100, 125, 150, 180 and again 180 MeV in the bins Z_{LP}=3-5, 6-8, 9-11, 12-14 and 15-17, respectively. These values of the energy have been chosen because the predicted multiplicities for Z=1 particles, the spectrum of which is dominated by evaporation, do not exceed the measured ones at any value of E_{sys}. The corresponding predictions of PACE for Z=2 particles exceed the measured values by a factor close to 2 in the vicinity of the Coulomb barrier. For Z=3 particles, PACE makes no predictions, while multiplicities predicted by other evaporation codes are smaller than our data by orders of magnitude.

To improve the quality of the fit, we have tentatively added a fragmentation contribution to the evaporation one. This is justified if one supposes that the light particles are emitted after reseparation, some of them going off before thermalisation has been reached so that their energy spectrum still reflects the Fermi motion. The others are evaporated later. The fragmentation component is indicated by the dashed curves and has

been calculated with the Goldhaber formalism [7] modified to take into account the velocity damping and the Coulomb repulsion between the emitted particle and the rest of the projectile:

$$dM/dE_{sys} = F \exp(-(p-p_0)^2/2\sigma^2)$$

where:

$$\sigma^2 = A_{part} (A_p - A_{part}) \sigma_0^2/ (A_p-1)$$

$$p = A_{part} m_N V/ c$$

$$p_0 = A_{part} m_N V_{coul} /c$$

$$V= (A_p-A_{part}) V_{sys} / A_p$$

$$E_{sys} = 1/2 \ A_{part} \ m_N V_{sys}^2$$

and A_{part} is the mass number of the particle, A_p that of the beam, c the velocity of light and m_N the nucleon mass. The factor F was adjusted to fit the data. The Coulomb velocities V_{coul} have been calculated for spherical nuclei and are equal to 3.57, 2.33 and 2.23 cm/ns for Z=1, 2 and 3 particles, respectively. To yield the best χ^2, the parameter σ_0 has been taken equal to 70, 85 and 100 MeV/c for the same Z values. A unique value of 85 MeV/c would have yielded nearly the same result.

The sum of the two components is indicated by the full curves. The success of our approach confirms that the mechanism of the reaction is basically a damping process analogous to the low bombarding energy regime, but that the difference appears in the deexcitation step [1]. Surprisingly, the Goldhaber's formalism applies to particles which are emitted sequentially, i.e. after a time longer than the interaction time. Even more surprising is the fact that the value found for σ_0^2 is close to the one which is used at much higher energies. This seems to show the influence of the Fermi motion on the deexcitation mechanism.

REFERENCES

(1) L. Stuttgé, J.C. Adloff, B. Bilwes, R. Bilwes, F. Cosmo, M. Glaser, G. Rudolf, F. Scheibling, R. Bougault, J. Colin, F. Delaunay, A. Genoux-Lubain, D. Horn,C. Le Brun, J.F. Lecolley, M. Louvel, J.C. Steckmeyer and J.L. Ferrero, accepted for publication in Nucl. Phys. (1992)

(2) G. Rudolf, J.C. Adloff, B. Bilwes, R. Bilwes, F. Cosmo, M. Glaser, A. Kamili, F. Scheibling and L. Stuttgé, Nucl. Instr and Meth. **A307** (1991) 325

(3) G. Bizard, A. Drouet, F. Lefebvres, J.P. Patry, B. Tamain, F. Guilbault and C. Lebrun, Nucl. Instr. and Meth. **A244** (1986) 483

(4) A. Péghaire, B. Zwieglinski, E. Rosato, G.M. Jin, J. Kasagi, H. Doubre, J. Péter, F. Guilbault, C. Lebrun, Y. Cassagnou and R. Legrain, Nucl. Instr. and Meth. **A295** (1990) 365

(5) G. Rudolf et al., Nouvelles de Ganil N°41 (1991)

(6) A. Gavron, Phys. Rev. **C21** (1980) 230

(7) A.S. Goldhaber, Phys. Lett. **53B** (1974) 306

Figure 1: dM / dE_{sys} spectra for the sequentially emitted particles. The dotted curves indicate the evaporation component, the dashed curves the fragmentation one and the full curves the sum of the two.

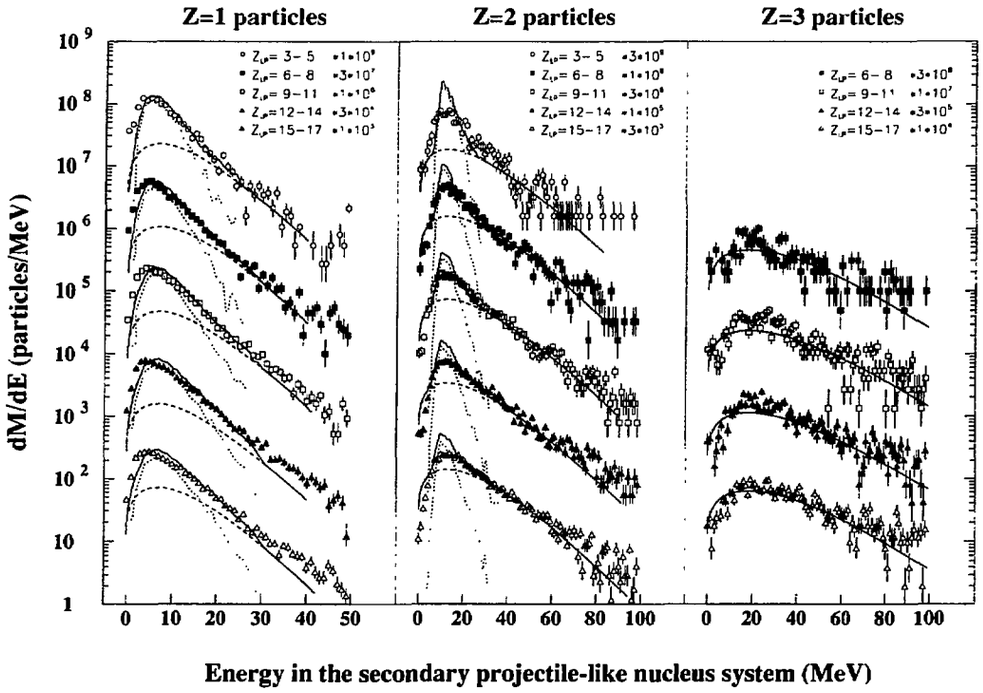

Fission and Competing Decay Mechanisms in ^{40}Ar-Induced Reactions on Au and Th at 27 to 77 MeV/u of Incident Energy

E. Schwinn[a], U. Jahnke[a], J.L. Charvet[c], B. Cramer[a], H. Doubre[b], J. Fréhaut[c], J. Galin[b], B. Gatty[d], D. Guerreau[b], G. Ingold[a], D. Jacquet[d], D.X. Jiang[e], B. Lott[f], M. Morjean[b], C. Magnago[c], Y. Patin[c], Y. Pranal[c], A. Sokolov[b], and J.L. Uzureau[c]

a *Hahn-Meitner-Institut Berlin, D 1000 Berlin 39, Germany*

b *GANIL, B.P. 5027, F 14021 Caen Cedex, France*

c *CE Bruyères-le-Châtel, B.P. 12, F 91680 Bruyères-le-Châtel, France*

d *IPN Orsay, B.P. 1, F 91460 Orsay Cedex, France*

e *Dept. of Phy. Technics, Univ. of Beijing, Beijing, China*

f *CRN Strasbourg, B. P. 20 CRO, F 67037 Strasbourg Cedex, France*

We report here on a series of experiments with the reactions ^{40}Ar + Au, Th using beams of 27, 35, 44 and 77 MeV/u from the GANIL-accelerator. These investigations have been motivated by the unexpected and very puzzling result of a fission correlation study by the Saclay-Darmstadt group [1] and others [2], namely the disappearence of the high-linear momentum transfer (LMT) peak from the folding angle distribution of correlated fission fragments for incident energies in excess of 35 MeV/u.

In order to probe further the mechanism of these reactions in this energy range we have supplemented the customary experimental set-up by a 4π-neutron multiplicity detector [3, 4] (actually, two different scintillator tanks have been used in the course of this investigation, a small reconstructed 500 l detector from CE Bruyères-le-Châtel, followed by a 1500 l detector from Hahn-Meitner-Institut). These detectors surround the reaction chamber with the charged particle detectors inside and allow to count the neutrons which are evaporated in each reaction with a high efficiency (approaching 75 to 90%, respectively, for 2 MeV neutrons), thereby providing a sensitive filter on the total energy dissipation in the reaction, which is in turn related to the centrality or the impact parameter of the collision. Moreover, and contrary to the folding angle method, this filter does not depend on the specific decay properties (binary fission) of the highly excited complex formed in the reaction.

In Fig. 1 we exhibit the inclusive neutron multiplicity distributions obtained with these detectors for Ar + Th at the four different bombarding energies, and in doing so we confront them at the same time with the corresponding folding angle spectra. The latter ones are from the Saclay-Darmstadt collaboration, supplemented, however, at 27 and 77 MeV/u by our own data. The neutron number spectra on the left side of the figure have been calibrated, i.e. corrected for the detector efficiency and normalized to give absolute cross sections. The shape of these spectra shows the same composition from peripheral and central reactions as do the folding angle distributions, at least for the lower bombarding energies (the neutron number scale has been inverted in the figure in order to emphasize the analogy to the folding angle spectra). However, whereas the correlation angle spectra experience the aforesaid decline and disappearence of the central collision bump with increasing incident energy, the corresponding maximum at high multiplicity in the neutron data persists unaffected throughout the whole range of incident energy. The cross section for these central and very dissipative reactions amounts invariably to nearly half of the reaction cross section.

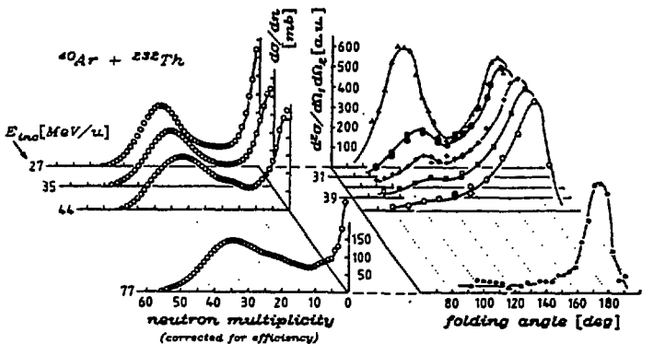

Fig. 1 : Comparison of neutron multiplicity spectra and folding angle distributions for Ar + Th over the whole range of incident energy from 27 to 77 MeV/u.

The central collisions thus do not forfeit their capability for massive energy dissipation, as one might have concluded from the loss of the high-LMT peak in the fission correlation spectra. The reason for this disappearence has therefore to be searched for in the exit channel, i.e. in a variation of the decay properties of the reaction complex.

In order to investgate the decay properties we have made two kinds of measurements : (i) cross measurements between in- and out-of-plane folding angle (Θ_{fold}) and the multiplicity of the associated neutron evaporation, and (ii) at 44 and 77 MeV/u, measurements of the angular distribution of fission- and heavier fragments, once more in coincidence with the neutron emission.

In Fig. 2 we present as examples for (i) the in-plane folding distribution for Ar + Th recorded at the lowest bombarding energy, 27 MeV/u, where we still have the double-humped LMT-profile and at 44 MeV/u, where the high-LMT component has diappeared. The figure shows also the average neutron multiplicity $\langle M_n \rangle$, as accumulated for small bins in Θ_{fold}. In the two examples as well as at the other energies and also for Ar + Au, $\langle M_n \rangle$ increases strongly when going from large folding angles near 180° towards smaller ones. The initial steep rise diminishes beyond the peripheral peak when the competition of charged particles in the evaporation chain sets in, and finally $\langle M_n \rangle$ bends over into a plateau.

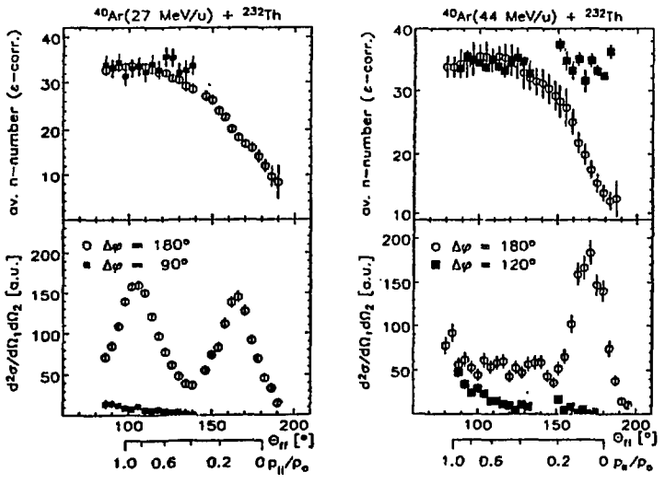

Fig. 2 : Coplanar ($\Delta\varphi$= 180°) and non-coplanar ($\Delta\varphi$= 90°, 120°) folding angle distributions for Ar(27 and 44 MeV/u) + Th and the associated neutron multiplicity (corrected for efficiency). The LMT-scale applies to the coplanar data only.

From this evolution of ⟨Mn⟩ with Θ_{fold} we see that, indeed, the energy dissipation increases with LMT and vice versa, as one would expect. When ⟨Mn⟩ becomes constant in the high-LMT region this may indicate that the energy thermalization has effectively saturated by then and that smaller folding angles are not due to larger LMT's but rather originate from broadening effects introduced by particle emission and by the fragments mass asymmetry.

The disappearence of the fusion-like maximum in the folding angle distribution for $E_{inc} \geq 35$ MeV/u has no obvious effect on the relation between ⟨Mn⟩ and Θ_{fold}. ⟨Mn⟩ still increases for smaller Θ_{fold} beyond the peripheral bump, showing that events in this region come from more violent collisions. There are, however, some features in our measurements which exhibit a discontinuity for $E_{inc} \geq 35$ MeV/u: Whereas at 27 MeV/u we observe a regular increase of the sum energy of the two detected fragments with decreasing folding angle, this relation gets lost beyond the peripheral bump at higher bombarding energy. Also, folding angle measurements made out of plane (with a relative azimuthal angle of 60, 90 and 120 degree between the same type of position-sensitive solid state detectors which have been used in plane and which do not discriminate against lighter or intermediate mass fragments, IMF) exhibit a yield which becomes more and more important with increasing bombarding energy. From this observation we conclude that the binary character of the decay gets lost in the considered energy interval by the emission of a third (or even a fourth) heavier fragment or IMF prior or simultaneously with the fission decay.

So as to consolidate this hypothesis we have (ii) studied the fission decay also with simple time-of-flight detectors, which do not impose a condition on the spatial correlation between two fragments. With these detectors we do indeed observe at E_{inc}= 44 and 77 MeV/u a large yield of fission-like fragments not only from peripheral but notably also from central reactions. Fig. 3 displays their laboratory angular distribution at E_{inc}= 44 MeV/u. The yield is strongly forward focused in both cases due to the recoil momentum imparted in the reaction. The integrated cross section amounts to about 1000 mb for Au and much higher, 3000 mb, for Th, because of the important contribution from sequential fission.

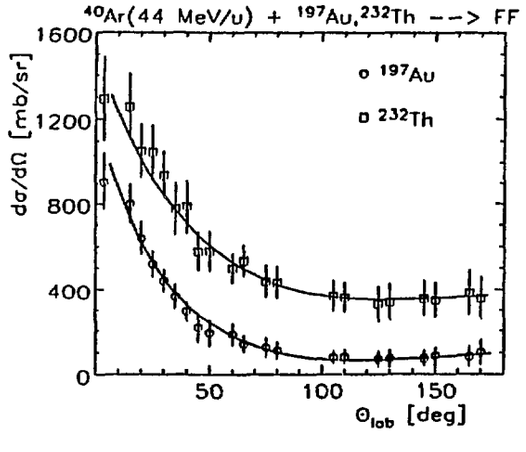

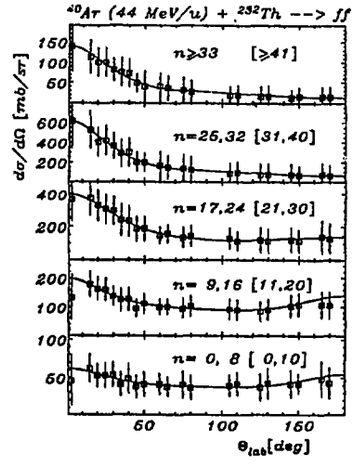

Fig. 3 (left) : Lab. angular distribution of fission fragments from Ar(44 MeV/u) + Au, Th
Fig. 4 (right) : Lab. angular of fission fragments from Ar(44 MeV/u) + Th, selected for five bins in the number of simultaneously detected neutrons n (the neutron numbers after efficiency correction are quoted in brackets).

The full extent to which different LMT's contribute to the fission process becomes evident, when we decompose the angular distribution according to the associated neutron multiplicity. This has been done for the distribution from Ar (44 MeV/u) + Th in Fig. 4 for five consecutive bins in neutron number and we can see that the character of these distributions changes noticeably with the neutron number. The lowest neutron window selects mostly sequential fission. The average LMT in this window, as determined from the condition that the emission has to be symmetric with respect to 90° in the reference system of the emitting source, is only 5% and the angular anisotropy is very weak. With increasing neutron number both quantities, LMT and anisotropy increase and in the upper two neutron bins, which comprise only central reactions, the LMT arrives at 42%. The total fission cross section for central reaction (defined here by the evaporation of 29 or more neutrons, or equivalently by $\Theta_{fold} \leq 150°$, see Fig. 2) is 1300 mb.

When nearly doubling the incident energy to 77 MeV/u, we find that the LMT for the bulk of the central reactions for Ar + Th has dropped to slightly below 30% and the respective fission cross section has also diminished to about 1000 mb. The two values for the LMT at 44 and 77 MeV/u translate within the massive transfer picture to an excitation energy of 630 and 770 MeV, respectively, which is fully consistent with what has been deduced [5] from the evaporated particle multiplicities registered in the same experiment.

Simultaneously with the fission fragments we have observed another group of still heavier residues (HR), which had been recognized before [6]. Their main characteristics are: average masses of 140 to 150 amu (for Ar + Au), a strongly forward peaked emission, high associated neutron multiplicity, as high as in the central collision maximum of the inclusive neutron number spectra, and a very broad energy distribution. The energy distribution extends up to 150 MeV, its maximum, however, is cut off on the low energy side by the detection thresholds. Due to this truncation only lower limits for the production cross section can be given: about 950 mb for Ar + Au and 300 mb for Ar + Th at E_{inc}= 44 MeV/u and similarly at 77 MeV/u. These features suggest, that the HR may be released when IMF-emission depletes the reaction complex so thoroughly in mass and charge as to hinder the fission decay.

In summary we find, that in the reactions Ar (27 to 77 MeV/u) + Au, Th fission and heavy residue production exhausts the central collision cross section to a large extent. True multifragmentation marked by exclusively small reaction debries can therefore, in spite of the observed ample IMF-emission, be only of secondary importance. The IMF-emission, however, destroys the binary character of the decay in the fission branch and this could presumably also explain the disappearence of the high-LMT peak from the folding angle distributions.

[1] M. Conjeaud et al., Phys. Lett. 159B (1985) 244
[2] S. Leray, J. de Phys. (France) C4-47 (1986) 275 and references therein
[3] U. Jahnke et al., Lecture Notes in Phys. 178 (1983) 179, Springer Verlag
[4] J. Galin et al., Proc. 2nd IN2P3-Riken Symp., Obernay (World Scientific 1990)
[5] D.X. Jiang et al., Nucl. Phys. A503 (1989) 560
[6] G. Bizard et al., Nucl. Phys. A465 (1986) 173

PRODUCTION OF INTERMEDIATE MASS FRAGMENTS IN HEAVY ION REACTIONS AT INTERMEDIATE ENERGY

M. Cavinato[1], A.M.J. Ferrero[1], F. Gulminelli[1], I. Iori[1], L. Manduci[1], A. Moroni[1], R. Scardaoni[1], M. Bruno[2], M. D'Agostino[2], M.L. Fiandri[2], E. Fuschini[2], P.M. Milazzo[2], A. Cunsolo[3], A. Foti[3], G. Sava[3], F. Gramegna[4], P. Buttazzo[5], G.V. Margagliotti[5], G. Vannini[5], G. Auger[6], E. Plagnol[6]

[1]*Dip. di Fisica dell'Universita' and I.N.F.N., Milano, Italy*
[2]*Dip. di Fisica dell'Universita' and I.N.F.N., Bologna, Italy*
[3]*Dip. di Fisica dell'Universita' and I.N.F.N., Catania, Italy*
[4]*I.N.F.N., Legnaro, Italy*
[5]*Dip. di Fisica dell'Universita' and I.N.F.N.,Trieste,Italy*
[6]*GANIL, Caen, France*

1. Motivation

The production of Intermediate Mass Fragments (IMF) in intermediate energy heavy ion collisions has been extensively studied in recent years (1). In this respect a clear signal of the multifragmentation mechanism has been experimentally observed by some groups (2).

From the theoretical point of view different approaches have been proposed to explain the origin of these IMF, but the inclusive data are well described by all of them. Therefore, to distinguish between different mechanisms, it is necessary to perform exclusive experiments collecting as much as possible information : an event-by-event coincidence measurement with a large solid angle acceptance is required to try to understand fragment formation mechanism.

We have started experiments using reverse kinematics reactions with a multi-element detector of high efficiency for a wide range of masses. The first measurement, performed at Ganil laboratories, consisted in a 45 MeV/A ^{129}Xe beam impinging on a ^{64}Cu target. IMF (Z>2) were completely measured, while light particles were partially undetected. To overcome this problem we plan to couple our apparatus to a high efficiency light particles detector.

A first comparison between experimental three-fold events and the prediction of a statistical binary decay model (GEMINI code (3)) has been performed.

2. The Experiment

The detecting system (4) is made of 48 telescopes covering from ±3° to ±23° in and out of plane. Each telescope has a front cross section of 50x50 mm^2 and it is made of an axial ionization chamber filled by flowing CF_4 gas, followed by a two-dimensional position sensitive solid state detector (5), 500 μm thick, and a CsI(Tl) scintillator, 2.5 cm thick. The gas pressure inside the ionization chamber and the voltage of the detectors are controlled and kept constant during the experiment with a VME control system (6). The front face of each telescope is tangent to a sphere 50 cm in radius centered on the target; the array was mounted inside the scattering chamber Nautilus. Within the covered solid angle, the geometrical efficiency (7) of the array is 72%; the loss is mainly due to the dimension of the detector frames.

The energy calibration of the detectors has been performed with a Xe beam at two different incident energies; the position calibration of the Silicon detectors has been made following a method described in Ref.(5). The obtained energy resolution is of the order of 1% for Silicon detectors and of the order of few percent for ionization chambers and for CsI scintillators. The position resolution has been measured with a suitable mask; the resolution resulted of the order of 1 mm in the central region, which corresponds in our configuration to approximately 0.1°. The resolution worsen to 3 mm (0.3°) close to the sides of the detector . The energy threshold of the detector is essentially given by the ionization chamber and confirms the calculated value of about 2 MeV/A for all the detected fragments.

In Fig.1 a typical ΔE-E spectrum for fragments stopped in the silicon detector is shown and compared with calculated values from energy loss tables. Fig.2 shows a plot of a particle identification function (PIF) for the fragments stopped in CsI. A good Z resolution is achieved.

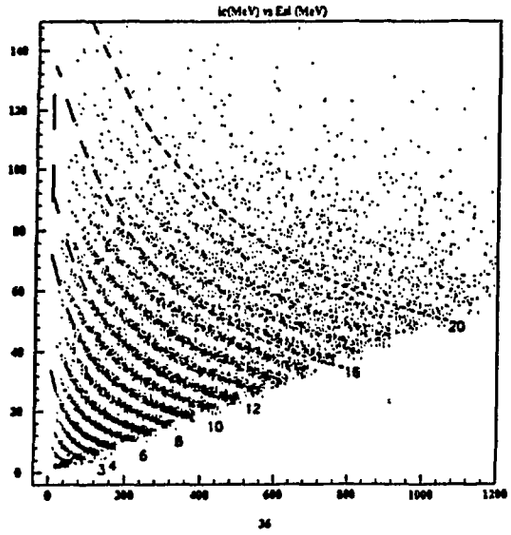

Fig.1- ΔE-E matrix from IC-Si data.

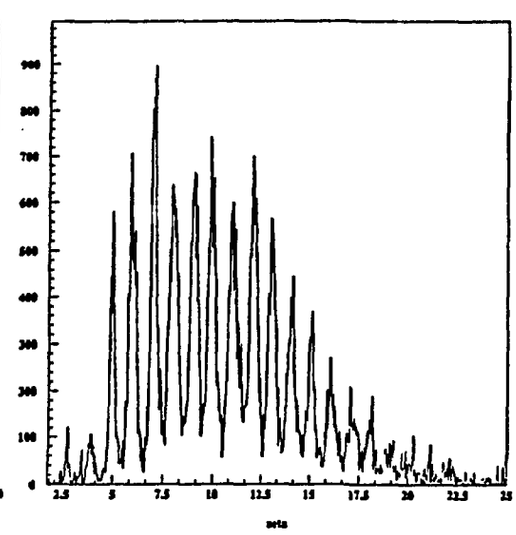

Fig.2- PIF for fragments stopped in CsI.

3. Results

The performances of the apparatus show that it is a powerful instrument for the study of the IMF emission in reverse kinematics experiments. The analysis of the experimental data is in progress. The very preliminary results, over a few percent of the collected data, show a total charge of the IMF, detected for the two- and three-fold events, of about 36, slightly less than the total charge predicted by the Gemini code, based on the statistical binary decay model with the inputs from the Viola systematics.

For the three-fold events we plotted the experimental distribution of the highest Z values as a function of the lowest one, normalized for each event to the total charge and we compared this bidimensional spectrum to that obtained from three-fold events generated by the Gemini code. While the calculation shows that the most populated regions correspond to fission-evaporation deexcitation mechanism (see Fig.3), experimentally the region of the 3 nearly equal masses is highly populated (see Fig.4).

This seems to indicate that a different mechanism in the IMF production is involved with respect to Gemini code assumptions. To investigate the origin of these fragments and to state if a prompt multifragmentation exists or ., one has to do a more sophisticated analysis, where for example relative angles and velocities are calculated, quantities which seem to be sensitive to the mechanism (8).

We stress that the good position resolution of the apparatus allows for a precise reconstruction of the kinematics. Calculations based on dynamical models (Landau-Vlasov) are in progress.

A comparison with experimental data could give more information on the dynamics of the IMF production and in particular on the impact parameters involved for this kind of mass distribution for three-fold events.

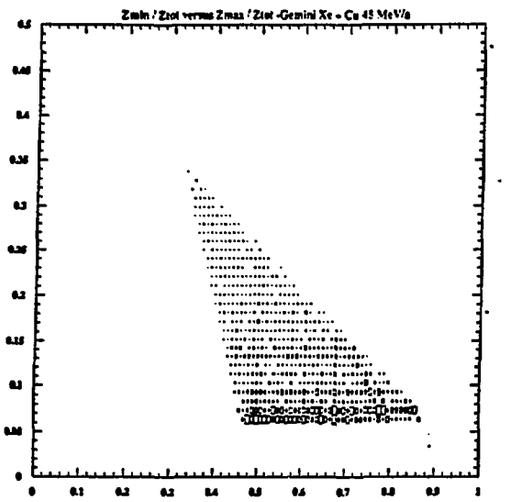

Fig.3 Zmin/Ztot versus Zmax/Ztot for three fold events from Gemini code.

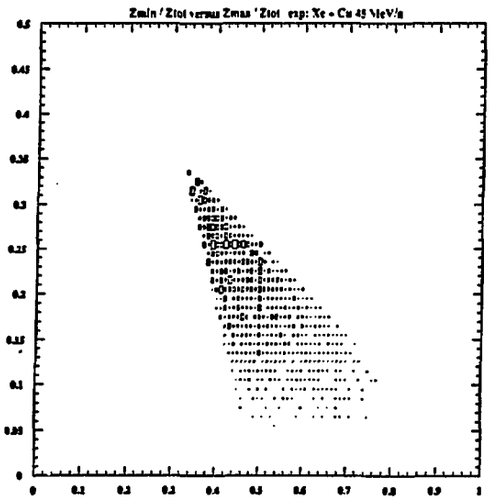

Fig.4 Zmin/Ztot versus Zmax/Ztot for three fold experimental events.

REFERENCES

(1) XXIX International Winter Meeting On Nuclear Physics, Bormio,1991, ed.by I.Iori, and references quoted therein.
(2) D. R. Bowman et al., Phys.Rev.Lett. 67(1991)1527.
J. Hubele et al.,Z.Phys.A340(1991)263.
(3) R.J.Charity et al., Nucl. Phys. A483(1988)371.
(4) A. Moroni et al., I.N.F.N./BE 91/06.
(5) M.Bruno et al., to be published on Nucl. Instr. and Meth.(1992).
(6) R. Bassini et al., Nucl.Instr.and Meth.A267(1988)499.
(7) M.Bruno et al., Nucl.Instr.and Meth. A305(1991)410.
(8) M.Bruno et al., submitted to Lett. Nuovo Cim.

ORIGIN OF PRE-EQUILIBRIUM EMISSION IN ^{40}Ar ON ^{27}Al COLLISIONS AT 45 AND 65 MeV/u

J. Péter [a], G. Bizard [a], R. Brou [a], Y. Cassagnou [c], E. Crema [b] [l], D. Cussol [a], H. Doubre [b], K. Hagel [b] [f], S.C. Jeong [i], G.M. Jin [b] [k], J. Kasagi [j], C. Lebrun [d], S.M. Lee [i], R. Legrain [c], M. Louvel [a], R. MacGrath [g], T. Motobayashi [a] [b] [k], Y. Nagashima [i], T. Nakagawa [i], M. Ogihara [i], J.P. Patry [a], A. Péghaire [b], R. Régimbart [a], E. Rosato [e], F. Saint-Laurent [b], J.C. Steckmeyer [a], J.P. Sullivan [a], B. Tamain [a]

a) LPC Caen ; b) GANIL ; c) DPhN/SEPN, CEN Saclay ; d) LPN Nantes ;
e) Univ. di Napoli (Italy) ; f) Cyclotron, Texas A&M Univ. (USA) ;
g) SUNY, Stony Brook (USA) ; h) Inst. of Modern Physics, Lanzhou (China) ;
i) Inst. of Physics, Tsukuba (Japan) ; j) Tokyo Inst. of Technology (Japan) ;
k) Rikkyo University, Tokyo (Japan) ; l) Inst. de Fisica, Sao Paulo (Brazil)

1 - MOTIVATIONS

Mid-rapidity nucleons and clusters are emitted in the first stage of the nucleus-nucleus encounter. At relativistic energies, they are issued from the decay of a very excited participant zone (fireball) separated from the spectators. They can also be issued from collisions of the projectile nucleons on the target nucleons in the initial interaction volume. These processes are expected to vary as a function of the initial interaction volume, which is directly related to the impact parameter value b . In order to reach meaningful and detailed conclusions, it is necessary to sort the events as a function of b . This pre-equilibrium emission must be distinguished from the particles issued from the equilibrated fusion nucleus.

We have performed an exclusive experiment in which the charge and velocity of nearly all charged products were measured on an event by event basis. We have chosen the ^{40}Ar+^{27}Al system.

The 4π detector array Mur+Tonneau is described in contribution : "*Charged particles calorimetry of ^{40}Ar+^{27}Al reactions from 36 to 65 MeV/u* ". The selection of well measured events is described in "*Using global variables for impact parameter determination...*"as well as the impact parameter sorting based on the average parallel velocity of detected products.

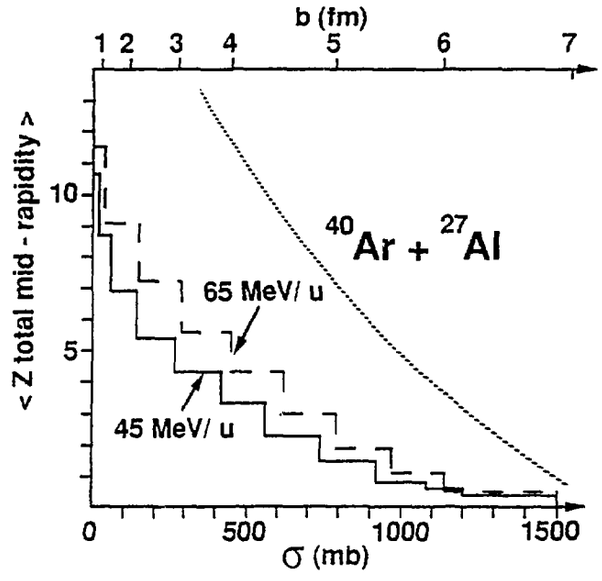

Fig. 1 :
Average mid-rapidity charge per event, versus the impact parameter value b. The dotted curve is the charge of the participant zone in the abrasion geometry (fireball).

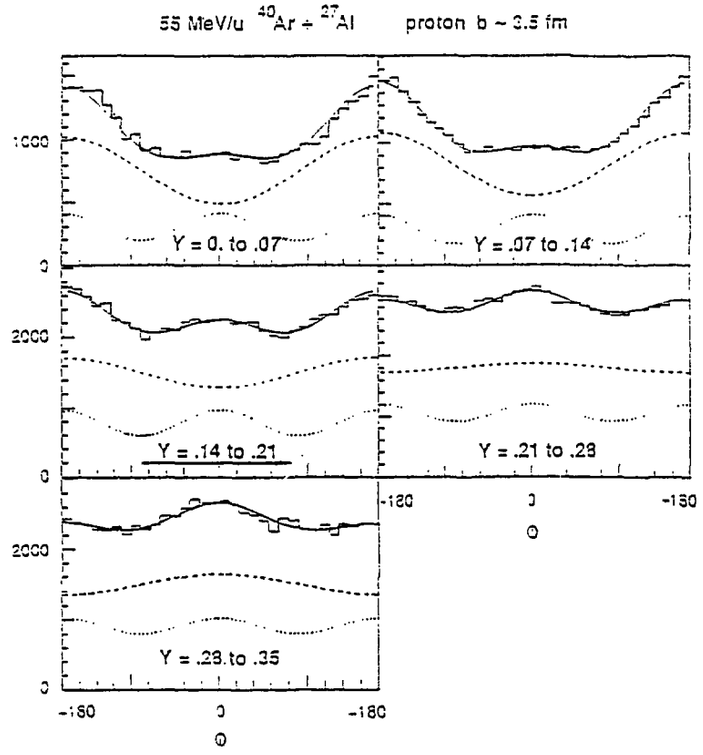
55 MeV/u 40Ar + 27Al proton b ~ 3.5 fm
Y = 0. to .07
Y = .07 to .14
Y = .14 to .21
Y = .21 to .28
Y = .28 to .35
1000
2000
0
-180
Θ

Fig 2

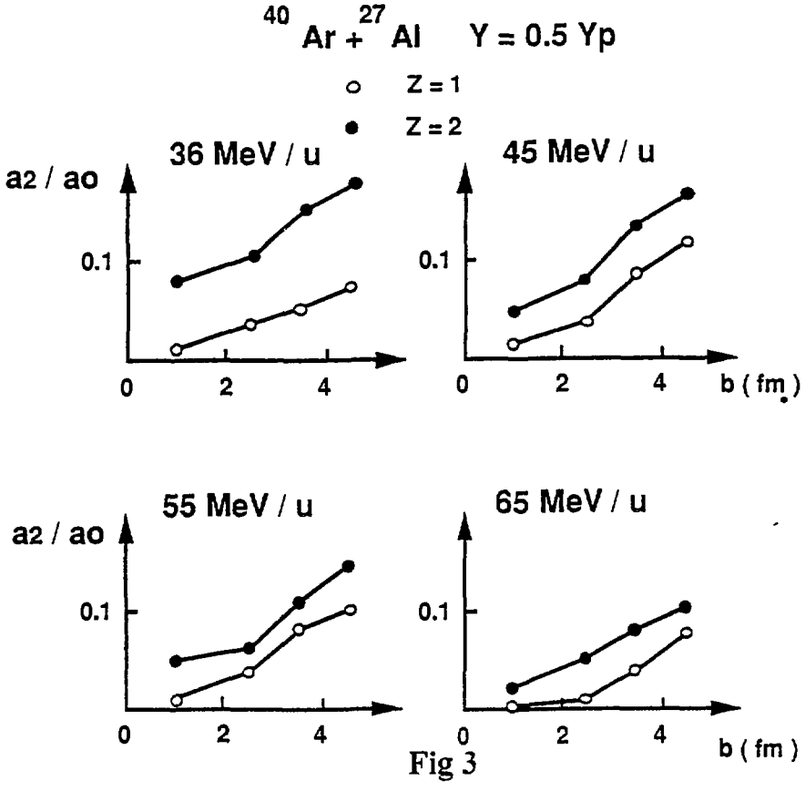
40 Ar + 27 Al Y = 0.5 Yp
Z = 1
Z = 2
36 MeV / u
45 MeV / u
55 MeV / u
65 MeV / u
a2 / ao
0.1
0
2
4
b (fm)

Fig 3

2 - PRE-EQUILIBRIUM EMISSION AS A FUNCTION OF IMPACT PARAMETER

Contour plots of the invariant cross sections versus ß// and ß+ exhibit an equilibrium component (discussed in contribution "*Charged particles calorimetry of $^{40}Ar+^{27}Al$ reactions from 36 to 65 MeV/u* ") and, for Z=1 and 2 , a component around half the projectile rapidity. The total number of charges in this component is shown in Fig. 1 versus the impact parameter, at 45 and 65 MeV/u . In central collisions, it reaches one third of the total charge of the system, (i.e. the nucleus issued from fusion between the remnants of the projectile and target nuclei is very far from complete fusion). At variance with relativistic energies, this number of emitted nucleons is very much lower than the number of participants in the geometrical abrasion model (dotted line in Fig. 2). As expected, it increases with the incident energy.

3 - NUCLEON-NUCLEON COLLISIONS OR SEPARATED PARTICIPANT ZONE ?

In Ref. 1, we attributed this mid-rapidity component to emission after one (or two) collisions of a nucleon on nucleons of the other nucleus. But it could also be attributed to emission from a separated participant zone, especially for clusters.

Another piece of information is given by the azimuthal direction of these pre-equilibrium particles. The direction of the reaction plane has been determined with the transverse momentum analysis method (Danielewicz and Odyniec) for studying the flow (see contribution *"Inversion of flow and equation of state"*). The azimuthal distribution of mid-rapidity protons is shown in Fig. 2. 0° is the impact parameter vector direction. The distribution is fitted with a function $a_0+a_1\cos\phi+a_2\cos2\phi$.

a_1 is related to the in-plane flow. The bottom line is the $a_2\cos2\phi$ contribution (shifted up by $0.25a_0$). a_2 is positive, reflecting a preferential emission in the reaction plane (minima at $\pm$ 90°), as would result from an angular momentum perpendicular to the reaction plane. In this interpretation, the lifetime of the source is not negligible, i.e. it is not consistent with direct emission after one collision. This angular momentum effect should increase with the mass of the emitted particle and with the impact parameter. Such a behaviour is indeed observed : Fig. 3, showing the ratio a_2/a_0 for mid-rapidity particles. More data can be found in Ref. 2.

4 - CONCLUSION

Cluster emission and azimuthal distributions agree with the formation of a participant zone in collisions above the Fermi energy. Its volume increases strongly with decreasing impact parameter and slightly with increasing incident energy. At 65 MeV/u , it is still much smaller than the geometric abrasion value. However, the possibility of minima at ±90° in the azimuthal distributions resulting from nucleon-nucleon collisions remains to be studied.

PUBLICATIONS

1) J. Péter et al ; Phys. Lett. B237 (1989) 187
2) W.Q. Shen et al ; submitted to Nucl. Phys. A

INVERSION OF COLLECTIVE MATTER FLOW AND EQUATION OF STATE

J.P. Sullivan[a)m)], J.Péter[a)], G. Bizard[a)], W.Q. Shen[a)n)], R. Brou[a)], D. Cussol[a)], M. Louvel[a)], J.P. Patry[a)], R. Regimbart[a)], J.C. Steckmeyer[a)], B. Tamain[a)], E. Crema[b,i)], H. Doubre[b)], K. Hagel[b,f)], G.M. Jin[b)h)], A. Péghaire[b)], F. Saint-Laurent[b)], Y. Cassagnou[c)], R. Legrain[c)], C. Lebrun[d)], E. Rosato[e)], R. MacGrath[g)], S.C. Jeong[i)], S.M. Lee[i)], Y. Nagashima[i)], T. Nakagawa[i)], M. Ogihara[i)], J. Kasagi[i)], T. Motobayashi[a)b)k)]

a) LPC Caen, ISMRA, 14050 Caen, France, b) GANIL Caen, c) DPhN/BE CEN, Saclay 91191, d) LPN Nantes, e) Dipart. di Scienze Fisiche, Univ. di Napoli, Italy, f) Present address : Cyclotron Institute Texas A&M Univ. , USA, g) SUNY, Stony Brook, USA, h) Inst. of Modern Physics, Lanzhou, China, i) Inst. of Physics, Tokyo, Japan, Inst. of Technology, Tokyo, k) Rikkyo University, Tokyo, Japan, l) Permanent address : Inst. de Fisica, Univ. de Sao Paulo, Brazil, m) Present address : P2 Division, Los Alamos National Laboratory, USA, n) Permanent address : Institute of Nuclear Research, Shanghaï, China.

1 - MOTIVATION

The study of mid-rapidity particles provides information on nuclear matter in the interaction region (the overlap volume of the two nuclei, also called participant nucleons). The flow of matter in the reaction plane (sidewards flow) is a signature of this interaction.

At high energies, the flow parameter is positive and attributed to a repulsive momentum transfer in the compressed interaction region. Conversely, at a few tens of MeV/u , the interaction is dominated by the attractive mean field. There, fragments have been shown to be deflected to negative angles. The continuous evolution from negative to positive flow values as a function of incident energy has been studied with the Boltzmann equation (Bertsch et al) and the microscopic Landau-Vlasov model (F. Sebille et al) : the flow values are sensitive both to the nucleon-nucleon cross section σ_{NN} in nuclear medium and to the equation of state through the incompressibility modulus K of infinite nuclear matter. In order to disentangle the respective influences of two parameters (σ_{NN} and K) by comparing the results of such calculations to experimentally determined flow values, the flow should be measured as a function of two variables, namely the incident energy and the impact parameter.

We have performed measurements on the system ^{40}Ar on ^{27}Al from 25 to 85 MeV/u . For the experimental set-up (charged product 4π array Mur+Tonneau), see contribution *"Charged particle calorimetry..."*. For the exclusion of badly measured events (in very peripheral reactions) and the sorting of events versus the impact parameter value, see contribution "*Using global variables...*".

2 - EXPERIMENTAL RESULTS

The method created by Danielewicz and Odyniec has been used to find the location of the reaction plane.

Figures 1 shows the measured average transverse momentum in the reaction plane $< p^{x'}/A >$ versus the particle rapidity (y) obtained at 45 MeV/u for Z=2 , in bins corresponding to impact parameter values centered at 6, 4.5, 2.6 and 1.6 fm . The rapidities of the projectile, y_p , the center-of-mass, y_{cm} , and the nucleon-nucleon center-of-mass $y_{NN}=y_p/2$, are shown by arrows. The location of the "spectator" equilibrated nuclei is shown by a rectangle (projectile-like fragment in peripheral collisions, incomplete fusion nucleus in central collisions). At 6 and 1.6 fm , the rapidity distribution of Z=2 particles is shown-helping to see where participants and "spectators" contribute.

The flow parameter of the participants is the slope at $y_p/2$ multiplied by $(y_p-y_p/2)$. This is shown at 6 fm . The variation of the flow parameter versus b is plotted in figure 2 at 55 MeV/u for Z=1 and Z=2 . Other energies are shown in Ref. 1 and 2. Larger flow values are

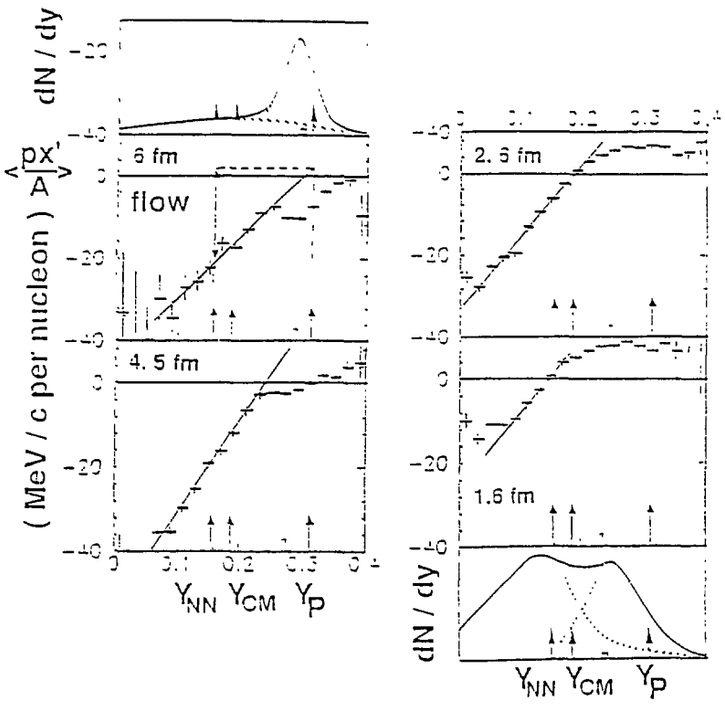
dN / dy
6 fm
flow
4. 5 fm
2. 6 fm
1.6 fm
(MeV / c per nucleon)
Y_{NN} Y_{CM} Y_P

Fig 1

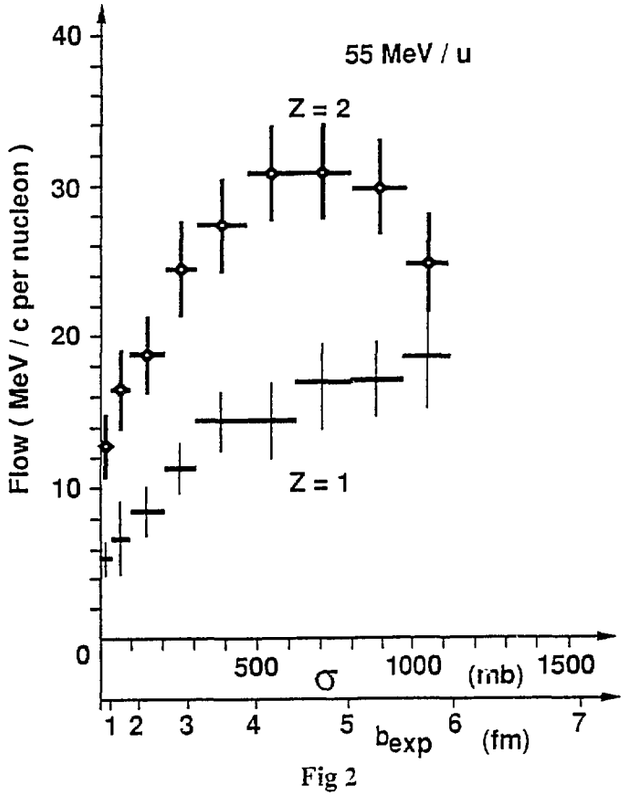
55 MeV / u
Z = 2
Z = 1
Flow (MeV / c per nucleon)
σ
(mb)
b_{exp}
(fm)

Fig 2

observed for Z=2 than for Z=1 . This effect has already been observed. It has been attributed to the role of thermal motion which tends to reduce the alignment into the reaction plane due to collective motion : An objection to this explanation is that thermal motion should not modify the average value of $< p^x/A >$ (which is used to get the flow parameter) as is confirmed by the simulation described below. It has been shown that Coulomb repulsion is, at least partially, responsible for this increase of flow with Z (F. Sébille et al).

3 - REAL AND MEASURED FLOW VALUES

An experimental value of the flow parameter is normally less than the true value because the experimentally determined direction of the reaction plane is not exactly the real one. It is important to understand that this deviation from the real reaction plane is not caused only by the experimental resolution, it is due to the thermal energy which leads to the emission of particles having a randomly oriented momentum, superimposed to the flow momentum. If the thermal momentum is small relative to the flow momentum, the final direction of the particles remain close to that of the reaction plane and Danielewicz's method will lead to a good location of the reaction plane. In the opposite case, the influence of the flow momentum on the direction of the particle is washed out by the large thermal momentum.

Simulated events were used to study this problem on the system $^{40}Ar+^{27}Al$ at E/A=45 MeV .Fig. 3 (left) shows the distributions that would be measured by a perfect detector which gives the exact mass, charge, velocity and angle of all particles, including neutrons. The top part of the figure shows the distribution when the flow parameter is 0, the middle part is for a value of 40 MeV/c , and the bottom part shows 100 MeV/c . The solid lines indicate the shapes of the $< p^x >$ distribution which was put into the simulation. The points are the value determined with Danielewicz's method. There is a large difference in the slope (in-plane flow) when its value is small. The reason for this behaviour is that the method used to determine the reaction plane assumes that there is flow.

The right side of Fig. 3 shows that the reaction plane determination is not much broadened by the actual detector limitations. The reason is that MUR + TONNEAU, although far from being perfect, has several good points : it is axially symmetric, its geometrical efficiency is 85% , and the momenta per nucleon, used here, are directly measured.

The ratio between the real and measured flow parameters is needed when analyzing data so that the measured flow parameter can be corrected to give the true value before the effects of the method and detector limitations have changed it. There are several different methods for estimating this correction factor first formulated by Danielewicz's and co-workers. They give reasonnably accurate factors (publication 3).

However, instead of correcting the experimental data, it is much better to analyse the theoretical calculations in a way similar to the experimental data : one forgets that the reaction plane is known and one finds its direction with the Danielewicz's method, firstly for a perfect detector, secondly after applying a software filter which reproduces the detector limitations. One must perform separately these two steps and watch their effect.

CONCLUSIONS

Fig. 4 shows the flow measured at different energies for an impact parameter value b around 3 fm , for Z=1 (open circles). E_{bal} (3fm) appears to lie in the range 90-100 MeV/u . Similar plots for Z=1 and Z=2 indicate that E_{bal} (1fm) is in the range 70-80 MeV/u and E_{bal} (5 fm) is above E_{bal} (3 fm). This increase of E_{bal} with b is in qualitative agreement with theoretical predictions.

The values corrected for the difference between the true and measured reaction plane are shown as closed circles . The right hand part shows the values calculated with a Boltzmann equation (Bertsch et al). Experimental results are in agreement with a nucleon-nucleon cross section in mesium slightly lower than the value for free nucleons ; however Coulomb repulsion is not included in this calculation and the comparison is not valid for charged particles. The left hand part shows calculations based on the Landau-Vlasov equation using a Gogny force and including Coulomb effects (B. Remaud et al) ; experimental results indicate that the effective nucleon-nucleon cross section in medium is equal on slightly lower than the value used in the calculation.

PUBLICATIONS

1) J.P. Sullivan & al ; Phys. Lett. B249 (1990) 8
2) J. Péter et al ; Proc. of XXIX Winter Meeting on Nuclear Physics, Bormio (1991), edited by I. Iori, p. 1-15
3) J.P. Sullivan and J. Péter ; Nucl. Phys. A (accepted for publication (nov. 1991).

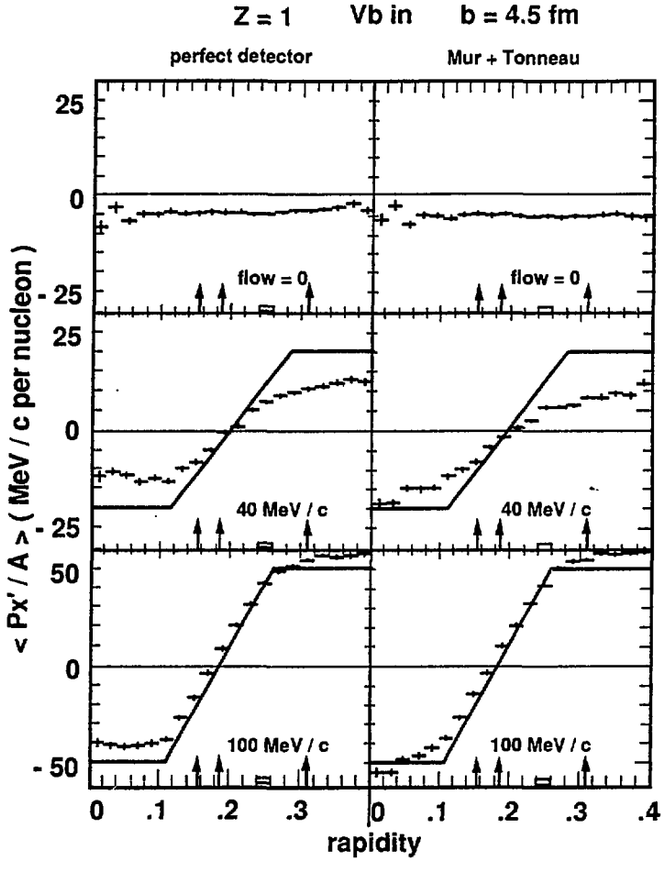

Fig 3

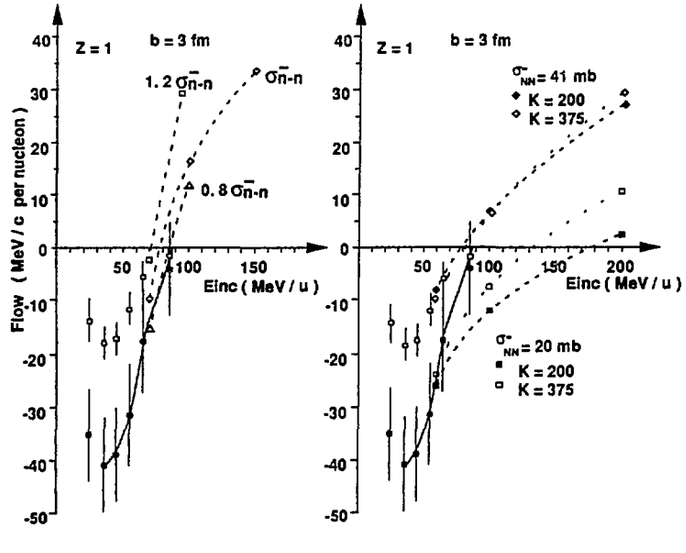

Fig 4

SEARCH FOR TIME DEPENDENCE IN THE DECAY OF AN EVAPORATIVE SOURCE, USING TWO-PARTICLE CORRELATIONS

P. Lautridou[1], D. Ardouin[4], R. Boisgard[1], H. Dabrowski[4], D. Durand[2], P. Eudes[4], D. Goujdami[1,4], F. Guilbault[4], C. Lebrun[4], A. Péghaire[3], J. Québert[1], F. Saint Laurent[3]

[1] *CEN de Bordeaux Gradignan, Le Haut Vigneau, 33175 Gradignan Cedex, France*
[2] *LPC de Caen, Boulevard Maréchal Juin, 14032 Caen Cedex,France*
[3] *GANIL, BP 5027, 14021 Caen Cedex, France*
[4] *LPN de Nantes, 2 rue de la Houssiniere, Nantes Cedex, France*

Backward angle detection of light particles emitted in the collision of asymmetric systems like ^{16}O + Au (94 MeV/A) or ^{40}Ar + Au (44 MeV/A) allowed us to disentangle a clear evaporation process of the quasi-target from other source contributions like projectile fragmentation present in forward angle measurements. In studying two-particle correlations in an evaporation process like this, at intermediate energy, our aim was to measure two quantities essentially: i) the range of time which controls particle evaporation, ii) the temperature of the source, by another way than measuring the slopes of singles spectra.

- Concerning the time which characterizes particle emission and particularly this process, the following questions can be addressed: Are particles emitted simultaneously or, in the same way as γ bands deexcite, are particles sequentially emitted? In the latter case, what is the characteristic time involved in the sequence?

Two-particle correlations, performed for particles collinearly emitted, are a way to control the sequence of emission from a source. Such properties are particularly known in pion interferometry. With heavier particles, final state interactions which are prominent, could also play the role of a clock of the process. In our experiments, we measured such kinds of amplitudes of final state interactions between two light particles like: 2p $=^2$He, αd$=^6$Li, etc...Depending on the lifetime of such resonances and the lifetime of the initial state of the source, the sequential or the simultaneous nature of the process can be derived through the resonance strength.

- The other feature, in a clean evaporation process like this emission from the quasi-target, is a good justification of the temperature, which should be determined accurately. This value can be drawn from the ratio of the population of two states of a light cluster which belongs to the initial thermal bath, prior to the decay in a two-particle channel. As will be shown below, we have found a rather low temperature ($\simeq$ 2.5 MeV), compared to previous measurements performed in the forward direction, where projectile fragmentation can be the source of a significant part of the yield.

On figure 1, we show an invariant distribution of single protons (the different circles locate a source which slightly shifts on the rapidity axis). The coincidence rate of two protons was simultaneously recorded at small relative angles in the same region to yield the p-p correlation function. Such detections were performed by using a close-packed multidetector of ICs scintillators. The correlation function is displayed for different values of the sum of two proton energies. From these measurements we conclude the following main points:

The higher the energies of the two protons collinearly detected, the stronger the nuclear interaction at Q=20 MeV/c (s-state of ^{2}He at 400 keV); this emission corresponds

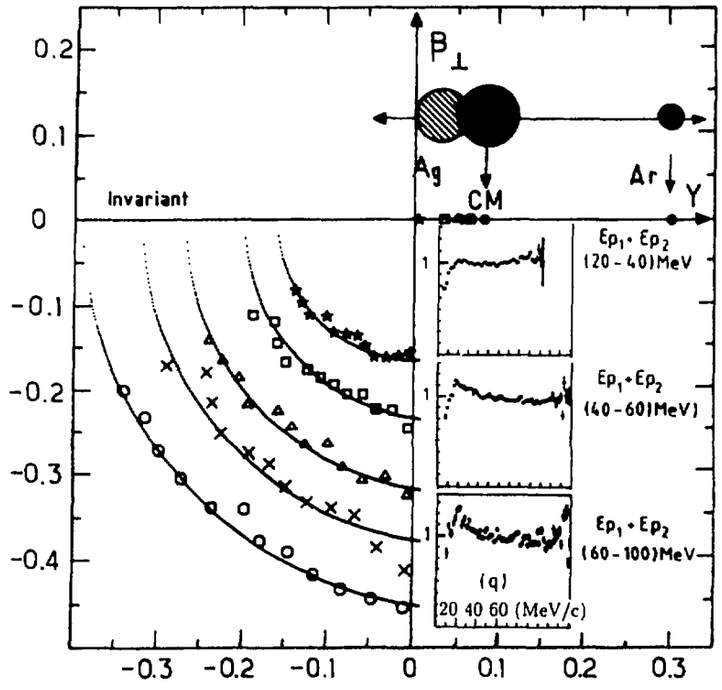

Figure 1: p-p correlation functions against proton energies and source excitation. The nuclear correlation at 20 MeV/c only occurs for a highly excited source. There is no nuclear correlation for a weakly excited quasi-target

to a high excited source, i.e., to a source which is close to the CM rapidity. On the other hand, the lower the proton energies, the weaker their nuclear interaction; the source has in this case, a velocity close to the target one, indicating a weakly excited target. This feature shows that the amplitude of a final state interaction depends on the excitation energy of the source and that, in this specific case, the scattering length of two protons of low energy is surely larger than the usual one ($\simeq$ -7.5 fm) known in decays of few nucleon systems. This can be due to the occurence of a large space-time effect when the source has lost its large excitation.

A conclusion of this is that, when using the yield of a peak due to a final state interaction in a correlation function, we should keep in mind that this quantity only reflects an average value over the excitation energy of the source or, alternatively, over the decaying time.

We used such resonance yields to draw the temperature of this source. On figure 2 we display the p-t correlation function which allowed us[1] to draw the relative population between the 20.1 MeV state and the ground state of ^{4}He. The same procedure was done for the 2.18 MeV state and the 4.31 state of ^{6}Li. In both cases we find temperatures which are respectively: T= 2.2 $^{+0.3}_{-0.2}$ MeV and T= 2.9 $\pm$0.7 MeV.

Time effects are more difficult to draw quantitatively from correlation measurements. As the results show on figure 1, there is a fingerprint (such as the resonance reduction) of time effects. Nevertheless, they are difficult to quantify without ambiguity and are model dependent.

One of the possibilities, formerly suggested in the study of p-p correlation functions,

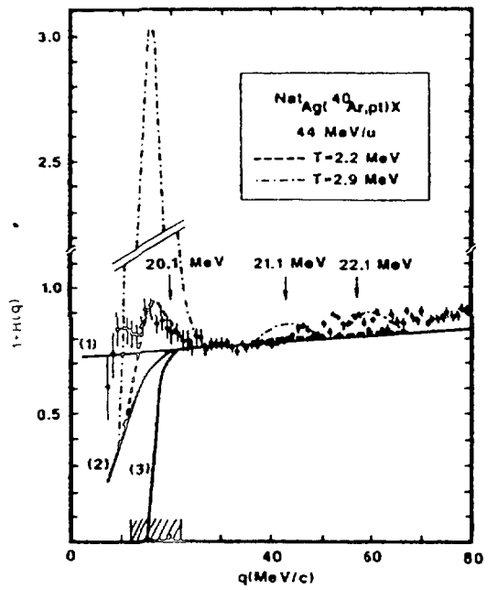

Figure 2: Relative population of the 20.1, 21.1, 22.1 MeV ^{4}He excited states in p-t correlations. A temperature of 2.2 MeV is found.

is to search for a possible anisotropy in the decay of two protons in the CM of the ^{2}He resonance, either in the direction of flight of the composite system or perpendicularly to it.

On figure 3 we display the results[2] of this procedure. Due to the poor directional sensitivity, it is hard to conclude that a lifetime effect, in the sense of the proposed analysis, is clearly observed.

Further studies[6,5] are necessary to understand the clear reduction and even the disappearance of the ^{2}He resonance. Let us recall that such a reduction was also found versus the increasing average angle of detection in ^{16}O + Au at 94 MeV/A[3]. This feature is certainly reminiscent of a large space-time extent of the source.

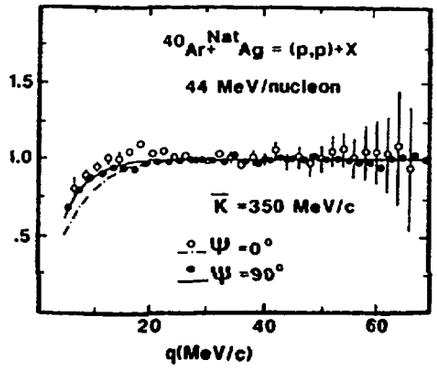

Figure 3: Search for directional effects in the pp correlation function. The results are displayed for a low total momentum and two directions of emission in the cm system of ^{2}He (notice that this is the case of a strong resonance reduction). The sensitivity is very low, as predicted by theory (full line and dashed line).

References

[1] H. Dabrowski et al., Phys. Letters 247(1990)223

[2] D. Goujdami et al., Z. Phys. A 339(1991)293

[3] J. Québert et al, Bormio meeting, Supp. 69(1989)220, ed. I.Iori, Milano

[4] D. Ardouin et al, Nucl. Phys A495(1989)57c

[5] D. Ardouin et al, Proc. of the E. Fermi School, Varenna (1989)

[6] J. Québert et al, Nuclear dynamics and nuclear disassembly; Dallas- World Scient., ed. J.B. Natowitz 1989 p.337

[7] D. Ardouin et al., Second IN2P3-RIKEN Symposium on H.I. Collisions, World Scient., ed. B. Heusch, M. Ishihara 1990 p.186

[8] J. Québert et al; CORINNE 90; Nantes- World Scient., ed. D. Ardouin 1990 p.134

[9] P. Lautridou, Tours Symposium on Nucl. Physics (1991)

PB INDUCED FISSION AT 29 MEV/NUCLEON ON A SERIES OF TARGETS: C, AL, NI, AU

L.Pienkowski[a,b], S.Bresson[a], R.Bougault[c], J.Colin[c], E.Crema[a,d], J.Galin[a], B.Gatty[e], A.Genoux-Lubain[c], D.Guerreau[a], D.Horn[c,f], D.Jacquet[e], U.Jahnke[g], J.Jastrzebski[b], A.Kordyasz[h], C.Le Brun[c], J.F.Lecolley[c], B.Lott[i], M.Louvel[c], M.Morjean[a], C.Paulot[a], E.Piasecki[h], J.Pouthas[a], B.Quednau[j], W.U.Schroeder[j], E.Schwinn[g], W.Skulski[b], J.Töke[j]

[a]*GANIL, B.P. 5027, 14021 Caen-Cedex France*

[b]*Heavy Ion Laboratory, Warsaw University, ul. banacha 4, 02-097 Warszawa, Poland*

[c]*Laboratoire de Physique Corpusculaire, Bd du Maréchal Juin, 14032 caen-Cedex France*

[d]*Instituto de Fisica, Universidade de Sao Paulo, Brazil*

[e]*Institut de Physique Nucléaire B.P.1, 91406 Orsay-Cedex France*

[f]*Chalk River Laboratories, Atomic Energy of Canada Limited, Chalk River, Ontario,Canada KOJIJO*

[g]*Hahn Meitner Institut,D1000 Berlin 39, Germany*

[h]*Institut of Experimental Physics, Warsaw University, Hoza69, 00-681 Warszawa, Poland*

[i]*Centre de Recherches Nucléaires Strasbourg, B.P. 20 CRO, 67037 Strasbourg France*

[j]*University of Rochester, Rochester, New York 14627 USA*

1. Motivations

Fission has been often used as a means to probe either the reaction mechanisms or the properties of nuclei formed in intermediate energy heavy ion reactions. However, for the fission process to occur, rather severe constraints exist on the mass, excitation energy, spin, isospin of the nucleus. Therefore, most often, one probes a limited part of the reaction cross section through this process and thus, it is of great importance to know which part of the reaction has been probed. One typical example has been already given with Ar induced reactions studied at several bombarding energies[1], but in the present contribution one wants to investigate the influence of mass asymmetry in the entrance channel on the fission properties.

A 29 MeV/nucleon Pb beam has been used in order to bombard targets as different as C, Al, Ni and Au. From the amounts of available energy in these systems, 330 MeV for Pb+C or nearly 3 GeV for Pb+Au, it can be easily guessed that fission will be a dominant channel in the first reaction and rather marginal in the second, as already shown elsewhere[2]. In all cases, and due to the pretty large fission barriers of Pb-like nuclei, it is obvious that the most peripheral collisions cannot be investigated through fission. But here, we are interested in all other collisions which are more dissipative than the very peripheral ones.

2. The experimental approach.

By using a heavy ion beam on lighter targets, the fission fragments get strongly forward focused that makes them easy to catch with a single detector of limited aperture. Moreover, their large energy facilitates their identification. A position-sensitive telescope subtending an opening of 16 deg., from 6 to 20 deg., was utilized for this purpose. It consisted of two silicon detectors (.2 mm ad .5 mm thick for dE and E respectively), each divided into strips which provided us with the emission angle of the fragment with respect to the beam axis. Atomic numbers could be resolved up to Z=50. In addition, the neutron multiplicity was counted over 4 pi with the ORION detector in order to provide, eventwise, a reliable information on the violence of the collision.

3. The experimental data.

An overview of all detected nuclei is given as a function of associated neutron multiplicity for the four targets (Fig.1). Due to the small grazing angle for the three lighter targets (C, Al, Ni) and the position of the telescope, the projectile-like nuclei having not undergone fission in very peripheral collisions could not be seen. Only for Au, some of these high Z nuclei could be registered in the inner strips of the telescope.

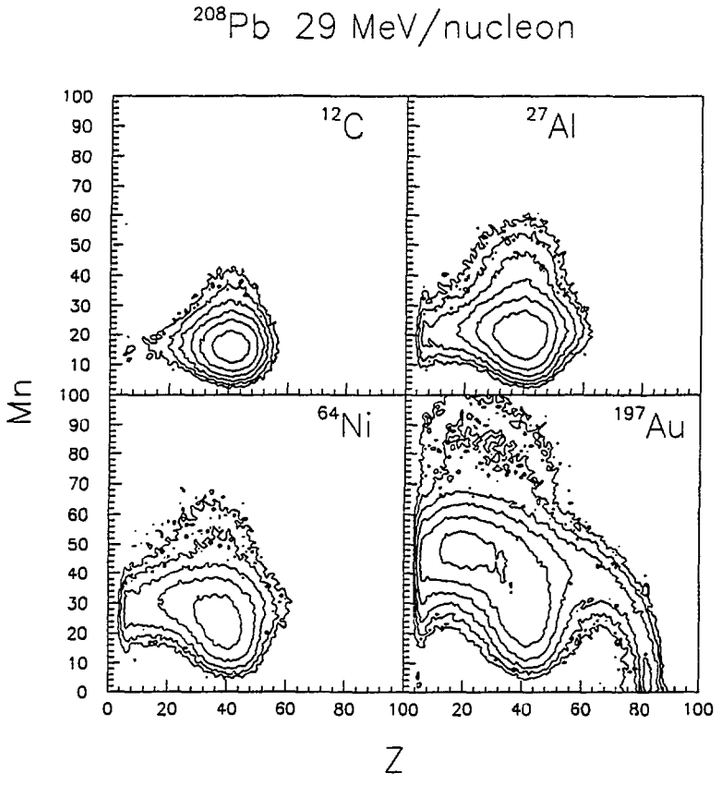

Fig.1 Distribution of nuclei detected from 6 to 20 deg. as a function of neutron multiplicity in Pb induced reactions on several targets. The intensities are given in arbitrary units.

The most interesting part of the data, in so far as fission is considered, comes from Z<60. For the C target, fission fragments appear very distinctly and cannot be confused with anything else. For the Au target, as already stressed elsewhere[2], fission fragments of the projectile-like nucleus are far from being dominant and moreover they are not well separated from fragments of a distinct origin especially for large neutron multiplicities. A continuous evolution between the C and Au patterns can be seen on these plots for intermediate targets like Al and Ni. Clearly, intermediate mass fragments appear to be, on the average, more selective of highly dissipative collisions than binary fission

As it has been explained in some details in another contribution[3], it is possible to infer the properties of the fissioning nuclei from the analysis of a single fission fragment provided the violence of the collision, or the energy dissipation, has been filtered before by using the neutron multiplicity information. The data relative to the recoil velocity of the fissioning nuclei are presented

in Fig.2 for different neutron multiplicity gates. There is a rather general behaviour for all considered targets, showing that, the larger M_n, the slower the fissioning nuclei appear to be. This

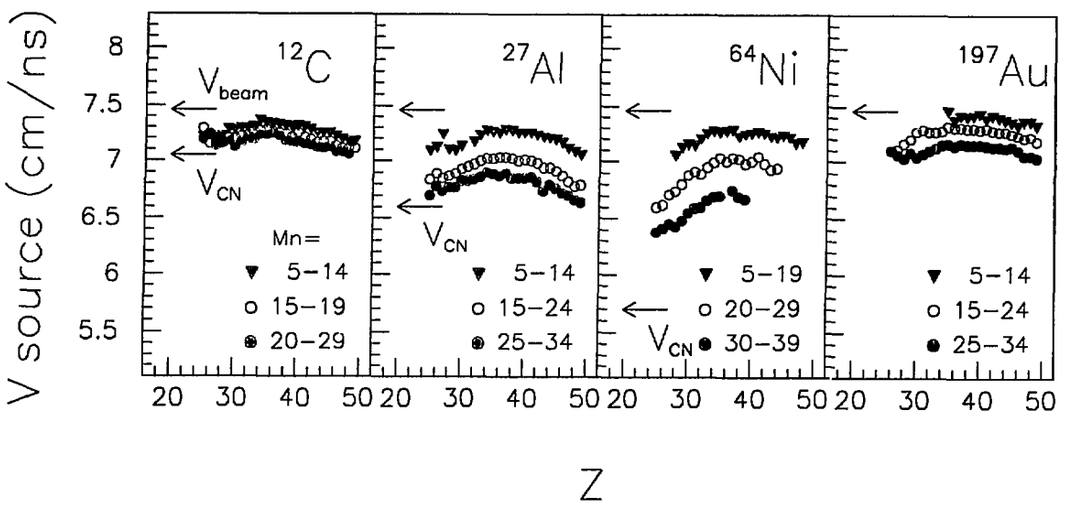

Fig.2 Velocities of the fissioning nuclei as derived from a fit of fragment invariant cross sections as a function of Z of the fragments for different neutron multiplicity gates (as measured). The beam velocity and compound nucleus velocity are shown to suggest the amount of transferred momentum.

slowing down in "reverse" kinematics is simply due to energy dissipation and the analogous effect, in "direct" kinematics, would simply be the acceleration of the fissioning nuclei. It is interessing to note that, for the two ligher targets, the most dissipative collisions are consistent with moment transfers of roughly 3/4 of the maximum they would reach in an ideal compound nucleus formation process. This data agree fairly well with the systematics[4]. However, for heavier targets, such as Ni, one observes a deviation from this systematics. At best, for the most dissipative collisions leading to a fission-like fragment the momentum transfer amounts , on the average, to 50% of the possible maximum value i.e. somewhat less than given by Volant et al[5] for a similar system. Fusion of Ni with Pb is far from being complete when investigating the fission channel. This is even better shown when considering the Au target. The most dissipative collisions appear to be too much violent for the heavy, heated nuclei to survive and undergo binary fission.

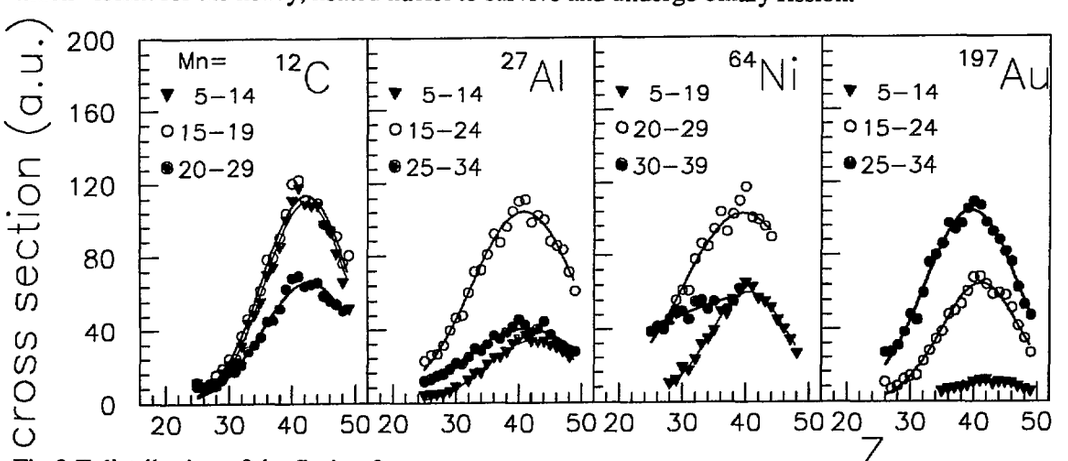

Fig.3 Z distribution of the fission fragments.

Another interesting piece of information is provided by the Z distributions of the fragments. The distributions have been constructed by integrating the data for each measured Z over the whole space. It is found that these distributions remain centered close to half the projectile Z, whatever the considered target, as though the fissioning nuclei had not gained much mass from the target. This low gain in Z is easily understandable in the case of C. At the other extreme, with the nearly symmetric Pb+Au system for which one does not expect flow of matter, on the average, these Z distributions are also easily understandable. For Al or Ni targets the transfer of matter in the first step of the reaction can be partially washed out by subsequent evaporation. In particular, at high excitation energy, charged particle evaporation has been shown to become noticeable, even for heavy, neutron rich, sytems. For example, from Kr+Au studies, with estimated excitation energies of 670 MeV, one measured 4 evaporated-like particles with Z=1 and 2.5 with Z=2, making altogether the evaporation of 9 charged units. This number amounts to 15 for an estimated E* of about 1 GeV[6]. Then, there is a delicate balance between gain by mass and Z transfer and loss by evaporation which leads to fission fragments of similar mass, irrespective of the violence of the collision. It is worth noting that if the first moment of the Z distributions remains almost constant, the second moment increases noticeably with excitation energy. This effect is probably more related to a broadening of the initial mass and Z distribution of the fissioning nuclei than to a thermal effect on the fission process itself.

4 Conclusions

This systematic studies of fission induced by Pb on a series of target has shown that the fission probe was very well suited to study the most dissipative collisions induced on light targets like C and possibly Al. However when increasing the target mass and by keeping constant the beam energy, more and more energy becomes available in the considered system and binary fission becomes less and less likely for the most dissipative collisions. This has been clearly shown in the extreme case of the Pb+Au interaction, but this is also quite noticeable in the case of Pb+Ni. As already shown elsewhere[1,7], the emission of intermediate mass fragments becomes enhanced at high excitation energies and this has a strong effect on fission barriers of the residual nuclei. The fission process which is a good probe of both linear and angular momentum effects should be used with great caution when dissipative phenomena are at stake. A nucleus must meet rather restrictive conditions on mass, Z, spin and excitation energy in order to undergo fission. This makes of fission both a powerful tool, but also a rather difficult tool to be used in the study of reaction mechanisms.

REFERENCES

1 E.Schwinn et al., to be published and contribution to this volume
2 E.Piasecki et al., Phys. Rev. Lett. **66** (1991) 1291
3 S.Bresson et al., submitted to Phys. Rev. Lett. and contribution to this volume
4 M.Fatyga et al., Phys. Rev. Lett. **55** (1985) 1376
5 C.Volant et al., Phys. Lett. **B195** (1987) 22
6 E.Crema et al., Phys. Lett. **B258** (1991) 266
7 A.Sokolov et al., to be published and contribution to this volume

THE EMISSION OF COMPLEX FRAGMENTS IN THE REACTION Ar+Au AT 44 AND 77 A.MEV

A.Sokolov [1], D.Guerreau[1], J.L Charvet[2]*, B.Cramer[3], H.Doubre[1], J.Fréhaut[2]
J.Galin[1], B.Gatty[4], G.Ingold[3], D.Jacquet[4], U.Jahnke[3], D.X.Jiang[1,5]
B.Lott[6], C.Magnago[2]*,M.Morjean[1], Y.Patin[2], E.Piasecki[7], J.Pouthas[1], E.Schwinn[3]

1- GANIL, BP 5027 14021 Caen Cedex, France
2- CE Bruyères-Le_Chatel, B.P 12, 91680 Bruyères-le-Chatel, France
3- Hahn Meitner Institute, D-1000 Berlin 39, Germany
4- IPN, BP 1, 91406 Orsay Cedex, France
5- Dept. of Phys. Technics, Univ. of Beijing, Beijing, China
6- CRN Strasbourg, BP 20 CRO, 67037 Strasbourg Cedex, France
7- Inst. of Exp. Phys, Warsaw Univ.,Hosa 69 00-681 Warsaw Poland

1. Motivations

One of the main features of heavy ion induced reactions in the intermediate energy range (above 25 A.MeV) is the increasing emission of the so-called "intermediate mass fragments" (IMF) or "complex fragments". This problem has attracted much interest as it was first connected with the possibility to give evidence for the existence of a transition towards a new decay mode usually called "multifragmentation". Such a transition would be observed when selecting more and more violent colllisions. As it appears reasonable to not rely on the characteristics of the exit channels which are a priori unknown, it is desirable to choose an observable, connected with the degree of violence of the collision, which introduces the least possible bias in the interpretation of the data. In that sense, the measurement of the neutron multiplicities M_n appears to be a quite appropriate choice. Complex fragment emission from the 44 and 77 A.MeV $^{40}Ar + ^{197}Au$ reaction has been investigated. Equilibrium and non-equilibrium components have been identified which are discussed in terms of statistical emission from the hot target-like fragment and of a deep-inelastic process.

2. Experimental approach

In this experiment, we have performed coincidence measurements between neutrons and intermediate mass fragments (IMF) in the reaction $^{40}Ar+^{197}Au$ at 44 and 77 A.MeV. The choice of a heavy system insures that neutron emission is strongly favoured with respect to l.c.p. emission. The knowledge of the neutron multiplicity (Mn) is then a good guide of the degree of violence of the collision (and to some extent of the impact parameter)[1]. Through this study we aimed to isolate the different components in the IMF emission and discuss their possible origins.

The 4π Gd loaded liquid scintillator detector (from HMI Berlin) was used in order to get an event by event measurement of the neutron multiplicity[2]. Its efficiency is close to 80% for those neutrons isotropically emitted from a hot TLF moving with a velocity of 1 cm/ns and 30% for 40 MeV neutrons. To first order, the detected neutrons will then be considered as evaporated ones from the TLF.The IMF have been measured using standard Si telescopes located at 3.7° (2.7° at 77 A.MeV), 20°, 40°, 60° and 160° .

3. Experimental results.

The evolution of the mean value <Mn> as a function of the coincident fragment Z (for different detection angles) is displayed in Fig 1 (the neutron multiplicity has been corrected for the efficiency of the detector).
Previous studies have demonstrated that, near the grazing angle, the observed products are mainly

* Present address: CEN Saclay, DPhN-SEPN, 91191 Gif sur Yvette CEDEX, France

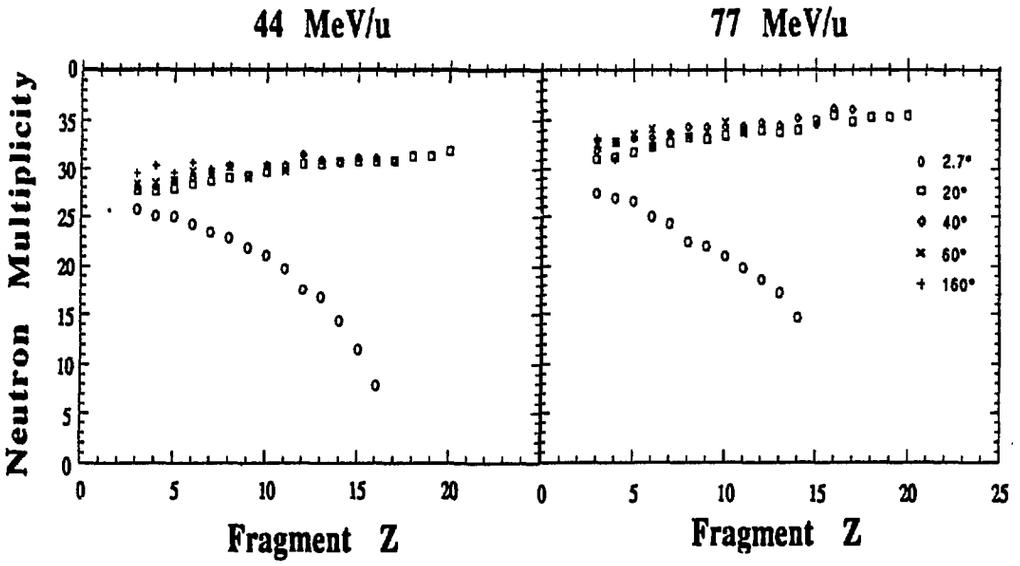

Fig. 1 Average neutron multiplicities (corrected for the efficiency of the detector) associated with IMF detected at various angles.

projectile-like fragments (PLF) originating from rather peripheral collisions and the sharp increase of <Mn> with decreasing Z is just the signature of an increasing energy dissipation[3]. It has been shown to be in qualitative agreement with a massive transfer process for not too high incident energies[3].

The main point is that, apart from these most forward angles (2.7°and 3.7°), the mean Mn values (as well as the second moments of the distributions, not represented in the figure) almost do not change with the detected Z. Moreover, *<Mn> rises by only about 3 units between 44 and 77* A.MeV. These mean values are very close to the ones associated with the high multiplicity bump in the inclusive neutron data. They are also similar to those observed for other exit channels (evaporated light charged particles or fission[1]). The detection of one IMF in the exit channel doesn't seem to reflect, on the average, the existence of more excited nuclei. It should be mentioned also that, apart from the grazing angle, <Mn> almost doesn't change with the fragment kinetic energy.

Very similar forward peaked angular distributions are also observed at both incident energies for those fragments having a velocity smaller that 80% of the beam velocity (i.e. excluding the PLF contribution) which ,once again, seems a strong indication for the IMF to have very close origin(s) in this energy range. If one excepts Z=3, the integrated charge distribution is also quite insensitive to the bombarding energy. All these products originate from very dissipative collisions as the associated neutron multiplicity is high and close to the most probable value of the high multiplicity bump in the inclusive neutron data. One may then define the average IMF multiplicity as the ratio of the total IMF cross section to the total cross section corresponding to "dissipative" collisions (the latter can be easily deduced from the inclusive neutron multiplicity distributions). Deduced values are close to 1 IMF per collision at 44 A.MeV and 1.2 IMF at 77 A.MeV.

Fig 2 shows the total IMF cross-sections (for Z=3-14) compared with those measured at 30 and 220 A.MeV[4]. Surprisingly, within the experimental uncertainties, the IMF cross section remains remarquably constant over this wide energy range.

What are the possible origins of the complex fragments? It is tempting to first assume that two components are present, a fast non-equilibrium component, strongly forward peaked and a slow one leading to a quite isotropic emission of the IMF. The equilibrium component is usually explained by a standard evaporative process from an equilibrated system.

In order to evaluate the maximum contribution from a thermally equilibrated source (the hot quasi target), all IMF emitted at 160° have been considered to come from this unique source. The shape of the energy spectrum has been parametrized according to Moretto prescription[5]. Energy

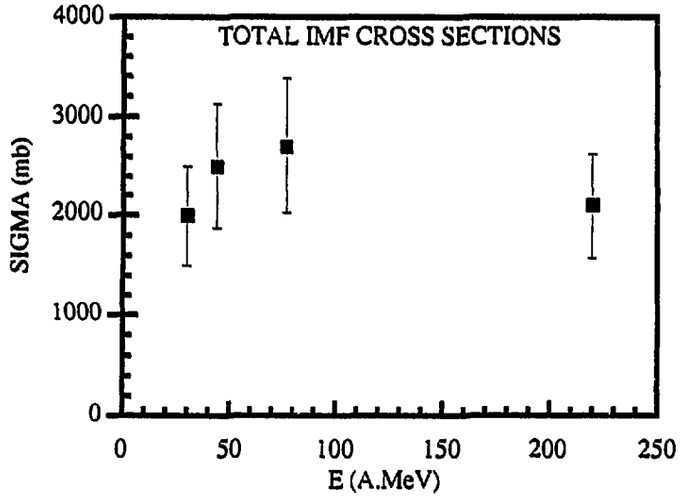

Fig.2 Integrated IMF cross sections for various incident energies between 30 and 220 A.MeV.

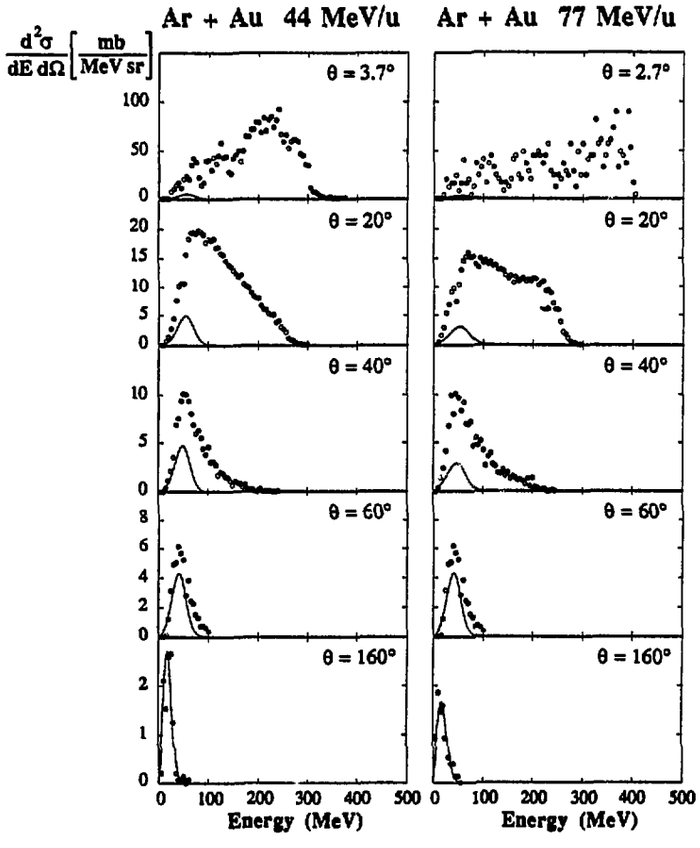

Fig.3 Comparison of experimental energy spectra for Z=3 (points) with calculated ones (solid curves) assuming an evaporation by the hot quasi-target

spectra have been calculated for each laboratory angle assuming a source recoil velocity of 1cm/ns and a temperature of 5 MeV. The calculated spectra for such an equilibrated component, assuming a $1/\sin\Theta$ angular distribution in the source rest frame, are compared to the experimental ones for Z=3 at the two bombarding energies (Fig.3).

It appears clearly that most fragments are not evaporated by the target like nucleus in thermal equilibrium. "Non equilibrium source(s)" are more and more dominant as one goes from backward to forward angles. The corresponding average IMF multiplicity for this equilibrium component amounts to about 0.15±0.05 IMF per "dissipative" collision at both incident energies (that is at least 5 times smaller than the "non equilibrium component"). This value is in agreement with a GEMINI calculation assuming a composite system ^{221}Th excited at 600 MeV.

Another explanation has to be put forward to account for the emission of slow fragments at small angles (<60°) which are also associated with a large energy dissipation, i.e high Mn values . The origin of such fragments, with an average multiplicity close to unity, is more puzzling and may be associated with shorter time-scales. Let us just say that the forward IMF emission may be qualitatively understood within a deep inelastic process. The persistence of such binary processes with strong energy damping, even at rather high incident energies, may result from a strong reduction of the energy relaxation time due to the increasing effect of the two-body collisions[6].

The bulk of the IMF cross-section seems then to be explained by "conventional" mechanisms. This doesn't exclude at these energies the possible occurence of more exotic but rare processes associated with higher multiplicities which however would require more exclusive measurements.

7. Conclusions

Complex fragments with Z≥3 have been detected in the Ar+Au reactions at 44 and 77 A.MeV together with the associated neutron multiplicity distributions[7].

Energy spectra and angular distributions for those complex fragments issued from strongly dissipative collisions indicate the existence of two contributions.The isotropic component may be explained by a statistical emission from the hot system after an incomplete fusion process. The average fragment multiplicity for such a process, which remains small (≈0.15) and constant at both incident energies can be accounted for by statistical calculations assuming an average excitation energy deposit in the system close to 600 MeV.

The origin of the other component which is strongly forward peaked is more puzzling and may be associated to shorter time scales. It corresponds to much larger cross-sections than the evaporative component , with a multiplicity close to unity. The properties of this component are not incompatible with the persistence of a deep inelastic process at these high energies.

REFERENCES

(1) D.X.Jiang et al, Nucl.Phys. A503(1989)560
(2) U.Jahnke et al, Lecture Notes in Physics, (Springer, Berlin, 1983), 170
(3) M.Morjean et al, Nucl.Phys. A524(1991)179
(4) U.Milkau et al, GSI Preprint 91-08
(5) L.Moretto, Nucl.Phys. A247(1975)211
(6) D.Jouan et al, Z.Phys. 340(1991)63
(7) A.Sokolov, Thèse de Doctorat, Université Paris VI(1990)
A.Sokolov et al, to be published.

HOT NUCLEAR SYSTEMS (T>6 MEV) INVESTIGATED IN 32 MEV/NUCLEON KR INDUCED REACTIONS ON AU

E.Crema[a,b], S.Bresson[a], H.Doubre[a], J.Galin[a], B.Gatty[c], D.Guerreau[a], D.Jacquet[c], U.Jahnke[d], B.Lott[e], M.Morjean[a], E.Piasecki[a,f], J.Pouthas[a], F.Saint-Laurent[a], E.Schwinn[d], A.Sokolov[a], X.M.Wang[a,g]

[a] GANIL, B.P.5027, F-14021 Caen Cedex, France
[b] Instituto de Fisica da Universidade de Sao Paulo, Sao Paulo, Brazil
[c] IPN, B.P.1, F91406 Orsay Cedex, France
[d] Hahn Meitner Institute, D1000 Berlin 39, Germany
[e] CRN Strasbourg, B.P.20 CRO, F-67037 Strasbourg Cedex, France
[f] Institute of Experimental Physics, Warsaw University, Hoza 69, PL-00-681 Warsaw, Poland
[g] Institute of Modern Physics, P.O.Box31, Lanzhou, China

1. Motivations

Heavy ion induced collisions at intermediate energy have proved to be very efficient means of studying the formation and decay of hot nuclei. After a series of measurements performed on the Ar+(Au,Th) systems[1] in order to study the influence of bombarding energy on energy dissipation, it was deemed relevant to complement this systematics by studying the effect of projectile mass (or entrance channel mass asymmetry) on energy dissipation. The beam velocity was kept close to 30 MeV/nucleon to compare with Ar data[1] at a similar velocity and the mass of the projectile was nearly doubled by choosing ^{84}Kr as a projectile.

The determination of T is not an easy task, especially for pretty heavy systems, due to the large variety of decay channels. Since the characteristics of these channels are not known a priori, it is desirable to choose for T an observable which introduces the least possible bias to the interpretation of the measurements. The evaporation of light particles is expected to fulfill this condition since such particles are always emitted whatever the decay process. Measurements of the multiplicities of neutrons and light charged particles (LCP) permits a rather direct estimate of the excitation energy[1-2].

2. The experimental set up.

The Au target was placed inside a small scattering chamber surrounded by the 4π neutron detector, ORIONI, providing the neutron multiplicity information (M_n). ORIONI, a Gd loaded liquid scintillator detector of a total volume of 3 m^3, has a large efficiency for low energy neutrons (87% at 2 MeV) that makes it a very good tool for counting the neutrons evaporated by slow moving heavy and hot nuclei. In addition to the neutron detector, two standard telescopes set at 109° and 159° allowed the identification of evaporated charged particles and provided the trigger signal for the event by event neutron numbering.

3. Experimental results

As already observed in Ar induced[1] reactions, the inclusive neutron multiplicity distribution exhibits two components which can be related to peripheral and central reactions collisions. As also shown elsewhere[2-3], for heavy nuclei, evaporated light charged particles are mostly emitted in the highly dissipative collisions, i.e. in coincidence with rather large neutron multiplicities. This is well illustrated when comparing the gated- and ungated neutron multiplicity spectra (Fig. 1b and 1a), or their relative quantity which is nothing but the differential particle multiplicity (Fig.1c).

Further insight on the origin of the backward emitted LCP has been obtained by constructing their energy spectra for each associated M_n. The most probable energies, E_{mp}, of such spectra, exhibit a very strong dependence with M_n, as displayed in Fig.2, which can be simply

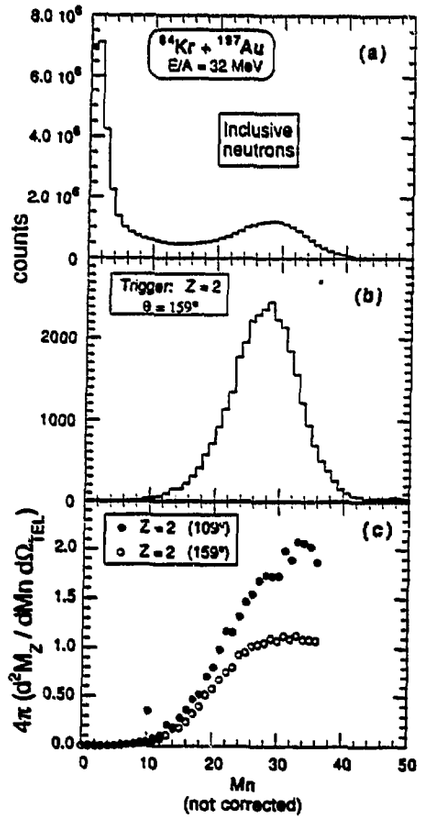

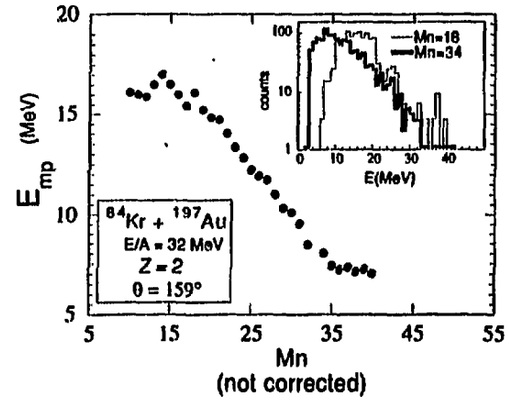

Fig.2 Evolution with M_n of the most probable kinetic energy E_{mp} of Z=2 detected at 159°. The insert displays the energy spectra measured for two different M_n values.

Fig.1. Neutron multiplicity distrbutions as measured in the inclusive mode (a), in coincidence with Z=2 detected at 159° (b). Differential multiplicities for Z=2 (without jacobian correction) detected at 159° and 109° (c). No correction has been applied for the detection efficiency of the neutron detector.

explained by kinematical considerations: the more violent the collision, the greater the recoil velocity of the emitter and the smaller E_{mp} of the backward emitted particles are. In order to interpret quantitatively this correlation between Emp and Mn, the very simple massive transfer picture has been employed. Details can be found in ref.[4]. It appears that, for the detection angles considered here, this method of determination of the recoil velocity is almost independent of the assumed mechanism. The analysis was performed on neutron multiplicity bins of 5 units from M_n=10 to 35. The most violent collisions (highest Mn bin) lead to a very high momentum transfer (85% of the initial momentum) in agreement with the results of ref.[5]. Once a recoil velocity of the emitter has been inferred, then it is possible to determine the total multiplicity of LCP from the measured differential multiplicities shown in Fig. 1c..An isotropic emission in the proper reference frame has been assumed. The neutron multipl...ities corrected for detection efficiency and associated LCP are listed in table I. It can be noticed that data measured at 109° and 159° lead to the same integrated alpha-particle multiplicities in agreement with the isotropic distribution hypothesis. It is also an a posteriori confirmation of the validity of the determination of the source velocities. The last step of the analysis consists in deriving the thermal excitation energies E* (and T from the relation $E^*=A/10T^2$) from the multiplicities of evaporated neutrons and LCP. The calculation was performed by removing step by step an energy equal to (B_n+2T) per emitted neutron and (B_{LCP}+V_B+2T) per emitted LCP. This was

done in an iterative way as the initial temperature is unknown. The deduced values for E* and T are shown in table I.

<Mn> (corrected)	v_S/v_{FMT}	$M_{Z=1}$	$M_{Z=2}$		E*	T	T_{fit}
		Θ=159°	Θ=159°	Θ=109°	(MeV)	(MeV)	(MeV)
18.3	.45	.5	.4	.4	300	3.5	3.3
24.6	.60	1.7	1.5	1.2	480	4.5	4.3
30.1	.70	3.9	2.5	2.4	670	5.2	5.1
36.2	.81	5.6	3.5	3.6	860	5.8	6.3
40.5	.90	7.3	4.0	4.1	1030	6.2	7.0

Table I For each neutron multiplicity bin, corresponding to an average value <Mn> corrected for detector efficiency, the following quantities have been deduced: the ratio of the source velocity v_S to the center of mass velocity, v_{FMT}, the multiplicities for Z=1 and Z=2 (as deduced from two independent measurements at 159° and 109°), E*, T and T_{FIT} (see text).

For the most probable recoil velocity, an excitation energy close to 900 MeV is then derived, much higher than for the Ar induced reaction at a similar incident velocity.[1]

In order to extract the spectral temperature parameters, the five He-energy spectra associated with the five M_n windows of table I were constructed in their respective center of mass reference system using the previously calculated jacobians. These spectra are displayed in Fig.3 which clearly highlights the strong evolution with Mn of the slopes. Surface emission was assumed and maxwellian fits where then used to extract the apparent temperatures indicated by T_{fit} in table I. These values, which should represent an average value along the cascade, match nevertheless nicely with the initial temperatures extracted from the particle multiplicities. This may be explained by the fact that α-particles are preferentially emitted at an early stage of the deexcitation process, i.e.when the nucleus is the hottest.

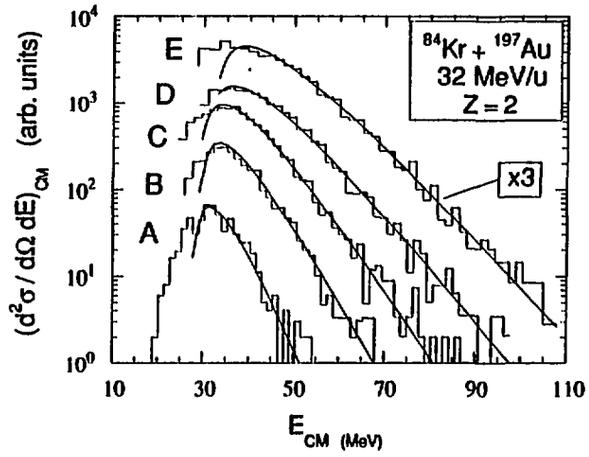

Fig.3 He-energy spectra, measured at 159° in the laboratory system, converted in their respective center of mass reference frame, associated with the five M_n windows of table I.

4. Conclusions

The consistent values of the temperatures which have been derived from two independent observables (multiplicities of particles and slope of energy spectra) give great confidence in the data thus obtained. For the most dissipative collisions in the Kr+Au reactions, composite systems can be formed for which about 85% of the projectile momentum has been transferred, leading to an excitation energy of ~1 GeV (or ~4 MeV/unucleon) and a temperature of ~6.2 MeV. Despite the fact that the decay lifetime for such hot systems is predicted to be very short ($<10^{-22}$s), i.e. comparable to the thermalization time, the excited systems behave like thermally

equilibrated nuclei would do. They emit a large number of light particles (up to 52, when including Z=1,2 and neutrons), with typical evaporative energy spectra.

REFERENCES:

(1) D.X Jiang et al. Nucl. Phys. A503 (1989) 560.
(2) W.A.Friedman Univ. Madison Preprint Mad/NT/90-08
(3) B.Lott et al., contribution to this volume
(4) C.Crema et a. Phys. Lett. B258 (1991) 266
(5) R.Bougault et al.Proc. XXVIII Int. Winter Meeting on Nuclear Physics (Bormio 1990)

CHARGED PARTICLES CALORIMETRY OF $^{40}AR + ^{27}AL$ REACTIONS FROM 36 TO 65 MEV/u.

D. Cussol [a], G. Bizard [a], R. Brou [a], D. Durand [a], M. Louvel [a], J.P. Patry [a], J. Péter [a], J.P. Sullivan [a], R. Regimbart [a], J.C. Steckmeyer [a], B. Tamain [a], E. Crema [b-l], H. Doubre [b], K. Hagel [b-f], G.M. Gin [b-h], A. Péghaire [b], F. Saint-Laurent [b], Y. Cassagnou [c], R. Legrain [c], C. Lebrun [d], E. Rosato [e], R. MacGrath [g], S.C. Jeong [i], S.M. Lee [i], Y.Nagashima [i], T. Nakagawa [i], M. Ogihara [i], J. Kasagi [i-j], T. Motobayashi [a-b-k]

a) LPC Caen, ISMRA, 14050 Caen, France; b) GANIL; c) DPhN/SEPN, CEN Saclay; d) LPN Nantes; e) Dipart. di Scienze Fisiche di Napoli, Italy; f) Cyclotron Institue Texas A&M University, USA; g) SUNY Stony Brook, USA; h) Inst. of Modern Physics, Lanzhou, China; i) Inst. of Physics University of Tsukuba, Japan; j) Dept. of Physics Tokyo Inst. of Technology, Japan; k) Rikkyo University, Tokyo, Japan; l) Inst. di Fisica Univ. di Sao Paulo, Brazil

I - MOTIVATIONS

An aim of the study of hot nuclei is to answer the question: what is the maximum amount of energy which can be thermalized in a nucleus ? Are there limiting values of the temperature or/and the excitation energy ? A lot of work has been already done, giving somewhat contradictory results. The main problem of most of these studies is that the temperature was determined from the value of the excitation energy or vice versa, using the well known relation $E^* = a T^2$, so that these two quantities are not measured independently. This is not a problem at low energies since the excitation energy is essentially thermal, but this prevents to track possible decorrelations between these two observables at higher energies. Particularly, it is impossible to track compression effects and/or variation of the density level parameter value if T and E^* are not independently determined. Such an independent measurement of T and E^* has been made by R.Wada et al. [Phys. Rev. C39 (1988) 497], showing a variation of a with E^*.

We present here the results of the analysis performed on the $^{40}Ar + ^{27}Al$ system from 36 to 65 MeV/u incident energy in which E^* and T are independently measured.

II - EXPERIMENTAL SETUP

In this reverse kinematics system, nearly 4π in the center of mass was covered by using two complementary multidetector systems which covers 2π in the laboratory (see figure 1). The forward angles between 3.2° and 30° were covered by the MUR. Angles between 30° and 90° were covered by a spherical half-barrel TONNEAU. All events with a multiplicity larger than 1 were recorded in order to avoid an uncontrolled bias on the reactions. The velocities of all particles were measured and the charges were identified up to $Z = 8$, the particles with a higher charge were taken as having a charge equal to 9. The masses of the particles were estimated from the value of their charges. This setup is particularly efficient when the reaction leads to light and energetic particles, the particle identification being better for particles with a large velocity. Neutrons were not detected and 10-15 % of charged particles are missed due to narrow dead areas between detectors and to the absence of detectors at backward and very forward angles.

III - SELECTION OF WELL MEASURED EVENTS AND IMPACT PARAMETER SORTING

See contribution: "Using global variables for impact parameter determination in nucleus-nucleus collisions below 100 MeV/u".

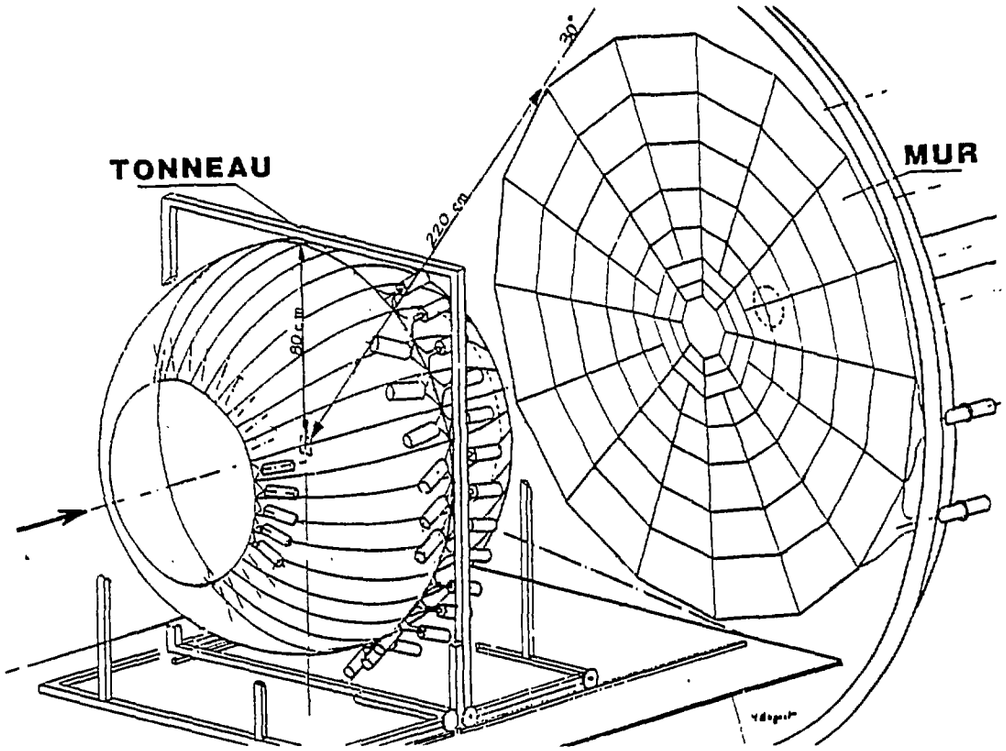

Figure 1: Experimental setup. The backward part of the TONNEAU was not present in this experiment.

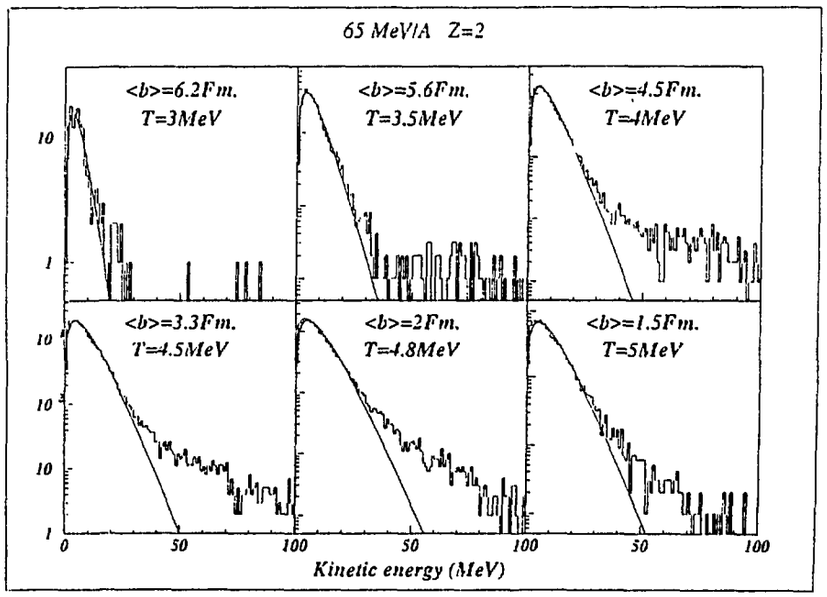

Figure 2: Kinetic energy distribution in the incomplete fusion nucleus frame for Z=2 particles at 65 MeV/u and for different impact parameter values. The black full line represents the fitted function used to determine the measured temperature.

IV - SOURCE IDENTIFICATION

To determine accurately the velocity of the equilibrated source, we fit the parallel velocity distribution of heavy particles ($Z > 6$), which has no preequilibrium component, by a gaussian function. The velocity of this source is then defined as the centroid of the gaussian. We verify afterwards that the velocity obtained is consistent with the parallel velocity distribution of the light particles . We determine this way the velocity V_{CN} of the equilibrated nucleus for each impact parameter bin.

V - MEASUREMENT OF THE TEMPERATURE PARAMETER

The temperature parameter is determined by a fit of the kinetic energy spectra of light particles *in the source frame*. In order to minimize the preequilibrium contribution, these spectra have to be taken at forward angles, but not too forward in order to be less sensitive to the uncertainty on the source velocity value. The kinetic energy spectra are then plotted at 50° in the source frame (see figure 2).

The value of T obtained this way is not the initial temperature of the hot compound nucleus. These spectra are the result of a long and complex decay chain in which the mass and the temperature of the emitter vary with time. To estimate this initial temperature, we used an event generator developped by D. Durand in which the so called "measured" temperature can be compared to the initial one.

VI - ESTIMATION OF E*/A

The basic method to determine the excitation energy per nucleon is to sum all the kinetic energies of all the emitted particles by the compound nucleus, taking into account the mass balance. For that, pre-equilibrium and evaporation components must be separated.The mass and charge of the reconstructed equilibrated nucleus take into account the estimated neutron multiplicity, the detector efficiency and the underestimation of the charge and mass of fragments with $Z > 9$.

VII - CORRELATIONS BETWEEN E*/A AND T

Figure 3 shows the evolution of the square of the initial temperature as a function of E*/A, for incident energies ranging from 36 to 65 MeV/u and for different impact parameter bin. We see that the obtained values are coherent from an energy to another one,and lead to the usual value of A/8 for the level density parameter at low excitation energies. At higher energies, this value shifts continuously to A/10 although the results at 65 MeV/u are still in agreement with A/8. These results are consistent with those obtained by the Grenoble-Texas A&M collaboration which show that the level density parameter should decrease to a value of A/13 at high excitation energies. The difference between the values obtained at high energies could be due to the different sizes of the two systems.

VIII - CONCLUSION

The estimations made here are not accurate enough to clearly establish if the initial value of T saturates or increases. Notice that the values obtained are average values for each impact parameter bin and that it can exist some events in which the excitation energy can reach higher values, especially in the most central collisions. Hopefully, the new generation of multidetectors and complementary measurements will give more accurate results.

We can summarize the three general properties of hot nuclei formed in the $^{40}Ar + ^{27}Al$ collisions :

- The temperature and the excitation energy per nucleon increase when the impact parameter decreases, for a given incident energy.
- For central collisions ($b < 2$ fm), the initial temperature reaches a value of 7 MeV.
- For these collisions, the excitation energy per nucleon increases when the incident energy increases and it reaches 5 MeV/u at 65 MeV/u.

PUBLICATIONS

•D.Cussol et al., preliminary data in "Les nouvelles du GANIL", n°37, mars 1991.
•D.Cussol et al., submitted to Nuclear Physics A.

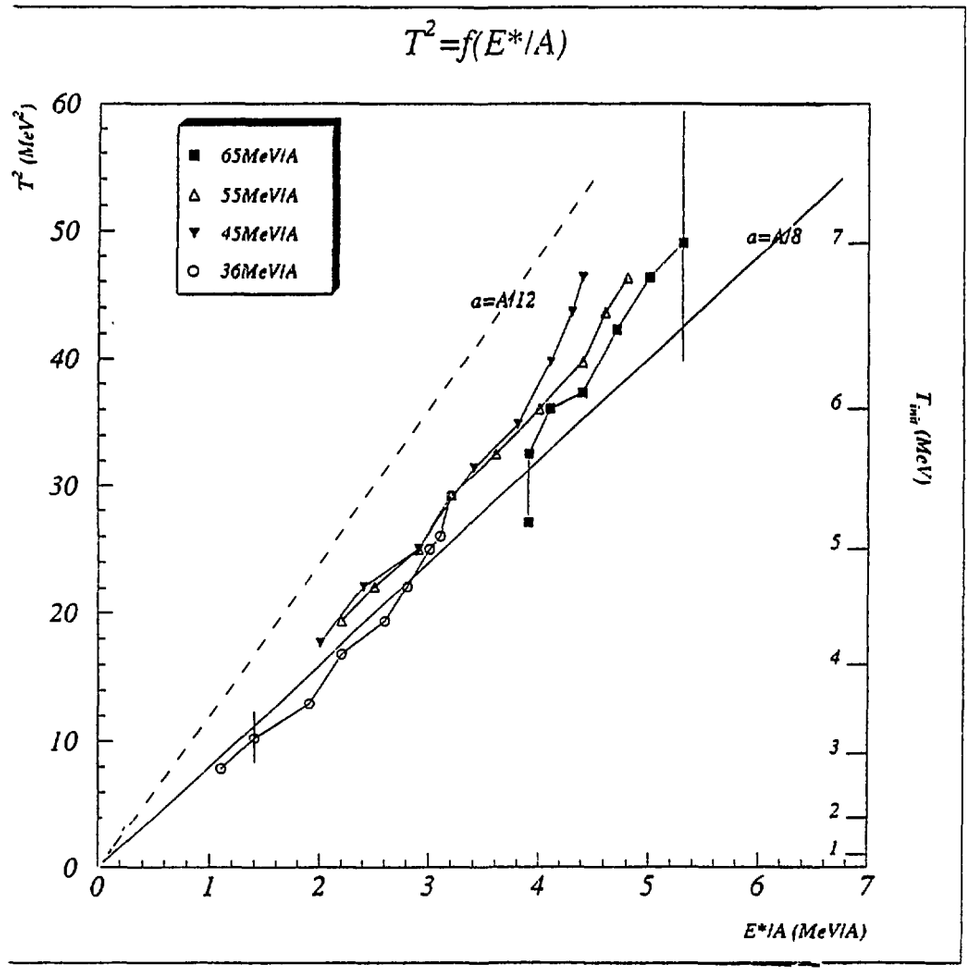

Figure 3: *Evolution of the square of the initial temperature with the excitation energy per nucleon for 36 MeV/u (open circles), 45 MeV/u (closed triangles), 55 MeV/u (open triangles) and 65 MeV/u (closed squares). Each point corresponds to an impact parameter.*

USING GLOBAL VARIABLES FOR IMPACT PARAMETER DETERMINATION IN NUCLEUS-NUCLEUS COLLISIONS BELOW 100 MeV/u

J. Péter [a], G. Bizard [a], R. Brou [a], Y. Cassagnou [c], E. Crema [b] [l], D. Cussol [a], H. Doubre [b], K. Hagel [b] [f], S.C. Jeong [i], G.M. Jin [b] [k], J. Kasagi [j], C. Lebrun [d], S.M. Lee [i], R. Legrain [c], M. Louvel [a], R. MacGrath [g], T. Motobayashi [a] [b] [k], Y. Nagashima [i], T. Nakagawa [i], M. Ogihara [i], J.P. Patry [a], A. Péghaire [b], R. Régimbart [a], E. Rosato [e], F. Saint-Laurent [b], J.C. Steckmeyer [a], J.P. Sullivan [a], B. Tamain [a]

a) LPC Caen ; b) GANIL ; c) DPhN/SEPN, CEN Saclay ; d) LPN Nantes ;
e) Univ. di Napoli (Italy) ; f) Cyclotron, Texas A&M Univ. (USA) ;
g) SUNY, Stony Brook (USA) ; h) Inst. of Modern Physics, Lanzhou (China) ;
i) Inst. of Physics, Tsukuba (Japan) ; j) Tokyo Inst. of Technology (Japan) ;
k) Rikkyo Univiversity, Tokyo (Japan) ; l) Inst. de Fisica, Sao Paulo (Brazil)

1 - MOTIVATIONS

When exclusive measurements are made with 4π arrays, the events have to be sorted according to their impact parameter value b , via the violence of the collision.

This is expressed through the value of one of the global variables which have been used in the study of reactions induced by relativistic heavy ions. **The purpose of this paper is to determine which global variable is the best one for determining b at energies below 100 MeV/u** , via simulated reactions and detectors. The choosen system is ^{40}Ar projectiles from 25 to 85 MeV/u on an ^{27}Al target, used with the multidetectors Mur and Tonneau. The maximum impact parameter is 8 fm, i.e. the reaction cross section is $\approx$2 barns .

2 - SIMULATION AND DETECTORS

The quality of the impact parameter determination is expressed by the correlation between the real b value and the experimentally determined value b_{exp} . It is affected by two factors ; firstly, the sensitivity of the global variable to the violence of the collision ; secondly, the distortion of the value of the global variable due to the characteristics of the detectors. We want to stress that **it is essential to clearly separate these two factors** in all calculations and simulations.

We have studied the correlation b_{exp} versus b_{real} for a perfect 4π array for charged products, i.e. a detector which would measure accurately the charge, mass, velocity, polar and azimuthal angles of all charged products. In the analysis we put a low velocity threshold. This is to avoid a constant value for some global variables (total detected charge, average parallel velocity). This threshold mostly eliminates the target-like spectator or residue.

Then, the events are filtered through the actual detector limitations : dead solid angles, velocity detection, threshold, finite resolution on the mass, charge, velocity, polar and azimuthal angles ; double hits. Two complementary multi-detector systems made of plastic scintillators with a 2 mm thickness have been used covering polar angles from 3.2 to 90° : Mur and Tonneau .

To be reliable, the sorting should be independent of the reaction mechanism. We have then used two extreme mechanisms. One of them is "incomplete fusion" or "massive transfer". A correction is to add some pre-equilibrium emission of particles at the beginning of the collision. The second one is a participant-spectator model, where the very excited interaction volume separates from the cold projectile-spectator and target-spectator nuclei. A correction is to give some excitation energy to these "spectators".

3 - SELECTION OF WELL MEASURED EVENTS

Due to the detector limitations, the information obtained on some events is incomplete to such an extent that their analysis would be meaningless. How to ensure that a sufficient information has been obtained ? The initial projectile linear momentum P_{proj} is equal to the sum $P_{//}$ of the components parallel to the beam direction of all final products. With a perfect charged particle detector, the sum is lower than P_{proj} by about 10% , due to the emission of undetected neutrons. With our actual detector, a reduction occurs, since some particles are not detected or their charge is not correct (mostly Z>9 taken as 9). In central and mid-central collisions, most events have more than 60% of P_{proj} . In mid-peripheral reactions, two components show up. The very low momentum component is due to the non-detection of the projectile-like fragment. Indeed, the grazing angle is close to 1° and most of the projectile like fragments are emitted below 3.2° , minimun. detection angle in Mur. **The events whose $P_{//}$ is larger than 60% P_{proj} are "well measured" events which are kept for further analysis.**

4 - SIMULATED RESPONSE OF SEVERAL GLOBAL VARIABLES

The sorting of events versus their impact parameter value should fulfill the following requirements :
i) It should be independent of the incident energy (in the range 25-100 MeV/u).
ii) It should be independent of the reaction mechanism.
iii) A clear physical meaning of the value of the variable would help to check the absence of mistakes in real experimental data.

Method :

The method used to get the correlation between the real value of b and the experimentally determined one is illustrated in Fig. 1 for the multiplicity ν of charged products measured with a perfect 4π array (with threshold of 2 cm/ns (c/15) and the trigger condition $\nu \geq 2$) ; curve labelled 1 is the multiplicity distribution obtained for reactions with b_{real} from 0 to 1 fm, i.e. 31 mb . Curve 2 is obtained for b from 1 to 2 (95 mb) . And so on for curves 3 to 8 . The "observed" multiplicity distribution is the sum shown as the thick curve. b_{exp} between 0 and 1 corresponds to the summation of the highest multiplicities until 31 mb is reached : mark 1 on the thick curve. And so on for 2, 3, 4, ...fm. The correlation between b_{real} and b_{exp} is shown in Fig. 2, top left. The area of each square is proportionnal to the cross section, the largest square corresponding to 300 mb .

Results for usual global variables :

This correlation b_{exp} versus b_{real} is broad for the multiplicity and becomes worse when the software filter simulating experimental set-up is applied Fig. 2, (top right). **Such poor correlations are obtained with other global variables which, like the multiplicity, make use of a small part of the information obtained.** With the total detected charge the correlation is rather good with a perfect detector, but bad with an actual array. Indeed missing a product with $Z \geq 3$ makes the event looks like as one with a much higher b value. The same effect occurs with the mid-rapidity charge; in addition, this variable is sensitive to the reaction mechanism.

Total perpendicular momentum

This variable, or the total perpendicular kinetic energy, is often used in collisions at relativistic energies. We prefer to use momenta since our detectors measure velocities and charges. The largest values are attributed to central collisions. The correlation is rather good, both with the perfect detector and the actual one (Fig. 2, middle). It is not sensitive to the reaction.

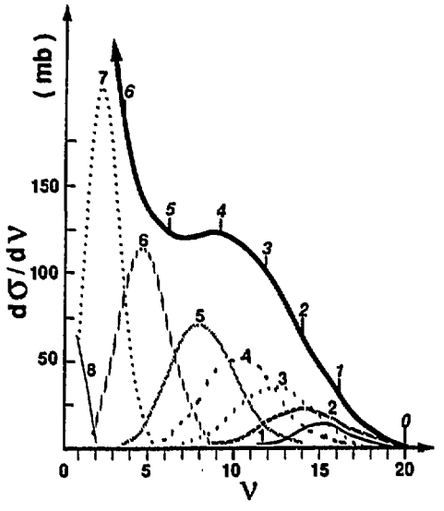

FIGURE 1

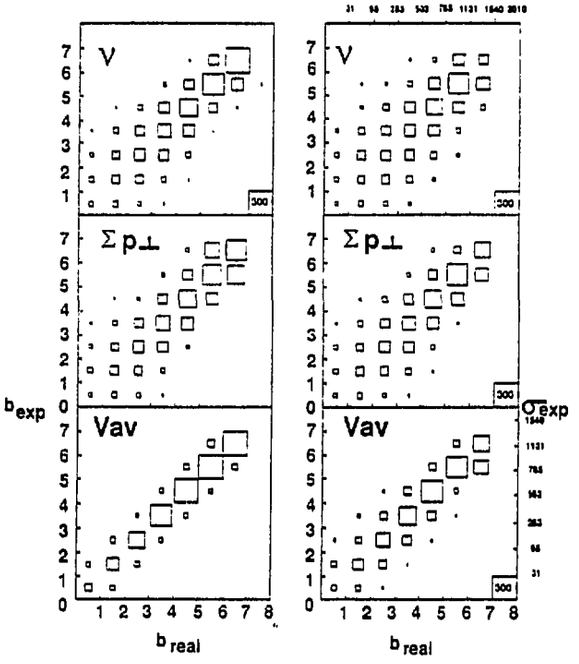

FIGURE 2

5 - A NEW GLOBAL VARIABLE : AVERAGE PARALLEL VELOCITY V_{AV}

The mass-weighted average parallel velocity is :

$$V_{av} = \sum_{i=1}^{\nu} m_i \gamma_i V_i \cos\theta_i / \sum_{i=1}^{\nu} m_i \gamma_i$$

Where m_i, γ_i, V_i and θ_i are the rest mass, relativistic factor, velocity and polar angle of particle i . It is simply the velocity which, when multiplied by the detected mass (denominator), gives the parallel momentum detected in the event (numerator).

This variable.needs to use a detection velocity threshold. Otherwise, with a perfect detector, it would always be equal to V_{cm} . With a real detector Mur and Tonneau, this threshold is produced by the aluminium foils preventing the detection of electrons.

V_{av} decreases from V_p (obtained in very peripheral reactions) down to a minimum value in central reactions (if the total mass of the system is involved, this minimum value is the center-of-mass velocity V_{cm}).

The correlation is better than with the other global variables : Fig. 2, bottom. The reason is that the errors in the numerator and the denominator due to the missed particles cancel each other to a large extent. It is not sensitive to the reaction mechanism.

In addition, the distribution of V_{av} provides a way to check the quality of the measurement in a real experiment as well as in a simulated one. Indeed, a direct observation of the experimental resolution is given by events with V_{av} lower than V_{cm}, or larger than V_p .

Note that for detectors which gives directly kinetic energies, the total transverse energy might give a better correlation.

PUBLICATIONS

J. Péter & al ; Nucl. Phys. A519 (1990) 611-630
J. Péter & al ; Proceedings IN2P3-RIKEN Symposium (1990) ; ed. Heusch and Ishihara ; World Scientific, 219-230 .

EXCITATION ENERGY DISTRIBUTIONS IN FUSION REACTIONS INDUCED BY Ar PROJECTILES at 50 and 70 MeV/u

E. Vient [1], A. Badala [1], R. Barbera [1], R. Bougault [1], R. Brou [1], D. Cussol [1], J. Colin [1], D. Durand [1], A. Drouet [1], D. Horn [1], J.L. Laville [1], C. Le Brun [1], J.F. Lecolley [1], C. Leflécher [1], M. Louvel [1], J.P. Patry [1], J. Péter [1], R. Régimbart [1], J.C. Steckmeyer [1], B. Tamain [1], G. Auger [2], A. Péghaire [2], P. Eudes [3], F. Guilbault [3], C. Lebrun [3], E. Rosato [4], A. Oubahadou [5], M. Gonin [6]

[1] Laboratoire de Physique Corpusculaire - ISMRA Caen FRANCE ;
[2] GANIL - Caen FRANCE ; [3] LPN - Nantes FRANCE ;
[4] INFN - Napoli ITALY ; [5] Université de Rabat MAROC ;
[6] Texas A & M - College Station USA

1 - Objective of the experiments

We have performed a 4π analysis of the charged particles emitted in the reaction Ar+Ag at 50 and 70 MeV/u . The first aim of this experiment was to study the "standard decay" of a hot nucleus. In other words, we mainly focused on fusion nuclei which undergo sequential decay leading to an evaporation residue. The system Ar+Ag has been chosen in order to reduce the fission contribution. The evaporation residue was identified in a forward silicon time of flight telescope insuring a very low velocity threshold. This telescope was the trigger of the experimental set up. The coincident light charged particles have been identified and their velocity measured in a 4π device (wall and barrel installed in the Nautilus chamber). Figure 1 is a mass-velocity plot of the nuclei detected in the forward telescope at 70 MeV/u : the low mass and large velocity nuclei correspond mainly to projectile like fragments and the evaporation residues are located in the mass range 50-100 amu and exhibit a rather wide velocity distribution : the very slow residues are associated with semi-peripheral collisions whereas the fastest ones correspond to more dissipative fusion reactions. The associated mass is relatively low because of the huge number of evaporated particles.

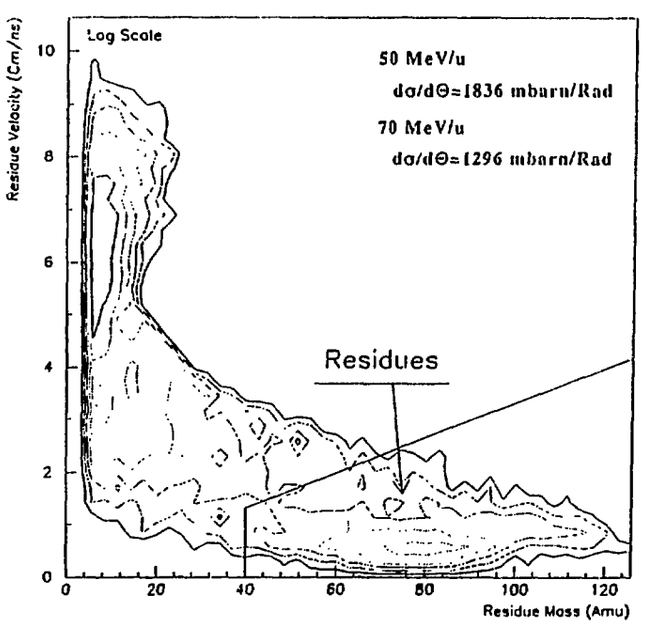

Figure 1 : *Mass velocity plot for the nuclei detected in the forward time of flight telescope for a bombarding energy of 70 MeV/u . The evaporation residues lie around mass 80 and their velocities reflect the centrality of the collision.*

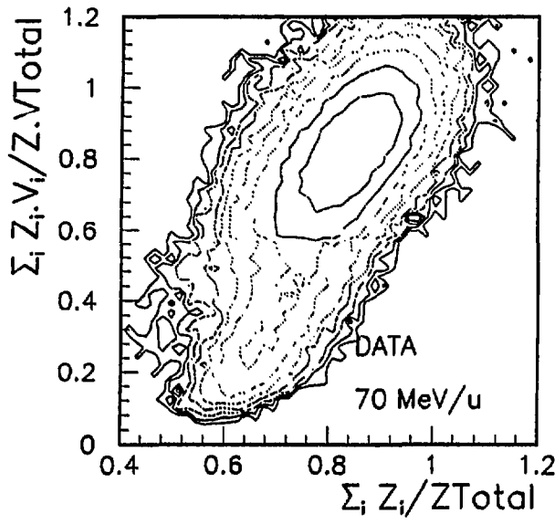

Figure 2 :
Contour plot for the total detected charge (abscissa) and the total linear momentum (ordinate) normalized to their maximum possible values. Trigger telescope at 11°9 . Incident energy : 70 MeV/u .

Figure 2 gives an indication of the quality of the whole set up : the quantities plotted are the total detected charge and the measured total linear momentum for each event triggering the forward telescope. They have been normalized to the total charge of the system (65 charge units) and to the projectile linear momentum. A perfect set up would lead to a concentration of points in the (1,1) region. The deviation from this ideal case is due to dead areas, thresholds and resolution effects of the 4π device. For most of the detected events, this deviation remains small (maximum of the contour plot located above the coordinates (0.8, 0.8). Badly analysed events correspond mostly to peripheral collisions for which the projectile like fragment has escaped through the forward 3° hole of the "wall" detector. We have checked that for the .astest evaporation residues for which no projectile like fragment is emitted, we have always detected more than 70% of the total charge of the system.

2 - Data analysis

The analysis has been performed on an event by event basis. It has been possible to reconstruct the initial hot nucleus corresponding to the detected evaporation residue. For this purpose, all the particles detected in coincidence with the residue have been kinematically analysed and their origin recognized : either evaporation from the hot fusion nucleus or faster emission (direct or pre-equilibrium). The hypothesis which have been used in this analysis are the following :

- the evaporation from the fusion nucleus is forward-backward symmetrical in the reference frame of the hot nucleus ;
- all the backward emitted particles (in the lab system) are evaporated from the hot nucleus ;
- the forward emitted particles can be either evaporated or promptly emitted. The probability for each process has been estimated from the evaporation contribution at backward angle ;
- in the event by event analysis, each forward emitted particle has been attributed to both evaporation and fast process with respective weights equal to the corresponding probabilities ;
- the results have been corrected for the neutron contribution in assuming that the number of evaporated neutrons is proportionnal to the number of evaporated protons and to the N/Z ratio of the system.

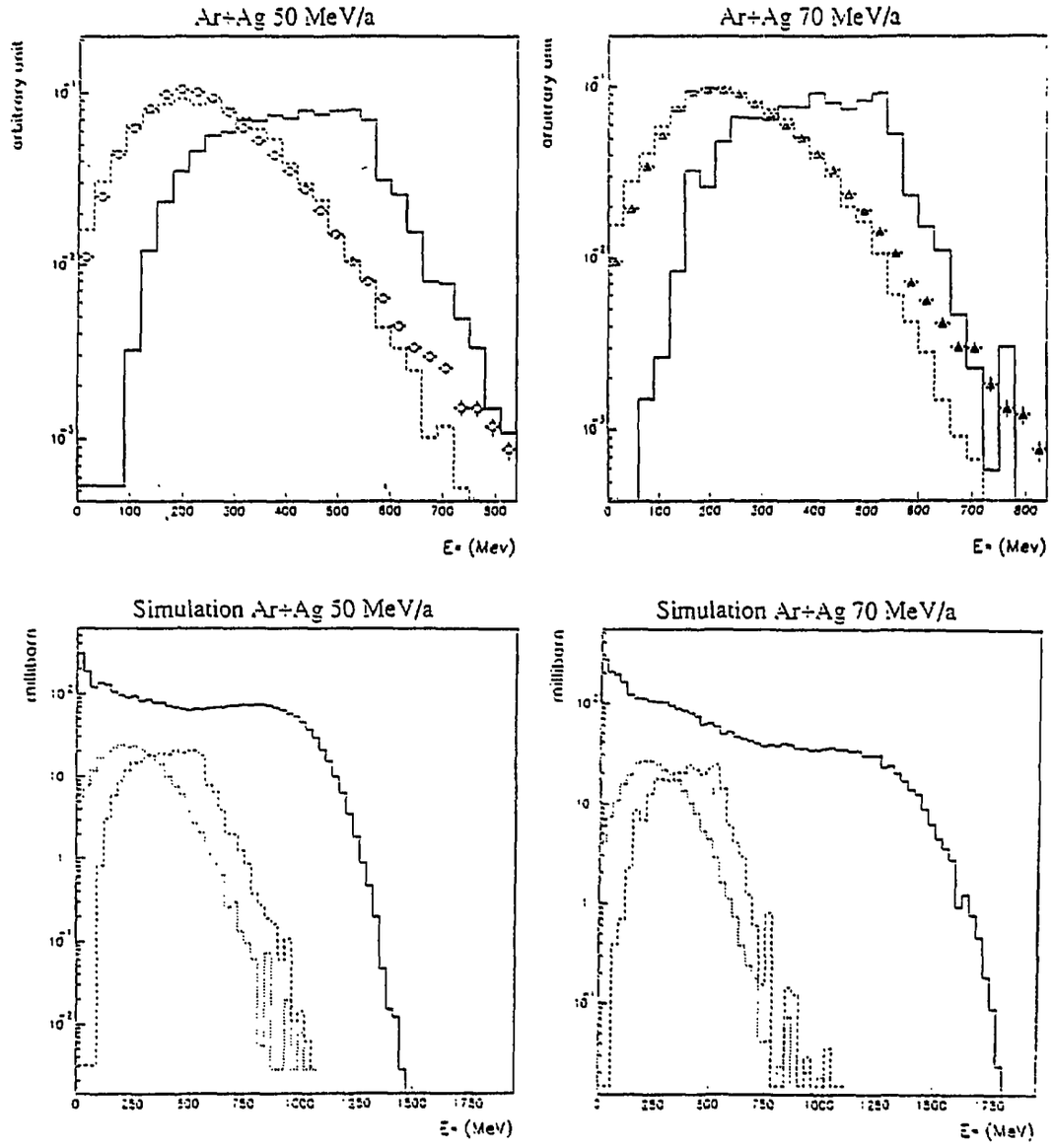

Figure 3 :
Excitation energy distributions for the Ar+Ag system at 50 (a, c) and 70 (b, d) MeV/u . The points are experimental. The corresponding triggering conditions are : detection of an evaporation residue at 11° . The dashed lines of figure a and b are the results of the simulation if the filtering effects of the detector are included. The full line of figures a and b are unfiltered results of the simulation. In figures c and d are given only simulated results : dotted line : filtered distribution when the trigger is an evaporation residue ; dashed line : corresponding unfiltered distribution (these two curves are already included in figures a and b) ; full line : simulated results for all the hot nuclei, whatever their decay process is.

3 - Results

From the event by event treatment, it has been possible to reconstruct, for each detected evaporation residue, the initial excitation energy of the primary hot nucleus. The corresponding distributions for a collection of events are shown in figure 3. Several curves are indicated for the two bombarding energies of interest. The points of figures 3a and b are experimental data and they are compared with the results of a simulation code [1] which describes the energy deposit in the entrance channel as a cascade process and the decay of the hot nuclei as a sequential process including dynamical aspects. The full curves are the raw results of the code. The dotted histogramm is obtained if the response function of the 4π device is included (dead areas, thresholds, double hit). Two main conclusions can be drawn. The first one is that the experimental distributions obtained at 50 and 70 MeV/u are quite similar. The second one is that the simulation code reproduces nicely the data : the maximum excitation energy leading to a sequential decay of the hot nuclei does not depend on the incident energy [1]. This result can be compared with the conclusions obtained at GANIL with the neutron ball which indicate a saturation of the deposited energy at large bombarding energies. However, one has to keep in mind that the results of figure 3a-b correspond to a given exit channel : the nuclei decay has been sequential and leads to evaporation residues. In figures 3c-d the predictions of the simulation indicate that the excitation energy distributions extend much further if the sequential evaporation requirement is relaxed [2].

4 - Conclusion

In this contribution, it has been shown that the excitation energy distribution of hot nuclei produced in the Ar+Ag collision are quite similar at 50 and 70 MeV/u if one restricts to the sequential decay channel leading to an evaporation residue. This result means that, if higher excitation have been reached, they do not feed this decay channel.

REFERENCES

1 - D. Durand ; accepted at Nucl. Phys. A.
2 - E. Vient et al ; submitted to Nucl. Phys.

B3 - MULTIFRAGMENT EMISSION

TRANSITION FROM BINARY FISSION TOWARDS MULTI-BODY DECAY FOR HEAVY EXCITED NUCLEI PRODUCED IN THE REACTION AR+AU AT 60 MeV/u

G. Bizard [1], R. Bougault [1], R. Brou [1], D. Durand [1], A. Genoux-Lubain [1], A. Hajfani [1]
J.L. Laville [1], C. Le Brun [1], J.F. Lecolley [1], M. Louvel [1], J.P. Patry [1], J. Péter [1]
N. Prot [1], R. Regimbart [1], J.C. Steckmeyer [1], B. Tamain [1], A. Badala [1-10]
H. Doubre [2], Y. El-Masri [3], H. Fugiwara [4], K. Hagel [1-5], F. Hanappe [6], S. Jeong [4]
G.M. Jin [2-7], S. Kato [4], S. Lee [4], T. Matsuse [8], T. Motobayashi [1-9], A. Péghaire [2]
F. Saint-Laurent [2]

1) LPC ISMRA, 14050 Caen Cedex, France
2) GANIL, 14021 Caen Cedex, France
3) FNRS-ULC, Louvain la Neuve, Belgium
4) Institute of Physics, University of Tsukuba, Ibaraki-ken 350, Japan
5) Cyclotron institute, Texas A&M University, College Station, TX77843, USA
6) ULB, Bruxelles, Belgium
7) Institute of Modern Physics, Lanzhou, China
8) Shinshu University, Japan
9) Rikkyo University, Toshima-ku, Tokyo 171, Japan
10) INFN Catania, Corso Italia, Catania, Italy

1. Motivations

When heavy nuclei produced in complete or incomplete fusion reactions are moderately excited, they usually decay by binary fission although a process leading to the survival of a heavy residue by the fast emission of light particles (mainly neutrons) may also compete. The question of the fate of these nuclei when the excitation energy is increased is widely debated. A transition towards the emission of three (or possibly more) large fragments is expected. The aim of the analysis presented in this contribution is to determine the excitation energy region where such a transition occurs.

2. Experimental set-up

The analysis uses part of the data recorded with the experimental set-up described in the contribution " Multifragment decay of heavy excited nuclei in Ar+Au reactions at 30 and 60 Mev/u". Several triggering conditions were used during the experiment. Here, we only concentrate on the case where one fragment was detected in the forward direction in the telescopes and at least two fragments with charge larger or equal to 8 detected in the Delf set-up at angles larger than 30°. Coincident light charged particles were detected in the "Mur" and in the "Tonneau".

3. Data summary and method of analysis

When selecting the trigger previously mentionned, we obtain the events displayed in the bi-dimensionnal spectrum velocity-atomic number of figure 1. Zone 1 and 3 correspond to fragments detected in the forward telescopes Most of them (zone 1) have a velocity and a charge close to the beam characteristics and are easily identified with projectile-like remnants while those located in zone 3 have a less well-defined origin (deep inelastic collisions?). These latter have not been used in the analysis. Zone 2 corresponds to fragments detected at large angles (more than 30°). Most of them have a velocity lower than 2 cm/ns and an atomic number around 35. Therefore, they can be identified as fission fragments resulting from the two body

decay of an excited target-like fragment. However, an other contribution is observed at lower charge (fragments called IMF for Intermediate Mass Fragments). The presence of such nuclei is an indication for the advent of collisions leading to target-like decay by an other mode than the usual binary fission, namely three fragment emission. What is the amount of such events?

To answer this question, we have used the kinematical coincidence method which has proven to be very usefull for determining whether events are complete or incomplete from a kinematical point of vue using a minimization procedure (for more details see ref 1). We mean by incomplete events, events where one slow fragment has been missed due to the limited acceptance of the detectors. By estimating the ratio of complete *vs* incomplete events, we have access to the probability of the two decay modes (binary fission *vs* three (or more) body decay). The next step in the analysis consists in sorting the events according to the excitation energy deposited in the target-like fragment.

To this end, we have used two different methods:

- 1) taking into account the total energy carried away by both the projectile-like fragment and the fast light particles which have not fused with the target (often called pre-equilibrium particles), the energy deposited in the target is then obtained by substraction
- 2) independently, this energy can also be estimated by correlating the dissipated energy with the recoil velocity of the slow fragments.

As shown in the following, it turns out that the two prescriptions lead to the same result. Last, the whole analysis procedure has been tested with help of simulations to estimate the possible biases of the method.

4. Results

The essential result of the analysis is displayed in figure 2. We observe that the three body contribution sets in around 3 MeV/u and becomes significant around 5 MeV/u. We stress that this result only concerns the decay by more than one large fragment, therefore not taking into acount the contribution of a possible final heavy residue in the total decay probability. Indeed, the experimental conditions did not allow to properly select this specific decay channel because of the insufficient angular coverage of the device.

Last, it is well known that the decay properties depend heavily on the angular momentum transferred to the excited nuclei. A rough estimation based on geometrical assumptions for the determination of the impact parameter coupled to the transferred linear momentum leads to values ranging from 0 to 110-120 $\hbar$ when increasing the excitation energy from 0 to 4-5 MeV/u.

5. Conclusions

The decay of excited nuclei produced in peripheral and mid-central collisions for the system Ar+Au at 60 MeV/u have been analysed by testing the completness of each recorded event.We have been able to extract the ratio of two *vs* three (or possibly more) body decay processes as a function of the excitation energy per nucleon using the kinematical coincidence method and sorting the events according to the dissipated energy by two different prescriptions. We conclude that the transition from a standard binary fission towards a multi-body decay occurs around 3 MeV/u for nuclei in the 200-220 mass number range.

REFERENCES

(1) M. Louvel Journées Théoriciens Saturne (1989) LNS/PH 90-09
(2) A. Badala et al. Winter Meeting on Nuclear Physics , Bormio (1990)
(3) E113 collaboration (to be published in Nuclear Physics)

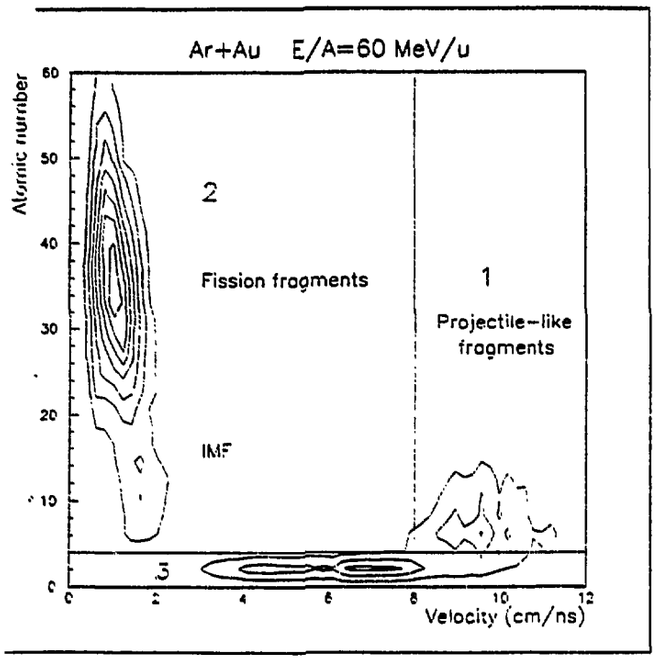

Figure 1) *Velocity vs atomic number for the products emitted in the reaction Ar+Au at 60 MeV/u when requiring one fragment in the forward direction (zone 1) and at least two fragments at large angles (zone 2). Events where one of the detected particles is in zone 3 have not been analysed*

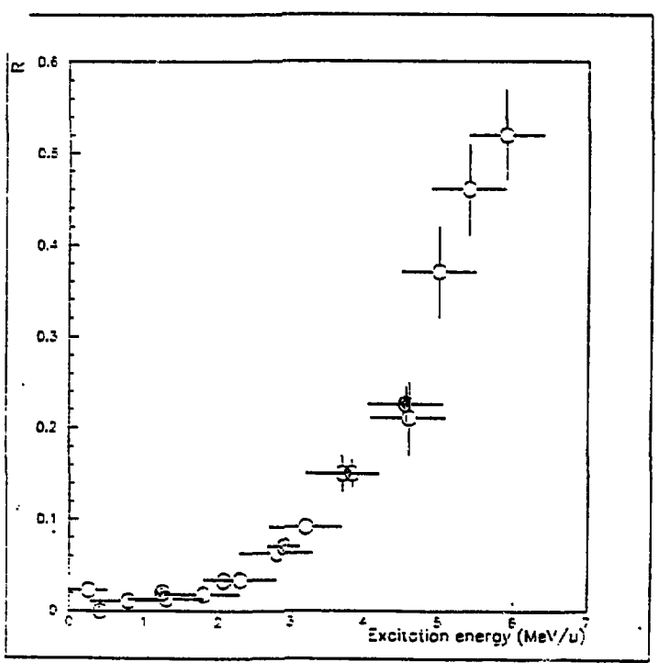

Figure 2) *Ratio between three and two + three decay fragments as a function of the excitation energy per nucleon.*
-filled points: E deduced from method 1 (see text)*
-open points: E deduced from method 2 (see text)*

MULTIFRAGMENT DECAY OF HEAVY EXCITED NUCLEI IN THE REACTION AR+AU AT 30 AND 60 MeV/u

G. Bizard [1], R. Bougault [1], R. Brou [1], A. Buta [1], D. Durand [1], A. Genoux-Lubain [1], A. Hajfani [1], T. Hamdani [1], J.L. Laville [1], C. Le Brun [1], J.F. Lecolley [1], M. Louvel [1] J.P. Patry [1], J. Péter [1], N. Prot [1], R. Regimbart [1], J.C. Steckmeyer [1], B. Tamain [1] A. Badala [1-10] H. Doubre [2], Y. El-Masri [3], H. Fugiwara [4], K. Hagel [1-5], F. Hanappe [6] S. Jeong [4], G.M. Jin [2-7], S. Kato [4], S. Lee [4], T. Matsuse [8], T. Motobayashi [1-9] A. Péghaire [2], F. Saint-Laurent [2]

1) LPC ISMRA, 14050 Caen Cedex, France
2) GANIL, 14021 Caen Cedex, France
3) FNRS-ULC, Louvain la Neuve, Belgium
4) Institute of Physics, University of Tsukuba, Ibaraki-ken 350, Japan
5) Cyclotron Institute, Texas A&M University, College Station, TX77843, USA
6) ULB, Bruxelles, Belgium
7) Institute of Modern Physics, Lanzhou, China
8) Shinshu University, Japan
9) Rikkyo University, Toshima-ku, Tokyo 171, Japan
10) INFN Catania, Corso Italia, Catania, Italy

1. Motivations

Intermediate energy heavy ion reactions (corresponding to incident energies between 10 and 100 MeV/u) are presently extensively used to investigate the properties of nuclear matter at high temperatures. As an example, the ^{40}Ar induced reactions on heavy targets have been widely studied with the help of various experimental set-ups. However, the information gained up to now depends drastically on the experimentally selected exit channels, and therefore on the ability of the apparatus to filter among various reactions, the most violent (but also rare) collisions. For example, experiments with heavy targets have shown that the cross section corresponding to central collisions leading to binary fission decreases with bombarding energy and that the linear momentum transfer saturates for incident energies larger than 30 MeV/u.Still, large cross sections corresponding to the production of heavy residues as well as fission fragments associated with large neutron multiplicities have been reported.

In this experiment , we have tried to answer the following questions:

-Does the incomplete fusion process disappear above the Fermi energy ?
- Is there a limit in the excitation energy deposited in the target ?
- Are there new decay channels opened around this incident energy ?
- If yes, can we characterize these new decay processes (time scales, dynamical properties...) ?

To this end, we have used the Ar beam delivered by the GANIL facility to bombard Au targets at 30 and 60 MeV/u.

2. Experimental set-up and triggering conditions

The experiment used three multidetectors (see fig 1): DELF for fragments with Z larger than 8 and velocity $v > 0,5$ cm/ns , emitted in the 30°-150° angular range, the Mur and Tonneau for light charged particles and light fragments in the 3°-150° polar angle range. In conjunction, four large area Silicon detectors were used to identify projectile-like fragments and four CsI scintillators at very backward angles to obtain the energy spectra of the evaporated light charged particles. The 18 DELF PPAC's cover 50% of the total solid angle. For each fragment, charge identification is achieved with an accuracy of 20% by combining the energy losses and the time of flight measurements. The four solid state telescopes were positionned at the same forward angle with respect to the beam axis: 9°4 and 5°5 respectively at 30 and 60 MeV/u. Each telescope was constituted of three elements of area 5 x 5 cm^2, and was mounted

one meter away from the target for TOF measurements between the timing signal provided by the first member and the radio frequency signal delivered by the machine. The identification of light charged products in the Mur and the Tonneau was achieved using the standard ΔE-TOF correlation. The PPAC's and the four telescopes were used to trigger the data acquisition system. In the experiment, the trigger required coïncidences between at least three fragments. These events can be roughly divided into two classes: the first one was obtained when one of the fragment was detected in one of the forward telescopes, while the second class was obtained when the three (or possibly more) fragments were detected in DELF (i.e at polar angles larger than 30). In the first case, provided that a velocity selection is performed on the detected fragment at forward angles, the selected events are mostly peripheral events while in the second case, more central collisions are selected. In the following, we concentrate on the second class of events, the first one is discussed in the contribution "Transition from binary fission towards multibody decay..."

3. Data summary

We first discuss the results concerning the heavy fragments detected in Delf. In table 1, we show the mean atomic number of the fragments (starting from the smallest) as a function of the detected multiplicity for the two incident energies. The total charge of the system corresponds to 97.

TABLE I

E/A	N_d	Mean atomic number				total
30 MeV/u	3	12.7	23.4	37.1		73.2
30 MeV/u	4	11.3	14.8	22.3	33.0	81.4
60 MeV/u	3	11.3	17.8	28.0		57.1
60 MeV/u	4	9.2	12.9	17.3	24.59	64.3

At 60 MeV/u, the total detected charge is significantly smaller as compared with 30 MeV/u. This is a first indication for the fact that more violent collisions have been selected at 60 MeV/u. We now try to characterize the events by kinematical correlations between the fragments. This is achieved by analysing the distributions of the relative velocities and relative angles. One way to cope with the possible biases of the experimental set-up is to compare the data with simulated events. In this case, the simulated events have been created using the sequential emission model coupled with a dynamical calculation of the Coulomb trajectories. By varying the time of emission of the fragments during the decay, we have access (by comparison with the data) to the time scale of the phenomenon. The results are shown in figure 2 and 3. In the 30 MeV/u case, we confirm the results of [5]: the process is correctly described by a succession of independent binary splittings. At 60 MeV/u, even by reducing significantly the time of emission, one cannot fully reproduce the data: the relative velocities between the fragments are too small in the simulation case. Such effects may be the signature for an expansion of the system during the decay process.

In table 2, we indicate some quantities related to the selected collisions. The linear momentum transfer (LMT) is in agreement with the systematics. The excitation (E*) has been deduced from the recoil velocity of the fragments using the massive transfer hypothesis. The cross section for such events is rather small but it increases with the incident energy. Concerning the light particles, their average multiplicity (Mult) is increasing with the beam energy as well as the apparent temperature (Tap) as deduced from a fit of the energy spectra. These values should be corrected to obtain the initial temperatures so that temperatures as high as 7-8 MeV have probably been reached at 60 MeV/u.

TABLE II

E/A	Pinc	LMT(%)	E*	Tap-Mev	Mult (Z=1+2)	Cross section
30 MeV/u	9456	75%	~ 650 MeV	5.± 0.3	8.4±0.3	100 mb
60 MeV/u	13372	50%	~ 1.1 GeV	6.7±0.3	15.4±0.5	300 mb

4. Conclusions

The temperature as well as the multiplicities of light charged particles increase with the incident energies indicating that the energy deposited increases as well (from 3 MeV/u at 30 MeV/u to around 5 MeV/u at 60 MeV/u). Dealing with the detected heavy fragments, we have shown that they originate from a thermalised very excited source. Their kinematical correlations exhibit different features depending on the incident energy. At 30 MeV/u, no significant deviations from a standard successive binary decay process are observed. At variance, at 60 MeV/u, the relative velocities between the fragments are in disagreement with the above-mentionned mechanism. This is an indication for the occurence of new phenomena in the decay processes. Studies are in progress to disentangle the various possible effects to be taken into account : shorter emission times, radial expansion due to compression ...

REFERENCES

(1) T. Motobayashi et al. NIM A284 (1989)
(2) G. Bizard et al Nouvelles du Ganil (Octobre 1989)
(3) G. Bizard et al International Conference on Nuclear Physics, Ierapetra (Greece) (1991)
(4) M. Louvel et al. Proceeding of the International Symposium, Nikko (Japan) (1991)
(5) G. Bizard et al. (accepted by Physics Letters)
(6) M. Louvel et al Winter Meeting on Nuclear Physics, Bormio (Italy) (1992)
(7) E113 collaboration (to be published in Nuclear Physics)

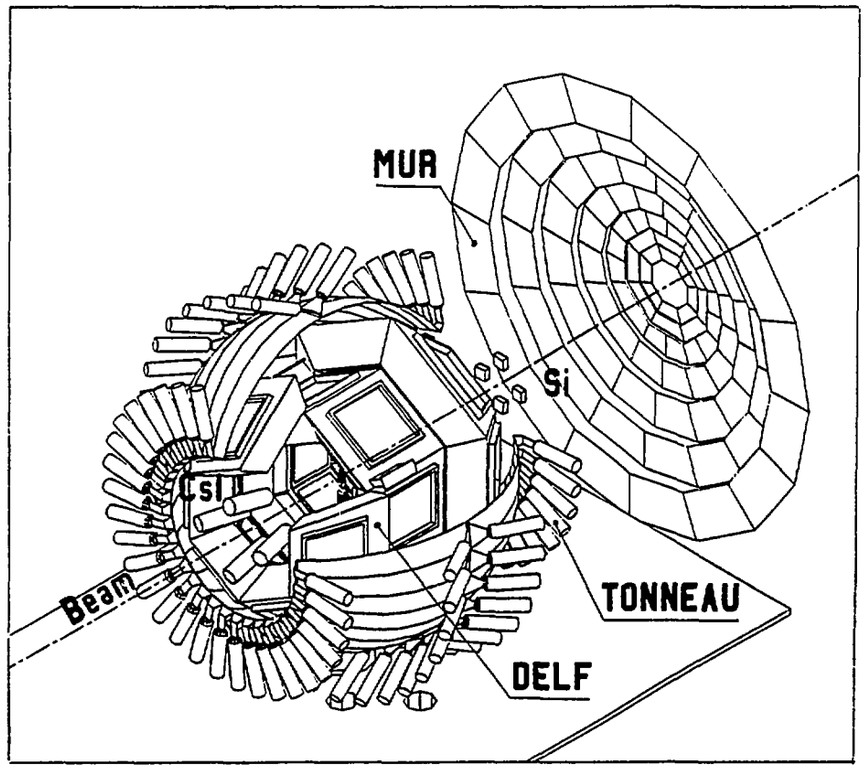

Figure 1) Experimental set-up

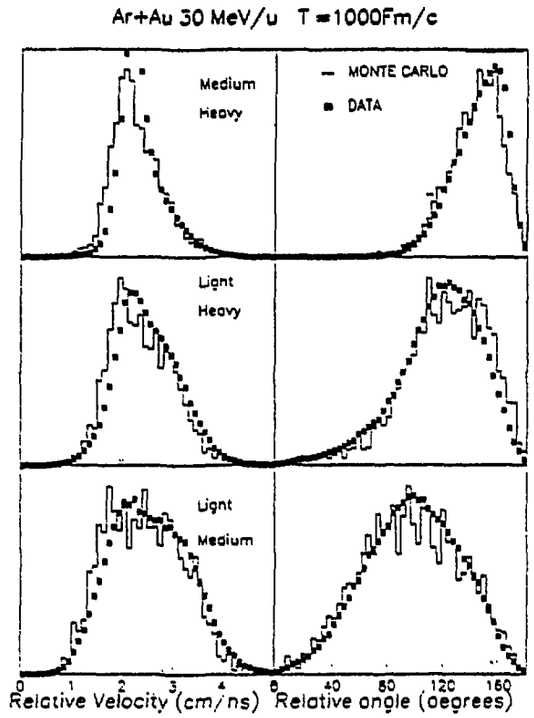

Figure 2) Relative velocity and relative angle distributions between two fragments sorted according to their atomic number. The dots are the experimental distributions. The histograms correspond to the simulation. The time between two successive decays is 1000 fm/c.

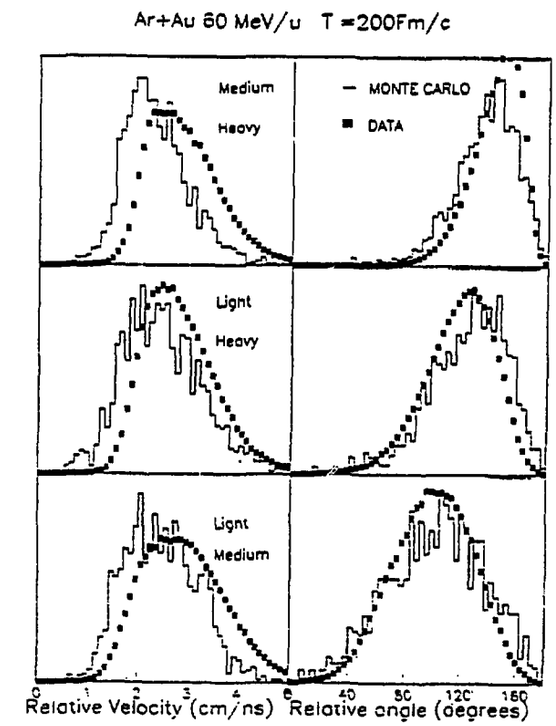

Figure 3) Same as figure 2) but at 60 MeV/u. In this case, the time between two successive decays is 200 fm/c.

Multifragment emission in reactions of ^{84}Kr on Ag and Au at 17.7, 27, and 35 MeV/n

M. Zamani,[a] M. Debeauvais,[b] J. Ralarosy,[b] J. C. Adloff,[b] F. Fernandez,[c] S. Jokic,[d] and D. Sampsonidis[a]

[a] *University of Thessaloniki, Thessaloniki, Greece*
[b] *Centre de Recherches Nucléaires, Strasbourg, France*
[c] *Universidad Autonoma de Barcelona, Barcelona, Spain*
[d] *University "Svetozar Markovic," Kragujevac, Yugoslavia*

For many years Solid State Nuclear Track detectors (SSNTD) have been used in the study of heavy ion interactions[1-3]. Using this technique there have been reported the so-called multi-pronged events where up to six correlated heavy fragments have been observed in ^{238}U + U, Pb, and Au reactions at 10 and 16.5 MeV/nucleon[4]. Similar information has also been reported more recently with other kinds of detection[5-8]. In général experimental data concerning 3-body production mechanisms are in agreement independently of the method of observation. The fact that the deep inelastic (DI) mechanism is progressively replaced by other mechanisms at higher bombarding energies makes it important to study the evolution of multifragment event cross-sections at higher energies. For less than 10 MeV/nucleon most of the events observed are binary or ternary ones[4] arising from fission after complete or incomplete fusion of the projectile with the target.

We have measured the cross section for multipronged events as a function of Kr projectile energy on Ag and Au targets for bombarding energies of 17.7, 27, and 35 MeV/nucleon. In this work we show that the contribution of events of higher multiplicity increases with increasing bombarding energy.

EXPERIMENTAL

The incident ^{84}Kr beams were delivered by the UNILAC of the GSI in Darmstadt, Germany at 17.7 MeV/nucleon and by GANIL in Caen, France at 27 and 35 MeV/nucleon with beam fluxes on the order of 10^6 Kr ions/cm^2. All Ag and Au targets were bombarded perpendicular to their surfaces. The targets consisted of layers of 1-2 mg/cm^2 of Ag or Au evaporated on one surface of the SSNTD type CR 39* detectors. This arrangement produced a 2π geometry in the laboratory system and a near 4π geometry in the c.m. The target thickness was determined with an accuracy of about 5 %.

*Manufactured by Pershore Mouldings Limited, Worcestershire WR 10 2DD, England.

RESULTS AND DISCUSSION

With our etching conditions the threshold of detection in CR 39 was about 8 MeV. cm^2/mg. In Fig. 1 we show the domain in which fragments can be detected with this threshold. All particles to the right of the boundary can be detected while those to the left (hatched region) escape detection.

Among all events, we have selected those with two or more visible fragments issued from the same reaction. As can be seen in Fig. 2, we have classified as 3-pronged events all reactions having three detected fragments as well as those having two fragments with relative projected angle on the detection plane less than 175° (indirect events). Due to momentum conservation, these latter events are associated with a third fragment which escapes detection. Also some 4- and 5-pronged events were found to be respectively 5-and 6-pronged events after the same analysis. The charge and energy of the fragments detected can be determined using our calibration based on the measurement of the geometrical track parameters (lengths, angles) and etched tip radius[9]. As an example, we give the relationship between the angle θ relative to the beam axis and the charge for indirect 3-pronged events in Fig.3 for the reaction Kr + Au and for events having three visible prongs in Fig.4. The grazing angle for this reaction at 17.7 MeV/nucleon is 12.9°. Fig. 3 shows a group of fragments at $\theta \approx 85°$, $Z \approx 75$. The range of each of the fragments in these events corresponds to a very low energy ($\approx$ 0.1 MeV/nucleon). They are identified as slow target-like fragments. Most of these events are associated with

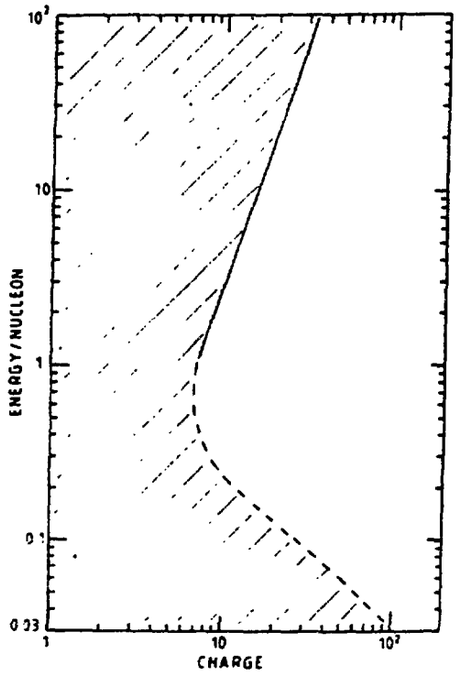

FIG. 1.

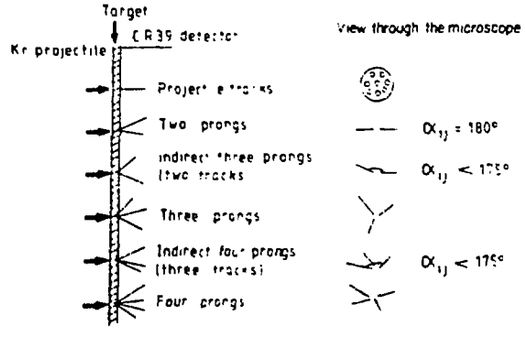

FIG. 2.

fast fragments lying around θ 14°, Z = 29 having an energy about 85 % of the total incident energy of 1.48 GeV. The missing energy corresponds to fragments that escape detection. These events are assumed to have their origin in DI reactions. Around θ ≈ 45°, Z ≈ 15 we observe a group with a different behavior. The two associated fragments have lower charges than before and larger emission angles. The total energy of the two fragments is about 200-600 MeV which implies that an important amount of energy escapes detection.

In Fig. 4 we show the events with three registered tracks. We also observe a small group (θ ≈ 85°, Z ≈ 75) assumed to come from DI reactions. The charge of the three associated fragments lies around 75, 30 and 14. Their total energy is slightly lower than 1.48 GeV.

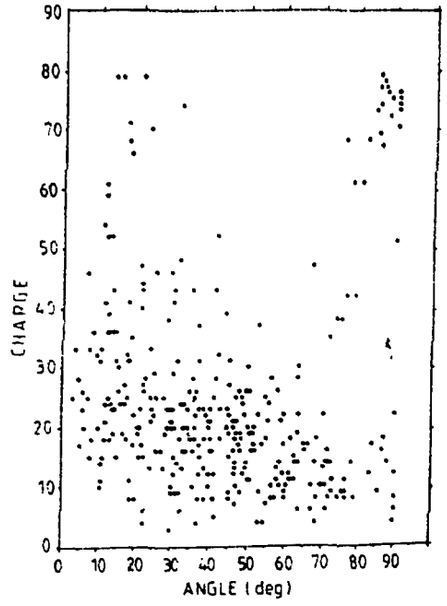

FIG. 3.

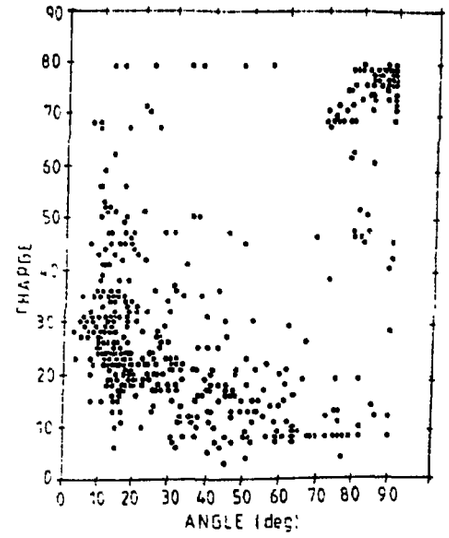

FIG. 4.

As can be seen from Figs. 5 and 6, the cross sections for multifragmentation processes leading to 3-, 4-, and (5 + 6)-intermediate mass fragments in the final state show a tendency to increase with bombarding energy. The smaller the multiplicity, the greater the cross section. Events with 5 and 6 intermediate mass fragments appear to have a threshold around 15 MeV/nucleon bombarding energy. As an internal check of our experimental procedure, we have measured the total reaction cross section of Kr + Au at 17.7 MeV/nucleon. Taking into account all 1-, 2-, 3-, 4-, 5- and 6-pronged events, we find 4.1 ± 0.5 b. The calculated cross section[11] is 4.6 b.

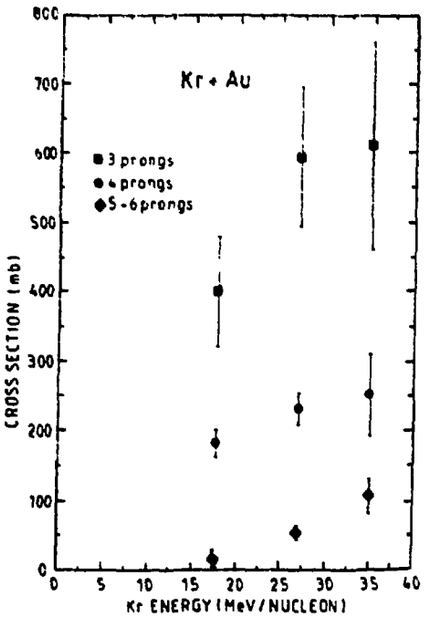

FIG. 5

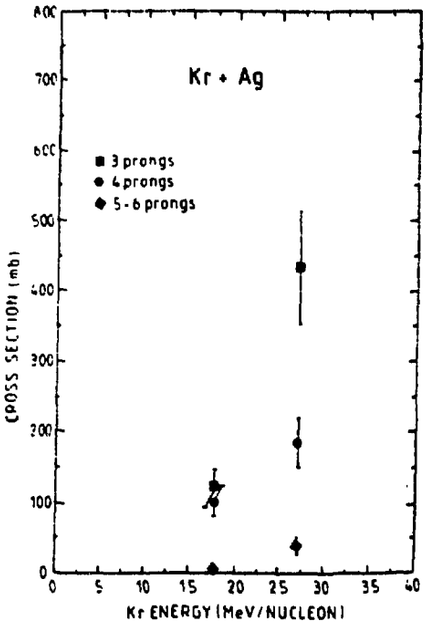

FIG. 6.

REFERENCES

[1] P.A. Gottschalk, P. Vater, H.J. Becker, R. Brandt and, G. Growert Phys. Rev. Lett. 42, 359(1979).

[2] H.A. Kahn, K. Rasghud, R.A. Akber, G. Hussaub, P. Vater, P.A. Gottschalk, and R. Brandt, Nucl.Instr.and Meth.173,155(1980).

[3] M. Debeauvais, S.Jokic, and J. Tripier, in *Proceedings of the 10th International Conference on Solid State Nuclear Track Detectors*, Lyon, 1979, edited by H. Francois et al. (Pergamon, London p. 927, (1980)

[4] M. Debeauvais, J Ralarosy, J. Tripier, and S. Jokic, Nuclear Tracks Radiat. Meas. 8, 515 (1984).

[5] M. Petrovici, J. Albinski, R. Bock, R. Cusson, A. Gobbi, G.Guarino S. Grotto,, K.D. Hildenbrand, W.F.J. Muller, A. Olmi, H. Stelzer and J. Toke, Nucl. Phys. A477 277 (1988).

[6] O. Garnier, C. Cerruti, S. Leroy, P.L'Henoret, R. Lucas, C. Mazur, J. Natowitz, C. Ngo, M. Rebaag, E. Tomasi, G. Imme, G. Raciti, G. Spinella, J. Albinski, A. Gobbi, N. Hermann, K.D. Hildenbrand, A. Olmi, Nucl. Phys. A481 109(1988).

[7] B Borderie, J.Phys.C4.251(1986).

[8] R. Bougault, F. Delaunay, A. Genoux-Lubain, C. Le Brun, J.F. Lecolley, F. Lefebvres, M. Louvel, J.C. Stockmeyer, J .C. Adloff, B. Bilwes, R. Bilwes, M. Glaser, G. Rudolf, F. Scheibling, L.Stuttge, J.L. Ferrero, Nucl. Phys. A488 255 (1988).

[9] M. Debeauvais, M. Zamani, J. Ralarosy, S. Jokic, and F. Fernandez, GSI Annual Report (1988)p.71.

[10] M. Zamani, F. Fernandez, S. Jokic, J. Ralarosy and M. Debeauvais, Nucl. Tracks Radiat. Meas.15.437 (1988).

[11] R. Bass, Nuclear Reactions with Heavy Ions - Springer Verlag.

[12] J. Tripier, G. Remy, J. Ralarosy, M. Debeauvais, R. Stein and D. Huss, Nucl.Instr. and Meth. 115,29(1974).

HEAVY FRAGMENT PRODUCTION IN Kr+Au, Th, Ag COLLISIONS AT 27 AND 43 MeV/n

J.C. Adloff[2], B. Bilwes[2], R. Bilwes[2], R. Bougault[1], J. Colin[1], F. Delaunay[1], A. Genoux-Lubain[1], M. Glaser[2], C. Masse[2], D. Horn[1], C. Le Brun[1], J.F. Lecolley[1], J. Lemière[1], M. Louvel[1], G. Rudolf[2], F. Scheibling[2], J.C. Steckmeyer[1], L. Stuttge[2]

[1]*Laboratoire de Physique Corpusculaire LA34 - ISMRA, IN2P3-CNRS*
Université de Caen - 14050 CAEN CEDEX France
[2]*CRN Strasbourg, IN2P3-CNRS - France*

1 - Motivations

In the GANIL energy range (25-100 MeV/A), the maximum excitation energy which may be deposited varies between 6.25 and 25 MeV/A ; a large fragment production has already been evidenced[1] and we may assume, extrapolating the Plastic Ball experiments[2] towards lower energy that the fragments will play a dominant role compared to the one of light particles. Therefore are of great interest in the study of heavy-ions collisions :

- their presence is a rough test of the limit reached by the excitation energy, it indicates that the nuclear matter is not totaly vaporized ;
- remnants of the primary interaction, their characteristics are strongly correlated to the dynamic of the collision ;
- the heavy fragments carry away at least the same number of neutrons and protons. Therefore an analysis based upon fragments detection will take into account a larger part of involved matter as compared to a light charged particle detection system. So their detection is required especially when dealing with heavy systems.

The experiments presented here was performed at GANIL with an ensemble of heavy fragment detectors covering a large solid angle. The detection system measured charges, angles, and velocities of fragments emitted in 27 and 43 MeV/A Kr collisions on Ag, Au and Th target.

The analysis of results from such detection system leads to new methods or unusual parameters for this energy range to evaluate the impact parameter and to look for equilibrated or unequilibrated decay modes of excited systems.

2 - Experiments

We will present an analysis of heavy nucleus collisions at 27 and 43 MeV/u based on as exclusive as possible detection of large fragments (Z>8) in the 3-150° angular range. The useful area of the detectors (DELF[3] and XYZT[4]) covered 55% of 4π. The measured parameters are the atomic number Z and the velocity vector $\vec{V}$ for each fragment in a detected event. Our first observation is a significant amount of events with a high number of detected fragments (up to 5 whatever the target is).

The data presented have been selected through a relative velocity ($V_{rel} = |\vec{V}_i - \vec{V}_j|$) analysis. The detected fragments (N_d) has been treated in sub-groups of three. In each sub-group the variable $Y_{3/3}$ is defined as $< V_{rel} > - V_{rel}^{min}$ (with $< V_{rel} >$ = mean value of the three relative velocities between the selected fragments and V_{rel}^{min} = minimum relative velocity in the considered sub-group).

		V_g cm/ns	V_g/V_{cm}	E*MeV/u
Kr + Ag	43 MeV/u	3.38	0.85	9.9
Kr + Au	43 MeV/u	2.	0.75	7.4
Kr +Th	43 MeV/u	1.8	0.75	6.8
Kr + Ag	27 MeV/u	3.15	0.99	6.6
Kr + Au	27 MeV/u	2.	0.93	5.4
Kr + Th	27 MeV/u	1.8	0.94	5.1

Table 1

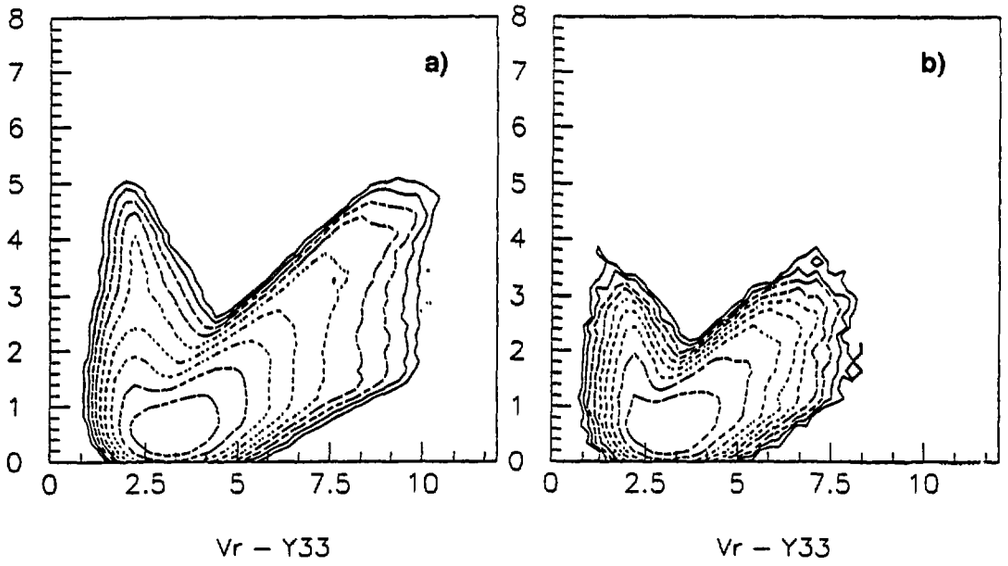

Fig. 1

Fig. 1 shows a logarithmic (Vrel, $Y_{3/3}$) plot for the gold target (N_d=4, E/A=43 MeV/u (fig. 1,a) and E/A=27 MeV/u (fig. 1,b). If all the $Y_{3/3}$ are lower than 2.5 cm/ns (fig. 1,a : E/A=43 MeV/n) and 1.5 cm/ns (fig. 1,b : E/A=27 MeV/n), the relative velocities are considered close compact and we are faced with a central event. We therefore confine our analysis to events fulfilling this criterion.

For the events selected as "central", the most probable value of the event recoil-velocity :

$$\vec{V}_g = \sum_{i=1}^{Nd} Z_i \vec{V}_i / \sum_{i=1}^{Nd} Z_i$$

remains inchanged, whatever N_d is and for a given system whatever the beam energy is (table 1). Furthermore these events present a strong similarity according to the relative velocity spectra whatever Nd is. All these facts allow to conclude at a common origin for these "central" events. Although high Nd are observed, global features of these events show that a fraction of Z remains missing (table 2). However for Nd>4, the majority of the involved matter is detected and the missing atomic number can be explain by pre-equilibrium and evaporation effects.

Kr 43 MeV/n	Au ΣZ_i %		Th ΣZ_i %		Ag ΣZ_i %	
Nd=3	53	46	57	45	39	47
Nd=4	64	56	69	55	45	54
Nd=5	73	63	80	63	50	60
Kr 27 MeV/u	**Au ΣZ_i %**		**Th ΣZ_i %**		**Ag ΣZ_i %**	
Nd=3	70	61	77	61	48	58
Nd=4	83	72	92	73	56	68
Nd=5	93	81	99	79	55	66

Table 2

Several methods to study directed collective motion has been used[5]. One is to calculate the event degree of isotropy in the momentum space. This global variable is measured by the ratio :

$$R = \frac{\frac{2}{\pi}\sum_{i=1}^{Nd}\left|\vec{P}_{\perp}^{(i)}\right|}{\sum_{i=1}^{N_d}\left|\vec{P}_{//}^{(i)}\right|}$$

The sums run over the number of detected fragments in the studied event, vector $\vec{P}_{\perp}^{(i)}$ and $\vec{P}_{//}^{(i)}$ are respectively the perpendicular and the parallel momentum of the i^{th} fragment. For each event, the calculation of transverse and parallel momenta are done in a a frame whose velocity is the event parallel recoil velocity $(\vec{V}_g)$. For an isotropically expending system, the R ratio is distributed around 1 ; if flow into transverse direction exists, R is larger than 1.

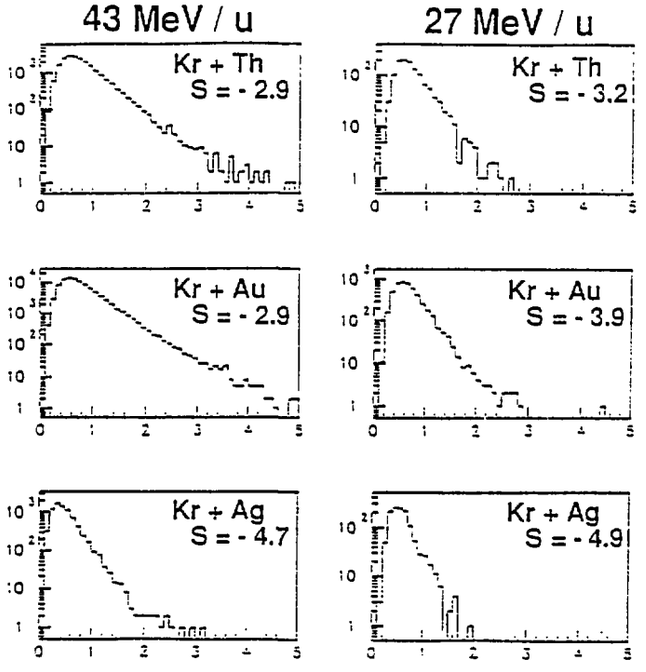

Fig. 2

In figure 2 we present the R spectra for the three studied systems at the two energies (27 and 43 MeV/n). A striking difference can be observed between the R plots for the Gold target and the Silver target (but not between the Gold and Thorium targets). For the heaviest targets we observe large R values at 43 MeV/n (not at 27 MeV/n). This indicates the appearance of momentum flow through an isotropic energy emission in a plane perpendicular to the beam direction. In order to characterize detection cuts (angle, atomic number and velocity) we performed a Monte Carlo simulation. It appears clearly that the experimental acceptance filter has no effect on the R slope.

In the central collisions selected by the relative velocity analysis the excitation energy, deduced from the recoil velocity reach values around 7 MeV/u and even for these large values we still observe large fragments. Moreover for a noticeable part (~10%) of the events all fragments are emitted in a plan perpendicular to the beam direction. So we may conclude that dynamical effects appears with increasing energy and mass system.and that heavy fragment production proves to be one way to extract the properties of non-equilibrated nuclear matter.

REFERENCES

1) E. Suraud et al, Progress of Nuclear and Particle Sciences, 23 (1989) 357
2) Gutbrod.h, Report on progress in Physics, 52 (1989) 1267
3).R. Bougault et al, NIM A259 (1987) 43
4) G. Rudolf et al, NIM A307 (1991) 325
5) R. Bougault et al, Symposium on Nuclear Dynamics and Nuclear Disassembly 197th ACS National Meeting - Dallas, Texas (USA) - April 9-14 (1989)
R. Bougault et al, Berkeley Workshop on multifragmentation - Asihomar, California (USA) october 1989
R. Bougault et al, 28th International Winter Meeting on Nuclear Physics - Bormio (Italy), 22-26 January 1990

NUCLEAR DISASSEMBLY OF THE PB + AU SYSTEM AT 29 MEV/NUCLEON

E.Piasecki[a,b], S.Bresson[b], B.Lott[c], R.Bougault[d], A.Chbihi[b], J.Colin[d], E.Crema[b,e], J.Galin[b], B.Gatty[f], A.Genoux-Lubain[d], D.Guerreau[b], D.Horn[d,g], D.Jacquet[f], U.Jahnke[h], J.Jastrzebski[i], A.Kordyasz[a], C.Le Brun[d], J.F.Lecolley[d], M.Louvel[d], M.Morjean[b], C.Paulot[b], L.Pienkowski[i], J.Pouthas[b], B.Quednau[j], W.U.Schroeder[j], E.Schwinn[h], W.Skulski[i], J.Tökej

[a] *Institut of Experimental physics, Warsaw University, Hoza 69, 00-681 Warszawa, Poland*
[b] *GANIL, B.P. 5027, 14021 Caen-Cedex France*
[c] *Centre de Recherches Nucléaires Strasbourg, B.P.20 CRO, 67037 Strasbourg France*
[d] *Laboratoire de Physique Corpusculaire, Bd du Maréchal Juin, 14032 Caen-Cedex France*
[e] *Instituto de Fisica, Universidade de Sao Paulo, Brazil*
[f] *Institut de Physique Nucléaire B.P. 1, 91406 Orsay-Cedex*
[g] *Chalk River Laboratories, Atomic Energy of Canada Limited, Chalk River, Ontario, Canada KOJ IJO*
[h] *Hahn Meitner Institut, D1000 Berlin 39, Germany*
[i] *Heavy Ion Laboratory, Warsaw University, ul. banacha 4, 02-097 Warszawa, Poland*
[j] *University of Rochester, Rochester, New York 14627 USA*

1. Motivations

Recent experiments[1] studying interactions of intermediate energy Ar projectiles with massive target nuclei have shown that, above a bombarding energy of about 30 MeV/nucleon, the measured most probable multiplicity of neutrons emitted from the reaction in dissipative collisions remains almost independent of the bombarding energy. Since for heavy systems the neutron multiplicity is a good measure of the total excitation energy introduced into the system, such a "saturation" effect could have represented a manifestation of limits to the temperature attainable by heavy nuclei[2]. However, in subsequent experiments[3] it has been observed that a further increase in excitation energy (and temperature) is possible when heavier projectiles such as Kr are used at similar velocities. Such a dependence on the projectile-target combination suggests that the limits reached in the above experiments are not yet those characteristic of nuclear systems in general but, are a reflection of the influence of the collision dynamics on the efficiency of heat-generation mechanisms.

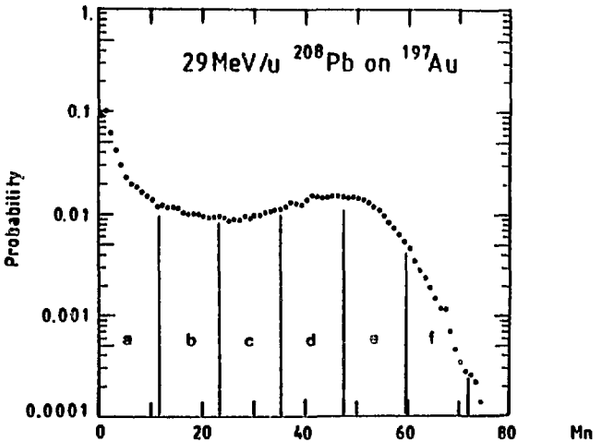

Fig.1 Neutron multiplicity distribution, with dead time correction but without detection efficiency corrections. Gates a, b, c, d, e, f refer to Fig.2

The purpose the present work was to extend the above systematics to very heavy and nearly symmetric projectile-target combinations and to search for changes in reaction mechanisms, at higher temperatures that can presumably be generated in such heavy systems.

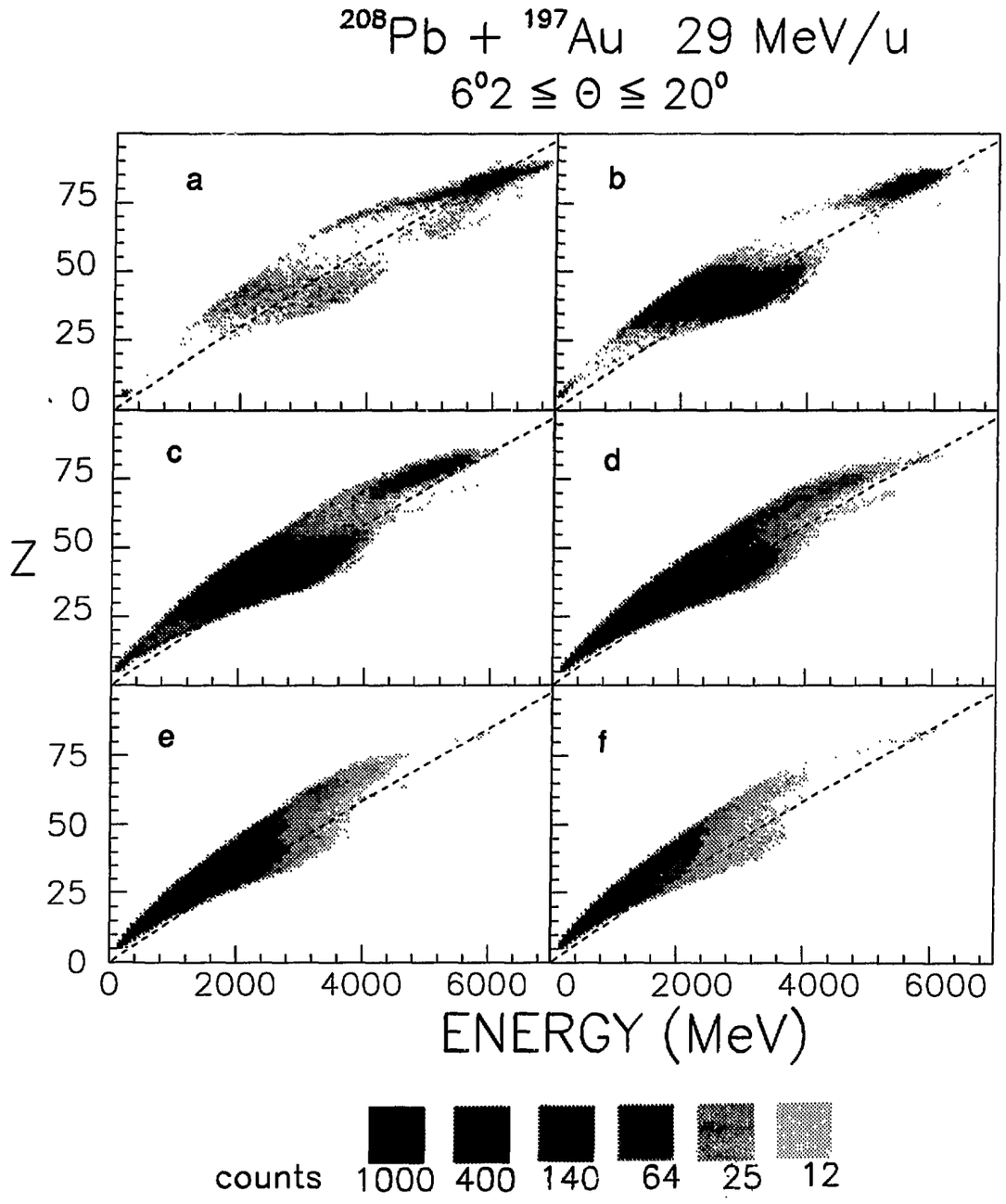

Fig.2 Distribution of the nuclei, detected from 6 to 20 deg., in the Z versus Energy space, for six contiguous neutron multiplicity gates, as mentioned in Fig.1. The dashed line represents the locus for reaction products at beam velocity. The detected products have a range, R, in silicon such that 200 μm <R< 700 μm.

2. The experimental approach

The experiment was carried out with the 29 MeV/nucleon Pb beam, impinging on a Au target. Charged products, ranging from protons to projectile-like nuclei, were measured with an array of different types of detector telescopes, ensuring a wide dynamic range and a broad angular coverage[4]. Simultaneously, the number of neutrons produced in a collision has been determined by means of the 4π ORION detector[5]. As demonstrated in previous studies[3], the multiplicity of neutrons emitted in a reaction provides a sensitive measure of the violence of a collision and, hence, the associated impact parameter.

3. The experimental data

A global information on energy dissipation in the measured reaction is given in Fig.1 by the inclusive neutron multiplicity distribution. It is similar to those measured earlier[1,3] with Ar and Kr beams at comparable velocity. The dominant features of these distributions are the presence of a narrow peak close to zero multiplicity, corresponding to the large impact parameters, and a broad bump at higher multiplicity associated with more central, dissipative collisions. For the present system, this latter bump is centered at a significant higher multiplicity of M_n=50, corresponding to approximately 78 neutrons when corrected for detection efficiency. This represents almost one-third of all neutrons of the system and almost 100% of the system neutron excess, much more than observed in reactions with Ar or Kr on the same Au target. This fact alone suggests that in the most central collisions the system disassembled into a large number of light fragments.

Experimental confirmation of this presumption is shown in Fig.2 where charged product-energy distributions (registered in the angular range 6-20 deg.) are presented for six contiguous bins of the associated observed neutron multiplicity M_n. One should stress that because of detector thresholds and kinematics one cannot see target-like fragments (not energetic enough) and that some of the lighest high energy fragments, punching through the front part of the telescope, could not be properly identified and were rejected. The most striking feature is the change in population with decreasing impact parameter (increasing M_n): from elastic and quasi-elastic collisions, through deep inelastic collisions and fission up to the most central collisions, when apparently only rather light particles and intermediate mass fragments survive the violent collision.

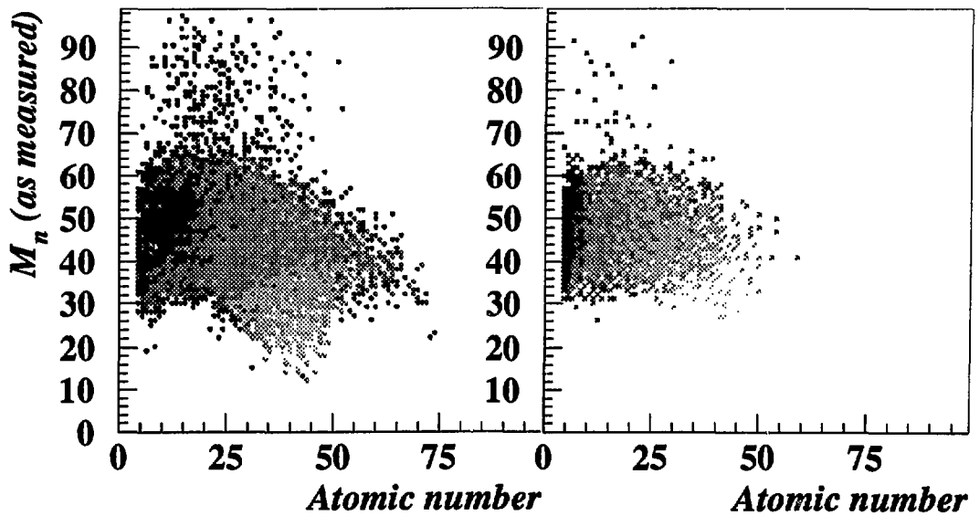

Fig.3-Left Differential multiplicities (arbitrary units) of light charged particles (lcp of Z=2) detected between 6 and 20 deg.in coincidence with a more massive nucleus, as a function of the Z of the latter and of the neutron multiplicity M_n. As expected, there are no lcp for quasi elastic events and rather low multiplicities accompanying sequential fission of the quasi-projectile (around Z=41). The lcp multiplicity peaks for high M_n values and rather low Z's.
Fig.3-Right : same as before with the second nucleus with Z>2, instead of Z=2.

The disassembly is also well shown in Fig.3-left where the differential multiplicity of light charged particles (Z=2) detected in the same array as the more massive fragments is presented as a function of size of the fragment (Z) and associated neuton multiplicity: The intermediate mass fragments are accompanied by the highest neutron and light charged particle multiplicities. The requirement of two IMF's detected in coincidence (Fig.3-right) leads to an even stronger focusing of events with large neutron multiplicities and relatively lighter IMF's.

4. Conclusions

Such a complete disassembly is known in high-energy induced reactions, but it is surprising that such events, comprising approximately one-fourth of the reaction cross section, occur also at so low relative velocity, when compressional effects are presumably not important. Coulomb forces might play a significant role in the disassembly if the two nuclei get confined for some time in a rather compact configuration. It would be premature to say now whether the observed disassembly is sequential or instantaneous. A detailed analysis of charged particles measured in coincidence is underway. Also it would be very helpful to perform similar experiments using a 4π charged product detector system and compare the results with model calculations[6-7].

REFERENCES

[1] D.X.Jiang et al., Nucl. Phys. **A503** (1989) 560

[2] E.Suraud, Nucl. Phys. **A462** (1987) 109, and references therein

[3] E.Crema et al., Phys.Lett. **B258** (1991)266

[4] Piaseki et al. Phys. Rev. Lett. **66** (1991) 1291

[5] J.Galin et al., Proceedings of the Second IN2P3-RIKEN meeting on Heavy-Ion Collisions, ed. by B.Heusch and M.Ishihara (World Scientific, Singapore, 1990), p102

[6] M.Blann et al., Phys. Rev. **C44** (1991) 431

[7] G.Peilert et al., Phys. Rev. **C39** (1989) 1402

DYNAMICS OF VIOLENT COLLISIONS FOR THE Ar+Ag SYSTEM BETWEEN 27 AND 57 MeV/nucleon

M. F. Rivet[1], B. Borderie[1], M. Dakowski[1], P. Box[1], C. Cabot[1], Y. El Masri[2], D. Gardes[1], F. Hanappe[3], D. Jouan[1], G. Mamane[1], X. Tarrago[1] and H. Utsunomiya[1]

[1] *Institut de Physique Nucléaire, F91406 Orsay Cedex*
[2] *Institut de Physique Nucléaire, UCL, B-1348 Louvain-la-Neuve*
[3] *Fonds National de la Recherche Scientifique et ULB, B-1050 Bruxelles*

1 Motivations

The dynamics of collisions producing an intermediate mass fragment (IMF) and a heavy residue in the outgoing channel has been thoroughly studied for the Ar+Ag system at 27 MeV/nucleon [1]. For peripheral and mid-central collisions dissipative binary reactions occur, with a progressive damping of the relative motion. In central collisions the two incident nuclei fuse together; in all cases but the very peripheral reactions an abundant preequilibrium emission was observed. This study was extended to higher incident energies (44 and 57 MeV/nucleon), to test the persistence of these mechanisms, and to search for eventual multifragment emission.

2 Experiment and first results

Heavy residues were detected by 11 low-resistivity silicon detectors located in the horizontal plane between 10 and 60° from the beam axis. Their mass was obtained via a time of flight measurement with respect to the RF pulse. On the other side of the beam and in the same plane, coincident intermediate mass fragments were identified in six telescopes made of a 40 or 10μ silicon detector backed by a 3.3 cm CsI cristal from the PACHA array, located between 10 and 120° from the beam direction.

The first results which are presented here concern the relative velocity of the two fragments and the recoil velocity of the system before the binary splitting. These quantities are calculated from average measured values as explained in [1].

The top part of figure 1 shows the evolution of the relative velocity of the two final fragments, expressed as $(V_{rel} - V_c)/(V_p - V_c)$, versus the emission angle of the light one (θ_{IMF}). In this expression V_p is the projectile velocity and $V_c = 3\ cm/ns$ the Coulomb repulsion. The behaviour of V_{rel} is the same for the three energies, one observes a gradual damping of the relative motion when θ_{IMF} increases; the Coulomb velocity is reached beyond 20-30°. We feel that the observed evolution signs the persistence of deeply inelastic processes up to 60 MeV/nucleon.

The bottom part of figure 1 presents the recoil velocity of the system before its binary break-up, normalized to the incident center of mass velocity. The recoil velocity was assumed to lie in the beam direction. Any deviation of the value of this ratio from 1 indicates the occurence of preequilibrium emission. At 44 MeV/nucleon as already noticed at 27 MeV/nucleon no preequilibrium emission is visible for the most peripheral collisions ($\theta_{IMF} \leq 10°$), which is no longer true at 57 MeV/nucleon. When going to more central collisions, V_{rec}/V_{cm} decreases strongly and more when the incident en-

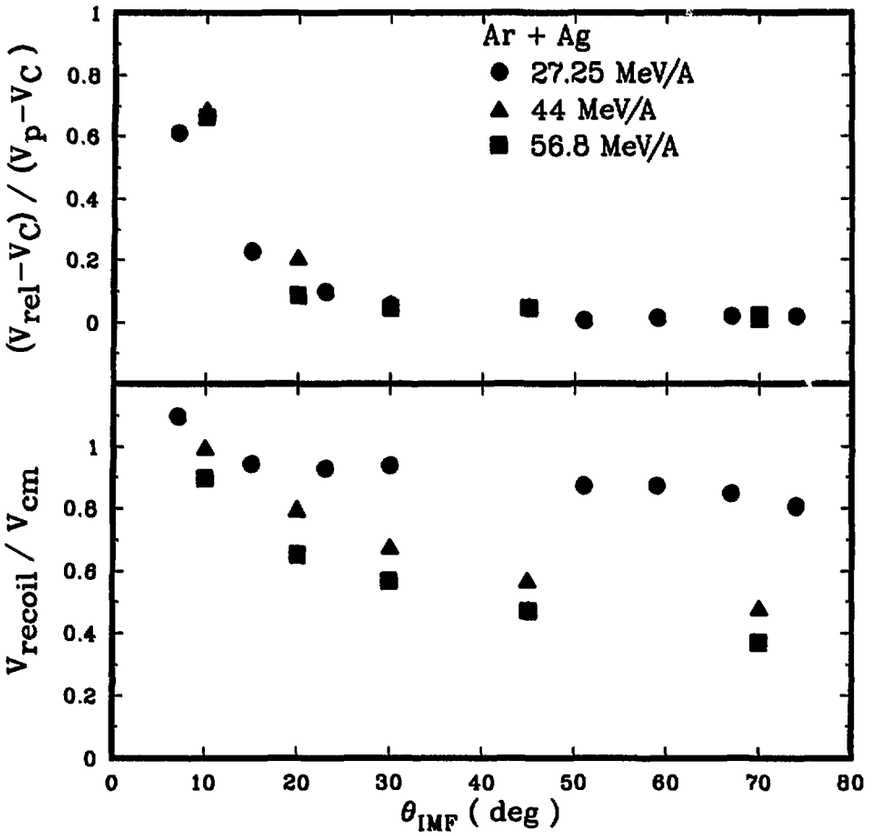

Figure 1: Evolution of the relative velocity of the two fragments (top) and of the recoil velocity of the system before splitting (bottom) versus the emission angle of the light fragment

ergy is higher. A large gap is however observed between 27 and 44 MeV/nucleon and a much smaller one between 44 and 57; for central collisions this would imply a fast rise of preequilibrium emission with incident energy followed by a slower increase. The parallel linear momentum transfer deduced from V_{rec} (in the massive transfer picture) is plotted in Figure 2 (points); the solid line shows the limit of momentum transfer due to momentum space considerations (P=180 MeV/c per projectile nucleon), which was shown to well fit most of the experimental data for a large number of systems. Our data at 44 and 57 MeV/nucleon lie well below this curve. A possible explanation for this observation would be the existence of a limiting temperature for nuclei; As a fisrt estimate, a crude value of the excitation energy can be derived from the momentum transfer in the framework of the massive transfer picture, and then a temperature (a=A/10). The limits imposed on the linear momentum by maximum temperatures equal to 6 and 7 MeV are indicated on Figure 2 by the dotted and dashed lines. Our experimental points lie between these two curves.

Comparisons with realistic dynamical simulations of nuclear collisions [2] will be

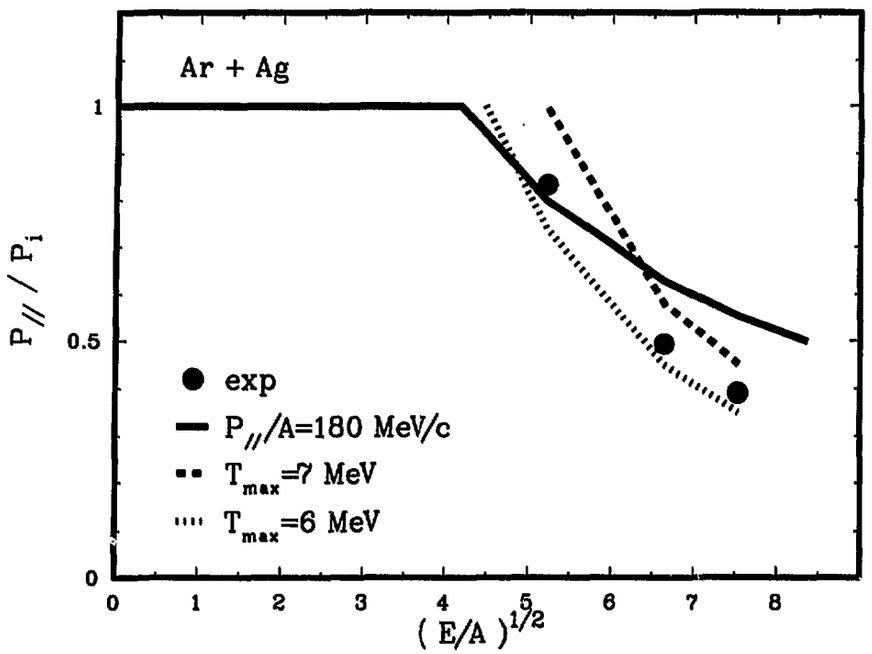

Figure 2: Experimental parallel linear momentum transfer compared to different limiting values (see text)

performed and may help to understand this experimental finding.

References

1. D. Jouan, B. Borderie, M.F. Rivet C. Cabot, H. Fuchs, H. Gauvin, C. Grégoire, F. Hanappe, D. Gardes, M. Montoya B. Remaud and F. Sébille Z. Phys.A-Hadrons and Nuclei **340** (1991) 63.

2. C. Grégoire, B. Remaud, F. Sébille, L. Vinet, Y. Raffray, Nucl. Phys. **A465** (1987) 317.

B4 - MESONS and PHOTONS

EXCLUSIVE MEASUREMENTS OF HIGH ENERGY PHOTON PRODUCTION IN THE $^{129}Xe + ^{197}Au$ REACTION AT 44 MeV/u

E.Migneco[1,2], C.Agodi[1], R.Alba[1], G.Bellia[1,2], R.Coniglione[1], A.Del Zoppo[1], P.Finocchiaro[1]
C.Maiolino[1], P.Piattelli[1], G.Russo[1,2], P.Sapienza[1], A.Badalá[3], R.Barbera[3], A.Palmeri[3]
G.S.Pappalardo[3], F.Riggi[2,3], A.C.Russo[2,3], R.De Leo[4], A.Peghaire[5]

(1) *Istituto Nazionale di Fisica Nucleare - Laboratorio Nazionale del Sud*
Viale A.Doria (angolo Via S.Sofia), 95123 Catania (ITALY)
(2) *Dipartimento di Fisica dell'Università di Catania (ITALY)*
(3) *Istituto Nazionale di Fisica Nucleare - Sezione di Catania (ITALY)*
(4) *Dipartimento di Fisica dell'Università di Lecce (ITALY)*
(5) *GANIL, Caen (FRANCE)*

1. Motivations

The high energy photon production ($E_\gamma \geq 30$ MeV) in heavy ion reactions at intermediate energy has been an intense field of research in the last years.[1,2]

Several theoretical models have been developed to explain the high energy γ production, but they can all be referred to three possible mechanisms:

nucleus-nucleus coherent bremsstrahlung models, in which the photons are produced by the deceleration of the two colliding ions during the first stages of the reaction; the hard γ-ray yield is expected to be proportional to the product of the colliding ion charges and the angular distribution to have a quadrupole pattern;

incoherent bremsstrahlung models, in which the photons are produced in the n-p collisions; the photon yield is expected to increase with increasing beam energy and the angular distribution should be isotropic plus a dipole component in the half-beam velocity reference;

statistical models, in which the photons are emitted by the decay of excited systems, which range from compound nucleus to the formation of a fireball for higher energies.

A quite large number of inclusive experimental data are available in a broad range of beam energies (10 MeV/u $\leq E_{beam} \leq$ 120 MeV/u) and for several projectile-target systems. The analysis of these data indicates the n-p bremsstralhung mechanism as the main responsable for the hard photon production. Up to now only a few exclusive experiments have been performed while it is of great interest to correlate the high energy photons to other observables of the reaction in order to achieve a deeper understanding of the hard photon production and of the heavy ion reactions.

2. The experiment

In the present experiment we have measured, on a event-by-event basis, hard photons in coincidence with the emitted light charged particles (p,d,t and He) in a close to 4π geometry. The experiment was performed at the GANIL laboratory by bombarding a ^{197}Au target with a 44 MeV/u ^{129}Xe beam and it was the first experiment run with

the MEDEA detector realized at the L.N.S. in Catania.[3]

In this experiment MEDEA consisted of 180 BaF_2 crystals, 20 cm thick, arranged in the shape of a hollow sphere with an inner radius of 22 cm and a forward wall made of 120 plastic phoswhich detectors placed at 55 cm from the target. The BaF_2 ball covers the polar angles between 30° and 170° while the phoswhich wall covers the angles between 10° and 30°. All the detector is placed under vacuum inside a large scattering chamber. The electronics was enabled by the presence in the event of at least one BaF_2 signal which passed a threshold level of an about 30 MeV γ-equivalent signal. After the conversion a further selection on the events was operated by a second level trigger.

3. Data analysis and results

The first part of the analysis aimed to the determination of the key parameters related to the high energy photon production; namely the inverse slope parameter E_o, the γ emitting source velocity β_s, the angular anisotropy and the hard γ emission probability from inclusive spectra at different laboratory angles.

The inverse slope parameter E_0=13.6±0.4 MeV is in good agreement with the systematics. A low anisotropy value α=0.23±0.05 has been found in agreement with other results from the heavier systems. The emitting source velocity β_s=0.15±0.05 is very close to the half beam velocity β=0.148 and therefore to the nucleon-nucleon center of mass velocity.

The probability P_γ of emitting an high energy photon ($E_\gamma \geq 30$ MeV) per n-p collision can be determined assuming that the γ cross section can be parametrized as

$$\sigma_\gamma = \sigma_R \cdot P_\gamma \cdot < N_{np} >$$

where σ_R is the reaction cross section and $< N_{np} >$ is the average number of first chance collisions, evaluated using the formula given in ref.4.

The value $P_\gamma \sim 6.07 \cdot 10^{-5}$ shows that even for the $^{129}Xe+^{197}Au$ system, that is the heaviest studied up to now, using the same scaling for the P_γ we get a good agreement with the overall systematics and the BUU calculations.[5]

In our experiment we have measured simultaneously the high energy photons and the light charged particles (p, d, t, He), and to characterize the events we have used the backward light charged particle multiplicity M_{lcp}. In fact several experimental and theoretical works have shown that low backward multiplicities are related to larger impact parameters (periferal collisions) while high backward multiplicities are related to lower impact parameters (central collisions).

The photon multiplicity for E_γ >40 MeV and for a given light charged particle fold m, defined as $M_\gamma(m) = \sigma_\gamma(m)/\sigma_R(m)$, is reported in fig.1a, showing a strong dependence on the *lcp* multiplicity. In fact the M_γ first increase steeply with increasing M_{lcp} then tends to saturate for the highest multiplicities. Since the M_γ varies over more than one order of magnitude, we deduce that the high energy photons are mostly produced in the more central reactions, and therefore the high energy photons represent a good centrality probe. This behaviour of the M_γ is in qualitative agreement with the results of BUU calculations performed for the reaction $^{40}Ar + ^{197}Au$ at 44 MeV/u.[6]

Another interesting result concerns the E_0 dependence on the centrality of the reaction. In fact the inverse slope parameter E_0 determined for events belonging to three

different multiplicity bins (low, intermediate and high multiplicities) is almost constant as shown in fig.1b. We have to mention that other experiments on lighter systems (^{36}Ar+^{27}Al, ^{40}Ar+^{159}Gd)[7,8] indicate an increase of E_0 with increasing centrality of the reaction. It will be interesting to verify if the observed different behaviour is related to the size of the interacting systems.

The proton spectra of the events producing high energy γ (fig.2a) is very similar to the proton spectra emitted in the high multiplicity events (fig.2b). The proton spectra at different angles can be simultaneously fitted with two sources: one with a $\beta_s=1/2\beta_{beam}$ and T=13 MeV that is characteristic of a preequilibrium emission and another with low velocity and low coulomb repulsion, which needs further investigations.

4. Conclusions

The inverse slope parameter E_0 and the γ emission probability per n-p collision P_γ are in good agreement with the systematics. The extracted source velocity $\beta_s=0.15$ is very close to the half beam velocity as expected in the n-p bremsstrahlung description. A strong dependence of the M_γ on the light charged particle multiplicity has been observed, confirming that the high energy photons are produced in the most central collisions.

In this experiment, at variance with previous measurements, we observe an independence of the slope parameter E_0 on the multiplicity. The proton spectra for the events producing high energy photons and for the high multiplicity events are very similar and indicate for the central collisions a strong preequilibrium emission.

References

(1) H. Nifenecker and J.A. Pinston, Annual Rev. Nucl. Part. Science, 40 (1990) 113.

(2) W. Cassing, V. Metag, U. Mosel, K. Niita, Phys. Rep. 188 (1990) 365.

(3) E. Migneco, C. Agodi, R. Alba, G. Bellia, R. Coniglione, A. Del Zoppo, P. Finocchiaro, C. Maiolino, P. Piattelli, G. Raia and P. Sapienza, Nucl. Instr. and Meth. A, in print.

(4) H. Nifenecker and J.P. Bondorf, Nucl. Phys. A442 (1985) 478.

(5) V. Metag, Nucl. Phys. A488 (1988) 483c.

(6) Riess, *Workshop on phisics related to TAPS*, GSI Report (1991) 52.

(7) R. Hingmann et al., Phys. Rew. Lett. 58 (1987) 759.

(8) M. Kwato Njock et al., Nucl. Phys. A489 (1988) 368.

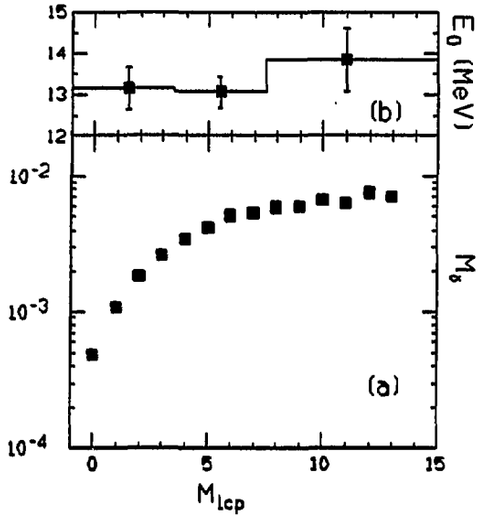

Fig.1 - (a) Photon multiplicity vs. light charged particle multiplicity M_{lcp}; (b) inverse slope parameter E_0 measured at θ_{lab}=112° vs. M_{lcp}. The M_{lcp} was evaluated with *lcp* emitted at backward angles ($\Omega \sim 2\pi$).

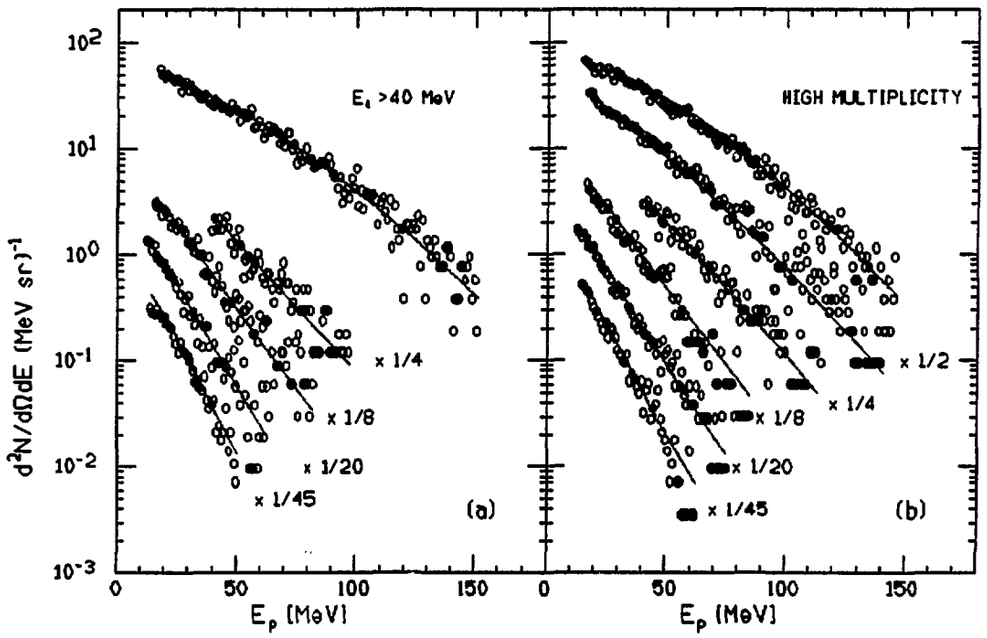

Fig.2 - (a) Proton energy spectra in coincidence with hard photons (E_γ >40 MeV) at different laboratory angles (θ=53°, 83°, 97°, 112° and 127°); (b) proton energy spectra for high multiplicity events at different laboratory angles (θ=53°, 68°, 83°, 97°, 112° and 127°). Solid lines are the data fits.

HARD PHOTON INTENSITY INTERFEROMETRY IN HEAVY ION REACTIONS.

R. Ostendorf[1], Y. Schutz[1], R. Merrouch[1], F. Lefèvre[1], H. Delagrange[1], W. Mittig[1], F.D. Berg[2], W. Kühn[2], V. Metag[2], R. Novotny[2], M. Pfeiffer[2], A.L. Boonstra[3], H. Löhner[3], L.B. Venema[3], H.W. Wilschut[3], W. Henning[4], R. Holzmann[4], R.S. Mayer[4], R. Simon[4], D. Ardouin[5], H. Dabrowski[5], B. Erazmus[5], C. Lebrun[5], L. Sézac[5], P. Lautridou[6], J. Québert[6], F. Ballester[7], E. Casal[7], J. Diaz[7], J.L. Ferrero[7], M. Marques[7], G. Martinez[7], H. Nifenecker[8], B. Fornal[9], L. Freindl[9], Z. Sujkowski[10], T. Matulewicz[11]

[1] *GANIL, BP 5027, 14021 Caen, France*
[2] *II Physikalisches Institut Universität Giessen, D-6300 Giessen, Germany*
[3] *KVI, 9747 AA Groningen, The Netherlands*
[4] *GSI, D-6100 Darmstadt, Germany*
[5] *LPN, 44072 Nantes Cedex 03, France*
[6] *CENBG, 33175 Gradignan Cedex, France*
[7] *IFIC 46100 Burjassot, Valencia, Spain*
[8] *ISN 38026 Grenoble, France*
[9] *INP, 31-342 Krakow, Poland*
[10] *SINS, Swierk, Poland*
[11] *Warsaw, University, Poland*

1. Introduction

It is rather well established, that the hard photon spectrum observed in heavy-ion collisions at several tens of MeV per nucleon mainly originates from the incoherent superposition of bremsstrahlung emitted during individual neutron-proton collisions. Calculations of BUU-type [1] reproduce rather well both qualitatively and quantitatively the observed characteristics of hard photons. They further conclude that due to Pauli-blocking only the first chance collisions effectively produce the hard photons. Therefore the average duration of the production should be of the order of 15 fm/c, which is the time for a single NN-collision. The extent of the photon source should be restricted to the overlap zone of two interacting nuclei at the very beginning of the collision. Since photons only interact weakly with the surrounding nuclear matter, they provide a unique undistorted probe of the early stage of nuclear reactions.

Not only is it a challenge to verify these theoretical deductions experimentally, but it also will be of prime importance to measure the dimensions of the interaction zone at the stage where the highest density is expected to be reached. We use a method that initially has been applied in astronomy to measure the size of stars. It is based on the principle of intensity interference leading to a pattern that is a measure for the photons' source size. In the case of incoherent production, pairs of hard photons will preferably be emitted at low relative momentum and the width of the enhancement reflects the size of the photon source.

2. The experiment

In order to optimize the photon production rate we selected a heavy system and a bombarding energy where the π^0 production rate is low enough not to hinder our measurement. The reaction was $^{129}Xe + {}^{197}Au$ at 44 MeV/u. The gold target was 9 mg/cm^2 thick.

To overcome the weak production rate of hard photons, the present experiment employed a multidetector consisting of 247 hexagonal BaF_2 detectors of various types. They were assembled in 13 blocks of 19 modules with a central detector surrounded by an inner ring of 6 and an outer ring of 12 modules. The blocks surrounded the target at a distance of 420 mm and covered 27% of 4π at θ angles spanning a nearly continuous range between 50° and 170° and almost a full coverage in φ [2].

The detectors were calibrated using radioactive sources and for a high energy calibration point ($\sim$ 40 MeV) using cosmic muons whose deposited energy was calculated in a Monte-Carlo simulation including the angular distribution of muons and the spatial distribution of the detectors. The cosmic events were recorded throughout the whole experiment (including the beam off periods) and were used to monitor the gain.

In the off-line data analysis, photons were identified by using the difference in the pulse shapes generated in the BaF_2 detectors in response to neutral or charged particles and the difference in time of flight between photons and massive particles. The energy and emission angles of the photons were obtained from a shower reconstruction method. For single photon emission the yield as well as the shape of the spectra followed the established systematics [1].

To extract pure 2-photon events, it becomes necessary to reject on an event by event basis the cosmic muons which can fire several detectors within a block or even in different blocks and consequently distort the 2-photon correlation function. During the experiment, they were recorded in random coincidence with the beam at a rate of nearly 30 cosmic events for every 2-photon event. To be recognized as a 2-photon event, we have imposed the following three conditions : the hadron multiplicity is larger than 1; two high-energy photons ($E_\gamma \geq 25$ MeV) are detected in two different blocks; and no more than 3 high-energy hits are present. These conditions were fulfilled by $\sim$14000 events.

3. The result

The correlation function, C_{12}, was constructed as the ratio of the 2-photon events with respect to their relative four-momentum, $\tilde{q}_+$, over an uncorrelated background:

$$C_{12}(\tilde{q}_+) = K \cdot \frac{N_{\gamma_1\gamma_2}(\tilde{q}_+ = \Delta\tilde{q}_{\gamma_1\gamma_2})}{N_{\gamma_1} N_{\gamma_2}(\tilde{q}_+ = \Delta\tilde{q}_{\gamma_1\gamma_2})}$$

where

$$\tilde{q}_+^2 = (E_{\gamma_1} - E_{\gamma_2})^2 + (\vec{p}_{\gamma_1} - \vec{p}_{\gamma_2})^2 \qquad (\hbar = c = 1)$$

and normalized to 1 in the region of $\tilde{q}_+ \sim 80$ MeV/c. The variable $\tilde{q}_+$ — note that it is not the invariant mass — is calculated in the nucleon-nucleon center of mass. Within this representation, the width of the correlation function is a direct measure of the space-time extent of the source assuming that the value for the lifetime and the radius are comparable. The denominator, or uncorrelated background, is constructed by mixing events. The experimental correlation function is shown in figure 1a. The peak around $\tilde{q}_+ = 130$ MeV/c is due to photons from the disintegration of π^0 mesons.

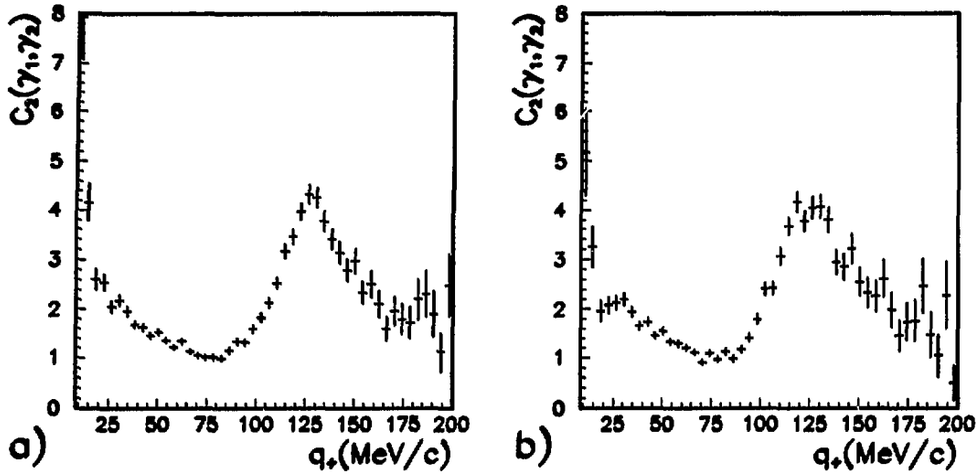

Figure 1: Correlation function versus the relative momentum $\tilde{q}_+$ constructed from two-photons events a) measured in the reaction ^{129}Xe + ^{197}Au at 44 MeV/u; b) simulated and including uncorrelated hard photons, π^0, e^+-e^- pairs and cosmic muons having the caracteristics observed experimentally.

In order to understand the structures observed at low relative momenta events have been simulated that included uncorrelated hard photons, π^0, cosmic muons and e^+-e^- pairs created by the conversion of photons passing through the scattering chamber, with characteristics and their relative production rate deduced from the experimental data. The events were folded with the response function of the detectors using the code GEANT3. The events were then analysed and filtered in exactly the same way as the experimental data and finally the simulated correlation function displayed in figure 1b was constructed.

The strong rise of the correlation function below $\tilde{q}_+ = 20$ MeV/c can be attributed to conversion e^+-e^- pairs and the cosmic muons. At intermediate relative momenta, between 20 and 75 MeV/c, the rise results from the way how the denominator is calculated in the presence of the π^0 peak. We have therefore developped a method which on an iterative basis calculates weight factors for the pairs of photons that have an invariant mass between 75 and 140 MeV/c^2, until the correlation function converges to one within the region of the π^0 peak. This method has been applied to the experimental (figure 2a) as well as to the simulated events (figure 2b). The gaussian like shape beyond 20 MeV/c up to 60 MeV/c is attributed to the expected interference between two independent photons. The height of the correlation function at $\tilde{q}_+ = 0$ as deduced from a fit to the gaussian $1 + \lambda \cdot \exp\left(-\tilde{q}_+^2/\Gamma^2\right)$ between $\tilde{q}_+ = 20$ MeV/c and $\tilde{q}_+ = 140$ MeV/c is equal to 1.9 ± 0.2. This is higher than the expected value of 1.5 [3], but it should not be taken too stricktly because of the strong e^+-e^- contamination. The width also deduced from this fit is 33 ± 3 MeV/c, being compatible with the maximum overlap size of R = 8 fm and the theoreticaly deduced duration of T = 15 fm/c.

It now should be questioned wether we realy measured the photon source size. We have not demonstrated that the observed rise towards low relative momenta in the correlation function is due to an interference effect and is sensitive to the source size. This can be demonstrated by measuring the correlation function for two systems entirely different in size.

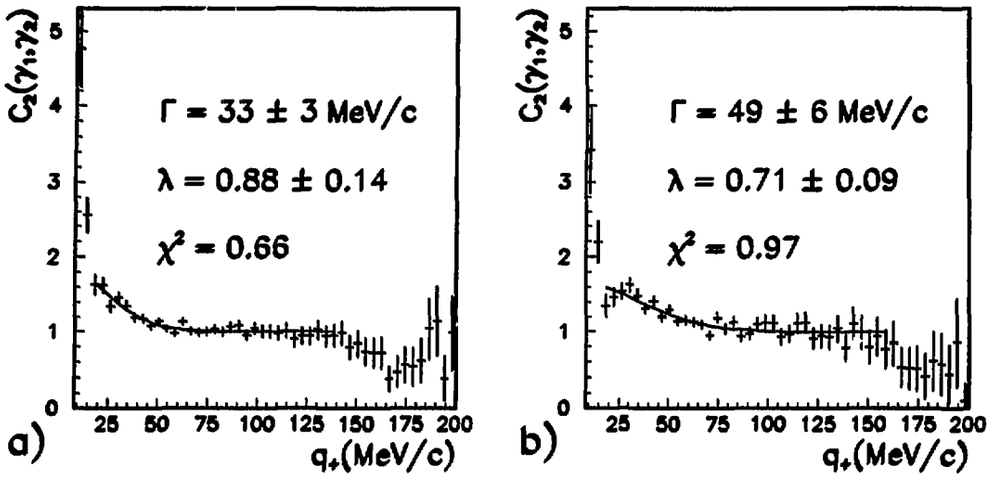

Figure 2: Correlation function obtained after weighting of events generating the π^0 peak for a) data events and b) simulated events. The solid line is the result of a fit to a Gaussian, $C_{12} = 1 + \lambda \cdot \exp\left(-\tilde{q}_+^2/\Gamma^2\right)$ with λ and Γ indicated on the figure.

Another open question is the influence of the cosmic muons, the analysis being unable to eliminate all of them. Although the two figures 2a and 2b are similar the difference in shape gives us a strong hint that in figure 2a we indeed observe the photon's intensity interference.

4. Conclusion

Hard photons produced in heavy ion collisions are believed to be a probe of the early phase of the reaction, the phase where the maximum density is reached. To measure the dimensions of the photon source, the technique of intensity interference was used. We have demonstrated that the TAPS multidetector has made this kind of experiment feasible as a result of its broad angular coverage and its energy resolution. The measured rise of the correlation function towards low relative momenta is tentatively attributed to the interference effect, which would be the first observation of the Hanburry-Brown Twiss effect in nuclear physics. This observation however should be confirmed with a new experiment, that enables a further background reduction and which correlates the width of the correlation function to the size of the system.

We wish to thank our colleagues at the Oak Ridge National Laboratory, J.R. Beene, F.E. Bertrand, M.L. Halbert, D. Horen, D. Olive and R. Varner for making their BaF_2 detectors available to us and for their help in the setup of the experiment.

References

[1] W. Cassing et al., Physics Reports **188** (1990) 363.

[2] R. Merrouch, thesis University of Caen, (1991)

[3] D. Neuhauser Phys. Lett **B182** (1986) 289.

Subthreshold K^+ Production in Heavy Ions Collisions

J. Julien[1], D. Lebrun[2], A. Mougeot[1], P. de Saintignon[2], N. Alamanos[1], Y. Cassagnou[1], C. Le Brun[3], J.F. Lecolley[3], R. Legrain[1], G. Perrin[2]

[1] DAPNIA/SPN CEN Saclay, 91191 Gif sur Yvette CEDEX, France

[2] ISN Grenoble, 53 avenue des Martyrs, 38026 Grenoble, France

[3] LPC ISMRA, 6 Bld. Juin, 14050 Caen CEDEX, France

Motivation

The emission of energetic photons and pions in collisions of heavy ions has been intensively investigated in recent years, as possible probes of the initial phase of the collision and as such was considered as a way of getting information on the equation of state. In that respect kaons appear as an even better choice than pions, since, due to strangeness conservation, they are very weakly reabsorbed in the nuclear medium, once they are produced. At subthreshold energies, nucleons have to undergo several collisions in the hot and compressed interaction zone to accidently gather up an energy high enough to produce one kaon (the free N-N threshold is 1.6 GeV) and thus kaon emission should be sensitive to the window in space and time associated with the largest energy densities.

K^+ production in heavy ions collisions has been studied with beams of 2.1 GeV/u [1], but no data exist for heavy ions at subthreshold energies. The present measurement of K^+ production in $^{36}Ar+^{48}Ti$ at 92 MeV/u [2] is an exploratory run, more data not yet analysed have recently been taken.

Experimental set-up

The titanium target was inserted between two copper slabs in which kaons produced in the target are stopped and decay into muons of 153 Mev energy, with a time constant of 12.4 ns. Muons are detected 30 cm away from the Cu absorbers in a range telescope made of a stack of 15 planes of segmented scintillators of different nature, their total number being forty. The range detector was divided in two parts: the trigger made of the first ten planes, and the absorber in which the range is measured.

The trigger consists in two hodoscopes, each with horizontal and vertical localization, which in total generated two times 25 zones in x-y directions. In between were 1.2 cm thick scintillating glasses and 4 cm thick plastic scintillators for energy loss measurements, a 0.5 cm thick NE102 scintillator used for time measurement versus the cyclotron RF signal and a plexiglass Cerenkov counter to reject particles with $\beta < 0.67$. The distance between the two hodoscopes was large enough to roughly reconstruct trajectories starting close to the target and Cu stoppers.

Good trajectories with only one hit in each hodoscope plane, plus a minimum energy loss of 2 MeV/g/cm^2 in the trigger planes, plus a narrow coincidence between these planes along with a delay larger than 4 ns relative to prompt events, plus a Cerenkov positive response made strongly restrictive conditions in the off-line analysis before absorber counters were read out.

The absorber was made of four 4 g/cm^2 thick glass (one) and NE102 scintillators (three), followed by veto counters out of the range to be measured. The range telescope was so designed that 153 MeV muons had to stop in the second or third of the four absorber counters. The total energy measured in the trigger + absorber amounted to 60 % of 153 MeV.

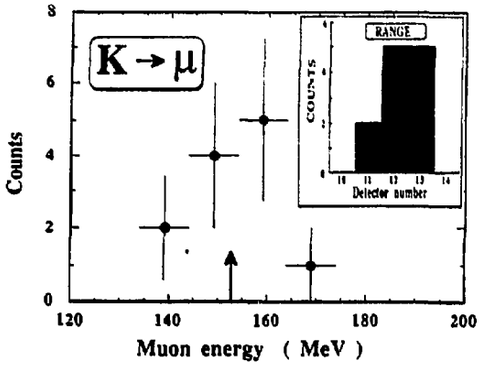

Fig. 1

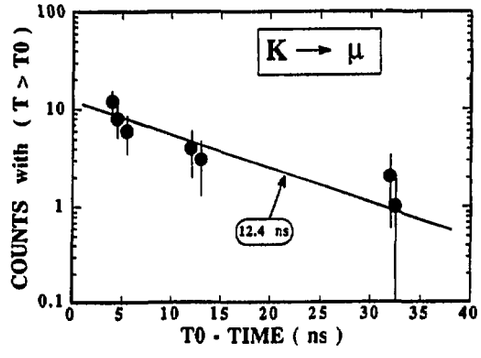

Fig. 2

Results and conclusions

With 10^{11} incident ^{36}Ar ions per second on the the 90 mg/cm^2 thick, 45° tilted ^{48}Ti target and after 24 hours of counting time, twelve good events were fulfilling the previous conditions. The total energy distribution of these 12 muons is shown in Fig 1 and their corresponding ranges appear in insert. The energy distribution shows a maximum at the expected place as indicated by the arrow, while the range distribution is flatter than anticipated, but remains within the detector resolution. Fig. 2 displays the time spectrum of these events; here is plotted the remnant population of events having a time of arrival greater than a given delay t_0 relative to prompt events. Data are compatible with the time distribution expected from kaon decay lifetime of 12.4 ns (solid line).

From these spectra we conclude to the evidence of kaon production. With an overall detection efficiency of 0.3% and assuming an isotropic distribution of the kaons, a total cross section of 240 ± 150 picobarns is infered for their production.

Theoretical calculations were, up to now, mainly concerned with incident energies of 500 MeV/u and above. However two recent works are giving predictions close to our result. The K+ production cross section in the ^{42}Ca + ^{42}Ca at 92 MeV/u has been estimated to 20-530 picobarns [3] using an analytical model based on the Boltmann Langevin equation. Another calculation [4] yielding a cross section of 152 picobarns has been done in the framework of a cooperative model [5] already used for subthreshold pion production. The first calculation shows that fluctuations increase subtstancially the K+ production cross section while the second one seems to imply that phase space constraints are important in K+ production.

References

[1] A good comprehensive review of subthreshold particle production can be found in: W. Cassing, V. Metag, U. Mosel and K. Niita, Phys. Rep. 188 (1990) 363.
[2] J. Julien, D. Lebrun, A. Mougeot, P de Saintigon, N. Alamanos, Y. Cassagnou, C. Le Brun, J.F. Lecolley, R. Legrain, G. Perrin, Phys. Lett. B264 (1991) 269.
[3] M. Belkacem, E. Suraud and S. Ayik, submitted to Phys. Rev. Lett.
[4] B. Gosh, Phys. Rev. C Rapid Communications (in press)
[5] R. Shyam and J. Knoll, Nucl. Phys. A426 (1984) 606

LIGHT PARTICLES EMITTED IN COINCIDENCE WITH PIONS AND ENERGETIC PROTONS IN HEAVY ION COLLISIONS AT 94 MeV/u

S.Aiello [1] ,A.Badala [1] ,R. Barbera [1],G.Bizard [2] ,R. Bougault [2]
D. Durand [2],A. Genoux-Lubain [2] ,G. M. Gin [3,4] ,J. L. Laville [2]
F. Lefebvres [2],A. Palmeri [1],G. S. Pappalardo [1] ,E. Rosato [3,5]
and F. Riggi [1]

[1] INFN ,Corso Italia,CATANIA, Italy
[2] LPC CAEN,ISMRA,IN2P3-CNRS,14050 CAEN,France
[3] GANIL,BP5027,14021 CAEN,France
[4] Inst. of Modern Physics,PO Box31,LANZHOU,China
[5] Dipart. di Scienze Fisiche,Univ. di NAPOLI,Italy

1-MOTIVATIONS

The production of pions in heavy ion collisions far below the free nucleon nucleon (N-N) threshold is an intriguing problem since a large amount of the available energy of the system has to be concentrated into one degree of freedom. Two types of theories have been proposed to describe the subthreshold pion emission:

- individual nucleon nucleon interaction boosted by the internal motion of the nucleons in the nuclei.
- collective effects such as thermal emission by an excited zone, nuclear bremsstrahlung, etc....

The results of inclusive experiments can be described either by microscopic (N-N collisions) or by statistical models. Hence, to proceed one step further and try to identify the production process, we decided to perform an exclusive experiment, detecting most of the light fragments emitted in coincidence with the pion. In the same experiment we performed also measurements of correlations between light fragments and high energy protons (Ep > 140 Mev) in order to compare the behaviour of the nuclear system when the same energy, but very different linear momenta, are subtracted by different probes[1].

2-EXPERIMENTAL SET-UP

The experimental set up is sketched in figure 1. The pions and high energy protons are detected and identified by a range telescope placed at three successive polar angles : 70°, 90°, 120°. The coincident light fragments are identified by two multidetectors : the `MUR` -plastic wall-(for forward angles) and the `TONNEAU` -plastic barrel- (for large angles). Three systems have been studied : O+Al, O+Ni and O+Au at 94 Mev / nucleon.

3-RESULTS AND INTERPRETATION

The most significative experimental results are:

-1)The observables measured by the multidetectors (multiplicity,velocity and angular distributions) are identical for the pion and high energy proton triggers. These two triggers select rather central interactions [1].

-2)The velocity spectra of particles detected in coincidence with the triggering particle (pion or proton), exhibit two emitting sources : one with a velocity slightly lower than that of the beam, the other with a velocity near that of the center of mass of the system (figure 2).

-3)For the proton trigger,the azimuthal distributions of the coincident particles are not isotropic. They have a maximum located opposite of the trigger telescope, with respect of the beam axis(figure 3).

-4)Both pions and protons are produced in collisions of similar nature as shown in figure 4 where the production rate of pions and protons for different targets are reported as a function of the total energy extracted from the system [7] (*i. e.* the kinetic energy in the proton case, the total energy in the pion case).

All these features can be well explained by a participant spectator scenario .To take into account the role of the intermediate energy corrections (Pauli blocking and one body dissipation) in the participant zone formation, a modified fireball model was developped [3,6,8]. The standard Weisskopf theory is applied to the fireball decay. The modified model predicts that the size of the fireball is smaller than in the geometrical model and does not increase considerably with the target mass[8]. This is in agreement with our data and can be explained by a strong interaction between participant and spectator zones[8]. This in turn is in agreement with the emission times of protons calculated by means of the BNV model[6,8]. This emission time of about 20 fm/c corresponds to covered distances of about 8 fm for a 100 Mev/nucleon ^{16}O ion which are comparable with the size of the interacting system. This means that a strong overlap of the nuclear matter can be expected while the energetic protons are being emitted.

4-CONCLUSION

We conclude that our exclusive data can be reasonably well explained in the frame of the participant spectator model, the pion being statistically emitted by the highly excited participant zone. Of course, this does not rule out a microscopic explanation, but, to our knowledge, no exclusive predictions have been made, up to now, using the nucleon nucleon collisions model.

PUBLICATIONS RELATED TO THIS EXPERIMENT

1)Light fragment emission in heavy ion reactions producing pions in O+Al collisions at 94 Mev/A
S.Aiello et al -Europhys. Lett. 6(1988),25

2)Semi exclusive pion production by heavy ions at energy below 100 Mev/u
A.Badala et al -Nucl. Phys.A482 (1988),511c

3)Light fragment emission correlated with large transverse momentum protons in 94 Mev/u ^{16}O induced reaction
D.Durand et al -Nucl. Phys. A511 (1990),442

4)Evidence of a two source emission for light charged particles in coincidence with pions produced in O+Al collisions at 94 Mev/u
R.Barbera et al -Nucl. Phys. A518 (1990),767

5)Subthreshold production of pions in coincidence with light particles.
R;Barbera et al. -Nucl. Phys. A519(1990)231c

6)Statistical and microscopic description of energetic products in the reactions induced by O on Al, Ni and Au at 94 Mev/u
A.Badala et al - Phys. Rev. C43 (1991),190

7)Energetic particle emission in heavy ion collisions around 100 Mev/u
A.Badala et al - Europhys. Lett. 15(1991),145

8)Proton helium correlation in 94 Mev/u O induced reactions on Al,Ni and Au targets
A.Badala et al - Phys. rev. C in press

Fig 1: experimental set-up

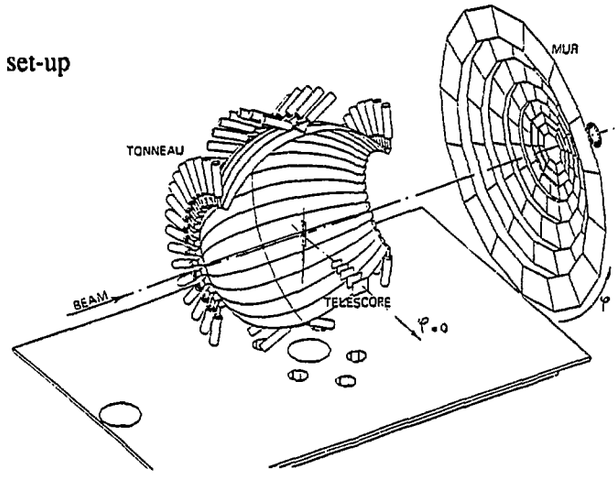

Fig 2 : an example of invariant velocity plot

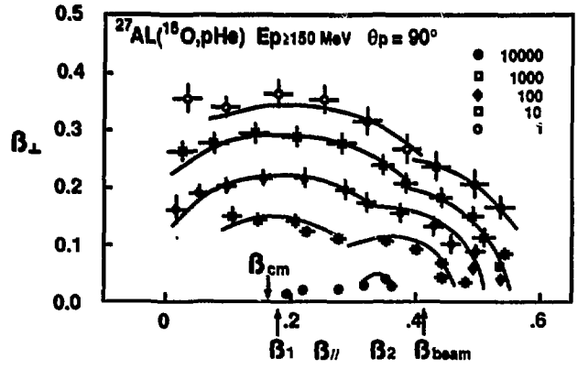

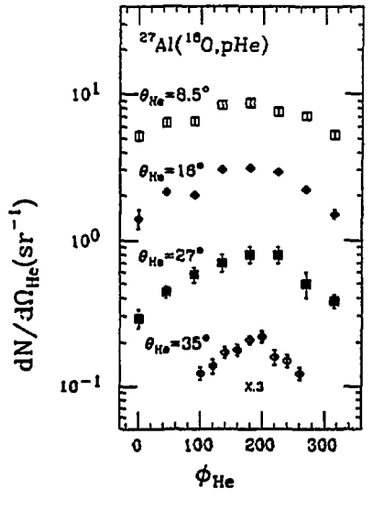

Fig 3 : azimuthal distributions of α particles in coincidence with a high energy proton in O + Al reaction

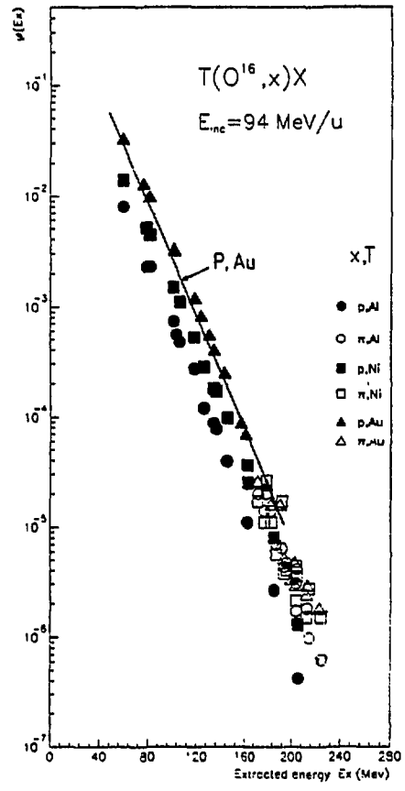

Fig 4 : production rate $\left(\frac{1}{pp^*}\frac{d\sigma}{d\Omega dE}\right)$ for pions(open symbols) and protons(black symbols). The straight line is the prediction of our model for proton production in the O + Au system

Investigation of Subthreshold π^0 Production in $^{129}Xe + ^{197}Au$ at 44 MeV/u[†]

R. Holzmann, R.S. Mayer, W.Henning, R. Simon
GSI, Darmstadt
H. Delagrange, F. Lefèvre, R. Merrouch, W. Mittig, R. Ostendorf, Y. Schutz
GANIL, Caen
F.D. Berg, W. Kühn, V. Metag, R. Novotny, M. Pfeiffer
Universität Gießen
A.L. Boonstra, H. Löhner, L.B. Venena, H.W. Wilschut
KVI, Groningen
D. Ardouin, H. Dabrowski, B. Erazmus, D. Lebrun, L. Sézac
LPN, Nantes
F. Ballester, E. Casal, J. Diaz, J.L. Ferrero, M. Marques, G. Martinez
IFIC, Valencia
H. Nifenecker (ISN, Grenoble), B. Fornal, L. Freindl (INP, Cracow)
Z. Sujkowski (SINS, Swierk), T. Matulewicz (Warsaw University)

1 Motivation

Like hard-photon emission, the production of pions has been shown to be a powerful probe of reaction dynamics in heavy-ion collisions[1,2]. In that respect, particularly subthreshold π^0 production has been extensively studied over the last decade. Indeed, below threshold where pions can only be produced by coupling the Fermi momenta to the momentum of relative motion of the colliding nuclei, the sensitivity to dynamical effects should be highest. While it is generally accepted that at intermediate energies pions are mainly produced in first-chance nucleon-nucleon collisions, collective or cooperative effects might still play a role far below threshold. Furthermore, pions interact strongly with the surrounding nuclear medium, i.e they rescatter and are reabsorbed with a high probability. Knowledge of the final-state interactions is therefore important for any comparison of theory and experiment. In order to address these questions and to extend the available experimental systematics to very heavy collision systems, we have measured neutral-pion production in the reaction $^{129}Xe + ^{197}Au$ at 44 MeV/u.

2 Experiment

We have detected high-energy γ rays in a large array of BaF_2 scintillators (TAPS) set up at SPEG. A total of 247 hexagonal detector modules, clustered in 13 blocks, ranged from 66° to 156° with respect to the beam axis, covering a solid angle $\Omega \simeq 0.30 \cdot 4\pi$. About half of the detectors were TAPS modules, the remaining ones, of somewhat different shapes, were supplied by GSI and ORNL respectively. For this experiment only one of the 13 blocks was equipped with plastic charged-particle veto detectors, the other blocks were shielded with 2 cm thick plexiglass plates. A detailed description of the set-up and the associated electronics can be found in Ref. 3. A 9 mg/cm^2 Au target was irradiated with a 44 MeV/u ^{129}Xe beam of 20-50 enA. Requiring coincidences of at least two high-energy hits in the array, it was possible to trigger selectively on $\gamma - \gamma$ and π^0 events. Scaled-down single hits were also registered for control and normalization purposes.

[†]This report describes part of the Ph.D. work of R.S. Mayer

3 Data analysis

The BaF_2 modules have been energy-calibrated with γ rays from radioactive sources (^{88}Y and AmBe) and with cosmic muons. After correcting the short-gated energy signals for non-linearities, a clean pulse-shape analysis could be performed. The time signals have been corrected for residual walk, for cross-talk effects in the fast electronics and for drifts of the RF reference, yielding finally an average intrinsic resolution of $\simeq$ 700 ps fwhm. Combining the pulse-shape analysis with the time of flight information, it has been possible to identify 'photon only' events with a high degree of selectivity, despite the absence of charged-particle veto detectors on all but one block. The intensive background of events produced by cosmic muons could be strongly reduced by putting cuts on the relative time and on the extension of the electromagnetic shower in the detector blocks. Within each block, the photon energies from adjacent modules have been summed in order to improve the overall response. In a final step, π^0 events have been identified by an invariant-mass analysis, and clean pion spectra could be constructed. In a similar way, from the singles trigger, hard-photon spectra have been generated. The detector efficiency and response functions have been obtained from GEANT simulations.

4 Results

We find an inclusive cross section of 5.4 $\pm$ 0.9 mbarn for the production of high-energy photons with $E_\gamma \geq 30$ MeV, in good agreement with the systematics[2]. From a moving-source analysis we obtain a source velocity of $\beta = 0.147 \pm 0.009$, very close to $\beta_{beam}/2$. A Legendre-polynomial fit to the angular distribution in the half-rapidity frame gives a coefficient $A_2 = -0.12$, corresponding to a maximum at 90°, compatible with dipole radiation. The two latter findings are indeed consistent with the picture describing hard photons as mainly bremsstrahlung produced in individual proton-neutron collisions.

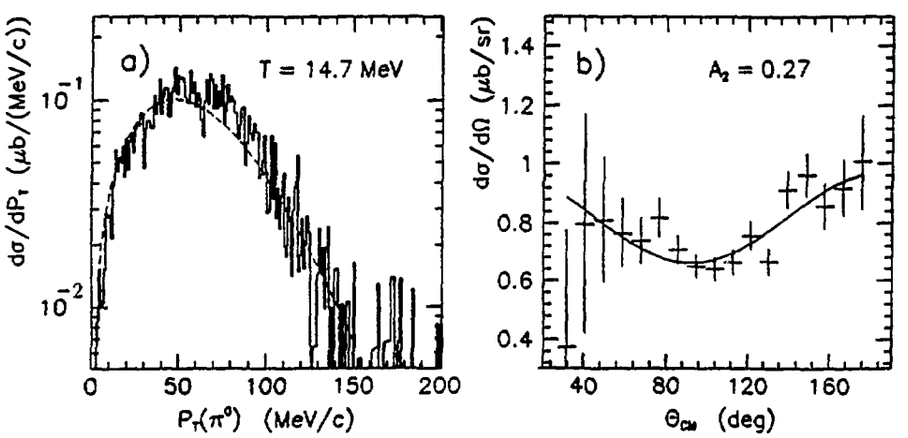

Fig. 1. (a) π^0 response-corrected transverse momentum spectrum. (b) Angular distribution in the nucleon-nucleon center-of-mass frame.

The invariant-mass analysis produces a cross section for inclusive π^0 production of 9.6 ± 1.7 μbarn. The quoted error consists of a 4% statistical and a 17% systematic error, mainly from the beam current normalization. Figure 1. shows a response-corrected π^0 transverse-momentum spectrum and an angular distribution in the nucleon-nucleon CM frame. A fit to the P_T spectrum gives a source temperature of 15 ± 1 MeV, in agreement with an existing systematic study[4]. The yield shows a minimum at 90°, indicative of the p-wave amplitude of pion production via the Δ resonance.

Our pion cross section can be compared to the body of inclusive data available around 44 MeV/u[5,6], extending from $^{12}C+^{12}C$ to $^{86}Kr+^{90}Zr$. Because of the very strong energy dependence of subthreshold pion production, we choose to scale the various data points to a common energy available above the Coulomb barrier[2], namely 40 MeV/u. Also, to the three smallest systems (with $A_{1,2} < 30$) an empirical correction has been applied to compensate for their reduced Fermi momenta. The rescaled cross sections are shown in Fig. 2(a) together with our Xe+Au point as a function of $\sigma_{reac} \cdot N_{NN}$, i.e. the reaction cross section times the impact-parameter averaged number of first-chance nucleon-nucleon collisions. Indeed, in the simplest picture one would expect that σ_{π^0} scales with this product, in analogy to hard-photon production scaling with the number of first-chance proton-neutron collisions[7]. For each system, the average number of participant nucleons has been computed in a Glauber approach[8]. An attempt to fit a straight line to the data (dashed curve in Fig. 2) shows that the expected proportional law does not hold. This deviation from linearity can be attributed to pion reabsorption, which is particularly strong in heavy systems. Only after having corrected the data with an appropriate pion escape factor does the linear scaling hold (solid line in Fig. 2). The escape factors have been calculated in a simple geometrical model[8] in which the pion absorption length is a free parameter. A best fit yields then the energy-averaged value of $\lambda_{abs} = 5.5^{+2.5}_{-1.5}$ fm. This is also apparent from Fig. 2(b) where the average π^0 multiplicity per NN collision nucleon is shown as a function of the mean distance the pions propagate in the nuclear medium before they can escape.

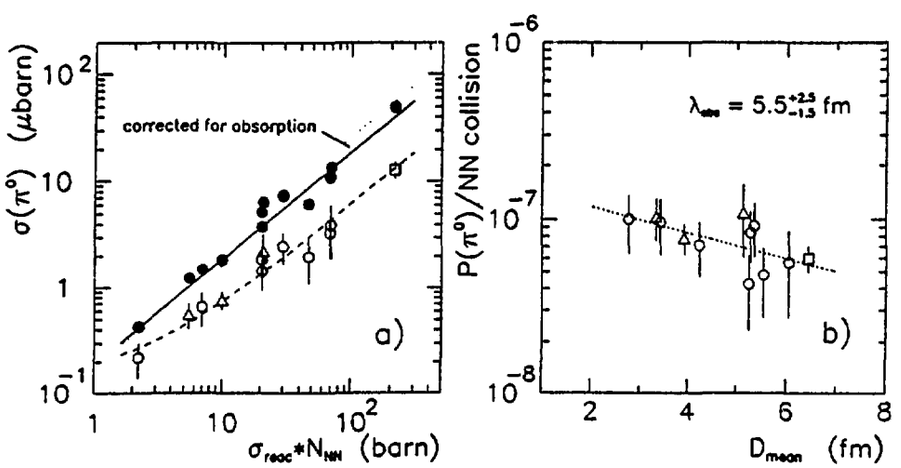

Fig. 2. (a) Systematics of inclusive π^0 cross sections scaled to an energy above the Coulomb barrier of 40 MeV/u (open symbols); the square point is Xe+Au, other data are from Refs. 5 and 6. Solid symbols represent the cross sections corrected for reabsorption (here error bars are omitted for clarity). The curves correspond to fits to the data (see text for details). (b) Inclusive π^0 multiplicity per NN collision vs. the mean distance to the nuclear surface, derived in a geometrical model[8].

Setting gates on the multiplicity of nucleons detected in TAPS, it is possible to achieve a certain degree of exclusivity. The impact-parameter calibration of the multiplicity bins has been deduced from FREESCO calculations done with a realistic experimental filter; the resolution is roughly 30%. In Fig. 3(a) the number of pn collisions, obtained[2] from the measured exclusive hard-photon multiplicities, is displayed vs. the impact parameter. Setting then $N_{NN}(b) \simeq 2 \cdot N_{pn}(b)$, one can extract the impact-parameter dependence of the π^0 multiplicity per nucleon-nucleon collision (Fig. 3(b)). Our data show that pion production is enhanced in central collisions and depleted in peripheral ones, although not completely suppressed.

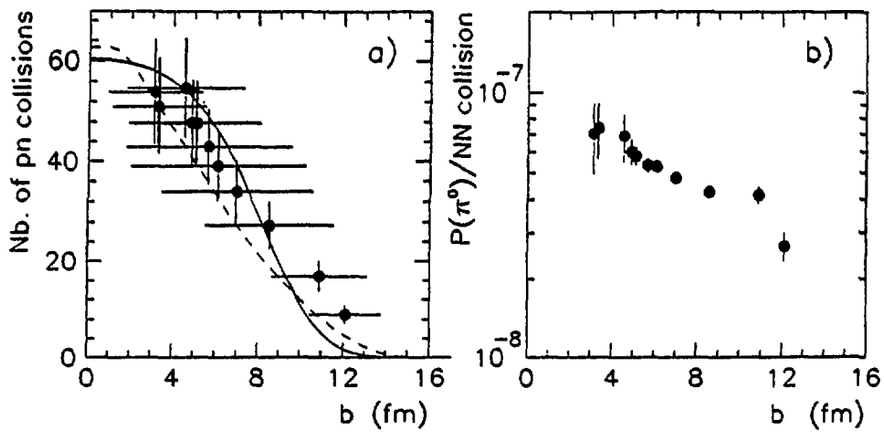

Fig. 3. (a) Measured number of pn collisions vs. impact parameter. The horizontal error bars represent the fwhm of the multiplicity bins. The solid curve is a Glauber calculation, the dashed one is computed with the equal-participant model of Nifenecker and Bondorf[7]. (b) π^0 multiplicity per NN collision vs. impact parameter.

In conclusion, our data support the picture of π^0 and hard-photon production in individual nucleon-nucleon collisions. It also appears that more exclusive experiments are necessary to extend our present knowledge about subthreshold particle production. However, reabsorption plays an important role and has to be investigated in order to obtain a consistent picture. One should finally realize that a more thorough study of final-state interactions could offer a new approach to the pion-nuclear potential.

References

(1) P. Braun-Münzinger and J. Stachel, Ann. Rev. Nucl. Part. Sci. **37** (1987) 1.
(2) W. Cassing, V. Metag, U. Mosel and K. Niita, Phys. Rep. **188** (1990) 365.
(3) R. Merrouch et al., Nouvelles du GANIL, N° 38, April 1991.
(4) T. Suzuki et al., Phys. Lett. **257B** (1991) 27.
(5) E. Grosse, in Proc. Intern. School of Physics Enrico Fermi (Varenna, Italy, 1987).
(6) J. Stachel et al., Phys. Rev. **C33** (1986) 1420.
(7) H. Nifenecker and J.P. Bondorf, Nucl. Phys. **A442** (1985) 478.
(8) W. Cassing, Z. Phys. **A329** (1988) 487.

AUTHOR INDEX

II

PUBLICATION LIST

1989

DIRECT MEASUREMENTS OF TOTAL REACTION CROSS SECTIONS IN THE INTERMEDIATE ENERGY RANGE USING STABLE AND NEUTRON-RICH HEAVY ION PROJECTILES

EL MASRI Y., HANAPPE F., COSTA G., BRUANDET J.F., KOX S., MUELLER A.C., BIMBOT R.
FNRS - BRUXELLES AND UNIV. CATHOLIQUE DE LOUVAIN - LOUVAIN-LA-NEUVE,
FNRS - BRUXELLES AND UNIV. LIBRE DE BRUXELLES, CRN - STRASBOURG, ISN - GRENOBLE,
GANIL - CAEN, IPN - ORSAY
DALLAS
NUCLEAR DYNAMICS AND NUCLEAR DISASSEMBLY

TRANSFER REACTIONS AND SEQUENTIAL DECAYS OF THE PROJECTILE-LIKE FRAGMENTS IN THE 60 MeV/NUCLEON 40 Ar + nat Ag, 197 Au REACTIONS

STECKMEYER J.C., BIZARD G., BROU R., EUDES P., LAVILLE J.L., NATOWITZ J.B., PATRY J.P., TAMAIN B., THIPHAGNE A., DOUBRE H., PEGHAIRE A., PETER J., ROSATO E., ADLOFF J.C., KAMILI A., RUDOLF G., SCHEIBLING F., GUILBAULT F., LEBRUN C., HANAPPE F.
LPC - CAEN, GANIL - CAEN, CRN - STRASBOURG, LSN - NANTES,
FONDS NATIONAL DE LA RECHERCHE SCIENTIFIQUE - BRUXELLES
NUCL. PHYS. A500 (1989) 372.

EXCITATION OF GIANT RESONANCES IN 20 Ne + 90 Zr AND 208 Pb INELASTIC SCATTERING AT 40 MeV/u

SUOMIJARVI T., BEAUMEL D., BLUMENFELD Y., CHOMAZ Ph., FRASCARIA N., GARRON J.P., JACMART J.C., ROYNETTE J.C., BARRETTE J., BERTHIER B., FERNANDEZ B., GASTEBOIS J., ROUSSEL-CHOMAZ P., MITTIG W., KRAUS L., LINCK I.
IPN - ORSAY, CEN - SACLAY, GANIL - CAEN, CRN - STRASBOURG
NUCLEAR PHYSICS A491 (1989) 314

EXCITATION OF GIANT RESONANCES IN HEAVY ION REACTIONS AT INTERMEDIATE ENERGIES

SUOMIJARVI T., BEAUMEL D., BLUMENFELD Y., CHOMAZ PH., FRASCARIA N., GARRON J.P., ROYNETTE J.C., SCARPACI A., BARRETTE J., FERNANDEZ B., GASTEBOIS J., ROUSSEL-CHOMAZ P., MITTIG W.
IPN - ORSAY, CEN SACLAY - GIF SUR YVETTE, GANIL - CAEN
RICERCA SCIENTIFICA ED EDUCAZIONE PERMANENTE 69 (1989) 97.
INTERNATIONAL WINTER MEETING ON NUCLEAR PHYSICS.27
BORMIO (IT)

HEAVY ION CHARGE EXCHANGE REACTIONS TO PROBE THE GIANT ELECTRIC ISOVECTOR MODES IN NUCLEI

BERAT C., BUENERD M., CHAUVIN J., HOSTACHY J.Y., LEBRUN D., MARTIN P., BARRETTE J., BERTHIER B., FERNANDEZ B., MICZAIKA A., MITTIG W., STILIARIS E., VON OERTZEN W., LENSKE H., WOLTER H.H.
ISN - GRENOBLE, CEN - SACLAY, GANIL - CAEN, HMI - BERLIN,
UNIVERSITY OF MUNICH - MUNICH
PHYSICS LETTERS B218, 3 (1989) 299

HEAVY IONS CHARGE EXCHANGE REACTIONS AS A PROBE OF THE ISOVECTOR ELECTRIC NUCLEAR RESPONSE

BERAT C., BUENERD M.
ISN - GRENOBLE
RICERCA SCIENTIFICA ED EDUCAZIONE PERMANENTE 69 (1989) 417.
INTERNATIONAL WINTER MEETING ON NUCLEAR PHYSICS.27

THE ONSET OF MULTIFRAGMENTATION IN THE 40 Ar + 27 Al SYSTEM BETWEEN 25 AND 85 MeV/u

HAGEL K., CUSSOL D., DOUBRE H., JIN G.M., PEGHAIRE A., PETER J., SAINT-LAURENT F., BIZARD G., BROU R., LOUVEL M., PATRY J.P., REGIMBART R., STECKMEYER J.C., TAMAIN B., CASSAGNOU Y., LEGRAIN R., LEBRUN C., ROSATO E., JEONG J.C., LEE S.M., NA GASHIMA Y., NAKAGAWA T., OGIHARA M., KASAGI J., MOTOBAYASHI T., Mc GRATH R.

GANIL - CAEN, LPC - CAEN, DPHN/CEN - SACLAY, L.N.S. - NANTES, DFNSMFA - NAPOLI, INST. OF PHYSICS - TSUKUBA - INST. OF TECHNOLOGY - TOKYO, RIKKYO UNIV. - TOKYO, SUNY - STONY BROOK

RICERCA SCIENTIFICA ED EDUCAZIONE PERMANENTE 69 (1989) 298.

INTERNATIONAL WINTER MEETING ON NUCLEAR PHYSICS.27

BORMIO (IT)

DYNAMICAL ASPECTS OF VIOLENT COLLISIONS IN Ar + Ag REACTIONS AT E/A = 27 MeV

RIVET M.F., BORDERIE B., GREGOIRE C., JOUAN D., REMAUD B.

IPN - ORSAY, GANIL - CAEN, LPN/UA - NANTES

PHYS. LETT. B215 (1988) 55

SPIN ALIGNMENT IN PROJECTILE FRAGMENTATION AT INTERMEDIATE ENERGIES

ASAHI K., ISHIHARA M., TCHIHARA T., FUKUDA M., KUBO T., GONO Y., MUELLER A.C., ANNE R., BAZIN D., GUILLEMAUD-MUELLER D., BIMBOT R., SCHMIDT-OTT W.D., KASAGI J.

RIKEN - SAITAMA, GANIL - CAEN, IPN - ORSAY, UNIV. GOETTINGEN - GOETTINGEN, TOKYO INST. OF TECHNOLOGY - TOKYO

WORLD SCI. (1989) p. 173.

INTERNATIONAL SYMPOSIUM ON HEAVY ION PHYSICS AND NUCLEAR ASTROPHYSICAL PROBLEMS TOKYO

BETA DECAY OF 22 O

HUBERT F., DUFOUR J.P., DEL MORAL R., FLEURY A., JEAN D., PRAVIKOFF M.S., DELAGRANGE H., GEISSEL H., SCHMIDT K.H., HANELT E.

CEN - BORDEAUX-GRADIGNAN, GANIL - CAEN, GSI - DARMSTADT, INST. FUR KERNPHYSIK - DARMSTADT

Z. PHYS. A333 (1989) 237.

BETA DELAYED PROTON DECAY OF 28 S : COMPLETION OF THE MASS-28 ISOSPIN QUINTET

POUGHEON F., BORREL V., JACMART J.C., ANNE R., DETRAZ C., GUILLEMAUD-MUELLER D., MUELLER A.C., BAZIN D., DUFOUR J.P., HUBERT F., PRAVIKOFF M.S., AUDI G., ROECKL E., BROWN B.A.

IPN - ORSAY, GANIL - CAEN, CEN - BORDEAUX-GRADIGNAN, CSNSM - ORSAY, GSI - DARMSTADT, MSU - EAST LANSING

RICERCA SCIENTIFICA ED EDUCAZIONE PERMANENTE 69 (1989) 50.

INTERNATIONAL WINTER MEETING ON NUCLEAR PHYSICS.27

BORMIO (IT)

BETA-DELAYED NEUTRON EMISSION OF THE ISOTOPES 20 C, 40,41,42 P, 43,44 S

LEWITOWICZ M., PENIONZHKEVICH YU.E., ARTUKH A.G., KALININ A.M., KAMANIN V.V., LUKYANOV S.M., NGUYEN HOAI CHAU, MUELLER A.C., GUILLEMAUD-MUELLER D., ANNE R., BAZIN D., DETRAZ C., GUERREAU D., SAINT-LAURENT M.G. BORREL V., JACMART J.C., POUGHEON F., RICHARD A., SCHMIDT-OTT W.D.

JINR - DUBNA, GANIL - CAEN, IPN - ORSAY, PHYSIKALISCHES INSTITUT DER UNIVERSITAT - GOTTINGEN

NUCL. PHYS. A496 (1989) 477.

MEASUREMENTS OF REACTION CROSS SECTION WITH NEUTRON AND PROTON-RICH RADIOACTIVE BEAMS

VILLARI A.C.C., ZHAN WENLONG, MITTIG W., AUDI G., BIANCHI L., CUNSOLO A., FERNANDEZ B., FOTI A., GASTEBOIS J., GILLIBERT A., PLAGNOL E., SCHUTZ Y., STEPHAN C., TASSAN-GOT L.

I.F.U.S.P. AND CNPQ - SAO PAULO, INST. OF MODERN PHYS. - LANZHOU, GANIL - CAEN, UNIV. PARIS-SUD - ORSAY, DPHN SACLAY - GIF SUR YVETTE, I.N.F.N. - CATANIA

RICERCA SCIENTIFICA ED EDUCAZIONE PERMANENTE 69 (1989) 74.

INTERNATIONAL WINTER MEETING ON NUCLEAR PHYSICS.27

BORMIO (IT)

OBSERVATION OF NEW NEUTRON RICH NUCLEI 29 F, 35,36 Mg, 38,39 Al, 40,41 Si, 43,44 P, 45-47 S, 46-49 Cl, AND 49-51 Ar FROM THE INTERACTIONS OF 55 MeV/u 47 Ca + Ta

GUILLEMAUD-MUELLER D., PENIONZHKEVICH Yu.E., ANNE R., ARTUKH A.G., BAZIN D., BORREL V., DETRAZ C., GUERREAU D., GVOZDEV B.A., JACMART J.C., JIANG D.X., KALININ A.M., KAMANIN V.V., KUTNER V.B., LEWITOWICZ M., LUKYANOV S.M., MUELLER A.C., HOAI CHAU N., POUGHEON F., RICHARD A., SAINT-LAURENT M.G., SCHMIDT-OTT W.D.

GANIL - CAEN, JINR - DUBNA, IPN - ORSAY, GOTTINGEN UNIV. - GOTTINGEN

Z. PHYS. A332 (1989) 193.

PRODUCTION AND STUDY OF VERY NEUTRON-RICH NUCLEI BY MEANS OF FRAGMENTATION OF 48 Ca PROJECTILE AT GANIL ENERGIES

GUILLEMAUD-MUELLER D.

IPN - ORSAY

RICERCA SCIENTIFICA ED EDUCAZIONE PERMANENTE.69 (1989) 36.

INTERNATIONAL WINTER MEETING ON NUCLEAR PHYSICS.27

BORMIO (IT)

PROSPECTS FOR THE STUDY OF EXOTIC NUCLEI AT GANIL

DETRAZ C.

GANIL - CAEN

WORLD SCI. (1989) p. 151.

INTERNATIONAL SYSMPOSIUM ON HEAVY ION PHYSICS AND NUCLEAR ASTROPHYSICAL PROBLEMS

TOKYO

SOME PROPERTIES OF THE BETA-DELAYED CHARGED PARTICLE EMISSION OF 39 Ti AND 40 Ti

LEWITOWICZ M., DETRAZ C., ANNE R., BRICAULT P., GUILLEMAUD-MUELLER D., MUELLER A.C., ZHANG Y., DUFOUR J.P., BAZIN D., FLEURY A., HUBERT F., PRAVIKOFF M.S., JACMART J.C., POUGHEON F., RICHARD A.

GANIL - CAEN, CEN - BORDEAUX-GRADIGNAN, IPN - ORSAY

RICERCA SCIENTIFICA ED EDUCAZIONE PERMANENTE 69 (1989) 65.

INTERNATIONAL WINTER MEETING ON NUCLEAR PHYSICS.27

BORMIO (IT)

DISINTEGRATION OF THE NUCLEAR SYSTEM FORMED IN THE 45 MeV/NUCLEON 84 Kr + 159 Tb REACTION

MAJKA Z., SOBOTKA L.G., STRACENER D.W., SARANTITES D.G., AUGER G., PLAGNOL E., SCHUTZ Y., DAYRAS R., WIELECZKI J.P., BARRETO J., NORBECK E.

WASHINGTON UNIV. - SAINT LOUIS, GANIL - CAEN, CEN - SACLAY, IPN - ORSAY, IOWA UNIV. - IOWA

DALLAS

NUCLEAR DYNAMICS AND NUCLEAR DISASSEMBLY

HOT NUCLEI STUDIED WITH A 4 PI-NEUTRON DETECTOR

GALIN J., CHARVET J.L., CRAMER B., CREMA E., DOUBRE H., FREHAUT J., GATTY B., GUERREAU D., INGOLD G., JACQUET D., JAHNKE U., JIANG D.X., LOTT B., MAGNAGO C., MORJEAN M., PATIN Y., PIASECKI E., POUTHAS J., SAINT-LAURENT F., SCHWINN E., SOKOLOV A., WANG X.D.

GANIL - CAEN, CEN - BRUYERES LE CHATEL, IPN - ORSAY, HMI - BERLIN, CRN - STRASBOURG

DALLAS

NUCLEAR DYNAMICS AND DISASSEMBLY

HOT NUCLEI : BINARY FISSION AND INTERMEDIATE MASS FRAGMENTS PRODUCTION
CASSAGNOU Y., CONJEAUD M., DAYRAS R., HARAR S., KLOTZ-ENGMANN G., LEGRAIN R., LIPS V., OESCHLER H., POLLACO E.C., VOLANT C.
CEN - SACLAY, GANIL - CAEN, INST. FUR KERNPHYSIK - DARMSTADT
DALLAS
NUCLEAR DYNAMICS AND NUCLEAR DISASSEMBLY

NUCLEAR MATTER FLOW IN THE Kr+Au COLLISIONS AT 43 MEV/U
BOUGAULT R., DELAUNAY F., GENOUX-LUBAIN A., LE BRUN C., LECOLLEY J.F., LEFEBVRES F., LOUVEL M., STECKMEYER J.C., ADLOFF J.C., BILWES B., BILWES R., GLASER M., RUDOLF G., SCHEIBLING F., STUTTGE L., FERRERO J.L.
LPC/ISMRA - CAEN, CRN - STRASBOURG, UNIVERSIDAD DE VALENCIA
DALLAS
NUCLEAR DYNAMICS AND NUCLEAR DISASSEMBLY

SATURATION OF THE THERMAL ENERGY DEPOSITED IN Au AND Th NUCLEI BY Ar PROJECTILES BETWEEN 27 AND 77 MeV/u
JIANG D.X., DOUBRE H., GALIN J., GUERREAU D., PIASECKI E., POUTHAS J., SOKOLOB A., CRAMER B., INGOLD G., JAHNKE U., SCHWINN E., CHARVET J.L., FREHAUT J., LOTT B., MAGNAGO C., MORJEAN M., PATIN Y., PRANAL Y., UZUREAU J.L., GATTY B., JACQUET D.
GANIL - CAEN, HMI - BERLIN, CEN - BRUYERES-LE-CHATEL, IPN - ORSAY
NUCL. PHYS. A503 (1989) 560.

SEARCH FOR NUCLEAR DISASSEMBLY IN THE Ne+Ag AND Ne+Au SYSTEMS AT 60 MeV/u
BIZARD G., CASSAGNOU Y., DAYRAS R., DELAGRANGE H., LEGRAIN R., LOUVEL M., MOTOBAYASHI S., PEGHAIRE A., PETER J., POLLACCO E.C., ROSATO E., SAINT-LAURENT F., VOLANT C., WIELECZKO J.P.
LPC - CAEN, CEN - SACLAY, GANIL - CAEN, INFN - NAPOLI
DALLAS
NUCLEAR DYNAMICS AND NUCLEAR DISASSEMBLY

THE ROLE OF TIME IN THE DAMPING OF SOME FINAL STATE INTERACTIONS IN TWO-PARTICLE CORRELATIONS
QUEBERT J., BOISGARD R., LAUTRIDOU P., ARDOUIN D., DURAND D., GOUJDAMI D., GUILBAULT F., LEBRUN C., TAMISIER R., PEGHAIRE A., SAINT-LAURENT F.
CEN - BORDEAUX-GRADIGNAN, LPN - NANTES, GANIL - CAEN
DALLAS
NUCLEAR DYNAMICS AND NUCLEAR DISASSEMBLY

TRANSITION FROM COLLECTIVE TO PARTICIPANT-SPECTATOR MECHANISMS IN THE REACTION Kr + Au AT 44 MeV/u
RUDOLF G., ADLOFF J.C., BILWES B., BILWES R., GLASER M., SCHEIBLING F., STUTTGE L., BIZARD G., BOUGAULT R., BROU R., DELAUNAY F., GENOUX-LUBAIN A., LEBRUN C., LECOLLEY J.F., LEFEBVRES F., LOUVEL M., STECKMEYER J.C., FERRERO J.L., CASSAGNOU Y., LEGRAIN R., GUILBAULT F., LEBRUN C., RASTEGAR B., JIN G.M., PEGHAIRE A., PETER J., ROSATO E.
CRN - STRASBOURG, LPC - CAEN, IFIC - VALENCIA, DPHN/BE - SACLAY, LSN - NANTES, GANIL - CAEN
DALLAS
NUCLEAR DYNAMICS AND NUCLEAR DISASSEMBLY

CORRELATIONS BETWEEN PROJECTILELIKE AND TARGETLIKE FRAGMENTS IN THE REACTION 27 Al + 44-MeV/NUCLEON 40 Ar
DAYRAS R., CONIGLIONE R., BARRETTE J., BERTHIER B., de CASTRO RIZZO D.M., CISSE O., GADI F., LEGRAIN R., MERMAZ M.C., DELAGRANGE H., MITTIG W., HEUSCH B., LANZANO G., PAGANO A.
CEN - SACLAY, GANIL - CAEN, CRN - STRASBOURG,
ISTITUTO NAZIONALE DI FISICA NUCLEARE - CATANIA
PHYS. REV. LETT. 62 (1989) 1017.

INCOMPLETE FUSION IN NUCLEUS-NUCLEUS CENTRAL COLLISIONS. STUDY OF 40 Ar ON 27 Al FROM 25 TO 85 MeV/u
HAGEL K., PEGHAIRE A., JIN G.M., CUSSOL D., DOUBRE H., PETER J., SAINT-LAURENT F., BIZARD G., BROU R., LOUVEL M., PATRY J.P., REGIMBART R., STECKMEYER J.C., TAMAIN B., CASSAGNOU Y., LEGRAIN R., LEBRUN C., ROSATO E., MACGRATH R., JEONG S.C., LEE S.M., NAGASHIMA Y., NAKAGAWA T., OGIHARA M., KASAGI J., MOTOBAYASHI T.
GANIL-CAEN, TEXAS A&M UNIV.-COLLEGE STATION, LPC-CAEN, CEN-SACLAY, LPN-NANTES, DIPARTIMENTO DI SCIENZE FISICHE-NAPLES, SUNY-STONY BROOK, TSUKUBA UNIV.-IBARAKI-KEN, TOKYO INST.TECH.-TOKYO, RIKKYO UNIV.-TOKYO, INST.MOD.PHYS.-LANZHOU
PHYS. LETT. B229 (1989) 20.

SEARCH FOR CHARACTERISTIC TIMES GOVERNING THE EMISSION OF TWO PARTICLES FROM AN EXCITED NUCLEUS
QUEBERT J., LAUTRIDOU P., LEBRUN C., GUILBAULT F., GOUJDAMI D., DURAND D., ARDOUIN D., PEGHAIRE A., SAINT-LAURENT F.
CEN - BORDEAUX-GRADIGNAN, LPN - NANTES, GANIL - CAEN
RICERCA SCIENTIFICA ED EDUCAZIONE PERMANENTE 69 (1989) 220.
INTERNATIONAL WINTER MEETING ON NUCLEAR PHYSICS.27
BORMIO (IT)

TIMESCALE OF PARTICLE EMISSION USING NUCLEAR INTERFEROMETRY
ARDOUIN D., LAUTRIDOU P., DURAND D., GOUJDAMI D., GUILBAULT F., LEBRUN C., PEGHAIRE A., QUEBERT J., SAINT-LAURENT F.
LPN - NANTES, CEN - BORDEAUX-GRADIGNAN, GANIL - CAEN
NUCL. PHYS. A495 (1989) 57c.
INTERNATIONAL WORKSHOP ON NUCLEAR DYNAMICS AT MEDIUM AND HIGH ENERGIES
BAD HONNEF

TOTAL CROSS SECTIONS OF REACTIONS INDUCED BY NEUTRON-RICH LIGHT NUCLEI
SAINT-LAURENT M.G., ANNE R., BAZIN D., GUILLEMAUD-MUELLER D., JAHNKE U., JIN GEN MING, MUELLER A.C., BRUANDET J.F., GLASSER F., KOX S., LIATARD E., TSAN UNG CHAN, COSTA G.J., HEITZ C., EL-MASRI Y., HANAPPE F., BIMBOT R., ARNOLD E., NEUGART R.
GANIL - CAEN, ISN - GRENOBLE, CRN - STRASBOURG,
FONDS NAT. RECH.SCI. - BRUXELLES AND UCL/ULB - LOUVAIN-LA-NEUVE, IPN - ORSAY,
MAINZ UNIV. - MAINZ
Z. PHYS. A332 (1989) 457.

CHARGED PION RATIO IN HEAVY ION REACTIONS AT 93 MeV/n
LEBRUN D., CHAUVIN J., REBREYEND D., PERRIN G., DE SAINTIGNON P., MARTIN P., BUENERD M., LEBRUN C., LECOLLEY J.F., CASSAGNOU Y., JULIEN J., LEGRAIN R.
ISN - GRENOBLE, LPC - CAEN, CEN - SACLAY
RICERCA SCIENTIFICA ED EDUCAZIONE PERMANENTE 69 (1989) 141.
INTERNATIONAL WINTER MEETING ON NUCLEAR PHYSICS.27
BORMIO (IT)

HEAVY ION COLLISION GEOMETRY AT 93 MeV/u FROM PI-/PI+ MEASUREMENT
LEBRUN D., CHAUVIN J., REBREYEND D., PERRIN G., DE SAINTIGNON P., MARTIN P., BUENERD M., LE BRUN C., LECOLLEY J.F., CASSAGNOU Y., JULIEN J., LEGRAIN R.
ISN - GRENOBLE, LPC - CAEN, DPHN/CEN SACLAY - GIF SUR YVETTE
PHYS. LETT. B223 (1989) 139.

IMPACT PARAMETER DEPENDENCE OF HIGH-ENERGY GAMMA-RAY PRODUCTION IN ARGON INDUCED REACTION AT 85 MeV/NUCLEON
KWATO NJOCK M., MAUREL M., MONNAND E., NIFENECKER H., PERRIN P., PINSTON J.A., SCHUSSLER F., SCHUTZ Y.
CEN - GRENOBLE, ISN - GRENOBLE, GANIL - CAEN
NUCL. PHYS. A489 (1988) 368

I - INSTRUMENTATION

A NE213 LIQUID SCINTILLATOR, NEUTRON DETECTOR DESIGNED FOR LIFETIME MEASUREMENTS OF VERY NEUTRON-RICH NUCLEI
BAZIN D., MUELLER A.C., SCHMIDT-OTT W.D.
GANIL - CAEN, UNIVERSITAT GOTTINGEN - GOTTINGEN
NIM A281 (1989) 117.

A TEST OF NEW POSITION SENSITIVE DETECTORS FOR SPEG
VILLARI A.C.C., MITTIG W., BLUMENFELD Y., GILLIBERT A., GANGNANT P., GARREAU L.
INST. DE FISICA DA UNIV. DE SAO PAULO - SAO PAULO, GANIL - CAEN, IPN - ORSAY, CEN SACLAY - GIF SUR YVETTE
NIM A281 (1989) 240.

SEMI-EMPIRICAL FORMULAE FOR HEAVY ION STOPPING POWERS IN SOLIDS IN THE INTERMEDIATE ENERGY RANGE
HUBERT F., BIMBOT R., GAUVIN H.
CEN - BORDEAUX-GRADIGNAN, IPN - ORSAY
NIM B36 (1989) 357.

T - THEORIE

COMPRESSIONAL EFFECTS IN HEAVY ION COLLISIONS. SPINODAL DECOMPOSITION AND THERMAL ENERGY SATURATION
SURAUD E., PI M., SCHUCK P., REMAUD B., SEBILLE F., GREGOIRE C., SAINT-LAURENT F.
ISN - GRENOBLE, LPN - NANTES, GANIL - CAEN
PHYSICS LETTERS B229 (1989) 359.

DETERMINATION OF NUCLEAR PROPERTIES BELOW NORMAL DENSITY FROM THE MULTIFRAGMENTATION PATTERN
SNEPPEN K., CUSSOL D., GREGOIRE C.
NIELS BOHR INST. - COPENHAGEN, GANIL - CAEN
PHYS. LETT. B220 (1989) 342.

DYNAMICAL INSTABILITIES IN HOT EXPANDING NUCLEAR SYSTEMS : A MICROSCOPIC APPROACH TO THE UNDERSTANDING OF MULTIGRAGMENTATION
SURAUD E.
GANIL - CAEN
DALLAS
NUCLEAR DYNAMICS AND NUCLEAR DISASSEMBLY

EXPLOSIONS IN LANDAU VLASOV DYNAMICS
SURAUD E., CUSSOL D., GREGOIRE CH., BOILLEY D., PI M., SCHUCK P., REMAUD B., SEBILLE F.
KERNFYSISCH VERNELLER INST. - GRONINGEN, GANIL - CAEN, ISN - GRENOBLE, NANTES UNIV. - NANTES
NUCL. PHYS. A495 (1989) 73c.
INTERNATIONAL WORKSHOP ON NUCLEAR DYNAMICS AT MEDIUM AND HIGH ENERGIES
BAD HONNEF

NUCLEAR DYNAMICS WITH THE (FINITE-RANGE) GOGNY FORCE : FLOW EFFECTS
SEBILLE F., ROYER G., GREGOIRE C., REMAUD B., SCHUCK P.
LSN - NANTES, GANIL - CAEN, IRESTE - NANTES, ISN - GRENOBLE
NUCL. PHYS. A501 (1989) 137.

THE BUU EQUATION AND FLUCTUATIONS
AYIK S., GREGOIRE C.
TENNESSEE TECHNOLOGICAL UNIVERSITY - COOKEVILLE AND ORNL - OAK RIDGE, GANIL - CAEN DALLAS
NUCLEAR DYNAMICS AND NUCLEAR DISASSEMBLY

THEORETICAL DESCRIPTION OF MULTIGRAGMENTATION BY CONNECTING LANDAU-VLASOV CALCULATIONS WITH THE COPENHAGEN STATISTICAL MULTIGRAGMENTATION MODEL
CUSSOL D., SNEPPEN K., GREGOIRE C., SURAUD E., REMAUD B., SEBILLE F.
GANIL - CAEN, NIELS BOHR INST. - BLEGDAMSVEJ, SUNY - STONY BROOK, NANTES UNIV. - NANTES
RICERCA SCIENTIFICA ED EDUCAZIONE PERMANENTE
INTERNATIONAL WINTER MEETING ON NUCLEAR PHYSICS.27
BORMIO (IT)

1990

COMPOUND AND PRECOMPOUND EFFECTS IN PHOTON DECAY OF THE GIANT DIPOLE RESONANCE

BEENE J.R., BERTRAND F.E., HOREN D.J., LISANTTI J.L., HALBERT M.L., HENSLEY D.C., MITTIG W., SCHUTZ Y., BARRETTE J., ALAMANOS N., AUGER F., FERNANDEZ B., GILLIBERT A., HAAS B., VIVIEN J.P., NATHAN A.M.

OAK RIDGE NAT. LAB. - OAK RIDGE, GANIL - CAEN, CEN - SACLAY, CRN - STRASBOURG, UNIV. OF ILLINOIS - CHAMPAIGN

PHYS. REV. C41, 4 (1990) 1332.

CORRELATIONS BETWEEN PROJECTILE-LIKE AND TARGET-LIKE FRAGMENTS IN THE REACTION 40 Ar + nat Ag AT 60 MEV/NUCLEON

CHARVET J.L., GADI F., BARRETTE J., DAYRAS R., FAURE B., LEGRAIN R., POLLACCO E.C., WIELECZKO J.P., LANZANO G., PAGANO A., DELAGRANGE H., HEUSCH B.

DPHN/CEN SACLAY, INFN - CATANIA, GANIL - CAEN, CRN - STRASBOURG

RICERCA SCIENTIFICA ED EDUCAZIONE PERMANENTE 78 (1990) 351.

INTERNATIONAL WINTER MEETING ON NUCLEAR PHYSICS.18

BORMIO (IT)

EXCITATION OF GIANT RESONANCES IN HEAVY-ION REACTIONS AT INTERMEDIATE ENERGIES - RESULTS FROM THE 40 Ar + 90 Zr AND 208 Pb EXPERIMENTS AT 41 MeV/u

SUOMIJARVI T., BEAUMEL D., BLUMENFELD Y., CHOMAZ PH., FRASCARIA N., GARRON J.P., ROYNETTE J.C., SCARPACI J.A., BARRETTE J., FERNANDEZ B., GASTEBOIS J., MITTIG W.

IPN - ORSAY, CEN - SACLAY, GANIL - CAEN

NUCL. PHYS. A509 (1990) 369.

GLOBAL FEATURES OF INTERMEDIATE MASS FRAGMENT CROSS SECTIONS IN Ne INDUCED INTERACTIONS

PAPADAKIS N.H., VODINAS N.P., CASSAGNOU Y., DAYRAS R., FONTE R., IMME G., LEGRAIN R., PANAGIOTOU A.D., POLLACCO E.G., RACITI G., RODRIGUEZ L., SAINT-LAURENT F., SAINT-LAURENT M.G., SAUNIER N.

UNIV. OF ATHENS - ATHENS, CEN - SACLAY, INFN - CATANIA, GANIL - CAEN

PHYS. LETT. B240, 3,4 (1990) 317.

HEAVY-ION COULOMB EXCITATION AND PHOTON DECAY OF THE GIANT DIPOLE RESONANCE IN 208 Pb

BEENE J.R., BERTRAND F.E., HOREN D.J., AUBLE R.L., BURKS B.L., GOMEZ DEL CAMPO J., HALBERT M.L., SAYER R.O., MITTIG W., SCHUTZ Y., BARRETTE J., ALAMANOS N., AUGER F., FERNANDEZ B., GILLIBERT A., HAAS B., VIVIEN J.P.

OAK RIDGE NAT. LAB. - OAK RIDGE, GANIL - CAEN, CEN - SACLAY, CRN - STRASBOURG

PHYS. REV. C41 (1990) 920.

STOPPING POWERS OF SOLIDS FOR 84,86 Kr? 100 Mo AND 129,132 Xe IONS AT INTERMEDIATE ENERGIES (20-45 MeV/u) AND THE CHARGE STATE DISTRIBUTIONS AT EQUILIBRIUM

GAUVIN H., BIMBOT R., HERAULT J., KUBICA B., ANNE R., BASTIN G., HUBERT F.

INP - ORSAY, GANIL - CAEN, CSNSM - ORSAY, CENBG - GRADIGNAN

NIM B47, 4 (1990) 339.

STUDY OF GIANT RESONANCES AND HIGH EXCITATION ENERGY STRUCTURES WITH COINCIDENT LIGHT CHARGED PARTICLES

ROYNETTE J.C., SCARPACI J.A., BLUMENFELD Y., CHOMAZ PH., FRASCARIA N., GARRON J.P., SUOMIJARVI T., ALAMANOS N., FERNANDEZ B., GILLIBERT A., VAN DER WOUDE A., LEPINE A.

IPN - ORSAY, DPHN/CEN SACLAY, KVI GRONINGEN, SAO PAULO

RICERCA SCIENTIFICA ED EDUCAZIONE PERMANENTE 78 (1990) 421.

INTERNATIONAL WINTER MEETING ON NUCLEAR PHYSICS.18

BORMIO (IT)

CHANGES IN TARGET FRAGMENTATION MECHANISMS WITH INCREASING PROJECTILE ENERGY IN INTERMEDIATE ENERGY NUCLEAR COLLISIONS
LOVELAND W., ALEKLETT K., SIHVER L., XU Z., CASEY C., MORRISSEY D.J., LILJENZIN J.O., de SAINT-SIMON M., SEABORG G.T.
OREGON STATE UNIV. - CORVALLIS, STUDSVIK NEUTRON RES. LAB. - NYKOPING, OREGON STATE UNIV. - CORVALLIS, NSCL/MSU - EAST LANSING, UNIV. OF OSLO - OSLO, LAB. RENE BERNAS - ORSAY, LBL - BERKELEY
PHYS. REV. LETT. 41 (1990) 973.

MEASUREMENTS OF TIME DELAYS FOR PROJECTILE-LIKE FRAGMENTS IN THE REACTION 40 Ar + Ge AT 44 MeV/NUCLEON
GOMEZ DEL CAMPO J., BARRETTE J., DAYRAS R.A., WIELECZKO J.P., POLLACCO E.C., SAINT-LAURENT F., TOULEMONDE M., NESKOVIC N., OSTOJIC R.
OAK RIDGE NAT. LAB. - OAK RIDGE, CEN - SACLAY, GANIL - CAEN, CIRIL - CAEN, BORIS KIDRIC INST. OF NUCL. SCI. - BELGRADE
PHYS. REV. C41 (1990) 139.

STRONG IMPACT PARAMETER DEPENDENCE OF PRE-EQUILIBRIUM PARTICLE EMISSION IN NUCLEUS-NUCLEUS REACTIONS AT INTERMEDIATE ENERGIES
PETER J., SULLIVAN J.P., CUSSOL D., BIZARD G., BROU R., LOUVEL M., PATRY J.P., REGIMBART R., STECKMEYER J.C., TAMAIN B., CREMA E., DOUBRE H., HAGEL K., JIN G.M., PEGHAIRE A., SAINT-LAURENT F., CASSAGNOU Y., LEGRAIN R., LEBRUN C., ROSATO E., MACGRATH R., JEONG S.C., LEE S.M., NAGASHIMA Y., NAKAGAWA T., OGIHARA M., KASAGI J., MOTOBAYASHI T.
LPC - CAEN, GANIL - CAEN, INST. OF MODERN PHYS. - LANZHOU, CEN - SACLAY, LPN - NANTES, UNIV. DI NAPOLI - NAPLES, SUNY - STONY BROOK, UNIV. OF TSUKUBA - IBARAKI-KEN, TOKYO INST. OF TECH. - TOKYO, RIKKYO UNIV. - TOKYO
PHYS. LETT. 237 (1990) 187.

TIME-SCALE ANALYSIS OF EVENTS WITH THREE HEAVY FRAGMENTS IN THE 22 Ne + Au COLLISIONS AT 60 MeV/u
BOUGAULT R., COLIN J., DELAUNAY F., GENOUX-LUBAIN A., HAJFANI A., LE BRUN C., LECOLLEY J.F., LOUVEL M., STECKMEYER J.C.
LPC - CAEN
PHYS. LETT. B232 (1989) 291.

TWO-PARTICLE CORRELATIONS AS A PROBE FOR COLLISION DYNAMICS
BASRAK Z., BOISGARD R., CARJAN N., DABROWSKI H., ERAZMUS B., EUDES P., GOUJDAMI D., GUILBAULT F., LAUTRIDOU P., LEBRUN C., PEGHAIRE A., QUEBERT J., SEBILLE F., REMAUD B., SCHUCK P.
CENB - GRADIGNAN, LPN - NANTES, GANIL - CAEN, ISN - GRENOBLE
IN2P3-RIKEN SYMPOSIUM ON HEAVY-ION COLLISIONS
OBERNAI (FR)

EXOTIC LIGHT NUCLEI
DETRAZ C., VIEIRA D.J.
GANIL - CAEN, LANL - LOS ALAMOS
ANNUAL REVIEW OF NUCLEAR AND PARTICLE SCIENCE
ANNUAL REVIEW OF NUCLEAR AND PARTICLE SCIENCE.39

FIRST OBSERVATION OF THE NEUTRON-RICH NUCLEI 42 Si, 45,46 P, 48 S, AND 51 Cl FROM THE INTERACTION OF 44 MeV/u 48 Ca + 64 Ni
LEWITOWICZ M., ANNE R., ARTUKH A.G., BAZIN D., BELOZYOROV A.V., BRICAULT P., DÆTRAZ C., GUILLEMAUD-MUELLER D., JACMART J.C., KASHY E., LATIMIER A., LUKYANOV S.M., MUELLER A.C., PENIONZHKEVICH YU.E., POUGHEON F., RICHARD A., SCHMIDT-OTT W.D., ZHANG Y.
GANIL - CAEN, JINR - DUBNA, CEN - BORDEAUX-GRADIGNAN, IPN - ORSAY, GOTTINGEN UNIVERSITAT - GOTTINGEN, MSU - EAST LANSING
Z. FUR PHYSIK A335 (1990) 117.

MEASUREMENT AND QRPA CALCULATION OF THE BETA-DELAYED NEUTRON EMISSION OF 21,22 N AND 23,24 O

MUELLER A.C., GUILLEMAUD-MUELLER D., JACMART J.C., KASHY E., POUGHEON F., RICHARD A., STAUDT A., KLAPDOR-KLEINGROTHAUS H.V., LEWITOWICZ M., ANNE R., BRICAULT P., DETRAZ C., PENIONZHKEVICH YU.E., ARTUKH A.G., BELOZYOROV A.V., LUKYANOV S.M., BAZIN D., SCHMIDT-OTT W.D.

IPN - ORSAY, MAX-PLANCK-INST.FUR KERNPHYSIK - HEIDELBERG, GANIL - CAEN, JINR - DUBNA, CENBG - GRADIGNAN, UNIV. GOTTINGEN - GOTTINGEN

NUCL. PHYS. A513 (1990) 1.

PARTICLE STABILITY OF THE ISOTOPES 26 O AND 32 Ne IN THE REACTION 44 MeV/NUCLEON 48 Ca + Ta

GUILLEMAUD-MUELLER D., JACMART J.C., KASHY E., LATIMIER A., MUELLER A.C., POUGHEON F., RICHARD A., PENIONZHKEVICH Yu.E., ARTUHK A.G., BELOZYOROV A.V., LUKYANOV S.M., ANNE R., BRICAULT P., DETRAZ C., LEWITOWICZ M., ZHANG Y., LYUTOSTANSKY Yu.
S., ZVEREV M.V., BAZIN D., SCHMIDT-OTT W.D.

IPN - ORSAY, JINR - DUBNA, GANIL - CAEN, MOSCOW PHYS. ENGENEER. INST. - MOSCOW, CEN BORDEAUX - GRADIGNAN, UNIVER. GOTTINGEN - GOTTINGEN

PHYS. REV. C41 (1990) 937.

ZERO DEGREE MEASUREMENTS OF ISOTOPIC DISTRIBUTIONS IN 44 MeV/u 86 Kr-INDUCED REACTIONS FOR THE PRODUCTION OF NUCLEI FAR FROM STABILITY

BAZIN D., GUERREAU D., ANNE R., GUILLEMAUD-MUELLER D., MUELLER A.C., SAINT-LAURENT M.G.

GANIL - CAEN, CENBG - GRADIGNAN, IPN - ORSAY

NUCL. PHYS. A515 (1990) 349.

90 33 C

A STUDY OF DISSIPATIVE PHENOMENA USING ORION, A 4 PI SECTORIZED NEUTRON DETECTOR

GALIN J., WANG X.M., CREMA E., GUERREAU D., JIANG D.X., MORJEAN M., POUTHAS J., SAINT-LAURENT F., SOKOLOV A., GATTY B., JACQUET D., LOTT B., JAHNKE U., SCHWINN E., PIASECKI E., CHARVET J.L.

GANIL - CAEN, IPN - ORSAY, CRN - STRASBOURG, HMI - BERLIN, WARSAW UNIV. - WARZAWA, CEN - BRUYERES-LE-CHATEL

IN2P3-RIKEN SYMPOSIUM ON HEAVY-ION COLLISIONS.2

OBERNAI (FR)

A STUDY OF THE DECAY MODES OF HOT SYSTEMS FORMED IN THE Ar + Au AND Ar + Th REACTIONS

LOTT B., CHARVET J.L., CRAMER B., DOUBRE H., FREHAUT J., GALIN J., GATTY B., GUERREAU D., INGOLD G., JACQUET D., JAHNKE U., JIANG D.X., MAGNAGO C., MORJEAN M., PATIN Y., PIASECKI E., POUTHAS J., SCHWINN E., SOKOLOV A.

CRN - STRASBOURG, CEN - BRUYERES LE CHATEL, HMI - BERLIN, GANIL - CAEN, IPN - ORSAY, WARSAW UNIV. - WARSZAWA

RICERCA SCIENTIFICA ED EDUCAZIONE PERMANENTE 78 (1990) 292.

INTERNATIONAL WINTER MEETING ON NUCLEAR PHYSICS.18

BORMIO (IT)

DEVIATIONS FROM PURE TARGET FRAGMENTATION IN 94 A MeV 16 O INDUCED HEAVY ION REACTIONS

GUSTAFSSON H.A., JAKOBSSON B., KRISTIANSSON A., OSKARSSON A., WESTENIUS M., ARVE P., HELGESSON J.W., WESTERBERG L., ALEKLETT K., KORDYASZ A.J., LAVERGNE-GOSSELIN L., STAB L.

UNIV. OF LUND - LUND, LUND INST. OF TECHNOLOGY - LUND, UNIV. OF UPPSALA - UPPSALA, STUDSVIK NEUTRON RES. LAB. - NYKOPING, UNIV. OF WARSAW - WARSAW, IPN - ORSAY

PHYS. LETT. B241 (1990) 322.

DYNAMICS AND THERMALIZATION IN VIOLENT COLLISIONS AROUND 30 MeV/u
BORDERIE B., JOUAN D., RIVET M.F., CABOT C., FUCHS H., GARDES D., GAUVIN H., JACQUET D., MONNET F., MONTOYA M.
IPN - ORSAY
IN2P3-RIKEN SYMPOSIUM ON HEAVY-ION COLLISIONS
OBERNAI (FR)

HEAVY RESIDUE LINEAR MOMENTA IN INTERMEDIATE ENERGY KRYPTON-GOLD COLLISIONS
ALEKLETT K., LOVELAND W., DE SAINT-SIMON M., SIHVER L., LILJENZIN J.O., SEABORG G.T.
STUDSVIL NEUTRON RES. LAB. - NYKOPING, OREGON STATE UNIV. - CORVALLIS, LAB. RENE BERNAS - ORSAY, CHALMERS UNIV. OF TECH. - GOTEBORG, LBL - BERKELEY
PHYS. LETT. 236 (1990) 404.

LIGHT FRAGMENT EMISSION CORRELATED WITH LARGE TRANSVERSE MOMENTUM PROTONS IN 94 MeV/u 16 O INDUCED REACTIONS
DURAND D., LAVILLE J.L., BIZARD G., BOUGAULT R., GENOUX-LUBAIN A., LEFEBVRES F., PATRY J.P., BADALA A., BARBERA R., PALMERI A., PAPPALARDO G.S., SCHILLACI A., JIN G.M., ROSATO E.
LPC - CAEN, ISTITUTO NAZIONALE DI FISICA NUCLEARE - CATANIA, GANIL - CAEN, INFN - NAPOLI
NUCL. PHYS. A511 (1990) 442.

MULTI-FRAGMENT EVENTS IN THE Ar + Au SYSTEM AT 30 AND 60 MeV/u
BADALA A.,BIZARD G.,BOUGAULT R.,BROU R.,DELAGRANGE H.,DOUBRE H.,DURAND D., EL MASRI Y.,FUGIWARA H.,GENOUX-LUBAIN A.,HAGEL K.,HAJFANI A.,HANAPPE F.,JEONG S.C., JIN G.,KATO S.,KERAMBRUN A.,KUGO H.,LAVILLE J.L.,LE BRUN C.,LECOLLEY J.F.,LEE S.M., LOUVEL M.,MATRUSE T.,MOTOBAYASH T.,PATRY J.P.,PEGHAIRE A.,PETER J.,PROT N., REGIMBART R.,SAINT-LAURENT F.,STECKMEYER J.C.,TAMAIN B.,YAMAHA T.
LPC - CAEN, GANIL - CAEN, UNIVERSITIES OF LOUVAIN-LA-NEUVE, TSUKUBA, RIKKYO, BRUXELLES
RICERCA SCIENTIFICA ED EDUCAZIONE PERMANENTE 78 (1990) 314.
INTERNATIONAL WINTER MEETING ON NUCLEAR PHYSICS.18
BORMIO (IT)

ON THE OBSERVATION OF A TRANSITION FROM FUSION TO MULTIGRAGMENTATION IN HIGH MULTIPLICITY 16 O INDUCED REACTIONS
JAKOBSSON B., JONSSON G., KARLSSON L., KOPLKAR V., NOREN B., SODERSTROM K., SCHUSSLER F., MONNAND E., NIFENECKER H., FAI G., BONDORF J.P., SNEPPEN K.
UNIV. OF LUND - LUND, ISN - GRENOBLE, KENT STATE UNIV. - KENT, NIELS BOHR INST. - COPENHAGEN
NUCL. PHYS. A509 (1990) 195.

PREEQUILIBRIUM PARTICLES AND MEAN-FIELD EFFECTS FROM PARTICLE-PARTICLE CORRELATIONS IN HEAVY-ION COLLISIONS
ARDOUIN D., BASRAK Z., SCHUCK P., PEGHAIRE A., SAINT-LAURENT F., DELAGRANGE H., DOUBRE H., GREGOIRE C., KYANOWSKI A., MITTIG W., PETER J., VIYOGI Y.P., QUEBERT J., GELBKE C.K., LYNCH W.G., MAIER M., POCHODZALLA J., BIZARD G., LEFEBVRES F., TAMAIN B., REMAUD B., SEBILLE F.
LPN - NANTES, ISN - GRENOBLE, GANIL - CAEN, VECC - CALCUTTA, CENBG - GRADIGNAN, MSU - EAST-LANSING, LPC - CAEN
NUCL. PHYS. A514 (1990) 564.

PRODUCTION AND DEEXCITATION OF HOT NUCLEI IN COLLISIONS OF 27 MeV/NUCLEON 40 Ar WITH 238 U
JACQUET D., PEASLEE G.F., ALEXANDER J.M., BORDERIE B., DUEK E., GALIN J., GARDES D., GREGOIRE C., GUERREAU D., FUCHS H., LEFORT M., RIVET M.F., TARRAGO X.
IPN - ORSAY, STATE UNIV. OF NEW YORK - STONY BROOK, GANIL - CAEN, HMI - BERLIN
NUCL. PHYS. A511 (1990) 195.

SEQUENTIAL OR SIMULTANEOUS BREAK UP INVESTIGATED IN A 3-BODY ANALYSIS
BOUGAULT R., COLIN J., DELAUNAY F., GENOUX-LUBAIN A., HAIFANI A., HORN D., LE BRUN C., LECOLLEY J.F., LOUVEL M., STECKMEYER J.C.
LPC - CAEN
IN2P2-RIKEN SYMPOSIUM ON HEAVY-ION COLLISIONS.2
OBERNAI (FR)

SIDEWARDS FLOW EFFECT IN Kr + Au CENTRAL COLLISIONS AT 43 MeV/u
BOUGAULT R., DELAUNAY F., GENOUX-LUBAIN A., LE BRUN C., LECOLLEY J.F., LEFEBVRES F., LOUVEL M., STECKMEYER J.C., ADLOFF J.C., BILWES B., BILWES R., GLASER M., RUDOLF G., SCHEIBLING F., STUTTGE L., FERRERO J.L.
LPC - CAEN, CRN - STRASBOURG, IFIC - VALENCIA
RICERCA SCIENTIFICA ED EDUCAZIONE PERMANENTE 78 (1990) 259.
INTERNATIONAL WINTER MEETING ON NUCLEAR PHYSICS.18
BORMIO (IT)

SIDEWARDS FLOW IN THE 43 MeV/u Kr + Au REACTION
BOUGAULT R., DELAUNAY F., GENOUX-LUBAIN A., LE BRUN C., LECOLLEY J.F., LEFEBVRES F., LOUVEL M., STECKMEYER J.C., ADLOFF J.C., BILWES B., BILWES R., GLASER M., RUDOLF G., SCHEIBLING L., FERRERO J.L.
LPC - CAEN, CRN - STRASBOURG, IFIC - VALENCIA
IN2P3-RIKEN SYMPOSIUM ON HEAVY-ION COLLISIONS.2
OBERNAI (FR)

TEMPERATURE MEASUREMENTS AT BACKWARD ANGLES IN 40 Ar INDUCED REACTIONS ON Ag AT E/A = 44 MeV
DABROWSKI H., GOUJDAMI D., GUILBAULT F., LEBRUN C., ARDOUIN D., LAUTRIDOU P., BOISGARD R., QUEBERT J., PEGHAIRE A., EUDES P., SEBILLE F., REMAUD B.
LPN AND UNIV. DE NANTES - NANTES, CENB AND UNIV. DE BORDEAUX I - GRADIGNAN, GANIL - CAEN
PHYS. LETT. 247, 2,3 (1990) 223.

USING GLOBAL VARIABLES FOR IMPACT PARAMETER DETERMINATION IN NUCLEUS-NUCLEUS COLLISIONS BELOW 100 MeV/u
PETER J., CUSSOL D., BIZARD G., BROU R., LOUVEL M., PATRY J.P., REGIMBART R., STECKMEYER J.C., SULLIVAN J.P., TAMAIN B., CREMA E., DOUBRE H., HAGEL K., JIN G.M., PEGHAIRE A., SAINT-LAURENT F., CASSAGNOU Y., LEGRAIN R., LEBRUN C., ROSATO E., MACGRATH R., JEONG S.C., LEE S.M., NAGASHIMA Y., NAKAGAWA T., OGIHARA M., KASAGI J., MOTOBAYASHI T.
LPC - CAEN, GANIL - CAEN, CEN - SACLAY, LPN - NANTES, UNIV. DI NAPOLI, SUNY - STONY BROOK, INST. OF MOD. PHYS. - LANZHOU, UNIV. OF TSUKUBA, TOKYO INST. OF TECHNOLOGY - TOKYO, RIKKYO UNIV. - TOKYO
IN2P3-RIKEN SYMPOSIUM ON HEAVY-ION COLLISIONS.2
OBERNAI (FR)

EVIDENCE OF A TWO-SOURCE EMISSION FOR LIGHT CHARGED PARTICLES IN COINCIDENCE WITH PIONS PRODUCED IN 16 O + 27 Al COLLISIONS AT 94 MeV/NUCLEON
BARBERA R., BADALA A., ADORNO A., BONASERA A., DI TORO M., PALMERI A., PAPPALARDO G.S., BIZARD G., BOUGAULT R., DURAND D., GENOUX-LUBAIN A., LAVILLE J.L., LEFEBVRES F., PATRY J.P., JIN G.M., ROSATO E.
ISTITUTO NAZIONALE DI FISICA NUCLEARE - CATANIA, LPC - CAEN, GANIL - CAEN, INFN - NAPOLI
NUCLEAR PHYSICS A518 (1990) 767

HARD PHOTON CORRELATIONS IN HEAVY-ION COLLISIONS
OSTENDORF R., SCHUTZ Y.
GANIL - CAEN
INTERNATIONAL WORKSHOP ON PARTICLE CORRELATIONS AND INTERFEROMETRY IN NUCLEAR COLLISIONS
NANTES
CORINNE 90

PION PRODUCTION AND SOURCE EFFECTS IN INTERMEDIATE ENERGY HEAVY ION COLLISIONS
LEBRUN D., PERRIN G., de SAINTIGNON P., BOUGAULT R., DURAND D., GENOUX-LUBAIN A., JULIEN J., LE BRUN C., LECOLLEY J.F., LOUVEL M.
ISN - GRENOBLE, LPC - CAEN, SPEN - SACLAY
IN2P3-RIKEN SYMPOSIUM ON HEAVY-ION COLLISIONS.2
OBERNAI (FR)

PI- PRODUCTION IN 16 O + 27 Al AT 38, 65 AND 93 MeV/u
LEBRUN D., CHAUVIN J., JULIEN J., LEBRUN C., LECOLLEY J.F., PERRIN G., REBREYEND D., de SAINTIGNON P.
ISN - GRENOBLE, CEN - SACLAY, LPC - CAEN
Z. FUR PHYSIK A335 (1990) 73.

MASS MEASUREMENTS WITH THE GANIL CYCLOTRONS
AUGER G., BAJARD, BARON E., BIBET D., BRICAULT P., CHABERT A., GILLIBERT A., MITTIG W., ORR N., PLAGNOL E., RICAUD C., SCHUTZ Y., VILLARI A.C.C.
GANIL - CAEN, CEN - SACLAY, IFN/USP - SAO PAULO
INTERNATIONAL CONFERENCE ON RADIOACTIVE NUCLEAR BEAMS.1
BERKELEY
RADIOACTIVE NUCLEAR BEAMS

INDRA : A NEW DETECTOR FOR HEAVY ION REACTION STUDIES
PLAGNOL E.
GANIL - CAEN
IN2P3-RIKEN SYMPOSIUM ON HEAVY-ION COLLISIONS.2
OBERNAI (FR)

LISE : A RECOIL-SPECTROMETER AT GANIL FOR THE PRODUCTION AND STUDY OF SECONDARY RADIOACTIVE BEAMS. PRESENT STATUS AND FUTURE
MUELLER A.C., ANNE R.
IPN - ORSAY, GANIL - CAEN
INTERNATIONAL CONFERENCE ON RADIOACTIVE NUCLEAR BEAMS.1
BERKELEY
RADIOACTIVE NUCLEAR BEAMS

PRODUCTION OF AND EXPERIMENTS WITH SECONDARY RADIOACTIVE BEAMS
MUELLER A.C.
IPN - ORSAY
IN2P3-RIKEN SYMPOSIUM ON HEAVY-ION COLLISIONS.2
OBERNAI (FR)

PRODUCTION OF RADIOACTIVE BEAMS AT GANIL AND THEIR USE FOR ASTROPHYSICAL PURPOSES
AGUER P.
CSNSM - ORSAY
INTERNATIONAL CONFERENCE ON RADIOACTIVE NUCLEAR BEAMS.1
BERKELEY
RADIOACTIVE NUCLEAR BEAMS

THE GANIL ACCELERATOR : NEW ENERGIES AND NEW DETECTORS
PLAGNOL E.
GANIL - CAEN
RICERCA SCIENTIFICA ED EDUCAZIONE PERMANENTE 78 (1990) 181.
INTERNATIONAL WINTER MEETING ON NUCLEAR PHYSICS.18
BORMIO (IT)

T - THEORIE

AMBIGUITIES IN THE CALCULATION OF HARD-PHOTON PRODUCTION IN DIFFERENT ESTIMATES OF THE COLLISION INTEGRAL
BONASERA A., GREGOIRE C.
UNIVERSITAT MUNCHEN - GARCHING, GANIL - CAEN
IL NUOVO CIMENTO 102A (1989) 1301.

EQUATION D'ETAT NUCLEAIRE ET SIMULATIONS NUMERIQUES DES REACTIONS D'IONS LOURDS
ISN - GRENOBLE, GANIL - CAEN, UNIV. DE NANTES - NANTES
LE COURRIER DU CNRS 74 (1989) 19.

EQUATION OF STATE SIGNATURES IN HEAVY-ION DYNAMICS AT INTERMEDIATE ENERGIES
DE LA MOTA V., SEBILLE F., REMAUD B., GREGOIRE C., SCHUCK P.
LPN - NANTES, IRESTE - NANTES, GANIL - CAEN, ISN - GRENOBLE, ISITEM - NANTES
RICERCA SCIENTIFICA ED EDUCAZIONE PERMANENTE 78 (1990) 88.
INTERNATIONAL WINTER MEETING ON NUCLEAR PHYSICS.18
BORMIO (IT)

KAON PRODUCTION IN LANDAU-VLASOV CALCULATIONS
BELKACEM M., AYIK S., STRYJEWSKI J., SURAUD E.
GANIL - CAEN
RICERCA SCIENTIFICA ED EDUCAZIONE PERMANENTE 78 (1990) 62
INTERNATIONAL WINTER MEETING ON NUCLEAR PHYSICS.18
BORMIO (IT)

L'EQUATION D'ETAT NUCLEAIRE
SURAUD E.
IN2P3
ECOLE JOLIOT-CURIE DE PHYSIQUE NUCLEAIRE 1990
MAUBUISSON
LA PHYSIQUE NUCLEAIRE DU LABORATOIRE AUX ETOILES

STATIC AND DYNAMICAL PROPERTIES OF HOT NUCLEI
SURAUD E.
GANIL - CAEN
IN2P3-RIKEN SYMPOSIUM ON HEAVY-ION COLLISIONS
OBERNAI (FR)

TOWARDS A DYNAMICAL DESCRIPTION OF INTERMEDIATE MASS FRAGMENT FORMATION IN HEAVY-ION COLLISIONS AT SOME TENS OF MeV/A
SURAUD E.
GANIL - CAEN
RICERCA SCIENTIFICA ED EDUCAZIONE PERMANENTE 78 (1990) 190.
INTERNATIONAL WINTER MEETING ON NUCLEAR PHYSICS.18
BORMIO (IT)

TRANSPORT THEORY OF FLUCTUATION PHENOMENA IN NUCLEAR COLLISIONS
AYIK S., GREGOIRE C.
TENESSEE TECHNOLOGICAL UNIV. - COOKEVILLE AND JINR - DUBNA, GANIL - CAEN
NUCL. PHYS. A513 (1990) 187.

1991

EXCITATION OF GIANT RESONANCES THROUGH INELASTIC SCATTERING OF 17 O AT 84 MEV/U. FISSION DECAY OF GIANT RESONANCES

CABOT C., BARRETTE J., MARK S.K., TURCOTTE R., WING J., ALAMANOS N., AUGER F., FERNANDEZ B., GASTEBOIS J., GILLIBERT A., LACEY R., LIGUORI-NETO R., ROUSSEL-CHOMAZ P., MICZAIKA A., BLUMENFELD Y., FRASCARIA N., GARON J.P., ROYNETTE J.C., SCAR
VAN DEN BERG A.M.
Mc GILL UNIV. - MONTREAL, SEPN/CEN SACLAY, IPN - ORSAY, KVI - GRONINGEN
RICERCA SCIENTIFICA ED EDUCAZIONE PERMANENTE.83 (1991) 273.
INTERNATIONAL WINTER MEETING ON NUCLEAR PHYSICS.XXIX
BORMIO

GLOBAL VARIABLES AND IMPACT PARAMETER DETERMINATION IN NUCLEUS-NUCLEUS COLLISIONS BELOW 100 MeV/u

PETER J., CUSSOL D., BIZARD G., BROU R., LOUVEL M., PATRY J.P., REGIMBART R., STECKMEYER J.C., SULLIVAN J.P., TAMAIN B., CREMA E., DOUBRE H., HAGEL K., JIN G.M., PEGHAIRE A., SAINT-LAURENT F., CASSAGNOU Y., LEGRAIN R., LEBRUN C., ROSATO E., MacGRATH R., JEONG S.G., LEE S.M., NAGASHIMA Y., NAKAGAWA T., OGIHARA M., KASAGI J., MOTOBAYASHI T.
LPC - CAEN, GANIL - CAEN, CEN - SACLAY, LPN - NANTES, UNIV. DI NAPOLI - NAPOLI, SUNY - STONY BROOK, INST. OF MODERN PHYSICS - LANZHOU, UNIV. OF TSUKUBA, TOKYO INST. OF TECHNOLOGY - TOKYO, RIKKYO UNIV. - TOKYO
NUCLEAR PHYSICS A519 (1990) 611.

HIGH-ENERGY TARGET EXCITATIONS IN HEAVY ION INELASTIC SCATTERING

THOENNESSEN M., BEENE J.R., BERTRAND F.E., HOREN D.J., HALBERT M.L., HENSLEY D.C., LISANTTI J.E., MITTIG W., SCHUTZ Y., ALAMANOS N., AUGER F., BARRETTE J., FERNANDEZ B., GILLIBERT A., HAAS B., VIVIEN J.P., NATHAN A.M.
OAK RIDGE NAT. LAB. - OAK RIDGE, GANIL - CAEN, CEN - SACLAY, CRN - STRASBOURG, UNIV. OF ILLINOIS - CHAMPAIGN
PHYS. REV. C43, 1 (1991) 12.

IMPACT PARAMETER AND ENERGY DEPENDENCE OF THE DYNAMICS OF NUCLEUS-NUCLEUS COLLISIONS BELOW 100 MeV/u

PETER J.
LPC - CAEN
INTERNATIONAL SYMPOSIUM ON HEAVY ION PHYSICS AND ITS APPLICATION
LANZHOU

ISOSPIN CHARACTER OF THE GIANT QUADRUPOLE TRANSITION IN 124 Sn

HOREN D.J., BERTRAND F.E., BEENE J.R., SATCHLER G.R., MITTIG W., VILLARI A.C.C., SCHUTZ Y., ZHEN WENLONG, PLAGNOL E., GILLIBERT A.
OAK RIDGE NAT. LAB. - OAK RIDGE, GANIL - CAEN, CEN - SACLAY
PHYS. REV. C44, 6 (1991) 2385.

ISOSPIN CHARACTER OF THE "ISOSCALAR" GIANT QUADRUPOLE RESONANCE IN 118 Sn

HOREN D.J., BERTRAND F.E., BEENE J.R., SATCHLER G.R., MITTIG W., VILLARI A.C.C., SCHUTZ Y., ZHEN WENLONG, PLAGNOL E., GILLIBERT A.
OAK RIDGE NAT. LAB. - OAK RIDGE, GANIL - CAEN, CEN - SACLAY
PHYSICAL REVIEW C42 (1990) 2412.

PROTON STRIPPING INDUCED BY 13 C AT 50 MeV/NUCLEON ON 12 C, 40 Ca AND 58 Ni

BRAEUNIG M., VON OERTZEN W., BOHLEN H.G., MICZAIKA A., STILIARIS E., BUENERD M., BERAT C., CHAUVIN J., LEBRUN D., HOSTACHY J.Y., MARTIN PH., MITTIG W., BARETTE J., BERTHIER B., FERNANDEZ B.
HMI - BERLIN, ISN - GRENOBLE, GANIL - CAEN, CEN - SACLAY
NUCLEAR PHYSICS A519 (1990) 631.

ENERGETIC PARTICLE EMISSION IN HEAVY-ION COLLISIONS AROUND 100 MeV/u
BADALA A., BARBERA R., BIZARD G., DURAND D., LAVILLE J.L., PALMERI A., PAPPALARDO G.S., RIGGI F.
ISTITUTO NAZIONALE DI FISICA NUCLEARE - CATANIA, LPC - CAEN
EUROPHYS. LETT. 15, 2 (1991) 145.

ENERGY DISSIPATION IN PERIPHERAL REACTIONS INDUCED BY 40 Ar BEAMS BETWEEN 27 AND 44 MeV/u
MORJEAN M., DOUBRE H., GALIN J., GUERREAU D., JIANG D.X., POUTHAS J., CHARVET J.L., FREHAUT J., LOTT B., MAGNAGO C., PATIN Y., PRANAL Y., JACQUET D., INGOLD G., JAHNKE U.
GANIL - CAEN, CEN - BRUYERES LE CHATEL, IPN - ORSAY, HMI - BERLIN
NUCL. PHYS. A524 (1991) 179.

EXCITATION ENERGY PARTITION IN DEEPLY INELASTIC COLLISIONS AT 27 MeV PER NUCLEON AS A PROBE OF THE EVOLUTION OF THE ENERGY RELAXATION TIME
BORDERIE B., RIVET M.F., CABOT C., FUCHS H., GARDES D., HANAPPE F., JOUAN D., MONTOYA M.
IPN - ORSAY, HMI - BERLIN, FNRS ET UNIV. LIBRE DE BRUXELLES, IPEN - LIMA
RICERCA SCIENTIFICA ED EDUCAZIONE PERMANENTE.83 (1991) 38.
INTERNATIONAL WINTER MEETING ON NUCLEAR PHYSICS.XXIX
BORMIO

EXCITATION ENERGY PARTITION IN DEEPLY INELASTIC COLLISIONS BETWEEN 40 Ar AND Ag AT 27 MeV PER NUCLEON
BORDERIE B., RIVET M.F., CABOT C., FUCHS H., GARDES D., HANAPPE F., JOUAN D., MONTOYA M.
HMI - BERLIN, FNRS/UNIV.LIBRE DE BRUXELLES, IPEN - LIMA
Z. PHYS. A338 (1991) 369.

PROJECTILE EXCITATION ENERGY EVOLUTION IN PERIPHERAL COLLISIONS FOR 16 O + 197 Au AT 32.5, 50 AND 70 MeV/N
POULIOT J., AUGER G., BRICAULT P., CHAN Y., DORE D., GROULT S., HORN D., HOUDE S., LAFOREST R., PLAGNOL E., ROY R., SAINT PIERRE C.
LPN/UNIV. LAVAL STE-FOY - QUEBEC, GANIL - CAEN, LBL - BERKELEY, LPC - CAEN, CHALK RIVER LABORATORY
PHYS. LETT. B263, No. 1 (1991) 18.

INTERMEDIATE ENERGY HEAVY ION REACTIONS AND THE PRODUCTION OF NUCLEI FAR FROM STABILITY
BAZIN D., GUERREAU D., ANNE R., GUILLEMAUD-MUELLER D., GRUNBERG C., MUELLER A.C., SAINT-LAURENT M.G., STEPHAN C., TASSAN-GOT L., BACHELIER D., BACRI C.O., BIMBOT R., BORDERIE B., BOYARD J.L., CLAPIER F., DONZAUD C., HENNINO T., RIVET M.F., ROUSSEL P., DISDIER D., LOTT B.
NSCL - EAST LANSING, GANIL - CAEN, IPN - ORSAY, CRN - STRASBOURG
WINTER WORKSHOP ON NUCLEAR DYNAMICS.7
KEY WEST (US)
ADVANCES IN NUCLEAR DYNAMICS

MASS MEASUREMENTS OF NUCLEI FAR FROM THE VALLEY OF BETA-STABILITY EXPLORING THE MASS SURFACE AT GANIL
ARTUKH A.G., AUDI G., BELOZVOROV A.V., BIANCHI L., CUNSOLO A., DUMONT H., FERNANDEZ B., FOTI A., GASTEBOIS J., GILLIBERT A., GREGOIRE C., LEWITOWICZ M., LUKYANOV S.M., MITTIG W., MORJEAN M., ORR N., PENIONZHKEVICH YU.E., PLAGNOL E., PRANAL Y., SCHUTZ Y., STEPHAN C., TASSAN-GOT L., VILLARI A.C.C., ZHAN WEN LONG
GANIL - CAEN, INFN - CATANIA, JINR - DUBNA, IMP - LANZHOU, CSNSM - ORSAY, IPN - ORSAY, CEN - BRUYERES, IFUSP - SAO-PAULO
INTERNATIONAL SCHOOL-SEMINAR ON HEAVY ION PHYSICS
DUBNA (URSS)

NEW MASS MEASUREMENTS OF NEUTRON-RICH NUCLEI NEAR N = 20
ORR N.A., MITTIG W., FIFIELD L.K., LEWITOWICZ M., PLAGNOL E., SCHUTZ Y., ZHAN WEN LONG, BIANCHI L., GILLIBERT A., BELOZYOROV A.V., LUKYANOV S.M., PENIONZHKEVICH YU.E., VILLARI A.C.C., CUNSOLO A., FOTI A., AUDI G., STEPHAN C., TASSAN-GOT L.
GANIL - CAEN, CEN - SACLAY, JINR - DUBNA, INST. DE FISICA DA USP - SAO PAULO, INFN - CATANIA, CSNSM - ORSAY, IPN - ORSAY
PHYS. LETT. B258, 1,2 (1991) 29.

OBSERVATION OF FORWARD NEUTRONS FROM THE BREAK-UP OF THE Li NEUTRON HALO
ANNE R., ARNELL S.E., BIMBOT R., EMLING H., GUILLEMAUD-MUELLER D., HANSEN P.G., JOHANNSEN L., JONSON B., LEWITOWICZ M., MATTSSON S., MUELLER A.C., NEUGART R., NYMAN G., POUGHEON F., RICHTER A., RIISAGER K., SAINT-LAURENT M.G., SCHRIEDER G., SORLIN O., WILHELMSEN K.
GANIL - CAEN, CHALMERS TEKNISKA HOGSKOLA - GOTEBORG, IPN - ORSAY, GSI - DARMSTADT, AARHUS UNIVERSITET - AARHUS, MAINZ UNIV. - MAINZ, INSTITUT FUR KERNPHYSIK - DARMSTADT
PHYSICS LETTERS B250 (1990) 19.

PRODUCTION AND STUDY OF VERY NEUTRON-RICH NUCLEI BY MEANS OF FRAGMENTATION OF 48 Ca PROJECTILE AT GANIL ENERGIES
GUILLEMAUD-MUELLER D.
IPN - ORSAY
INTERNATIONAL SCHOOL-SEMINAR OF HEAVY ION PHYSICS
DUBNA (URSS)

RADII OF RADIOACTIVE NUCLEI
MITTIG W., PLAGNOL E., SCHUTZ Y., LEWOTOWICZ M., VILLARI A.C.C., BIANCHI L., GILLIBERT A., STEPHAN C., TASSAN-GOT L., AUDI G., ZHAN WENLONG, CUNSOLO A., FOTI A., BELEZYOROV A., LUKYANOV S., PENIONZHKEVICH Y.
GANIL - CAEN, INSTITUTO DE FISICA DA USP - SAO PAULO, CEN - SACLAY, IPN - ORSAY, CSNSM - ORSAY, IMP - LANZHOU, DIPARTIMENTO DI FISICA AND INFN - CATANIA, LNP/INR - MOSCOW
THE FIRST INTERNATIONAL CONFERENCE ON RADIOACTIVE NUCLEAR BEAMS
BERKELEY
RADIOACTIVE NUCLEAR BEAMS

SEARCH FOR DIRECT TWO-PROTON RADIOACTIVITY FROM Ti ISOTOPES AT THE PROTON DRIP LINE
DETRAZ C., ANNE R., BRICAULT P., GUILLEMAUD-MUELLER D., LEWITOWICZ M., MUELLER A.C., ZHANG YU HU, BORREL V., JACMART J.C., POUGHEON F., RICHARD A., BAZIN D., DUFOUR J.P., FLEURY A., HUBERT F., PRAVIKOFF M.S.
GANIL - CAEN, IPN - ORSAY, CENBG - GRADIGNAN
NUCLEAR PHYSICS A519 (1990) 529.

THE BETA DECAY OF 18 C
PRAVIKOFF M.S., HUBERT F., DEL MORAL R., DUFOUR J.P., FLEURY A., JEAN D., MUELLER A.C., SCHMIDT K.H., SUMMERER K., HANELT E., FREHAUT J., BEAU M., GIRAUDET G., BROWN B.A.
CENBG - GRADIGNAN, GANIL - CAEN, GSI - DARMSTADT, INST. FUR KERNPHYSIK - DARMSTADT, CEN - BRUYERES-LE-CHATEL, MSU - EAST LANSING
NUCL. PHYS. A528 (1991) 225.

THE MASS AND RADIUS OF EXOTIC FRAGMENTS
SCHUTZ Y.
GANIL - CAEN
INTERNATIONAL CONFERENCE ON SPECTROSCOPY OF HEAVY NUCLEI
CRETE (GR)
INST. PHYS. CONF. SR. No 105 (1989)

THE NEUTRON HALO
HANSEN P.G.
UNIV. OF AARHUS - AARHUS
NUCL. PHYS. NEWS. 1, No 3 (1991) 21.

CENTRAL COLLISIONS AT THE FERMI ENERGY
HARAR S.
GANIL - CAEN
INTERNATIONAL SCHOOL-SEMINAR ON HEAVY ION PHYSICS
DUBNA (URSS)

DISAPPEARANCE OF FLOW AS A FUNCTION OF IMPACT PARAMETER AND ENERGY IN NUCLEUS-NUCLEUS COLLISIONS
SULLIVAN J.P., PETER J., CUSSOL D., BIZARD G., BROU R., LOUVEL M., PATRY J.P., REGIMBART R., STECKMEYER J.C., TAMAIN B., CREMA E., DOUBRE H., HAGEL K., JIN G.M., PEGHAIRE A., SAINT-LAURENT F., CASSAGNOU Y., LEGRAIN R., LEBRUN C., ROSATO E., MAcGRATH R., JEONG S.C., LEE S.M., NAGASHIMA Y., NAKAGAWA T., OGIHARA M., KASAGI J., MOTOBAYASHI T.
LPC - CAEN, GANIL - CAEN, INST. OF MOD. PHYS. - LANZHOU, CEN - SACLAY, LPN - NANTES, UNIV. DI NAPOLI - NAPLES, SUNY - STONY-BROOK, UNIV. OF TSUKUBA - IBARAKI, TOKYO INST. OF TECH. - TOKYO, RIKKYO UNIV. - TOKYO
PHYSICS LETTERS B249 (1990) 8.

DYNAMICS AND THERMALIZATION IN VIOLENT COLLISIONS BETWEEN 40 Ar AND Ag AT 27 MeV/NUCLEON
JOUAN D., BORDERIE B., RIVET M.F., CABOT C., FUCHS H., GAUVIN H., GREGOIRE C., HANAPPE F., GARDES D., MONTOYA M., REMAUD B., SEBILLE F.
IPN - ORSAY, GANIL - CAEN, FNRS ET UNIV. LIBRE DE BRUXELLES, LPN - NANTES
Z. PHYS. A340 (1991) 63.

EXCLUSIVE STUDY OF NUCLEUS-NUCLEUS REACTIONS AT INTERMEDIATE ENERGIES : IMPACT PARAMETER DEPENDENCE OF PRE-EQUILIBRIUM EMISSION, COLLECTIVE FLOW AND HOT NUCLEI FORMATION
PETER J., SULLIVAN J.P., CUSSOL D., BIZARD G., BROU R., LOUVEL M., PATRY J.P., REGIMBART R., STECKMEYER J.C., TAMAIN B., CREMA E., DOUBRE H., HAGEL K., JIN G.M., PEGHAIRE A., SAINT-LAURENT F., CASSAGNOU Y., LEGRAIN R., LEBRUN C., ROSATA E., MACGRATH R., JEONG S.C., LEE S.M., NAGASHIMA Y., NAKAGAWA T., OGIHARA M., KASAGI J., MOTOBAYASHI T.
LPC - CAEN, GANIL - CAEN, CEN - SACLAY, LPN - NANTES, UNIV. DI NAPOLI - NAPOLI, SUNY - STONY BROOK, INST. OF MODERN PHYS. - LANZHOU, UNIV. OF TSUKUBA, TOKYO INST. OF TECHNOLOGY, RIKKYO UNIV. - TOKYO
NUCLEAR PHYSICS A519 (1990) 127c.
INTERNATIONAL WORKSHOP ON NUCLEAR DYNAMICS
MARCIANA MARINA (IT)

EXCLUSIVE STUDY OF THE FORMATION AND THE DECAY OF HOT NUCLEI IN THE INTERMEDIATE ENERGY DOMAIN
SAINT-LAURENT F.
GANIL - CAEN
INTERNATIONAL SYMPOSIUM ON HEAVY ION PHYSICS AND ITS APPLICATION
LANZHOU

FORMATION AND DECAY OF HOT AND HEAVY SYSTEMS STUDIED WITH A 4pi NEUTRON DETECTOR
MORJEAN M., BRESSON S., CREMA E., GALIN J., GUERREAU D., PAULOT C., POUTHAS J., GATTY B., JACQUET D., PIASECKI E., KORDYASZ A., JASTRZEBSKI J., PIENKOWSKI L., SKULSKI W., LOTT B., BOUGAULT R., COLIN J., GENOUX-LUBAIN A., HORN D., LEBRUN C., LECOLLEY J.F., LOUVEL M., QUEDNAU B., SCHROEDER W.U., TOKE J., JAHNKE U.
GANIL - CAEN, IPN - ORSAY, INST.OF EXP.PHYS./WARSAW UNIV. - WARSZAWA, HEAVY ION LAB./WARSAW UNIV. - WARSZAWA, CRN - STRASBOURG, LPC - CAEN, UNIV. OF ROCHESTER - ROCHESTER, HMI - BERLIN
WINTER WORKSHOP ON NUCLEAR DYNAMICS.7
KEY WEST (US)
ADVANCES IN NUCLEAR DYNAMICS

HOT COMPOSITE SYSTEMS WITH A > 200 AND T > 6 MeV
CREMA E., BRESSON S., DOUBRE H., GALIN J., GATTY B., GUERREAU D., JACQUET D., JAHNKE U., LOTT B., MORJEAN M., PIASECKI E., POUTHAS J., SAINT-LAURENT F., SCHWINN E., SOKOLOV A., WANG X.M.
GANIL - CAEN, UNIV. DE SAO PAULO, IPN - ORSAY, HMI - BERLIN, CRN - STRASBOURG, WARSAW UNIV. - WARSAW, IMP - LANZHOU
PHYS. LETT. B258, 3,4 (1991) 266.

HOT NUCLEI
GUERREAU D.
GANIL - CAEN
NUCLEAR PHYSICS NEWS 1, No. 6 (1991) 13.

LES NOYAUX CHAUDS
PETER J., TAMAIN B.
LPC - CAEN
LA RECHERCHE 228 (1991) 28.
91 09 D

NUCLEAR DISASSEMBLY OF THE Pb + Au SYSTEM AT E lab = 229 MeV PER NUCLEON
PIASECKI E., BRESSON S., LOTT B., BOUGAULT R., COLIN J., CREMA E., GALIN J., GATTY B., GENOUX-LUBAIN A., GUERREAU D., HORN D., JACQUET D., JAHNKE U., JASTRZEBSKI J., KORDYASZ A., LE BRUN C., LECOLLEY J.F., LOUVEL M., MORJEAN M., PAULOT C.,
PIENKOWSKI L., POUTHAS J., QUEDNAU B., SCHRODER W.U., SCHWINN E., SKULSKI W., TOKE J.
WARSAW UNIV. - WARSZAWA, GANIL - CAEN, CRN - STRASBOURG, LPC - CAEN, UNIV. DE SAO PAULO, IPN - ORSAY, CHALK RIVER LAB. - CHALK RIVER, HMI - BERLIN, UNIV. OF ROCHESTER - ROCHESTER
PHYS. REV. LETT. 66, 10 (1991) 1291.

RESULTS ON TWO-, THREE-, AND FOUR-BODY EVENTS FROM THE 100 Mo + 100 Mo AND 120 Sn + 120 Sn COLLISIONS AROUND E/A = 20 MeV
CHARITY R.J., FREIFELDER R., GOBBI A., HERRMANN N., HILDENBRAND K.D., RAMI F., STELZER H., WESSELS J.P., CASINI G., MAURENZIG P.R., OLMI A., STEFANINI A.A., GALIN J., GUERREAU D., JAHNKE U., PEGHAIRE A., ADLOFF J.C., BILWES B., BILWES R., RUDOLF G., PETROVICI M., GNIRS M., PELTE D.
GSI - DARMSTADT, INFN AND UNIV. OF FLORENCE, GANIL - CAEN, CRN - STRASBOURG, INPE - BUCAREST, UNIVERSITAT HEIDELBERG
Z. PHYS. A341 (1991) 53.

TRANSFER AND FRAGMENTATION REACTIONS OF 14 N AT 60 MeV/u
LAHMER W., VON OERTZEN W., MICZAIKA A., BOHLEN H.G., WELLER W., GLASOW R., GRZONKA D., SANTO R., BLUMENFELD Y., FRASCARIA N., GARRON J.P., JACMART J.C., ROYNETTE J.C.
HMI - BERLIN, INSTITUT FUR KERNPHYSIK - MUNSTER, IPN - ORSAY
Z. PHYS. A337 (1990) 425.

ESTIMATION OF THE SIZES OF HOT NUCLEAR SYSTEMS FROM PARTICLE-PARTICLE LARGE ANGLE KINEMATIC CORRELATIONS

LAVILLE J.L., BADALA A., BARBERA R., BIZARD G., DURAND D., JIN G.M., PALMERI A., PAPPALARDO G.S., ROSATO E.
LPC - CAEN, INFN - CATANIA, GANIL - CAEN, INFN - NAPOLI
INTERNATIONAL WORKSHOP ON PARTICLE CORRELATIONS AND INTERFEROMETRY IN NUCLEAR COLLISIONS
NANTES
CORINNE 90

EXCLUSIVE STUDY OF LIGHT PARTICLE CORRELATIONS IN THE INTERMEDIATE ENERGY DOMAIN

SAINT-LAURENT F., FERRAGUT A.
GANIL - CAEN
INTERNATIONAL WORKSHOP ON PARTICLE CORRELATIONS AND INTERFEROMETRY IN NUCLEAR COLLISIONS
NANTES
CORINNE 90

LIFETIME EFFECTS OF AN EVAPORATIVE SOURCE VIA TWO-PROTON CORRELATIONS

GOUJDAMI D., GUILBAULT F., LEBRUN C., DABROWSKI H., ARDOUIN D., PRATT S., LAUTRIDOU P., BOISGARD R., QUEBERT J., PEGHAIRE A.
LPN - NANTES, UNIV. OF WISCONSIN - MADISON, CENBG - GRADIGNAN, GANIL - CAEN
INTERNATIONAL WORKSHOP ON PARTICLE CORRELATIONS AND INTERFEROMETRY IN NUCLEAR COLLISIONS
NANTES
CORINNE 90

NEUTRON MULTIPLICITY MEASUREMENTS AS A TEST OF THE CHARACTER OF THE COLLISION

JACQUET D., BRESSON S., BOUGAULT R., COLIN J., CRAMER B., CREMA E., GALIN J., GATTY B., GENOUX-LUBAIN A., GUERREAU D., HORN D., JAHNKE U., JASTRZEBSKI J., KORDYASZ A., LE BRUN C., LECOLLEY J.F., LOTT B., LOUVEL M., MORJEAN M., PAULOT C., PIASECKI E., PIENKOWSKI L., POUTHAS J., QUEDNAU B., SAINT-LAURENT F., SCHRODER W.U., SCHWINN E., SKULSKI W., SOKOLOV A., TOKE J., WANG X.M.
WARSAW UNIV. - WARSZAWA, GANIL - CAEN, LPC - CAEN, HMI - BERLIN, UNIV. OF ROCHESTER, IPN - ORSAY, CRN - STRASBOURG, UNIV. DE SAO PAULO, CHALK RIVER LAB. - CHALK RIVER
RICERCA SCIENTIFICA ED EDUCAZIONE PERMANENTE.83
INTERNATIONAL WINTER MEETING ON NUCLEAR PHYSICS.XXIX
BORMIO

PROJECTILE FRAGMENTATION AT INTERMEDIATE ENERGY

SAUVESTRE J.E., BERTHIER B., CHARVET J.L., DAYRAS R., LEGRAIN R., LUCAS R., MAZUR C., POLLACCO E.C., VOLANT C., LANZANO G., PAGANO A., SPARTI U., URSO S., BECK C., DJERROUD B.
CEN SACLAY - GIF-SUR-YVETTE, INFN - CATANIA, CRN - STRASBOURG
RICERCA SCIENTIFICA ED EDUCAZIONE PERMANENTE.83 (1991) 91.
INTERNATIONAL WINTER MEETING ON NUCLEAR PHYSICS.XXIX
BORMIO

SEARCH FOR LIFETIME EFFECTS OF AN EVAPORATIVE SOURCE USING TWO-PROTON CORRELATIONS

GOUJDAMI D., GUILBAULT F., LEBRUN C., ARDOUIN D., DABROWSKI H., PRATT S., LAUTRIDOU P., BOISGARD R., QUEBERT J., PEGHAIRE A.
LPN - NANTES, UNIV. OF WISCONSIN - MADISON, CENBG - GRADIGNAN, GANIL - CAEN
Z. PHYS. A339 (1991) 293.

SUBTHRESHOLD K+ PRODUCTION IN HEAVY ION COLLISIONS
JULIEN J., LEBRUN D., MOUGEOT A., de SAINTIGNON P., ALAMANOS N., CASSAGNOU Y., LE BRUN C., LECOLLEY J.F., LEGRAIN R., PERRIN G.
CEN SACLAY - GIF SUR YVETTE, ISN - GRENOBLE, LPC - CAEN
PHYS. LETT. B264, No. 3,4 (1991) 269.

EVIDENCE OF A TWO-SOURCE EMISSION FOR LIGHT CHARGED PARTICLES IN COINCIDENCE WITH PIONS PRODUCED IN 16 O + 27 Al COLLISIONS AT 94 MeV/NUCLEON
BARBERA R., BADALA A., ADORNO A., BONASERA A., DI TORO M., PALMERI A., PAPPALARDO G.S., BIZARD G., BOUGAULT R., DURAND D., GENOUX-LUBAIN A., LAVILLE J.L., LEFEBVRES F., PATRY J.P., JIN G.M., ROSATO E.
ISTITUTO NAZIONALE DI FISICA NUCLEARE - CATANIA, LPC - CAEN, GANIL - CAEN, INFN - NAPOLI
NUCLEAR PHYSICS A518 (1990) 767.

EXPERIMENTAL SEARCH FOR COHERENT SUBTHRESHOLD PION PRODUCTION
ERAZMUS B., GUET C., GILLIBERT A., MITTIG W., SCHUTZ Y., VILLARI A.C.C., KUHN W., RIESS S., NIFENECKER H., PINSTON J.A., GROSSE E., HOLZMANN R., VIVIEN J.P., SOYEUR M.
GANIL - CAEN, UNIV. GIESSEN, ISN - GRENOBLE, GSI - DARMSTADT, CRN - STRASBOURG, LNS/CEN SACLAY - GIF SUR YVETTE
PHYS. REV. C44, 3 (1991) 1212.

SUBTHRESHOLD PRODUCTION OF PIONS IN COINCIDENCE WITH LIGHT PARTICLES
BARBERA R., BADALA A., ADORNO A., BONASERA A., DI TORO M., PALMERI A., PAPPALARDO G.S., RIGGI F., RUSSO G., BIZARD G., DURAND D., LAVILLE J.L., JIN G.M., ROSATO E.
ISTITUTO NAZIONALE DI FISICA NUCLEARE - CATANIA, LPC - CAEN, GANIL - CAEN, INFN - NAPOLI
NUCLEAR PHYSICS A519 (1990) 231c.
INTERNATIONAL WORKSHOP ON NUCLEAR DYNAMICS
MARCIANA MARINA (IT)

TOWARD EXCLUSIVE EXPERIMENTS ON PION AND HIGH ENERGY PROTON EMISSION AT GANIL
BIZARD G., BOUGAULT R., DURAND D., GENOUX-LUBAIN A., LAVILLE J.L., LEFEBVRES F., PATRY J.P., BADALA A., BARBERA R., BONASERA A., DI TORO M., PALMERI A., PAPPALARDO G.S., RIGGI F., RUSSO G., JIN G.M., ROSATO E.
LPC - CAEN, INFN - CATANIA, INST.OF MOD.PHYS. - LANZHOU, UNIV.DI NAPOLI - NAPOLI
INTERNATIONAL SYSMPOSIUM ON HEAVY ION PHYSICS AND ITS APPLICATION
LANZHOU

- ARTICLES GENERAUX

GANIL
HARAR S., DOUBRE H.
GANIL - CAEN
NUCL. PHYS. NEWS. 1, No 3 (1991) 12.

LES TRACES DES IONS
POUR LA SCIENCE 162 (1991) 13.

THE DEVELOPMENT OF HEAVY-ION RESEARCH AT GANIL
DETRAZ C.
GANIL - CAEN
INTERNATIONAL SCHOOL-SEMINAR ON HEAVY ION PHYSICS
DUBNA (URSS)

- INSTRUMENTATION

A DOUBLE ZERO-DISPERSION MAGNETIC SPECTROMETER USED IN A TELESCOPIC MODE FOR VERY FORWARD HEAVY-ION STUDIES
BACRI CH.O., ROUSSEL P.
IPN - ORSAY
NIM A300 (1991) 89.

SISSI AND SECONDARY BEAMS AT GANIL
MITTIG W.
GANIL - CAEN
NUCLEAR PHYSICS NEWS VOL. 1, No 2 (1990) 30.

T - THEORIE

FINITE-SIZE EFFECT IN INTERMITTENCY
BOZEK P., PLOSZAJCZAK M.
INST. OF NUCL. PHYS. - CRACOW, GANIL - CAEN
PHYS. LETT. B264, No. 1,2 (1991) 204.

FROM ONE-BODY TO COLLECTIVE TRANSPORT MODELS
AYIK S., SURAUD E., STRYJEWSKI J., BELKACEM M.
TENNESSEE TECHNOLOGICAL UNIV. - COOKEVILLE AND JOINT INST. FOR HEAVY ION RESEARCH - OAK RIDGE, GANIL - CAEN
Z. PHYS. A 337 (1990) 413.

FROM ONE-BODY TO COLLECTIVE TRANSPORT MODELS
AYIK S., SURAUD E., BELKACEM M.
TENNESSEE TECHNOLOGICAL UNIV. - COOKEVILLE, GANIL - CAEN
WINTER WORKSHOP ON NUCLEAR DYNAMICS.7
KEY WEST (US)
ADVANCES IN NUCLEAR DYNAMICS

HIGH TEMPERATURE GIANT DIPOLE AND ISOSCALAR RESONANCES
GARCIAS F., BARRANCO M., NAVARRO J., SURAUD E.
UNIVERSITAT DE LES ILLES BALEARS - PALMA DE MALLORCA, UNIVERSITAT DE VALENCIA - BURJASSOT, GANIL - CAEN
Z. PHYS. A337 (1990) 261.

INTERMITTENCY AND CLUSTERING IN THE 1D LATTICE GAS MODEL
BOZEK P., BURDA Z., JURKIEWICZ J., PLOSZAJCZAK M.
INST. OF NUCLEAR STUDIES - CRACOW, JAGELLONIAN UNIV. - CRACOW, NIELS BOHR INST. - COPENHAGEN, GANIL - CAEN
PHYS. LETT. B265 (1991) 133.

L'EQUATION D'ETAT NUCLEAIRE
SURAUD E.
GANIL - CAEN
ANN. PHYS. FR. 16 (1991) 193.

POWER LAWS FOR RATIOS OF MOMENTS OF THE FRAGMENT SIZE DISTRIBUTION
PLOSZAJCZAK M., TUCHOLSKI A., BOZEK P.
GANIL - CAEN, INST. OF NUCLEAR PHYSICS - CRACOW, UNIV. FRANKFURT, SOLTAN INST. FOR NUCLEAR STUDIES - SWIERK
PHYS. LETT. B262, No. 4 (1991) 383.

SPATIOTEMPORAL INTERMITTENCY IN ULTRARELATIVISTIC NUCLEAR COLLISIONS
BOZEK P., PLOSZAJCZAK M.
INST. OF NUCL. PHYS. - KRAKOW, GANIL - CAEN
PHYS. REV. C44, 4 (1991) 1620.

THE BOLTZMANN-LANGEVIN EQUATION AND ITS APPLICATION TO INTERMEDIATE MASS FRAGMENT PRODUCTION
SURAUD E., AYIK S., STRYJEWSKI J., BELKACEM M.
GANIL - CAEN, TENNESSEE TECHNOLOGICAL UNIV. - COOKEVILLE
NUCLEAR PHYSICS A519 (1990) 171c.
INTERNATIONAL WORKSHOP ON NUCLEAR DYNAMICS
MARCIANA MARINA (IT)

TOWARDS STOCHASTIC EXTENSIONS OF QUANTAL AND SEMICLASSICAL DYNAMICAL THEORIES
REINHARD P.G., SURAUD E., AYIK S., BELKACEM M.
UNIVERSITAT ERLANGEN, GANIL - CAEN, TENNESSEE TECH. UNIV. - COOKEVILLE
INTERNATIONAL WORKSHOP ON GROSS PROPERTIES OF NUCLEI AND NUCLEAR EXCITATIONS.19
HIRSCHEGG
GROSS PROPERTIES OF NUCLEI AND NUCLEAR EXCITATIONS

WEIGHTED PARTICLE METHOD FOR SOLVING THE BOLTZMANN EQUATION
TOHYAMA M., SURAUD E.
MSU - EAST LANSING, GANIL - CAEN
PHYSICAL REVIEW C43, 4 (1991) 1518.

Imprimerie CAEN-REPRO
Dépôt légal juin 1992

H T085

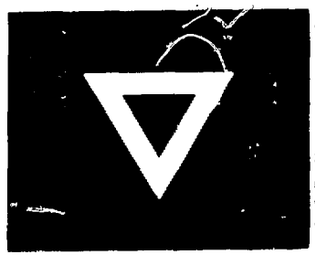

93.01.07

AD 94 05

CAL 840

GANIL

GRAND ACCELERATEUR D'IONS LOURDS
BP 5027 - 14021 CAEN CEDEX FRANCE - TEL. : 31 45 46 47
TELEX 170 533 F - FAX 31 45 46 65